

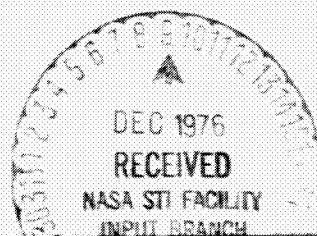
CR-15113

(NASA-CR-151113) SPACE SHUTTLE NAVIGATION
ANALYSIS (Analytic Sciences Corp.) 230 p HC
A11/MF AC1 CSCL 22A

N77-12112

Unclas

G3/16 55776



TASC

6 JACOB WAY/READING, MASSACHUSETTS 01867/(617) 944-6850

THE ANALYTIC SCIENCES CORPORATION

TR-548-2

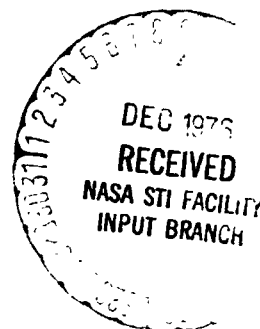
SPACE SHUTTLE NAVIGATION ANALYSIS

10 September 1976

**Prepared under:
Contract No. NAS 9-14203**

for

**NATIONAL AERONAUTICS AND SPACE ADMINISTRATION
Johnson Space Center
Houston, Texas**



Prepared by:

**Harold L. Jones
Gerd Luders
Gary A. Matchett
James E. Sciabarrasi**

Approved by:

**Donald R. Vander Stoep
Raymond A. Nash, Jr.**

**THE ANALYTIC SCIENCES CORPORATION
Six Jacob Way
Reading, Massachusetts 01867**

FOREWORD

The work for this report was performed under contract number NAS 9-14203. The authors acknowledge the guidance and assistance of the Contract Technical Monitors, Messrs. R. T. Savely and E. R. Schiesser of the Math Physics Branch of the Mission Planning and Analysis Division of NASA/JSC. Assistance and cooperation were also received from Messrs. T. J. Blucker and R. E. Eckelkamp.

This is the second of two reports submitted under the contract and represents work performed between September 1975 and July 1976. The results of work completed prior to September 1975 were presented in Ref. 1.

ABSTRACT

A detailed analysis of Space Shuttle navigation for each of the major mission phases is presented. A covariance analysis program for prelaunch IMU calibration and alignment for the Orbital Flight Tests (OFT) is described and a partial error budget is presented. The ascent, orbital operations and deorbit maneuver study considered GPS-aided inertial navigation in the Phase III GPS (1984+) time frame. The entry and landing study evaluated navigation performance for the OFT baseline system. Detailed error budgets and sensitivity analyses are provided for both the ascent and entry studies.

TABLE OF CONTENTS

	<u>Page No.</u>
FOREWORD	ii
ABSTRACT	iii
List of Figures	
List of Tables	
1. INTRODUCTION	1-1
1.1 Overview	1-2
1.1.1 Calibration and Alignment Analysis	1-3
1.1.2 GPS-Aided Navigation	1-5
1.1.3 Entry, Preland and Landing Navigation	1-8
1.2 ORGANIZATION OF THE REPORT	1-9
2. GPS-AIDED NAVIGATION	2-1
2.1 GPS Configuration	2-3
2.2 Trajectory and Measurement Schedule	2-10
2.3 Filter-Indicated Performance	2-16
2.4 Ascent Phase Truth Model	2-21
2.4.1 Ascent Phase Truth Model States	2-22
2.4.2 Truth Model Data Base	2-26
2.5 GPS-Aided Ascent Navigation Performance	2-28
2.6 Ascent Sensitivity Analysis	2-33
2.7 GPS-Aided Orbital and Deorbit Navigation	
Performance Projection	2-37
2.7.1 Deorbit Maneuver Study Baseline	2-38
2.7.2 Performance Projections	2-40
3. CALIBRATION AND ALIGNMENT COVARIANCE ANALYSIS	3-1
3.1 Calibration and Alignment Overview	3-1
3.2 Covariance Analysis Program Description	3-4
3.2.1 Program Overview	3-4
3.2.2 State and Covariance Equations	3-5
3.3 Truth Model Description	3-8
3.3.1 States and Error Sources	3-8
3.3.2 Truth Model Data Base	3-10
3.4 Partial Error Budget for Calibration and Alignment	3-14
4. ENTRY, PRELAND AND LANDING NAVIGATION	4-1
4.1 Trajectory and Measurement Schedule	4-1
4.2 Navigation Filter	4-5

TABLE OF CONTENTS (Continued)

	<u>Page No.</u>
4.3 Entry, Preland and Landing Phase Truth Model	4-9
4.3.1 Truth Model Definitions	4-9
4.3.2 Truth Model Data Base	4-11
4.4 Entry, Preland and Landing Navigation Performance	4-20
4.4.1 Navigation System Performance: Entry to 20,000 ft	4-20
4.4.2 Navigation System Performance: 20,000 ft to Touchdown	4-28
4.5 Entry, Preland and Landing Sensitivity Analysis	4-38
5. SUMMARY AND CONCLUSIONS	5-1
5.1 Ascent and Orbital Navigation	5-1
5.2 Prelaunch Calibration and Alignment	5-4
5.3 Entry, Preland and Landing Navigation	5-4
APPENDIX A - ANALYTIC EVALUATION OF TWO MECHANIZATIONS OF THE DRAG UPDATE FILTER	A-1
APPENDIX B - TRUTH MODEL DETAILS FOR THE CAL/ALIGN COVARIANCE ANALYSIS	B-1
APPENDIX C - ERROR CONTRIBUTION TIME HISTORIES: DEORBIT TO 20,000 FT	C-1
APPENDIX D - ERROR CONTRIBUTION TIME HISTORIES: 20,000 FT TO TOUCHDOWN	D-1
REFERENCES	R-1

LIST OF FIGURES

<u>Figure No.</u>		<u>Page No.</u>
1-1	Summary of TASC Studies Relative to Space Shuttle Navigation	1-2
1.1-1	TASC Approach to Calibration and Alignment Software Verification and Validation	1-4
1.1-2	Baseline Orbiter Radio Navigation Aids	1-9
2-1	Methodology for GPS/Shuttle Performance Projections	2-2
2.1-1	Elements of the NAVSTAR Global Positioning System	2-4
2.1-2	Typical User Measurement Error Statistics Due to Satellite Ephemeris and Clock Errors	2-8
2.2-1	Baseline GPS Satellite Coverage	2-11
2.2-2	Ascent Trajectory Acceleration Profile	2-13
2.2-3	Satellite Visibility Versus Time from Four User Positions	2-14
2.2-4	GPS Satellite Visibility Criterion	2-15
2.3-1	Typical GPS User Mechanization	2-16
2.3-2	Filter-Indicated Ascent Navigation Performance for First Eight GPS Measurements	2-20
2.4-1	Normalized RMS Phase Error for Quartz Crystal Clock Model	2-24
2.4-2	Quartz Crystal Clock Error Model	2-25
2.5-1	GPS-Aided Ascent Navigation: Overall Performance	2-30
2.6-1	RMS Position Error Sensitivity at Orbit Insertion to GPS Receiver Measurement Noise	2-35
2.6-2	RMS Position Error Sensitivity at Orbit Insertion to GPS Satellite Tracking Errors	2-35
2.6-3	RMS Velocity Error Sensitivity at Orbit Insertion to MTU Errors	2-36
2.6-4	RMS Downrange Misalignment Error Sensitivity at Orbit Insertion to Gyro Errors	2-37
3.1-1	Calibration and Alignment Schedule	3-3
3.2-1	Structure of Covariance Simulation for Performance Analysis	3-4

LIST OF FIGURES (Continued)

<u>Figure No.</u>		<u>Page No.</u>
4.1-1	Approach and Landing Ground Track for OFT-1 Mission	4-2
4.2-1	Schedule for Entry, Preland and Landing Phase Navigation Filter States	4-5
4.3-1	Deviation of Navigation Filter C_D Model From True C_D	4-15
4.3-2a	Time-Varying Density Bias for December-January Given as Percent Departure From 1962 Standard Atmosphere	4-16
4.3-2b	Time-Varying Density Bias for June-July Given as Percent Departure From 1962 Standard Atmosphere	4-16
4.3-3	Terrain Modeling Error for Approach Paths to Secondary Space Shuttle Landing Sites	4-18
4.4-1a	Overall Performance Down to 20,000 ft: Position	4-21
4.4-1b	Overall Performance Down to 20,000 ft: Velocity	4-21
4.4-2a	Overall Performance From 20,000 ft to Touchdown: Position	4-29
4.4-2b	Overall Performance From 20,000 ft to Touchdown: Velocity	4-29
4.5-1	RMS Vertical Velocity Error Sensitivity at 145,000 ft to Initial Position and Velocity Errors	4-39
4.5-2	RMS Crossrange Velocity Error Sensitivity at 145,000 ft to Initial Misalignment Errors	4-39
4.5-3	RMS Vertical Velocity Error Sensitivity at 20,000 ft to Baro Altimeter Bias, Scale Factor and Static Defect Errors	4-41
4.5-4	RMS Vertical Velocity Error Sensitivity at 100 ft to MLS Range Bias Error	4-41
4.5-5	RMS Downrange Velocity Error Sensitivity at 100 ft to MLS Range Second-Order Markov Error	4-42
4.5-6	RMS Crossrange Position Error Sensitivity at Touchdown to MLS Azimuth Bias Error	4-42
5-1	Velocity Performance During Landing - Complementary Mode Begins at T_{SW}	5-5

LIST OF TABLES

<u>Table No.</u>		<u>Page No.</u>
2.1-1	GPS Development Schedule	2-5
2.1-2	Phase III Satellite Initial Conditions	2-6
2.1-3	Ground Tracking Station Locations	2-6
2.1-4	Satellite Uploading Times	2-7
2.1-5	GPS Receiver Measurement Accuracy Specification	2-9
2.2-1	Trajectory Parameters at Key Events During Ascent	2-11
2.3-1	Navigation Filter States	2-17
2.3-2	Ascent Navigation Filter Initial Conditions	2-18
2.3-3	Filter-Indicated Performance During Ascent	2-21
2.4-1	Ascent Phase Truth Model States	2-22
2.4-2	Shuttle MTU Error State Definitions	2-25
2.4-3	Ascent Navigation Truth Model Data Base	2-27
2.5-1	Effect of GPS in Reducing Orbit Insertion Errors	2-31
2.5-2	Ascent Error Budget at Orbit Insertion	2-32
2.7-1	Comparison of Orbit Insertion and Deorbit Maneuvers	2-38
2.7-2	Navigation Filter Initial Conditions	2-40
2.7-3	Effect of GPS in Reducing Deorbit Errors	2-42
2.7-4	Projected Orbit Determination Accuracies for TDRSS and GPS	2-44
3.1-1	Errors Considered During the Cal/Align Phase	3-3
3.2-1	System and Covariance Error Equation Summary	3-6
3.3-1	IMU Truth Model States and Error Sources	3-9
3.3-2	IMU Truth Model Data Base for Calibrated Errors	3-11
3.3-3	IMU Truth Model Data Base for Noncalibrated Errors	3-12
3.4-1	Hangar Calibration Error Budget for Error Source Groups 18 and 23	3-16
3.4-2	Preflight Calibration Error Budget for Error Source Groups 18 and 23	3-16
4.1-1	Key Events for OFT-1 Mission	4-4
4.1-2	Sensor Locations with Respect to Touchdown Point	4-4

LIST OF TABLES (Continued)

<u>Table No.</u>		<u>Page No.</u>
4.2-1	Filter State and Measurement Error Statistics for Entry and Preland Navigation Filter	4-6
4.2-2	Landing Navigation Gains in Runway Coordinates	4-8
4.2-3	Filter-Indicated Performance	4-8
4.3-1	Entry Phase Truth Model States and Error Sources	4-10
4.3-2	Truth Model States and Error Sources for the Preland and Landing Phases	4-12
4.3-3	Truth Model Data Base for IMU-Related Error Sources	4-13
4.3-4	Truth Model Data Base for Drag-Related Error Sources	4-17
4.4-1	Baseline Error Budget for the Entry Navigation Phase	4-24
4.4-2	Alternative Contributions for the Entry Navigation Phase	4-26
4.4-3	Baseline Error Budget at 20,000 ft	4-27
4.4-4	Baseline Error Budget at T_{SW}	4-31
4.4-5	Baseline Error Budget at 100 ft Above Runway	4-33
4.4-6	Baseline Error Budget - Touchdown	4-35
4.4-7	Contribution of Terrain Modeling Error To Vertical Position Error at Touchdown	4-36
5-1	Effect of GPS in Reducing Orbit Insertion Errors	5-2
5-2	Projected Orbit Determination Accuracies for TDRSS and GPS	5-3

1. INTRODUCTION

The navigation system for the Space Shuttle will employ a variety of navigation aids in providing accurate navigation for the entire mission scenario from launch to landing. Previous studies by TASC have focussed on the development of error models for these navigation aids, the formulation of navigation software algorithms based upon the error models, and the generation of detailed performance projections for candidate navigation system implementations. As indicated in Fig. 1-1, these efforts have encompassed Space Shuttle navigation during each of the major mission phases. TASC has continued these activities in the current study with emphasis on evaluation of potential changes in the navigation system, including both software changes and new navigation aids, which could significantly improve Space Shuttle navigation performance.

The current study has considered three facets of navigation system performance:

- Prelaunch IMU calibration and alignment
- GPS-aided* navigation for the ascent, orbit and deorbit mission phases
- Entry, preland and landing navigation

The cal/align and entry studies addressed navigation system performance for the current Orbital Flight Test (OFT) baseline system. The GPS study evaluated the improvement

* NAVSTAR Global Positioning System

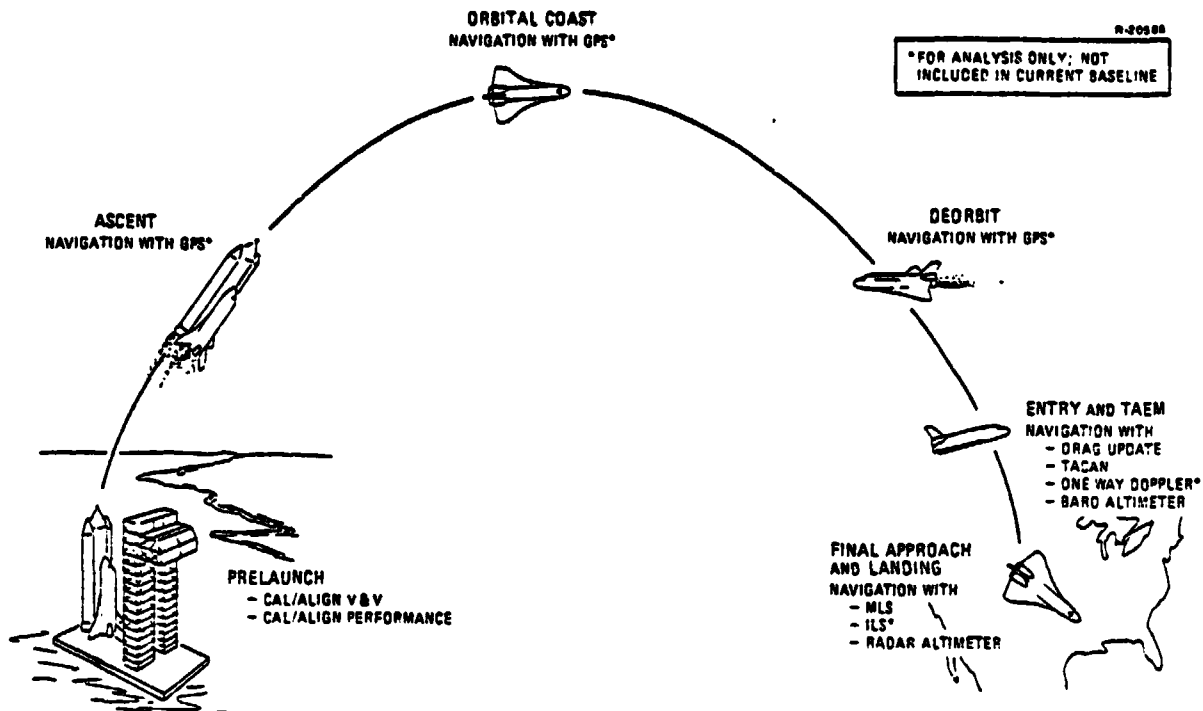


Figure 1-1 Summary of TASC Studies Relative to Space Shuttle Navigation (1973-1976)

in navigation accuracy which could be attained by using GPS as the primary navigation aid for the Space Shuttle. Each of these studies is discussed in more detail in the following section.

1.1 OVERVIEW

The guidance, navigation and control function for the Space Shuttle will be provided by the Operational Navigation Program (ONP). Those elements of the ONP which directly affect navigation performance are the:

- IMU Subsystem Operation Program (SOP)
- Navigation software
- Redundancy management software

The IMU SOP performs the basic ground function of calibrating and aligning the IMUs. During flight, it interrogates the IMUs and compensates the measured inertial velocities for the calibrated instrument errors. The inputs to the navigation software are the compensated inertial velocities as well as measurements obtained from the external navigation aids. The navigation software processes these inputs to generate estimates of vehicle position and velocity. The redundancy management software performs basic consistency checks on data generated at the subsystem level, e.g., IMU outputs, sensor outputs, position estimates, etc. The studies presented in this report deal only with the IMU SOP and the navigation software. The scope of the studies is outlined in the following subsections.

1.1.1 Calibration and Alignment Analysis

In January 1975, TASC initiated a verification and validation (V&V) program for the IMU software algorithm. The program was formulated in three phases (see Fig. 1.1-1) — analytical, functional and performance. As each phase was completed, a series of recommended algorithm modifications were delivered to NASA and, following approval by NASA, incorporated into the IMU software baseline. A summary of the first two phases, and part of the third phase, was presented in Ref. 1. A summary of subsequent progress on the performance phase is included in this report.

The performance phase of the V&V program applies three different techniques:

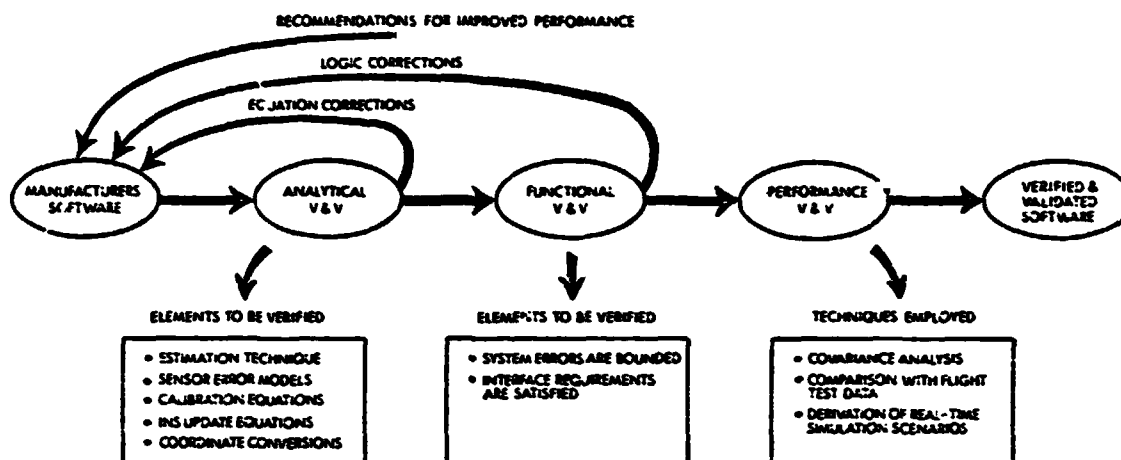


Figure 1.1-1 TASC Approach to Calibration and Alignment Software Verification and Validation

- Comparison of KT-73 calibration and alignment test data with the Shuttle performance specifications
- Monte carlo analysis
- Covariance analysis

Since the KT-73 IMU is generically related to the Space Shuttle IMU, and since the calibration programs are also similar, the KT-73 Data Bank (Ref. 19) developed and maintained by TASC for the U.S. Air Force is a valuable tool for evaluating the ability of the IMU software to calibrate and align the Space Shuttle IMUs in an operational environment. The Data Bank also provides a useful data source for updating the IMU error models and in many ways will complement the IMU test data currently being generated by NASA.

The monte carlo and covariance simulations provide complementary vantage points for computer-based analysis of the IMU software performance. The monte carlo simulation is a high fidelity simulation developed to ensure that the IMU

software algorithm can control the IMUs and execute the cal/align function. The simulation is extremely useful for generating coarse overall performance projections and for evaluating the effect of system nonlinearities on the software performance. Unfortunately, detailed sensitivity analyses or accurate overall performance projections can be prohibitively expensive with monte carlo simulations.

The covariance analysis simulation is based on a linearized IMU error model. Subject to the validity of this linearization, the covariance analysis simulation will yield a more accurate estimate of overall performance than is attainable with the monte carlo simulation and will also provide a detailed breakdown of the contribution of individual error sources to the calibration and alignment performance. The degree to which the nonlinearities alter the covariance analysis results can be inferred by comparison with the monte carlo results. Together, the two approaches will permit an accurate assessment of calibration and alignment performance and will provide a sound basis for recommending and evaluating software modifications which would improve overall performance.

The results of the KT-73 comparison and the monte carlo analysis were presented in Ref. 1. Development of the covariance analysis program was completed as part of the current effort. However, because of recent changes in the IMU software algorithm (Ref. 18), a complete error budget has not been generated. The error budget will be included in a subsequent report.

1.1.2 GPS-Aided Navigation

GPS is a satellite navigation system designed to provide accurate position and velocity fixes on a global

scale. The GPS network will become available on a limited basis by the end of 1977 (Phase I). The complete network will be operational in 1984 (Phase III). Because of its accuracy and its ability to provide navigation coverage during virtually all phases of a Space Shuttle mission,* NASA is currently evaluating the possibility of including GPS as a navigation aid. The objective of the GPS-aided navigation study was to provide NASA with an assessment of potential navigation accuracy in the operational GPS (post-1984) time frame. The study was restricted to those mission phases (ascent, orbit, deorbit) where no navigation aids are included in the current baseline, although GPS could also replace the current entry and preland navigation aids.

GPS is designed to satisfy the navigation requirements for both military and appropriately equipped civilian users. Seven classes of user requirements have been defined by the GPS Joint Program Office. Each class has its own unique requirements in terms of the type of user equipment needed and the navigation data required. The seven user classes are:

- Class A — High accuracy users such as strategic and reconnaissance aircraft
- Class B — Highly dynamic users such as fighter aircraft which require high accuracy updates
- Class C — Low-cost, low-accuracy users such as transport aircraft
- Class D — Land and sea-based surface vehicles

*No coverage will be available during radio-blackout. Also, the navigation accuracy may be marginal for landing.

THE ANALYTIC SCIENCES CORPORATION

- Class E — Manpacks
- Class F — Submarines
- Class M — Missiles

Two receiver types, the X and Y sets, are designed for users with high accuracy requirements. A third receiver type, the Z set, is intended for users with lower accuracy requirements.

The intent of the study was to evaluate GPS-aided navigation performance with the best available hardware. As a consequence, the Space Shuttle was assumed to be equipped as a Class B user. This included a multichannel X-receiver and processing of the high accuracy (P-code) satellite transmissions. However, it did not include a cesium time standard onboard the Space Shuttle. If the Shuttle Master Timing Unit (MTU) were replaced by a cesium time standard, navigation accuracy would be somewhat better than predicted in this study.

The GPS study had three basic objectives:

- Develop a navigation filter for GPS-aided navigation
- Formulate candidate GPS/Shuttle measurement scenarios
- Assess GPS-aided navigation

The emphasis in the navigation filter development was to retain the basic structure of the entry navigation filter (Ref. 45), with state definitions and parameter values suitably modified. The filter design as well as the performance analysis relied heavily upon GPS error models and GPS simulation programs developed by TASC in previous efforts (Refs. 1 and 5).

1.1.3 Entry, Preland and Landing Navigation

The Space Shuttle will employ a number of different navigation aids during the entry, preland and landing mission phases. In addition to the radio navigation aids indicated in Fig. 1.1-2, altitude measurements from a drag pseudo-measurement, a baro altimeter and a radar altimeter will be utilized at various points during the mission.

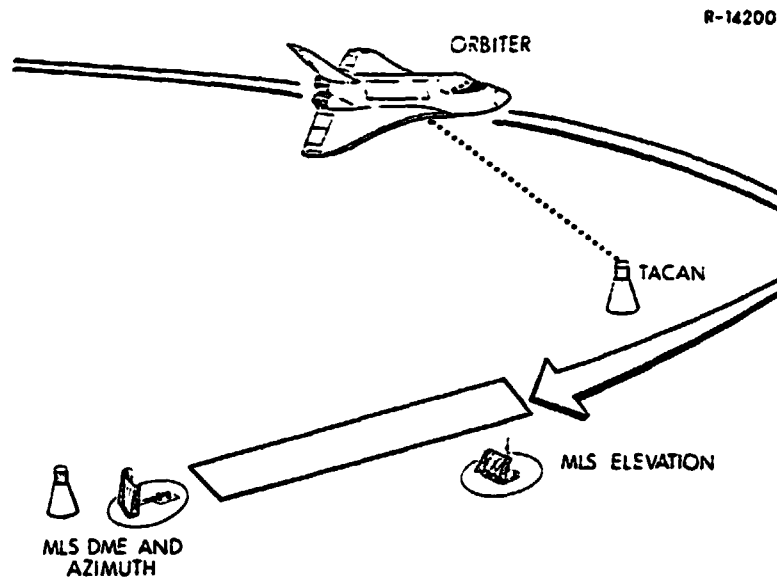


Figure 1.1-2 Baseline Orbiter Radio Navigation Aids

An accurate navigation performance analysis requires error models for the IMU and the navigation aids which adequately reflect instrument performance. Thus a major part of the entry, preland and landing study was the improvement of previously developed error models. Particular attention was given to the drag pseudo-measurement and radar altimeter error models, although recent performance data from the MLS manufacturer was also incorporated into the MLS error models.

1.2 ORGANIZATION OF THE REPORT

Chapter 2 summarizes the results of the GPS-aided navigation study. A candidate GPS measurement schedule is presented along with a description of a navigation filter suitable for processing GPS measurements during ascent, orbital operations and the deorbit maneuver. Navigation performance projections are presented for each of the mission phases for which the filter was designed. Performance sensitivity to the dominant error sources is also evaluated.

A description of the covariance analysis program to be used to analyze IMU calibration and alignment performance is provided in Chapter 3. Although a complete error budget is not given, calibration uncertainties due to certain key error sources are estimated. These estimates are compared with previous sensitivity analyses based upon TASC's monte carlo simulation.

The results of the entry, preland and landing study for the OFT-1 mission are contained in Chapter 4. Detailed error budgets are provided for the end of radio blackout, MLS acquisition and touchdown. The projected navigation performance is compared with results from previous studies and recommendations for improving performance are made.

A brief summary of results and conclusions is provided in Chapter 5.

2. GPS-AIDED NAVIGATION

The navigation error analysis for the Space Shuttle ascent phase provides an evaluation of navigation accuracy at orbit insertion if the baseline navigation system were modified to include the NAVSTAR Global Positioning System (GPS). The assumption in this study is that P-code (high accuracy) measurements from a GPS X-receiver are to be used periodically during ascent to update the navigation filter state estimates. The results are then extended to permit a preliminary evaluation of GPS-aided navigation performance during both the orbital and deorbit maneuver mission phases.

The methodology used for evaluation of the GPS-aided Space Shuttle navigation performance is summarized in Fig. 2-1. The first step in the process is the GPS segment simulation. This step is required to:

- Develop a time history of satellite orbital positions and velocities
- Generate the satellite position, velocity and clock error covariances

The GPS segment is performed using the TASC Navigation Error Sensitivity Analysis (NESA) program.

The second step is represented by the FLTCOV module in Fig. 2-1. The satellite ephemeris data, along with the Shuttle trajectory and measurement schedule, are used to generate a recursive solution of the navigation filter covariance propagation and update equations. This step is



Figure 2-1 Methodology for GPS/Shuttle Performance Projections

executed only once, with the filter gains being recorded on magnetic tape.

The third step (the SYSTEM module) is based on the system truth model and consists of the recursive solution of the linear system covariance equations. These equations are solved repeatedly to produce an error budget, the same gain file being used each time. The satellite error covariance generated in the NESA step is used to generate one line of the error budget and models for other error sources (IMU errors, MTU errors, etc.) are used to generate subsequent lines. An overall system performance projection is then calculated based on the detailed error-source-by-error-source breakdown.

The results of the ascent phase covariance analysis are summarized in this chapter. Section 2.1 describes the GPS configuration used in the NESA step and Section 2.2 discusses the relationship of the Orbiter trajectory and measurement schedule to the GPS satellite positions. The Shuttle navigation filter covariance generated in the filter gain step is discussed in Section 2.3. Section 2.4 summarizes the truth model used in the SYSTEM module. The performance assessment generated by that module is presented in Section 2.5 and a sensitivity analysis is presented in Section 2.6. A first-cut estimate of GPS-aided navigation performance during the orbital and deorbit maneuver phases is presented in Section 2.7.

2.1 GPS CONFIGURATION

GPS is a navigation satellite system under development by a multi-service Joint Program Office within the U.S. Air Force Space and Missile Systems Organization. The GPS satellites will each broadcast signals containing coded

information giving the time the signal was transmitted and the satellite position and velocity at that time. A user with an L-band antenna, a GPS receiver, and a clock synchronized with the satellite clocks will be able to compute the range to a satellite by measuring the time delay between signal transmission and reception, and he will be able to compute the range-rate to a satellite by measuring the signal's doppler shift (see Fig. 2.1-1). Since clock synchronization errors will enter into these measurements, they are termed pseudo-range and pseudo-range-rate measurements. Pseudo-range measurements to four different satellites will allow the user to solve for his three position coordinates and his clock phase synchronization error.* Similarly, pseudo-range-rate measurements to four different satellites will allow the user to solve for his three velocity coordinates and his clock frequency synchronization error. Measurements to more than four satellites can reduce the uncertainty of the results.

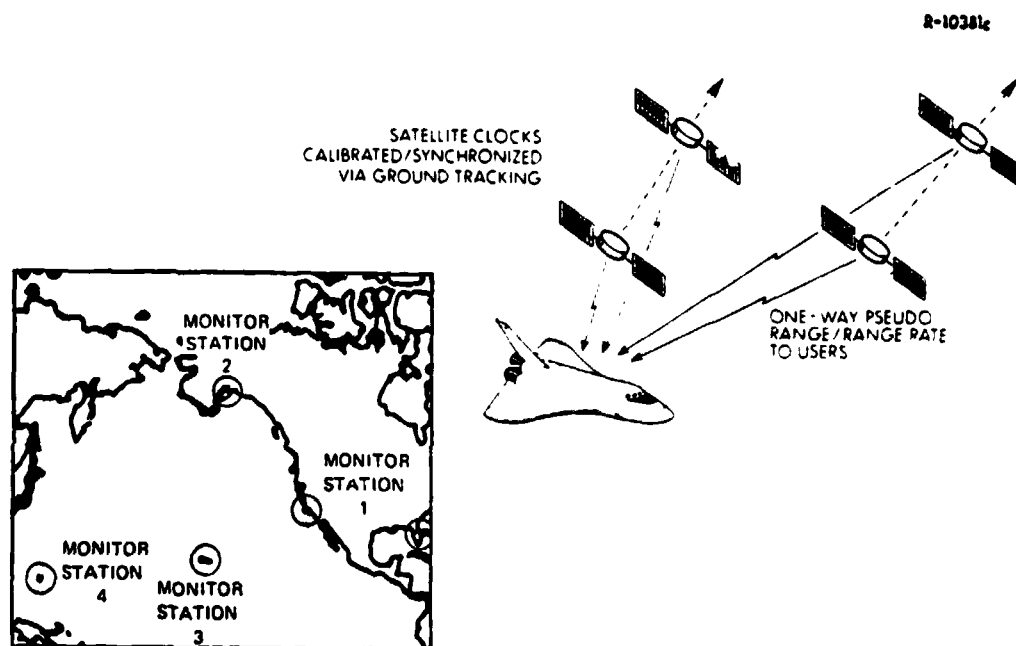


Figure 2.1-1 Elements of the NAVSTAR Global Positioning System (GPS)

*Provided the four satellites do not all lie on a cone with apex at the user location. See Appendix E of Ref. 4 for details.

THE ANALYTIC SCIENCES CORPORATION

Deployment of GPS is to be conducted in three phases (Table 2.1-1). The final configuration, Phase III, will consist of 24 satellites with cesium standard clocks and will provide full global navigation coverage for both ground-based and orbital users. Each satellite will have an orbital period of one-half a sidereal day (11 hours and 58 minutes). Thus, the satellites will nominally repeat the same ground track every two orbits, or once a day. Table 2.1-2 presents the orbital parameters of the Phase III satellites. A subset of these satellites that give good coverage over the Western Test Range (WTR) at the time of the Space Shuttle launch was used in the ascent phase navigation analysis. The eight satellites included in the subset have been denoted by asterisks in the tables.

TABLE 2.1-1
GPS DEVELOPMENT SCHEDULE

R-22802

	OPERATIONAL DATE	NUMBER OF SATELLITES	% TIME FOR WHICH 4 + SATELLITES ARE VISIBLE AT ORBITER ALTITUDE
PHASE I	LATE 1977	6	25
PHASE II	1981*	9*	90
PHASE III	1984	24	100

*A PROPOSAL TO ACCELERATE PHASE II DEVELOPMENT AND DEPLOY 12 SATELLITES IS UNDER CONSIDERATION.

The satellites will be tracked by four ground tracking stations located in United States territory. Pseudo-range measurements taken at each tracking station will be forwarded to the master tracking station at Vandenberg AFB for real-time satellite ephemeris estimation and clock calibration. The locations of the tracking stations are given in Table 2.1-3.

TABLE 2.1-2
PHASE III SATELLITE INITIAL CONDITIONS

Satellite No.	Semimajor Axis	Eccentricity	Inclination	Right Ascension of the Ascending Node	Argument of Perigee	Mean Anomaly
	a (earth radii)	e	i (deg)	Ω (deg)	ω (deg)	M (deg)
1	4.16449	0	63	0	0	15
2	4.16449	0	63	0	0	60
3	4.16449	0	63	0	0	105
4*	4.16449	0	63	0	0	150
5*	4.16449	0	63	0	0	195
6	4.16449	0	63	0	0	240
7	4.16449	0	63	0	0	285
8	4.16449	0	63	0	0	330
9	4.16449	0	63	120	0	345
10	4.16449	0	63	120	0	30
11*	4.16449	0	63	120	0	75
12*	4.16449	0	63	120	0	120
13*	4.16449	0	63	120	0	165
14	4.16449	0	63	120	0	210
15	4.16449	0	63	120	0	255
16	4.16449	0	63	120	0	300
17*	4.16449	0	63	240	0	0
18*	4.16449	0	63	240	0	45
19	4.16449	0	63	240	0	90
20	4.16449	0	63	240	0	135
21	4.16449	0	63	240	0	180
22	4.16449	0	63	240	0	225
23	4.16449	0	63	240	0	270
24*	4.16449	0	63	240	0	315

TABLE 2.1-3
GROUND TRACKING STATION LOCATIONS

Station No.	Name	Latitude (deg)	Longitude (deg)
1	Vandenberg AFB	34.7	-120.5
2	Elmendorf AFB	61.3	-149.5
3	Hawaii	20.0	-158.0
4	Guam	13.0	145.0

GPS requires periodic uploading of the satellite ephemeris and clock calibration parameters in order to maintain navigation accuracy. Uploading of a satellite with its currently estimated ephemeris will occur once a day when that satellite makes its closest approach to Vandenberg AFB. The time of the uploading to each satellite is given in Table 2.1-4. These times are relative to the initial time assumed in Table 2.1-2.

TABLE 2.1-4
SATELLITE UPLOADING TIMES

Satellite No.	Time of Uploading min	Satellite No.	Time of Uploading min
1	870	13*	1260
2	750	14	1140
3	615	15	1020
4*	495	16	915
5*	405	17*	90
6	1230	18*	1410
7	1140	19	825
8	1005	20	720
9	315	21	615
10	210	22	480
11*	105	23	360
12*	1395	24*	225

The net satellite contribution to pseudo-range and range-rate measurement error is not simply related to the satellite-transmitted ephemeris errors, because satellite clock errors are also involved, and the clock errors and ephemeris errors are highly correlated. In the case of pseudo-range measurements, the net error to the user is typically much smaller than the satellite position error itself. This happens because the combination of clock errors and position errors important to the user is nearly

the same combination measured by the ground tracking stations. While the ground network lacks good information to correctly allocate satellite position errors and clock errors independently, it has good information on the combination of these errors important to the user.

An example of the satellite contribution to user measurement errors and the importance of the ephemeris upload in maintaining measurement accuracy is provided in Fig. 2.1-2. Prior to the upload, the user measurement errors due to satellite errors alone are on the order of 5 ft and 0.003 fps. Immediately following the upload the errors are reduced to less than 2 ft and 0.001 fps. These errors define the fundamental limit of GPS measurement accuracy if all user-related errors (receiver errors, propagation errors, clock errors) could be eliminated.

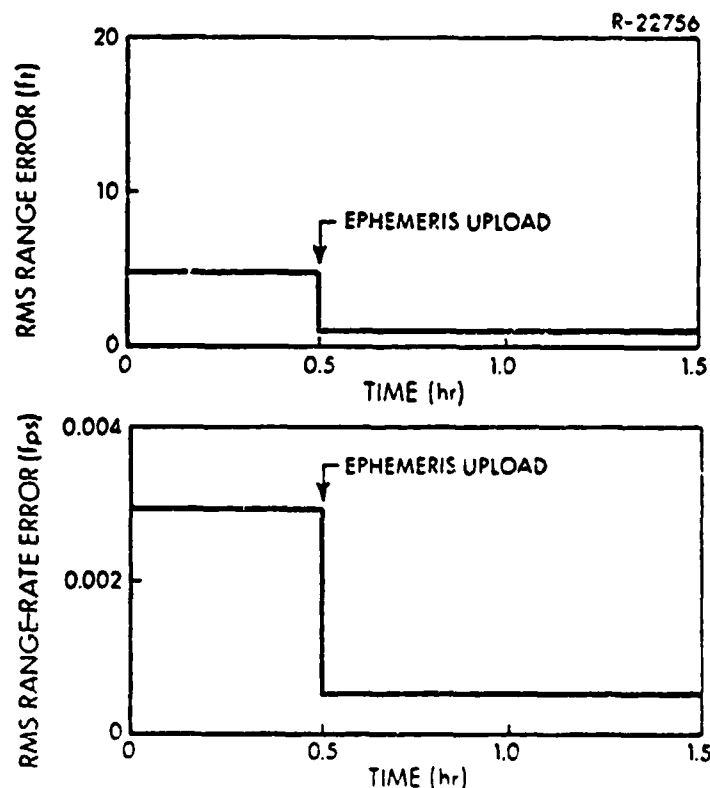


Figure 2.1-2 Typical User Measurement Error Statistics Due to Satellite Ephemeris and Clock Errors (Phase III GPS)

The user-furnished equipment for GPS measurement processing consists of an L-band antenna, a GPS receiver and a clock. In addition to GPS satellite ephemeris errors, GPS measurement accuracy is a function of the particular receiver (and clock) selected by the user. Several classes of GPS receiver have been defined. The principal difference from a performance vantage point is whether the receiver can process the P-code (high accuracy) or C/A-code (medium accuracy) GPS signals — the multichannel X-receiver can process both signal types while the single channel Z-receiver can process only the C/A-code. The receiver single-measurement performance specifications for a 0.1 sec integration time are summarized in Table 2.1-5. Greater accuracy can be achieved by averaging successive measurements.

The design specifications for the GPS X set require a user clock of comparable accuracy to the Shuttle Master Timing Unit (MTU) — short-term accuracy of 1 part in 10^{10} and an aging rate of 1 part in 10^9 per day. The user clock error model presented in Section 2.4 is based upon MTU test data.

TABLE 2.1-5
GPS RECEIVER MEASUREMENT ACCURACY SPECIFICATION (REF. 8)

CODE TYPE	1 σ RANGE ERROR (ft)	1 σ RANGE-RATE ERROR (fps)
Military (P) Code	5	0.2
Clear/Acquisition (C/A) Code	50	0.2

2.2 TRAJECTORY AND MEASUREMENT SCHEDULE

The GPS Navigation Error Sensitivity Analysis (NESA) computer program performs a statistical covariance analysis of the satellite system interacting with the ground tracking stations. Beginning with some initial condition statistics, to which this process is quite insensitive, the NESA program was used to simulate two days of GPS operation, achieving a close approximation to steady state conditions. The simulation correctly accounts for the fact that each satellite has its own "idea" of its ephemeris, clock synchronization, etc., based on the daily uploading from the master tracking station at Vandenberg AFB. Because each satellite's ground track and the time of its data uploading repeat every sidereal day, so do the statistics of the associated error processes, once the transient effects of the initial statistical conditions have faded. The steady state situation referred to above thus exhibits time variations within the day.

After the two day settling period, a 90 min segment of the statistical simulation was run with output at one minute intervals. This 90 min segment of GPS simulation was the input to the filter covariance program and to the truth model program for the GPS-aided Space Shuttle ascent navigation study. In order to do this, it was necessary to make a time connection between the Shuttle ascent trajectory and the NESA output.

The Shuttle trajectory used for this study was reference mission 3B with a launch from Vandenberg AFB. The ground track for the ascent trajectory, along with the location of the eight GPS satellites used in the simulation (assuming a launch at $t=0$) is shown in Fig. 2.2-1. Its key events are summarized in Table 2.2-1. From liftoff to

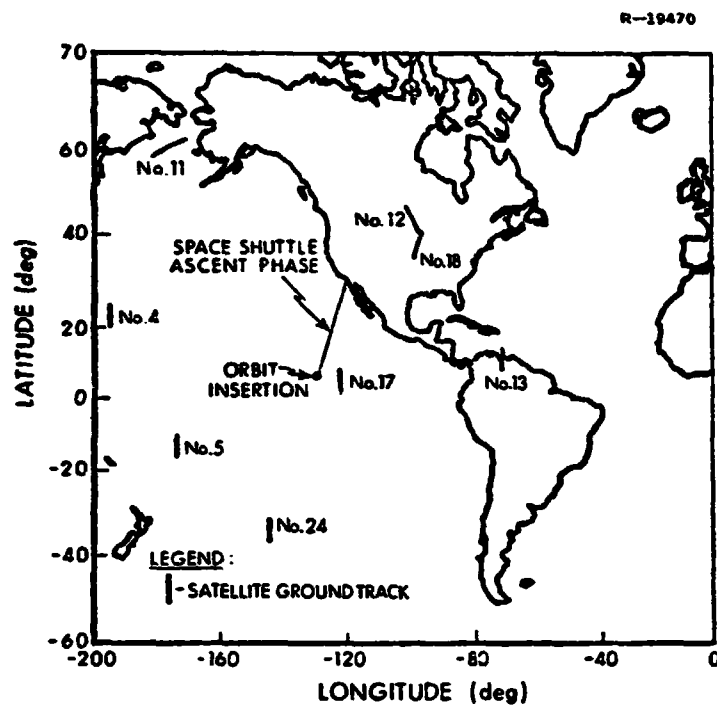


Figure 2.2-1 Baseline GPS Satellite Coverage
(Space Shuttle Ascent Phase)

TABLE 2.2-1
TRAJECTORY PARAMETERS AT KEY EVENTS DURING ASCENT

T-0068

Event	GET (sec)	Inertial Velocity (fps)	Relative Flight-Path Angle (deg)	Altitude (ft)	Geodetic Latitude (deg)	Longitude (deg)
Lift-off	0.0	1,251.3	0.00	0.25	35.000	239.500
Initiate Pitchover	5.0	1,257.1	90.00	297.0	35.000	239.500
Begin Gravity Turn Phase	20.0	1,350.5	86.18	5,159.0	34.999	239.500
Staging	116.4	4,183.2	65.61	189,910.0	34.850	239.432
Begin Con- stant 3g Accelera- tion Phase	383.4	15,454.4	-1.40	584,412.0	29.873	237.488
Begin Coast Phase	486.5	25,250.2	0.06	562,667.0	24.440	235.467
Begin OMS* to Orbit Phase	516.5	25,250.5	0.01	561,474.0	22.482	234.762
Orbit Insertion	771.0	25,597.1	0.12	551,798.0	5.673	229.225

*Orbit Maneuvering System

orbit insertion, the ascent takes only 771.0 sec, or less than 13 min; and the measurement taking portion of the trajectory, scheduled between 630.0 and 768.0 sec after liftoff, takes less than 138 sec, or 2.3 min. This period covers the second half of the final OMS insertion maneuver and should permit sufficient time for the aided navigation filter to improve the state estimates and for the guidance system to refine the insertion parameters. Thus, no apparent advantage would be obtained by starting the measurement processing earlier.

The measurement schedule calls for sequential processing of GPS measurements at the rate of one each 6 sec* starting with Satellite No. 4. Thus, over the 138 sec measurement interval, three measurements from each of the eight visible satellites are used to update the navigation filter state estimates. The measurement interval is shown relative to the ascent acceleration profile in Fig. 2.2-2. It is worth noting that the measurements were scheduled during a low acceleration portion of the mission. This was done to ensure that acceleration-sensitive errors in the Space Shuttle Master Timing Unit (MTU) would not significantly degrade the GPS measurement accuracy; however, the results in Section 2.5 suggest that the navigation accuracy is reasonably independent of the acceleration profile during the measurement sequence.

In order to connect the Orbiter trajectory to the NESA output, it is only necessary that the measurement interval of

*GPS receivers are capable of generating measurements at a much higher data rate. The slower measurement rate was selected to reduce computer requirements.

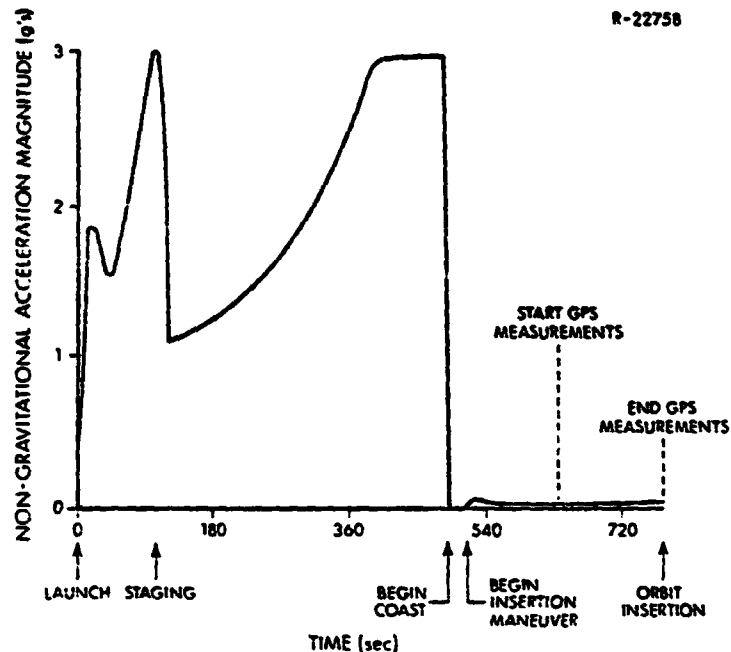


Figure 2.2-2 Ascent Trajectory Acceleration Profile

2.3 min fall somewhere within the 90 min of NESAs output. The Phase III GPS constellation provides good satellite coverage on a continuous basis. Because the NESAs run was made with a subset of eight satellites, however, the results are representative of Phase III GPS coverage in the WTR for only a short period each day. In order to determine where the measurement interval should fall within the NESAs output for simulation purposes, it was necessary to investigate satellite visibility from the Orbiter. Figure 2.2-3 indicates satellite visibility over the output period from four points. The four points are

- V) on the ground at Vandenberg AFB:
- B) on the Orbiter at 630.0 sec after liftoff, the beginning of the measurement interval;
- M) on the Orbiter at 702.0 sec after liftoff, about midway into the measurement interval;
- E) on the Orbiter at 768.0 sec after liftoff, the end of the measurement interval.

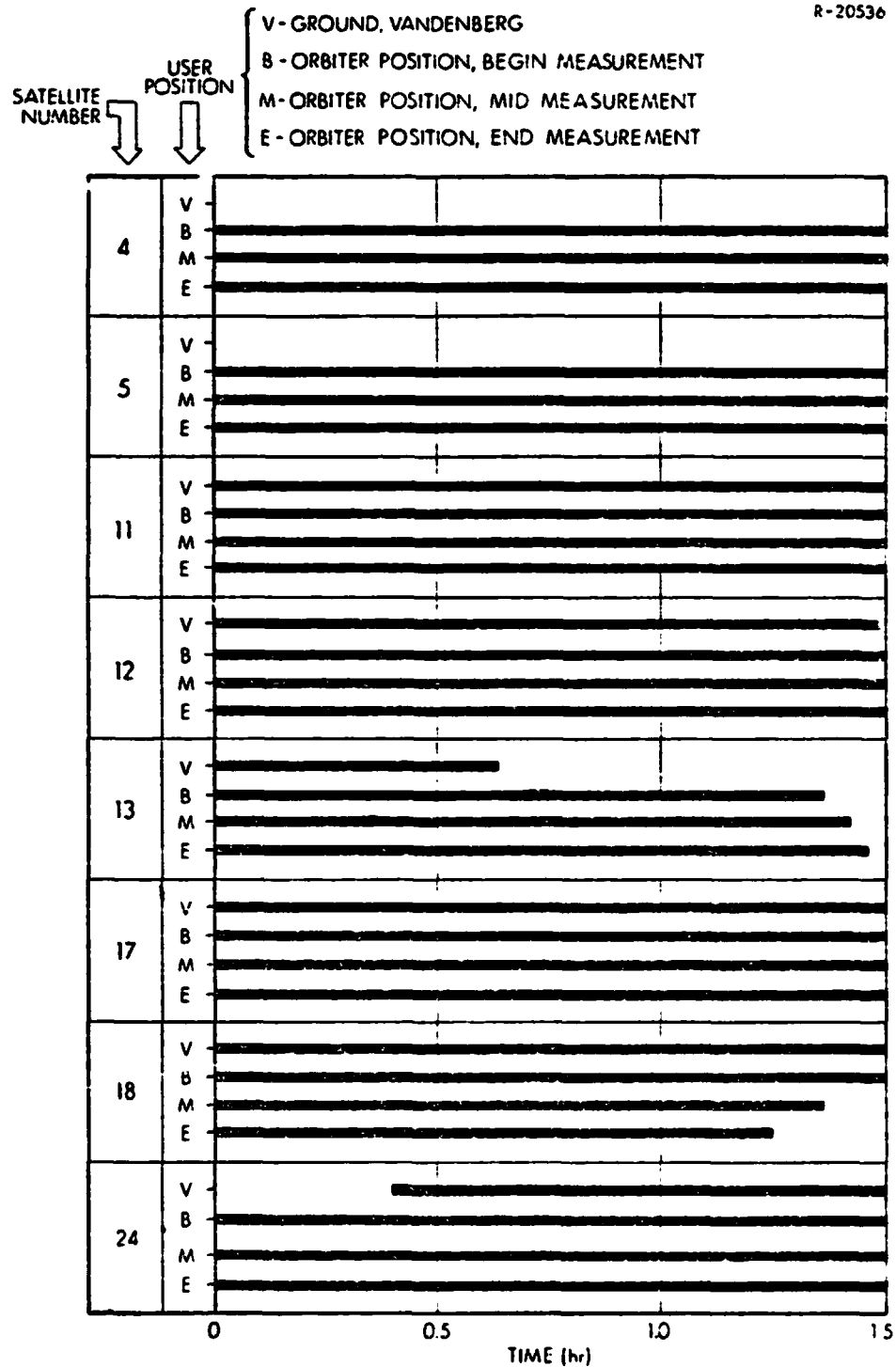


Figure 2.2-3 Satellite Visibility Versus Time from Four User Positions

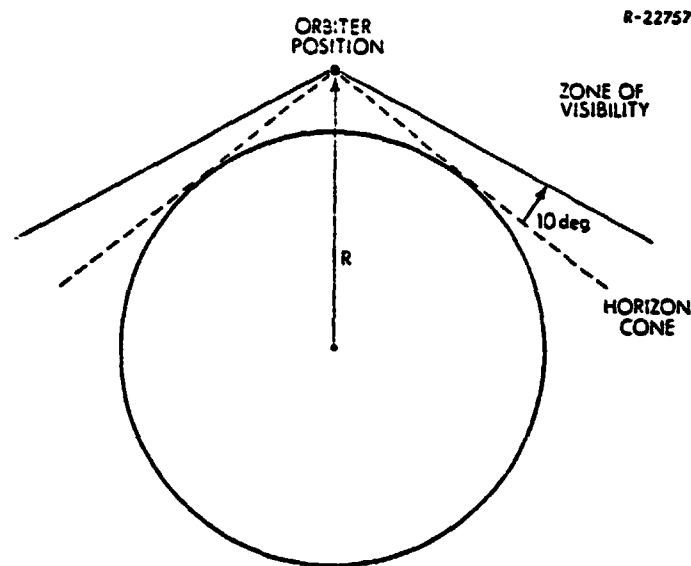


Figure 2.2-4 GPS Satellite Visibility Criterion

The criterion used for satellite visibility was the same in each case. To be visible, it was assumed that the satellite must be 10 deg or more above the horizon as viewed from the user location (Fig. 2.2-4). On the ground, the horizon is 90 deg below the zenith, so the half cone angle for satellite visibility is 80 deg. Above the earth on the Orbiter, however, the horizon is over 100 deg below the zenith, so the half cone angle for satellite visibility is increased to more than 90 deg.

As Fig. 2.2-3 shows, it makes little difference, in terms of visibility, where the Orbiter measurement interval interfaces with the NESA output. Satellites No. 13 and 18 disappear from view of the Orbiter near the end of the 90 min window, but the remaining six satellites should be capable of providing good coverage. Based on Fig. 2.2-3, the Shuttle launch time was synchronized with 0 hrs in the GPS time frame.

2.3 FILTER-INDICATED PERFORMANCE

The 11-state Kalman filter used during the GPS-aided ascent phase predicts pseudo-range and range-rate measurements ($\hat{\rho}_{iu}, \hat{\dot{\rho}}_{iu}$) based on the before-measurement estimates of Orbiter position, velocity and clock states, combined with the satellite delivered estimates of the corresponding satellite states. Differences between the actual measurements ($\rho_{iu}, \dot{\rho}_{iu}$) and the predicted measurements drive the filter and cause post-measurement updates in the Orbiter state estimates (see Fig. 2.3-1). The filter gains used for the updates are based upon a filter-generated covariance matrix which reflects the filter's confidence in its before-measurement state estimates. The filter-indicated performance implied by this covariance matrix is summarized in this section.

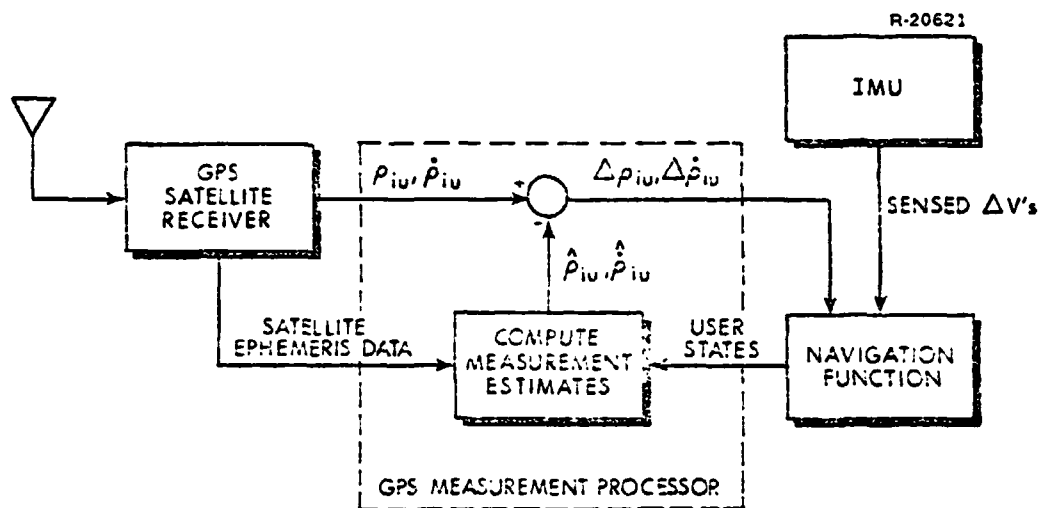


Figure 2.3-1 Typical GPS User Mechanization

The general structure of the 11-state filter used in the ascent phase study is presented in Table 2.3-1.

TABLE 2.3-1
NAVIGATION FILTER STATES

State Number	State Definition
1-3	Position*
4-6	Velocity*
7-9	IMU Misalignment Angles*
10	Receiver Clock Phase Error
11	Receiver Clock Frequency Error

The initial system covariance matrix, $P_F(t_0)$, and continuous process noise matrix, Q_{F_c} , are both diagonal. Initial standard deviations for the filter states and spectral densities for their associated process noises are presented in Table 2.3-2.

The initial velocity error uncertainty specified in Table 2.3-2 is based on the preflight vehicle motion model given in Section 3.2 of Ref. 1. The initial misalignment and the velocity and misalignment process noise values are based on the IMU performance specification of Ref. 28. The values for the clock states (States 10 and 11) were selected under the assumption that the oscillator in the onboard receiver will have operating characteristics similar to those of the Shuttle MTU and that it will be calibrated prior to launch. The MTU errors are discussed in Section 2.4.

The measurement covariance matrix, R , for the GPS measurement is diagonal. RMS values of 12 ft and 0.05 fps are assumed for the position and velocity measurements - the 12 ft value assumes that the P-code (high accuracy) GPS transmissions are used on the Space Shuttle. Additional measurement

* These states are expressed in the I (Inertial) coordinate frame of Appendix A of Ref. 1.

TABLE 2.3-2
ASCENT NAVIGATION FILTER INITIAL CONDITIONS

T-0044

State No.	Description	Initial Filter Standard Deviations		Filter Process Noise Spectral Densities	
		Value	Units	Value	Units
1	X Position Error	10	ft	--	ft ² /sec
2	Y Position Error	10	ft	--	ft ² /sec
3	Z Position Error	10	ft	--	ft ² /sec
4	X Velocity Error	0.01	fps	0.001	(fps) ² /sec
5	Y Velocity Error	0.01	fps	0.001	(fps) ² /sec
6	Z Velocity Error	0.01	fps	0.001	(fps) ² /sec
7	X Platform Misalignment	60	sec	0.035	sec ² /sec
8	Y Platform Misalignment	60	sec	0.035	sec ² /sec
9	Z Platform Misalignment	60	sec	0.035	sec ² /sec
10	Receiver Clock Phase Error	100	ft	0.1	ft ² /sec
11	Receiver Clock Frequency Error	0.1	fps	3 × 10 ⁻⁵	(fps) ² /sec

errors, such as ionospheric propagation uncertainties, plus unmodeled satellite errors are assumed to be included in the 12 ft and 0.05 fps values.

As a preliminary study of filter performance, the filter was simulated twice, once as an optimal Kalman filter, and once with measurement underweighting.* The purpose of underweighting is to prevent the filter from making sudden large changes in the state estimates when a new sensor is first acquired. This reduces the possibility of filter divergence as well as reducing the sensitivity of the filter to a single bad measurement. In an optimal Kalman filter, the gain matrix for a measurement is computed as:

$$K = PH^T [HPH^T + R]^{-1} \quad (2.3-1)$$

With underweighting, this equation is modified to read:

*Underweighting is discussed in Ref. 1 and is included in the Shuttle baseline for entry (Ref. 45).

$$K = PH^T[u_{70}HPH^T + R]^{-1} \quad (2.3-2)$$

where u_{70} is the underweighting factor, a scalar larger than unity. For the results presented here, an underweighting factor of 1.2 was used until the root sum of the position variances [the square root of the sum of $P(1,1)$, $P(2,2)$ and $P(3,3)$] was less than 1000 ft.

When the filter was run with measurement underweighting, the underweighting was turned off after 3 measurements, but its influence continued to be significant until about the eighth measurement. After the 8 measurements, the optimal and underweighted filters had nearly identical performance. Since measurement underweighting did not appear to sacrifice any navigation accuracy at orbit insertion, it was used for the baseline filter.

The filter covariance results are presented in Fig. 2.3-2 for the first 8 measurements. No measurements are made until 630 sec after liftoff; the filter covariance propagates in an open loop manner until that time. The first measurement is from Satellite No. 4, which has a line-of-sight approximately perpendicular to the Shuttle trajectory (Fig. 2.2-1). Consequently, the first update results in a significant decrease in the filter-indicated rms crossrange position and velocity error. Subsequent measurements provide significant decreases in the rms downrange and radial errors. After eight updates, the filter-indicated rms errors have decreased from approximately 2400 ft to 20 ft per axis in position and from approximately 7 fps to 0.2 fps per axis in velocity. Although measurements are taken until orbit insertion (771.0 sec, 24 updates), there is no significant reduction in the filter-indicated covariance after the eighth update.

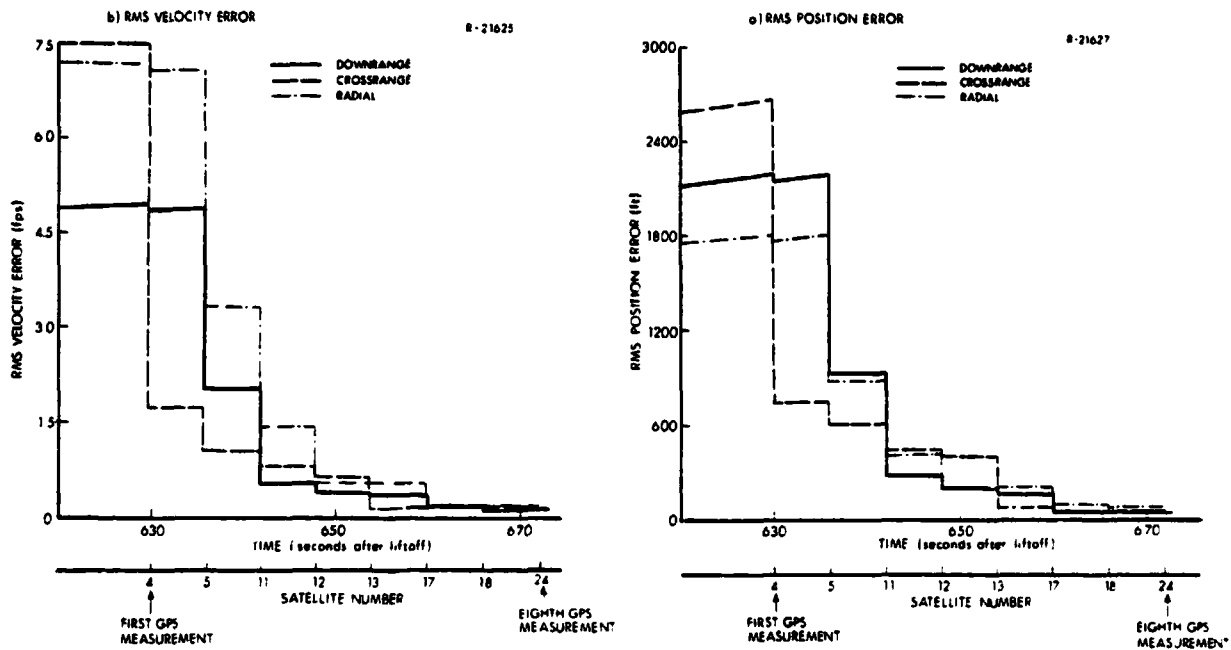


Figure 2.3-2 Filter-Indicated Ascent Navigation Performance for First Eight GPS Measurements

The filter covariance data for all 11 filter states is summarized in Table 2.3-3. The data is presented at four times:

- Liftoff ($t = 0$ sec)
- prior to the first GPS measurement ($t = 630^-$ sec)
- after the eighth GPS measurement ($t = 672^+$ sec)
- at orbit insertion ($t = 771$ sec)

In addition to improving the position and velocity estimates, it is interesting to note that the filter-indicated results suggest that GPS-aiding during ascent can estimate IMU misalignments to an accuracy better than that obtained from ground alignment. Although the filter is somewhat optimistic in its estimates, this capability is confirmed in Section 2.5.

TABLE 2.3-3
FILTER-INDICATED PERFORMANCE DURING ASCENT

Event	T (sec)	RMS Position Errors (ft)			RMS Velocity Errors (fps)			RMS Misalignment Errors (sec)			RMS Clock Errors	
		DR	CR	R	DR	CR	R	DR	CR	R	Phase (ft)	Freq. (fps)
Launch	0.	10.0	10.0	10.0	0.01	0.01	0.01	60.0	60.0	60.0	100.0	0.10
Before First Measurement	630.(-)	2184.6	2667.9	1803.3	4.96	7.46	7.19	60.2	60.2	60.2	128.4	0.17
After Eighth Measurement	672.(+)	9.9	19.0	28.6	0.07	0.16	0.17	12.0	6.6	12.4	19.9	0.10
Orbit Insertion	771.0	5.0	6.7	12.5	0.08	0.16	0.13	11.0	6.8	13.4	7.5	0.06

2.4 ASCENT PHASE TRUTH MODEL

The ascent phase truth model provides a detailed description of the environment in which the navigation filter must operate. As such, it is the basic element of the SYSTEM module (Fig. 2-1) which is used to analyze the performance of the candidate filter. The error sources included in the truth model fall into five general classes:

- Receiver measurement noise
- IMU errors
- Shuttle MTU errors
- Gravity modeling errors
- GPS satellite position, velocity and clock errors

The mathematical details of the models for these error sources were presented in Ref. 1. A brief description of the models and a summary of the numerical values used for the performance analysis are presented in this section.

2.4.1 Truth Model Definitions

With the exception of receiver measurement noise, each of the error models included in the ascent phase truth model requires that a set of error states be defined. A total of 128 error states are included in the truth model; the states are identified in Table 2.4-1. Except for the eleven filter states, the error states are grouped in terms of the error source classes defined above. The total of 88 GPS-related states includes eleven for each of the eight visible GPS satellites.

TABLE 2.4-1
ASCENT PHASE TRUTH MODEL STATES

Error Source	Individual Error Sources	Total Error Sources
I. Filter States	11	11
II. IMU Errors		20
Accelerometer		
Biases	3	
Scale Factors	3	
Asymmetries	3	
Non-Orthogonalities	3	
Gyroscope		
Bias Drift	2	
Mass Unbalances	5	
III. Shuttle MTU Errors	6	6
IV. Gravity Model Errors	3	3
V. GPS Satellite Errors		88
Position	3*	
Velocity	3*	
Clock	3*	
Solar Pressure	1*	
Gravitational Uncertainty	1*	
Total		128

*Number of Error States Per Satellite

The eleven filter states are identical to those in the navigation filter mechanization; however, the position,

velocity and misalignment states are not driven by process noise as was implied in Table 2.3-1. Instead, these states are driven by the appropriate error sources in the truth model, e.g., IMU and gravity model errors. (The filter treats these unmodeled errors as process noise.) Also, whereas states 10 and 11 reflect the filter estimates of the MTU phase and frequency errors, the actual MTU errors are specified in Group III of Table 2.4-1.

The states defined for the IMU error model are a subset of those included in the detailed error model used for the preflight calibration and alignment analysis (Ref. 1). Only those IMU error sources which can make an appreciable contribution to the navigation errors at orbit insertion were retained. Thus, the original model was reduced to 20 key states for this application.

The gravity error model is based on Ref. 44 and consists of two vertical deflection states (downrange and cross-range) and one gravity anomaly state. The error magnitudes are typical of those expected for an onboard gravity model which does not account for high frequency gravitational effects. The model parameters are determined as a function of altitude and velocity by table look-up. As altitude increases, the error magnitude decreases.

The Shuttle MTU error model is the 5-state model developed in Ref. 1, except that an acceleration-sensitive error state has been added to reflect the most recent test data available (Ref. 50). The resulting 6-state model conforms with a NASA generated specification for normalized

rms phase error, $\sigma_{\delta\phi}(\tau)/\tau$, and maximum random aging rate for the MTU. The specifications are:

- Normalized rms phase error of 10^{-10} over the interval $0.5 \text{ sec} \leq \tau \leq 10 \text{ sec}$.
- A maximum random aging rate of 10^{-9} per day. This is equivalent to an rms aging rate of 3.3×10^{-10} per day.

The NASA specification and the 6-state approximation to this specification (assuming zero acceleration) are shown in Fig. 2.4-1. The model was developed based on the approach presented in Ref. 10. Figure 2.4-1 also demonstrates the normalized rms phase error for the 2-state model developed for the navigation filter.

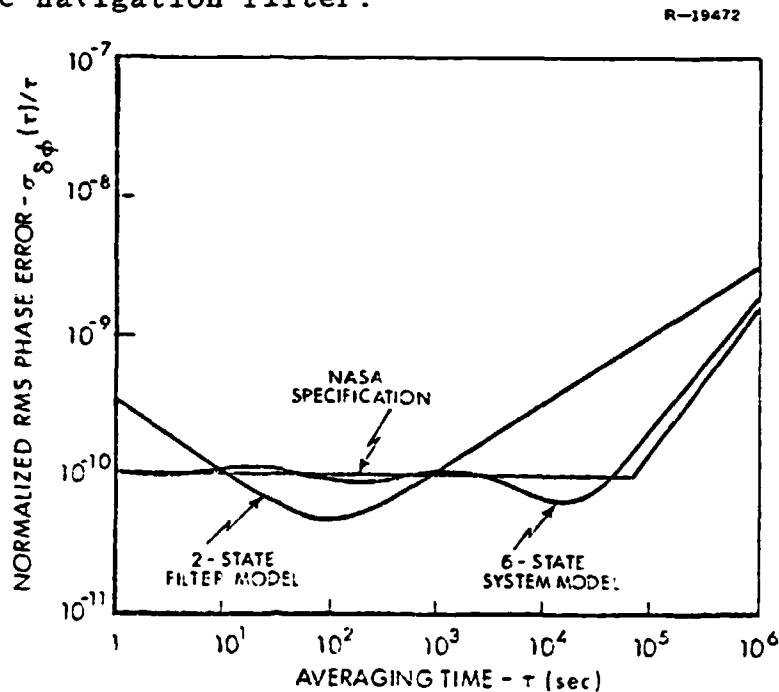


Figure 2.4-1 Normalized RMS Phase Error for Quartz Crystal Clock Model (Assuming Zero Acceleration)

*The MTU specification (Ref. 11) does not clearly indicate whether the oscillator performance is to be evaluated using Allan variances or normalized rms phase error. For a given numerical value, the latter is a less stringent specification and was therefore assumed for this study.

The linear system block diagram for the 6-state clock model is presented in Fig. 4.2-2. The parameters K_1 and K_2 assume values of 1.01×10^{-1} and 1×10^{-4} , respectively, and a is the Shuttle acceleration along the major thrust axis. Table 2.4-2 contains a description of the six clock model states.

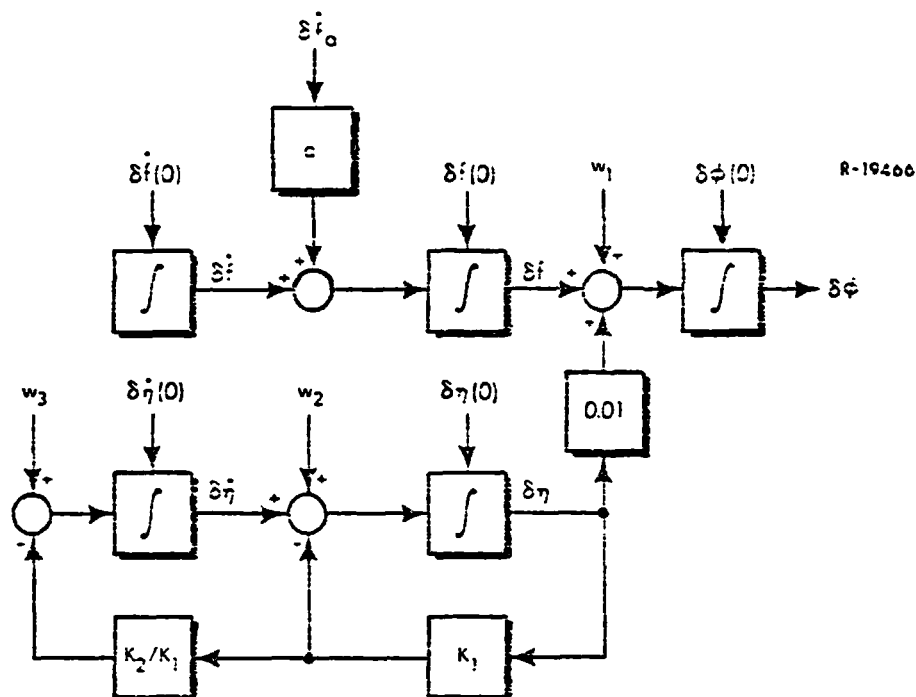


Figure 2.4-2 Quartz Crystal Clock Error Model

TABLE 2.4-2

SHUTTLE MTU ERROR STATE DEFINITIONS

Symbol	Error Source Definitions	Units
$\delta\phi$	Phase Error	ft
δf	Frequency Error	fps
$\delta\dot{f}$	Aging	ft/sec ²
$\delta\eta$	Flicker Frequency Error	fps
$\delta\dot{\eta}$	Random Frequency Rate Error	ft/sec ²
$\delta\dot{f}_a$	Acceleration Sensitivity	ft/sec ² /g
w_1	White Process Noise	fps
w_2		ft/sec ²
w_3		ft/sec ³

The GPS satellite error model was implemented in the NESAs program (see Section 2.2), which produced a data tape with an 88×88 covariance matrix and an associated state transition matrix for each measurement time. Although the NESAs program used more than 88 states in its error model (tracking station clock errors, survey errors, etc.), the 88 states defined in Table 2.4-1 are sufficient to characterize the GPS satellite contributions to user measurement errors.

2.4.2 Truth Model Data Base

The data base for the ascent phase truth model consists of the numerical data required to evaluate the filter performance in an environment defined by the truth model. In most cases this consists of initial covariances, process noise spectral densities, and measurement variances, but in certain instances it also includes time constants for correlated error sources. The data base for all error sources except the GPS satellite errors is presented in Table 2.4-3. The GPS satellite errors are characterized in the text of this section.

The measurement errors specified in the table assume that a multichannel X-receiver is used to process the P-code (high accuracy) on the Space Shuttle. Additional measurement errors, such as ionospheric propagation uncertainties, plus unmodeled satellite errors are assumed to be included in the 12 ft and 0.05 fps values.

The standard deviations assigned to the IMU errors (including IMU misalignment) are based on the IMU performance specification (Ref. 28). The position and velocity uncertainty values were derived from a model of wind-induced oscillations of the Shuttle on the launch pad (Ref. 1). It is important to note that these error sources are modeled as independent

TABLE 2.4-3
ASCENT NAVIGATION TRUTH MODEL DATA BASE

T-0268

Error Source	Standard Deviation	Time Constant	Process Noise Spectral Density
0. Uncorrelated GPS Receiver Measurement Errors			
Pseudo-Range	12	0	0
Pseudo-Range-Rate	0.05 fps	0	0
I. Filter States			
Position	10 ft	-	0
Velocity	0.01 fps	-	0
Misalignments	60 sec	-	0
II. IMU Errors			
Accelerometer			
True Biases	50 μ g	-	0
Scale Factors	40 ppm	-	0
Asymmetries	40 ppm	-	0
Nonorthogonalities	15 sec	-	0
Gyro			
True Bias Drifts	0.015 deg/hr		
Mass Unbalance	0.025 deg/hr/g		
III. Shuttle MTU Errors			
Phase Error	100 ft	-	Eq.(2.4-2)
Frequency Error	0.01 fps	-	
Aging	3.86×10^{-6} ft/sec ²	-	
Random Frequency Error	20.2 fps	-	
Random Frequency Rate Error	1.37 ft/sec ²	-	
Acceleration Sensitivity	0.1 ft/sec ² /g	-	
IV. Gravitational Deflections and Anomalies	8 sec 67 mgal	Function of Altitude and Vehicle Speed	Function of Altitude and Vehicle Speed
V. GPS Satellite Errors	Computed Using NESA Programs	See text	See text

rather than correlated errors. The IMU errors resulting from the preflight calibration will be correlated, but the effort presently underway at TASC to estimate those correlations is not complete. When they become available, these correlations can be added to the truth model.

Except for acceleration sensitivity, the values shown for the MTU are those used in generating Fig. 2.4-1. The MTU has a preferred axis along which the acceleration sensitivity is significantly smaller than for the other two axes. In selecting the $0.1 \text{ ft/sec}^2/\text{g}$ (1 part in 10^{10} per g) value in Table 2.4-3, it was assumed that this axis will be oriented along the major thrust axis for the Shuttle, but the results of Section 2.5 indicate that, for the selected measurement schedule, acceleration sensitivity would not be a dominant error source even if the MTU orientation were arbitrarily chosen.

The process noises w_1 , w_2 and w_3 for the MTU model (Fig. 2.4-2) are linearly dependent. The process noise spectral density used to generate Fig. 2.4-1 is

$$Q = \begin{bmatrix} 4.56 \times 10^{-3} & 0 & 0 & 4.14 \times 10^{-1} & 4.51 \times 10^{-3} & 0 \\ 0 & 0 & 0 & 0 & 0 & 0 \\ 0 & 0 & 0 & 0 & 0 & 0 \\ 4.14 \times 10^{-1} & 0 & 0 & 3.77 \times 10^1 & 4.10 \times 10^{-1} & 0 \\ 4.51 \times 10^{-3} & 0 & 0 & 4.10 \times 10^{-1} & 4.47 \times 10^{-3} & 0 \\ 0 & 0 & 0 & 0 & 0 & 0 \end{bmatrix}$$

with units specified in Table 2.4-2.

(2.4-2)

The covariance matrix for the GPS satellite error sources was generated by the NESA program. The satellite contributions to measurement error vary as a function of Orbiter/satellite geometry, time since last ephemeris update, etc., but Fig. 2.1-2 provides a general indication of the magnitude of the errors involved. For satellites which were uploaded immediately prior to the launch time, e.g., satellite No. 18, the satellite-contributed measurement errors would be on the order of 2 ft and 0.001 fps. For satellites with less recent updates, the errors could be a factor of 2 or 3 greater.

2.5 GPS-AIDED ASCENT NAVIGATION PERFORMANCE

The previous sections of this chapter have defined the proposed navigation filter for GPS-aided ascent navigation

and a stochastic model (truth model) of the real world environment in which the filter is designed to operate. The performance of the navigation filter in this environment is analyzed via covariance analysis in this section. The results of the analysis are presented in the form of both a time history of overall navigation performance during the GPS measurement interval and as a detailed error budget at orbit insertion.

The first GPS measurement is taken at 630 sec, midway through the final OMS insertion burn. Prior to that time the navigation mode is pure-inertial. The rms navigation errors at 630 sec are approximately 2000 ft and 7 fps along each axis, which roughly corresponds to the current specification for orbit insertion accuracy (Ref. 17). The dominant contributor to this error is initial IMU misalignment, but various gyro and accelerometer error sources are also significant.

The overall performance of GPS-aided navigation with the 11-state navigation filter is indicated in Fig. 2.5-1. At the time of the first measurement, there is an immediate decrease in both position and velocity errors. Because of the relative geometry of the Shuttle and the GPS satellite (Satellite No. 4) for this measurement, the greatest initial reduction is in crossrange errors. As subsequent measurements from different satellites are processed, however, the improvement in all three components of position and velocity is both uniform and dramatic. After measurements from all eight visible satellites have been processed (at 672 sec), the rms navigation errors are on the order of 20-30 ft and 0.2 fps along each axis, with the vertical errors being slightly larger because of the lack of a GPS satellite directly overhead of the Orbiter. Over the remainder of the measurement interval, the navigation errors slowly decrease so that they are less than 20 ft and 0.2 fps rms

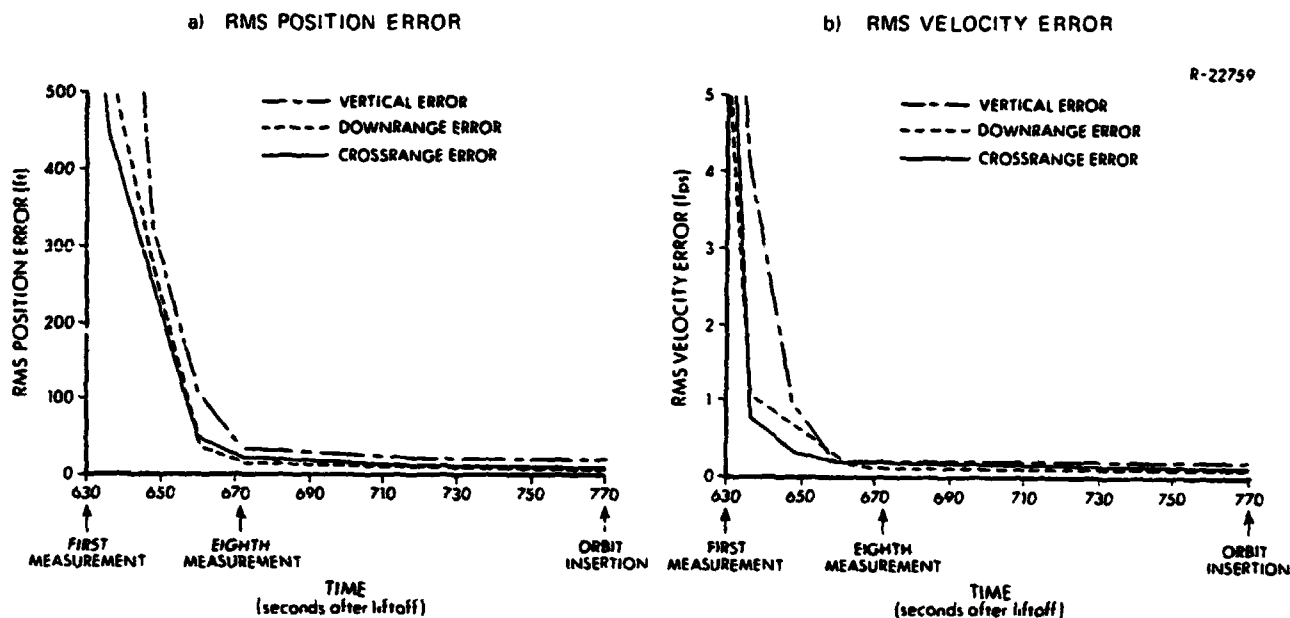


Figure 2.5-1 GPS-Aided Ascent Navigation: Overall Performance

along each axis at orbit insertion. These errors are somewhat larger than those of the GPS receiver and suggest that error sources other than the receiver errors (e.g., satellite ephemeris and clock) remain important.

The conclusion to be drawn from Fig. 2.5-1 is that the proposed navigation filter can effectively incorporate GPS measurements into the navigation solution. The degree to which GPS-aiding improves navigation performance is further illustrated by Table 2.5-1 which compares the navigation errors prior to the first GPS measurement with those at orbit insertion. The table indicates that GPS-aiding has decreased the rms position errors by better than a factor of 100 and the rms velocity errors by better than a factor of 30. Furthermore, the table indicates that the filter has used GPS measurements to align the IMU during powered flight. Whereas the rms IMU misalignments were

TABLE 2.5-1
EFFECT OF GPS IN REDUCING ORBIT INSERTION ERRORS

T-0269

Implementation	RMS Position Errors (ft)			RMS Velocity Errors (fps)			RMS Misalignment Errors (sec)			RMS Clock Errors	
	DR	CR	R	DR	CR	R	DR	CR	R	Phase (ft)	Freq. (fps)
Pure Inertial Navigation*	2280	2730	1864	5.2	7.6	7.4	64	62	61	132	0.20
GPS-Aided Navigation	7	9	16	0.1	0.1	0.2	25	13	15	4	0.14

*Errors at midpoint of final Orbital Maneuvering System (OMS) insertion burn, 142 sec prior to insertion

slightly greater than 60 sec prior to the first measurement, they are approximately 13 sec about the orthogonal (cross-range and vertical) axes and 25 sec about the downrange axis. This capability for accurate inflight alignment could significantly reduce the importance of the current system specifications for IMU alignment prior to launch and the deorbit burn.

One measure of navigation filter performance is the degree to which the filter covariance reflects the actual navigation accuracy. Comparison of Table 2.5-1 with Table 2.3-2 indicates that the filter was somewhat optimistic relative to the true position and velocity accuracy, but the difference was not significant. The filter was considerably over-optimistic in its estimate of IMU misalignments, however, which suggests that it might be desirable to increase the process noise which the filter uses to account for gyro errors.

The detailed error budget at orbit insertion is presented in Table 2.5-2. The most prominent feature of the table is that the navigation performance is completely dominated by GPS-related errors. The IMU is the major contributor

TABLE 2.5-2
ASCENT ERROR BUDGET AT ORBIT INSERTION

T-0270

Error Source	Position (ft)			Velocity (fps)			Misalignment (sec)		
	DR	CR	R	DR	CR	R	DR	CR	R
Initial Conditions	0.0	0.0	0.1	0.00	0.00	0.00	1.6	0.3	2.7
Measurement Noise	4.8	6.3	11.8	0.04	0.05	0.06	0.9	0.4	1.5
Accelerometer:									
Quantization	0.1	0.1	0.2	0.00	0.01	0.01	0.6	0.3	0.8
Bias	0.1	0.6	0.5	0.01	0.04	0.03	4.1	6.9	7.2
Scale Factor	0.0	0.1	0.2	0.00	0.00	0.01	0.3	3.6	0.2
Asymmetry	0.0	0.1	0.2	0.00	0.00	0.01	0.3	3.7	0.2
Nonorthogonality	0.0	0.1	0.4	0.00	0.00	0.00	2.6	3.8	7.0
Gyroscope:									
Bias	0.0	0.0	0.1	0.00	0.00	0.00	0.3	7.6	6.8
Mass Unbalance									
Input Axis	0.0	0.0	0.1	0.00	0.00	0.00	18.8	3.9	6.5
Spin Axis	0.0	0.0	0.0	0.00	0.00	0.00	4.0	1.1	2.6
MTU (Clock):									
Five State Model	2.5	4.3	6.5	0.08	0.10	0.17	1.7	1.1	3.1
Acceleration Term	0.0	0.0	0.2	0.00	0.00	0.01	0.0	0.1	0.1
Gravity Model	0.0	0.0	0.0	0.00	0.00	0.00	0.8	0.5	0.3
GPS Satellite Errors	4.4	4.2	8.7	0.00	0.00	0.01	0.2	0.2	0.3
RSS Total	6.9	8.7	16.0	0.08	0.12	0.19	25.7	12.8	14.7

to the remaining misalignment uncertainty, but the velocity estimation accuracy is dominated by the frequency errors in the MTU and the position estimation accuracy is dominated by the combination of GPS receiver measurement noise and GPS satellite ephemeris (and clock phase) errors. This dominance of GPS-related error sources implies that navigation performance is insensitive to an increase in the magnitude of any other error source as long as GPS is available.

The most important conclusion to be drawn from Table 2.5-2 is that, when GPS-aiding is used, ascent navigation accuracy may not be sensitive to the quality of the IMU. The role of the IMU is to provide an inertial reference with short term stability so that GPS measurements taken at different times can be "tied together" to generate an accurate navigation estimate. The IMU need not have good long term stability

performance characteristics and, more important in a Space Shuttle context, it need not be accurately calibrated or aligned.

A second important observation is that the acceleration-sensitive MTU error had a negligible effect on the navigation accuracy. This is partly due to the fact that the GPS measurements were processed during a low acceleration phase of the mission (approximately 0.1 g), but the error budget suggests that even during 3g acceleration the velocity error due to this error source would be less than 0.3 fps. Thus, the possibility exists for utilizing GPS-aided inertial navigation during the entire ascent mission phase.

The importance of the MTU frequency errors in limiting velocity accuracy is reflected in Table 2.5-1. Although GPS-aiding improved the position and velocity estimates, it could not improve the clock frequency error estimates significantly, primarily because of short-term instabilities in the MTU frequency (see Table 2.4-3). In effect, the residual MTU frequency estimation error establish the lower limit for the velocity errors. Any attempt to further decrease the velocity errors would require an onboard clock with improved frequency stability characteristics.

2.6 ASCENT SENSITIVITY ANALYSIS

The error budget in Section 2.5 was generated under the assumption that the truth model presented in Section 2.4 is an accurate statistical representation of the real world error sources which would affect navigation system performance. Since many of the models are based upon performance projections for hardware which has not yet been built, it is necessary

to evaluate the sensitivity of the navigation filter to unknown variations in the rms values of the dominant error sources. Sensitivity curves for the ascent navigation filter are presented in this section.

The error budget in Table 2.5-1 indicates that position errors at orbit insertion are dominated by GPS-related errors, primarily receiver noise and GPS satellite errors. The performance sensitivities to variations in these error sources are presented in Figs. 2.6-1 and 2.6-2, respectively. As an example of how to interpret the results, consider Fig. 2.6-1. The error budget indicates that, for the baseline error model, the radial position error at orbit insertion is 16 ft. If the receiver noise were a factor of 5 worse than predicted by the error model, however, and if the filter parameters were not adjusted to reflect the increase, then the radial error would increase to 60 ft.

Both Figs. 2.6-1 and 2.6-2 indicate a strong performance sensitivity to the GPS error sources. However, the error magnitudes anticipated in the model are not likely to be significantly in error for Phase III GPS. If the Space Shuttle were to process the C/A-code (low accuracy) signal rather than the P-code (high accuracy) signal, the receiver errors would be a factor of 10 greater than indicated in the error model, but this would be a known degradation for which the filter could be adjusted. The resulting position errors would be greater than those indicated in the error budget, but quite likely would be considerably less than the $\times 10$ numbers indicated in Fig. 2.6-1.

The only major contributor to velocity errors is the MTU frequency stability. As a result, the velocity error will exhibit a nearly linear dependence on unknown variations

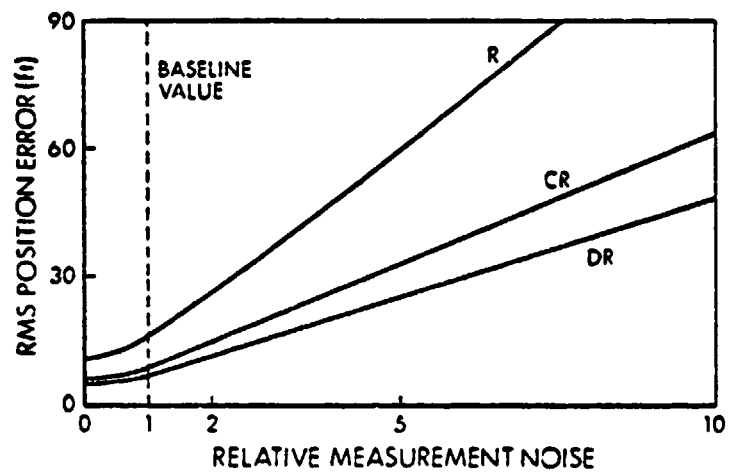


Figure 2.6-1 RMS Position Error Sensitivity at Orbit Insertion to GPS Receiver Measurement Noise

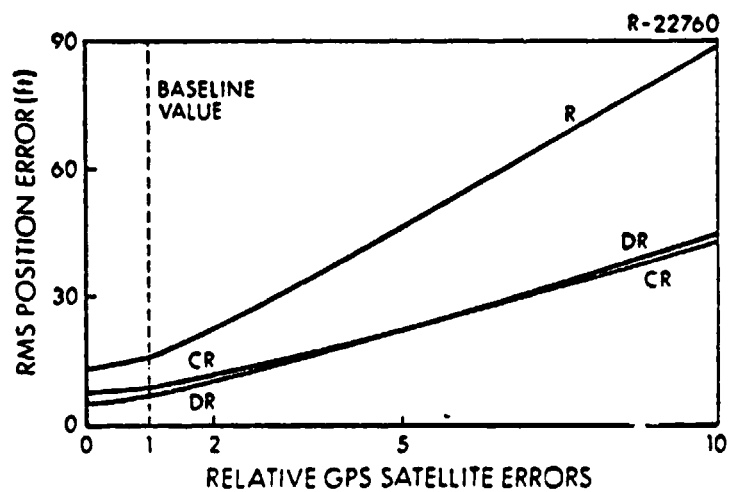


Figure 2.6-2 RMS Position Error Sensitivity at Orbit Insertion to GPS Satellite Tracking Errors

in the MTU errors. Figure 2.6-3 indicates that, if the MTU were replaced by a more accurate clock, the velocity errors could be significantly decreased even without adjusting the filter parameters. If velocity accuracies of 0.2 fps are adequate, however, the MTU will suffice as a time reference as long as it meets the established performance specifications.

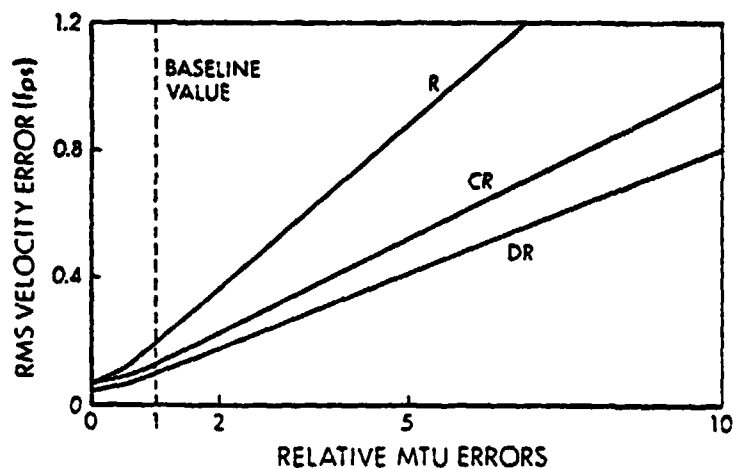


Figure 2.6-3 RMS Velocity Error Sensitivity at Orbit Insertion to MTU Errors

The principal contribution of IMU-related error sources to navigation performance at orbit insertion is to the residual misalignment error. This error will be important only if reentry is to be performed without GPS measurements and without realigning the IMU - constraints which potentially could be applied to short duration missions such as 3B. Because of geometric effects, the largest residual misalignment is about the downrange axis. The results in Fig. 2.6-4 indicate that, even if the IMU calibration were a factor of 5 worse than expected, the downrange alignment error (also crossrange and radial) would still be less than 100 $\hat{\text{sec}}$ at orbit insertion. Since initial conditions are a negligible contributor to the error budget, the performance at orbit insertion would be even less sensitive to large initial azimuth misalignments at launch.

THE ANALYTIC SCIENCES CORPORATION

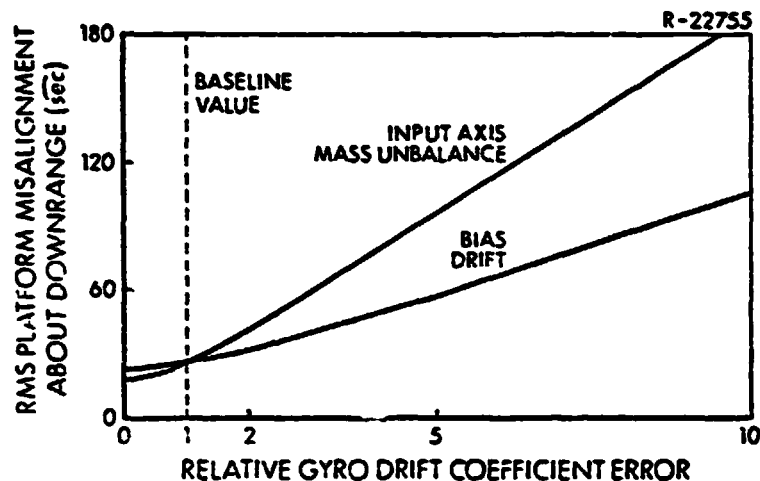


Figure 2.6-4 RMS Downrange Misalignment Error Sensitivity at Orbit Insertion to Gyro Errors

2.7 GPS-AIDED ORBITAL AND DEORBIT NAVIGATION PERFORMANCE PROJECTION

All major changes to the Space Shuttle orbit, including both the orbit insertion and deorbit maneuvers, will be accomplished with the OMS (Orbital Maneuvering System) engines. The thrust magnitudes as well as the burn durations will be similar for the final orbit insertion and the deorbit maneuvers (Table 2.7-1). Consequently, the orbit insertion maneuver and the techniques discussed in the previous sections can be used to gain insight into potential GPS-aided navigation performance for the deorbit maneuver.

As discussed in Section 2.5-2, the position and velocity errors for GPS-aided navigation at orbit insertion are entirely due to GPS-related error sources. Since the GPS-related errors are not acceleration sensitive*, the

* The MTU does have an acceleration sensitive error component, but it was shown to be a negligible error source for the acceleration magnitudes of interest.

TABLE 2.7-1
COMPARISON OF ORBIT INSERTION AND DEORBIT MANEUVERS

EVENT	MAXIMUM ACCELERATION (ft/sec ²)	MANEUVER DURATION (sec)
Orbit Insertion Maneuver (Mission 3B)	1.5	255
Deorbit Maneuver (Mission OFT-1)	2.1	212

position and velocity estimation accuracy is essentially independent of the presence (or absence) of OMS thrusting. Thus, the orbit insertion and deorbit maneuver performance evaluations can also be used to predict GPS-aided orbital navigation accuracy with two different sets of initial condition errors.

Performance projections for both GPS-aided orbital and deorbit navigation are presented in this section. The necessary changes to the navigation filter and the truth model for deorbit are discussed in Section 2.7-1 and the performance estimates are presented in Section 2.7-2.

2.7.1 Deorbit Maneuver Study Baseline

For the most part, the baseline used for the deorbit study is the same as that used for the ascent study. The principal differences are in the duration of the measurement sequence, the parameter values in the navigation filter, and the initial conditions (both filter and truth model). These differences are summarized in this section.

The measurement schedule for the ascent study specified a total of 24 GPS measurements at 6 sec intervals over the final 138 sec of the insertion maneuver. Because the initial navigation errors will generally be worse for deorbit than for ascent, and because the navigation filter is suboptimal, the measurement schedule for deorbit was extended to 36 measurements over 210 sec — approximately the duration of the deorbit maneuver.

The initial conditions for orbit insertion navigation are a consequence of IMU cal/align and MTU errors propagated through ascent. By contrast, the initial conditions for deorbit navigation are a function of the most recent navigation fix. For the deorbit study, the initial position, velocity and alignment errors assumed for the truth model are the same as those used for entry in Chapter 4 (Ref. 47). These errors correspond to an IMU alignment with the onboard star tracker and an uploaded navigation fix, both two hours prior to the deorbit maneuver, and then open loop propagation to the time of the maneuver. The resulting navigation errors are primarily in-plane errors — approximately 12,000 ft and 13 fps rss. The misalignments are 285 $\widehat{\text{sec}}$ per axis.

The MTU initial conditions assume an accurate calibration at the time of the startracker alignment and subsequent open loop propagation. The calibration errors assumed are those existing at orbit insertion for the GPS-aided ascent study (Table 2.5-1). At the time of the deorbit maneuver, the resulting MTU errors are 1129 ft in phase and 0.25 fps in phase rate.

The initial filter covariance matrix and the filter parameter values are shown in Table 2.7-2. The covariance is diagonal except for correlations between downrange and

TABLE 2.7-2
NAVIGATION FILTER INITIAL CONDITIONS

T-0044a

State No.	Description	Initial Filter Standard Deviations		Filter Process Noise Spectral Densities	
		Value	Units	Value	Units
1	X Position Error	16,700	ft	—	ft ² /sec
2	Y Position Error	16,700	ft	—	ft ² /sec
3	Z Position Error	16,700	ft	—	ft ² /sec
4	X Velocity Error	18.7	fps	0.001	(fps) ² /sec
5	Y Velocity Error	18.7	fps	0.001	(fps) ² /sec
6	Z Velocity Error	18.7	fps	0.001	(fps) ² /sec
7	X Platform Misalignment	900	sec	0.035	sec ² /sec
8	Y Platform Misalignment	900	sec	0.035	sec ² /sec
9	Z Platform Misalignment	900	sec	0.035	sec ² /sec
10	Receiver Clock Phase Error	1130	ft	0.1	ft ² /sec
11	Receiver Clock Frequency Error	0.25	fps	3×10^{-5}	(fps) ² /sec

radial errors*. Except for the addition of the clock errors, the filter data base is the same as that used in Chapter 4. These values are somewhat pessimistic relative to the truth model errors, particularly in crossrange position and velocity, in order to account for the effect of unmodeled errors. When coupled with measurement underweighting, the net effect of this pessimism is to require a longer measurement sequence than would be required if a more optimistic initial filter covariance were selected.

2.7.2 Performance Projections

The error budget in Section 2.5 indicated that position and velocity errors for GPS-aided navigation were due almost exclusively to:

*Downrange and radial navigation errors will be coupled due to the effect of orbital dynamics — a downrange velocity error at orbital perigee will generate a radial position error at orbital apogee, etc. The filter accounts for this effect by assuming -1 correlations between downrange velocity and vertical position and between downrange position and vertical velocity.

- measurement noise
- MTU errors
- GPS satellite errors

In addition, if "initial conditions" are redefined to mean the position, velocity and misalignment errors at the beginning of the measurement sequence, including the effect of IMU errors up to that time, then the misalignment errors at orbit insertion are dominated by:

- initial conditions

Because of the degree to which they dominate the ascent study results, these four error groups are sufficient to characterize navigation performance for the orbital and deorbit navigation studies. The performance projections summarized in this section are based on these error groups.

The results of the deorbit study are presented in Table 2.7-3. Even though the true initial errors were considerably larger than for the ascent study, and the filter initial covariance was not representative of the true errors, the position and velocity errors at the end of the deorbit measurement sequence were virtually identical to those at orbit insertion. This suggests that, at the very least, the 11-state filter can yield good navigation performance over the range of operating conditions expected for exoatmospheric mission phases. A future effort will investigate the filter performance during atmospheric flight.

The disappointing aspect of the deorbit results is the inability to estimate IMU misalignments. Whereas the misalignments were estimated to better than 25 $\widehat{\text{sec}}$ for the

TABLE 2.7-3
EFFECT OF GPS IN REDUCING DEORBIT ERRORS

T-0462

EVENT	RMS POSITION ERRORS (ft)			RMS VELOCITY ERRORS (fps)			RMS MISALIGNMENT ERRORS (sec)		
	DR	CR	R	DR	CR	R	DR	CR	R
Begin Deorbit	11265	866	1036	1.1	0.9	12.4	285	285	285
End Deorbit	7	9	17	0.1	0.1	0.2	283	256	257

ascent study, there was minimal improvement in the estimates during the deorbit measurement sequence. The principal difference is that the misalignments were highly correlated with the position and velocity errors during ascent, and hence readily recoverable from range and range-rate measurements. By contrast, the navigation errors during orbital operations are independent of IMU misalignments. Even though the deorbit acceleration will introduce a small correlation between misalignment and velocity errors, the table suggests that the acceleration level will not be large enough to make accurate (60 sec) misalignment estimates unless the duration of the deorbit maneuver (and measurement sequence) is increased.*

Although IMU misalignment errors apparently cannot be significantly reduced during deorbit, it is possible that the misalignments can be estimated with sufficient accuracy to provide a consistency check of the IMU alignments. This capability could eliminate the redundancy management problem of detecting the occurrence of major shifts in gyro parameters in the two hours between IMU alignment and deorbit. A more thorough investigation is required to determine the performance capability of such a consistency check.

*The true acceleration level for deorbit will be somewhat greater than that used for this study (2.2 vs 1.5 ft/sec²), but this would not significantly improve misalignment estimation accuracy.

The present baseline for operational Space Shuttle missions specifies the Tracking and Data Relay Satellite System (TDRSS) as the principal navigation aid for orbit determination. TDRSS can provide both range and range-rate information, but it suffers a number of operational disadvantages relative to GPS. Because TDRSS consists of only two satellites, TDRSS/user geometry is a more important factor in orbit determination accuracy than it would be for Phase III GPS. Also, utilization of only two satellites means that longer measurement sequences must be processed in order to generate a navigation solution. Finally, orbit determination using TDRSS requires ground processing and subsequent uploading of the navigation solution. This will tend to decrease the operational flexibility of TDRSS-aided navigation relative to an autonomous GPS navigation system.

Table 2.7-4 compares orbit determination accuracy for TDRSS and GPS. The TDRSS data was taken from Ref. 15;* the GPS performance projections are based on the orbit insertion and deorbit results after two min of data processing. The table clearly implies that GPS can provide significantly better navigation accuracy than TDRSS from shorter measurement sequences. In contrast to TDRSS, which requires a relatively long trajectory arc to estimate orbital parameters (5 min was the shortest arc considered in Ref. 15), GPS could attain the indicated accuracy with only a few seconds of data if the navigation filter were suitably optimized.

*The error analysis presented in Ref. 15 considered only receiver noise. It did not consider the effects of receiver oscillator instability, user dynamics, etc. As a consequence, the results in Ref. 15 are perhaps overly optimistic.

TABLE 2.7-4
PROJECTED ORBIT DETERMINATION ACCURACIES FOR
TDRSS AND GPS

NAVIGATION AID	LENGTH OF MEASUREMENT SEQUENCE (min)	RSS POSITION ERRORS (ft)	RSS VELOCITY ERRORS (fps)
TDRSS	5	200*	Not Specified
GPS	2	20	0.2

*See footnote on previous page.

3. CALIBRATION AND ALIGNMENT COVARIANCE ANALYSIS

The performance analysis for the Space Shuttle calibration and alignment algorithm is being conducted in two phases. The first phase, completed in the previous contract period (Ref. 1), used monte carlo techniques to generate an overall performance projection for the Approach and Landing Test (ALT) algorithm (Ref. 51) and to identify potential risk areas. The second phase, currently in progress, uses covariance analysis techniques to develop a detailed error budget for the Orbital Flight Test (OFT) algorithm (Ref. 18) and to identify the major error mechanisms which limit calibration and alignment performance. For those error parameters for which the algorithm cannot provide the required calibration accuracy, the results of this phase will provide a clear indication as to the modifications which must be made in order to achieve the desired performance.

An overview of the calibration and alignment mechanization for OFT is presented in Section 3.1. Section 3.2 contains a general description of the mathematical structure used in the covariance simulations and Section 3.3 summarizes the truth model states and error sources used in the covariance analysis. A partial error budget for the cal/align software is presented in Section 3.4.

3.1 CALIBRATION AND ALIGNMENT OVERVIEW

The calibration and alignment of the Space Shuttle inertial measurement units (IMUs) consists of two parts:

the hangar calibration and the preflight calibration and alignment. The hangar calibration will be performed in a low-vibration environment within 5* to 14* days prior to launch, and will have a total duration of 8.6* hr. The preflight calibration and alignment will be initiated at the launch pad within 3* to 15* hr before launch, and will have a total duration of 2.8* hr. The calibration and alignment schedule during both the hangar and the preflight mission phases is illustrated in Fig. 3.1-1.

The cal/align procedure consists of steering the platform to a series of discrete positions at which torquing rates are applied to compensate for earth rate, and in some cases "excess" rates are applied to torque the platform through a prescribed trajectory relative to a local vertical (North, West, Up) coordinate system. At each of these positions, the accelerometer outputs (in a few cases also the resolver outputs) are sampled and a least squares fit (LSF) filter is used to estimate the acceleration along the up axis and the platform tilts and tilt rates about the north and west axes. Once the data (vertical accelerations, tilts and tilt rates from the various positions) necessary to evaluate the required IMU error parameters has been collected, these are computed and the compensation parameters are updated. Between discrete positions, the platform is slewed at a high rate and no data is collected during this motion.

The cal/align mechanization comprises six different sequences. Each of these consists of several positions and is used for the calibration, alignment or verification of several IMU errors as outlined in Table 3.1-1.

*These times are approximate and subject to modification.

THE ANALYTIC SCIENCES CORPORATION

A-150455

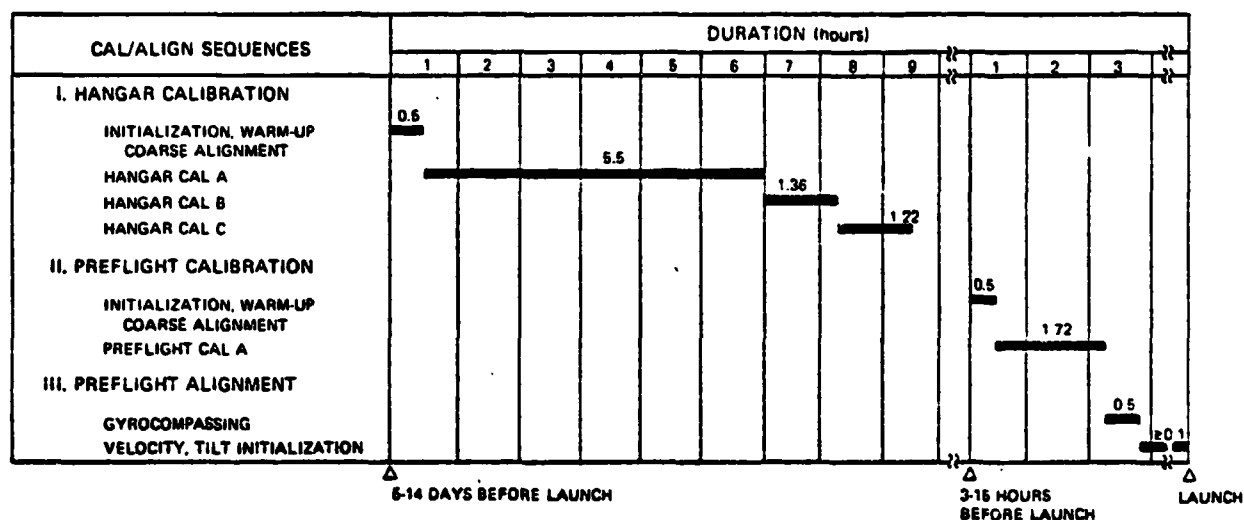


Figure 3.1-1 Calibration and Alignment Schedule

TABLE 3.1-1
ERRORS CONSIDERED DURING THE CAL/ALIGN PHASE

T-0040

IMU Errors		Hangar Phase			Preflight Phase		
Name	No. of Errors	Cal A	Cal B	Cal C	Cal A	Gyro-compass	VTI
Accel. Bias High Gain	3	1			1		
Accel. Scale Factor High Gain	3	1			1		
Accel. Bias Low Gain	3	1			1		
Accel. Scale Factor Low Gain	3	1			1		
Gyro Bias Drift Rate	3	1			1		
Gyro Mass Imbalance	5	1			4		
Accel. Asymmetry	3	1					
Accel. Nonorthogonality	3	1					
Gyro Torquer Scale Factor	3	1					
Gyro Misalignment	6	1					
Resolver Offset	3		1				
Gimbal Nonorthogonality	1		1				
Accel. and Gyro to Platform Misalignments	2		1				
Relative Cluster Attitude	-			3		4	5
Tilt Misalignments	2					5	
Azimuth Misalignment	1					5	

Key: 1 - Compute and calibrate
2 - Compute and, if commanded, calibrate
3 - Compute and store
4 - Compute and check for reasonableness
5 - Compute and align

3.2 COVARIANCE ANALYSIS PROGRAM DESCRIPTION

3.2.1 Program Overview

The structure of the covariance analysis program is the same as for the OFT IMU software. The program is organized into seven separate sequences with an executive program which defines the interface between those sequences (Fig. 3.2-1). The input to the Coarse Alignment sequence is a data file which defines the IMU status (values for all error coefficients, gyro torquing rates, etc.), a priori calibration and alignment estimates, and the transformation matrices between the platform coordinate system and the vehicle-, earth- and inertially-fixed coordinate systems. The output of the Coarse Alignment sequence is a new data file updated by the Coarse Alignment estimates. This file is then the input to Hangar Cal A and so on.

The program preserves the correlation between estimation errors in different sequences and has the capability of simulating a complete calibration and alignment procedure

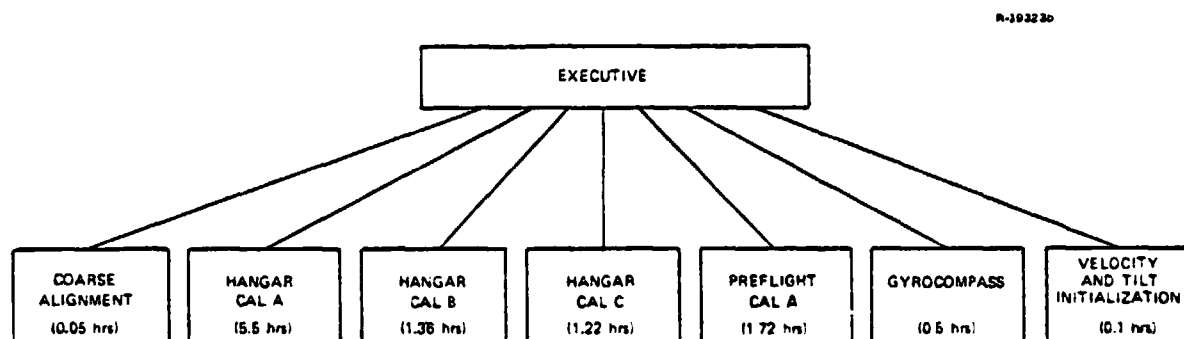


Figure 3.2-1 Structure of Covariance Simulation for Performance Analysis

from beginning to end. Alternatively, the initial condition data for any sequence can be used (and modified if desired) for performing special studies for a given sequence.

3.2.2 State and Covariance Equations

The LSF filter used in the cal/align software is a recursive filter, i.e., the tilt and tilt rate estimates generated at a particular time are a function only of the current accelerometer outputs and the estimates generated at the previous time. This recursive property permits the estimation procedure to be modeled as a (suboptimal) state estimator for the IMU error parameters based on a linearized model of the system dynamics. Because of the fact that the IMU parameter estimates are updated only at the end of each cal/align sequence, however, it is necessary to introduce temporary storage states into the filter equations. The form of these equations and the approach used in the program to generate the accompanying covariance equations are discussed in this section.

The state and covariance error equations are summarized in Table 3.2-1. Equation (3.2-1) found in the table models the error propagation for the linearized IMU system. The equation represents the fundamental operational mode of the IMU including its associated software during the hangar and preflight phases (the Ground Operation Sequence, Ref. 18). The state vector \underline{x} is composed of three parts:

\underline{x}_1 - the least squares fit (LSF) filter states used to estimate the platform accelerations (tilts) and acceleration rates (tilt rates) by measuring the platform velocity outputs, and/or to estimate the platform attitude and attitude rate by measuring the gimbal angles.

TABLE 3.2-1
SYSTEM AND COVARIANCE ERROR EQUATION SUMMARY

7-0016

CAL/ALIGN STEP	STATE EQUATION	COVARIANCE EQUATION
ESTIMATE TILTS AND DRIFTS PROPAGATE IMU ERRORS	$\dot{\underline{x}} = \underline{F} \underline{x} + \underline{w}$ (3.2-1)	$\dot{\underline{P}} = \underline{F} \underline{P} + \underline{P} \underline{F}^T + \underline{Q}$ (3.2-2)
TORQUE OUT TILTS RESET FILTER	$\underline{x}^+ = \underline{L} \underline{x}^-$ (3.2-3)	$\underline{P}^+ = \underline{L} \underline{P}^- \underline{L}^T$ (3.2-4)
STORE ESTIMATES RESET FILTER	$\underline{x}^+ = \underline{C} \underline{x}^-$ (3.2-5)	$\underline{P}^+ = \underline{C} \underline{P}^- \underline{C}^T$ (3.2-6)
UPDATE IMU PARAMETERS RESET STORAGE STATES	$\underline{x}^+ = \underline{D} \underline{x}^-$ (3.2-7)	$\underline{P}^+ = \underline{D} \underline{P}^- \underline{D}^T$ (3.2-8)

where the vectors are defined by

$$\underline{x} = \begin{bmatrix} \underline{x}_1 \\ \underline{x}_2 \\ \underline{x}_3 \end{bmatrix} = \begin{bmatrix} \text{LSF Filter States} \\ \text{Storage States} \\ \text{IMU Error States} \end{bmatrix} \quad \underline{w} = \begin{bmatrix} \underline{w}_1 \\ 0 \\ \underline{w}_3 \end{bmatrix} = \begin{bmatrix} \text{Measurement Noise} \\ - \\ \text{Process Noise} \end{bmatrix}$$

and the matrices are given by

IMU DYNAMICS	ERROR COVARIANCE	NOISE COVARIANCE
$\underline{F} = \begin{bmatrix} 0 & 0 & \underline{K} \underline{H} \\ 0 & 0 & 0 \\ 0 & 0 & \underline{F}_3 \end{bmatrix}$	$\underline{P} = \begin{bmatrix} P_{11} & P_{12} & P_{13} \\ P_{21} & P_{22} & P_{23} \\ P_{31} & P_{32} & P_{33} \end{bmatrix}$	$\underline{Q} = \begin{bmatrix} R_{11} & 0 & 0 \\ 0 & 0 & 0 \\ 0 & 0 & Q_{33} \end{bmatrix}$ (3.2-9)
PLATFORM LEVELING	DATA STORAGE	PARAMETER UPDATL
$\underline{L} = \begin{bmatrix} 0 & 0 & 0 \\ 0 & 1 & 0 \\ -\underline{L}_3 & 0 & 1 \end{bmatrix}$	$\underline{C} = \begin{bmatrix} 0 & 0 & 0 \\ C_2 & 1 & C_3 \\ 0 & 0 & 1 \end{bmatrix}$	$\underline{D} = \begin{bmatrix} 0 & 0 & 0 \\ 0 & D_2 & 0 \\ 0 & -D_3 & 1 \end{bmatrix}$ (3.2-10)

\underline{x}_2 - the dummy or storage states, used to store some of the filter estimates, \underline{x}_1 , which are required to update IMU error parameters at the present or at a future time.

\underline{x}_3 - the system states, including the platform velocity errors, misalignments and all IMU error states being considered in the present cal/align evaluation.

Equation (3.2-1) is driven by white process noise represented by the vector \underline{w} . The components of \underline{w} are resolver measurement error \underline{w}_1 and the IMU process noise \underline{w}_3 . There are no errors associated with the transfer of filter states \underline{x}_1 into storage states \underline{x}_2 . The propagation of the statistics associated with the state vector \underline{x} is governed by Eq. (3.2-2). The details about the elements in F_3 and H are given in Appendix B of Ref. 7. Details about K , L_3 , C_2 , D_2 and D_3 are given in Appendix D of Ref. 1 and in Appendix B of this report, and about Q and $P(0)$ in Section 3.3.2 of this report.

At the end of each estimation period some of the filter estimates \underline{x}_1 are stored in the temporary memory states \underline{x}_2 and, simultaneously, the filter states are reset to zero. This storage and reset is represented by Eqs. (3.2-5) and (3.2-6). Depending on the particular point in the cal/align process, the next step will be one of the following:

- Update one or more of the IMU errors, \underline{x}_3 , using one or more of the estimates stored in \underline{x}_2 , and reset the storage states in \underline{x}_2 which are not required for future IMU error updates. This step is represented by Eqs. (3.2-7) and (3.2-8).
- Rotate the platform about the horizontal axes by an amount equal and opposite to the filter estimates of the platform misalignments from level. This step is represented by Eqs. (3.2-3) and (3.2-4).
- Initiate the next estimation of platform tilts and drifts and IMU error propagation, as described above and represented by Eqs. (3.2-1) and (3.2-2).

The cal/align evaluation performed by TASC is based on computation of the covariance Eqs. (3.2-2), (3.2-4), (3.2-6) and (3.2-8). Since the corresponding state Eqs. (3.2-1), (3.2-3), (3.2-5) and (3.2-7) are all linear, it is

possible to initialize the matrices P and Q with only those error sources of interest at a particular time and to obtain, at the end of the run, the sensitivity of the cal/align process to that particular error source or group of errors.

3.3 TRUTH MODEL DESCRIPTION

Generation of an error budget for the cal/align software requires that a "truth model"* describing the real world error sources for the cal/align process be defined. The description must include a complete list of states and error sources, and a data base. The truth model to be used to evaluate the Space Shuttle cal/align software is presented in this section.

3.3.1 States and Error Sources

The truth model states and error sources used in evaluating the IMU cal/align mechanization are listed in Table 3.3-1, which divides them into three major categories:

- Category I - Platform misalignments and calibrated IMU error states
- Category II - Noncalibrated IMU error states
- Category III - Random and quantization errors

These three categories contain the error sources which will be used to generate the baseline error budget. The first category corresponds to the platform misalignments

*The "truth model" is a mathematical model of all potentially significant error sources and the way they affect the cal/align performance in the real world.

TABLE 3.3-1
IMU TRUTH MODEL STATES AND ERROR SOURCES

T-0011

ERROR SOURCE NAME AND GROUP NUMBER	NUMBER OF STATES	NUMBER OF ERROR SOURCES	ERROR MNEMONIC
I. PLATFORM MISALIGNMENTS AND CALIBRATED ERRORS			
1. Platform Misalignments	3	0	
2. Gyro Bias Drifts	3	3	DFX,Y,Z
3. Gyro Mass Unbalances	5	5	DIX,Z,DSX,Z,DOZ
4. Gyro Torquer Scale Factors	3	3	KTX,Y,Z
5. Gyro Misalignments	6	6	BXY,XZ,...,ZY
6. Accel. Biases - Low Gain	3	3	KOX,Y,Z
7. Accel. Scale Factors - Low Gain	3	3	KIX,Y,Z
8. Accel. Biases - High Gain	3	3	KOHX,Y,Z
9. Accel. Scale Factors - High Gain	3	3	KIHX,Y,Z
10. Accel. Scale Factor Asymmetries	3	3	KSX,Y,Z
11. Accel. Nonorthogonalities	3	3	DELTYX,ZX,ZY
12. Accel. and Gyro Misalignments	2	2	MXZ,NYZ
13. Resolver Offsets, Gimbal Nonorthogonalities	4	6	IRO,PO,AZO,DP,a,b
II. NONCALIBRATED IMU ERRORS			
14. Gyro Anisoeasticities	11	11	D12X,Z,DS2X,Y,Z D1SX,Z,DOSA,Z,DIOX,Z
15. Gyro Output Axis Mass Unbalances	2	2	DOX,Y
16. Gyro Heading Sensitive Drifts	3	3	HSN,W,U
17. Gyro Thermal Transient Drift	3	3	TTX,Y,Z
18. Accel. Nonlinearities - 2 nd Order	3	6	K2X,Y,Z,XZ,YZ,ZX
19. Accel. Nonlinearities - 3 rd Order	3	3	K3X,Y,Z
20. Accel. Heading Sensitive Biases	3	3	KOHSN,W,U
21. Accel. Heading Sensitive Scale Factors	3	3	K1HSN,W,U
22. Outer Roll Offset and Misalignments	3	3	ORO,AY,AZ
23. Resolver Harmonics	24	24	1 st ,4 th ,6 th ,7 th
III. RANDOM AND QUANTIZATION ERRORS			
24. Gyro Randomness and Quantization	3	6	
25. Accel. Randomness and Quantization		6	
26. Resolver Randomness and Quantization		7	
27. Vehicle Motions	7	2	
TOTALS	115	124	

and those IMU error sources which are calibrated during one or more calibration sequences. Category II corresponds to additional IMU error sources which are not estimated or calibrated during either the hangar or the preflight calibrations. Category III contains those states which are driven by random

errors, including instrument randomness, quantization effects and vehicle motions induced by wind gusts.

All error source categories are divided into smaller sets, each of which is associated with a group number. These group numbers were quite useful in defining the detailed truth model equations in Appendix B of Ref. 7. In addition, each line of the error budget that will be generated in this study will correspond to the contribution from all error sources in one particular group rather than each error taken one at a time. This simplifies the error budget table and places the various error source groups in better perspective.

3.3.2 Truth Model Data Base

Generation of a detailed error budget requires the numerical values for all truth model error sources. Two sets of errors must be specified: the initial calibration error (instrument error minus software compensation term) at the beginning of the hangar calibration phase, and the changes of the instrument errors during the time elapsed between the hangar calibration and the preflight calibration due to the turn-off turn-on errors. This data is summarized in Tables 3.3-2 and 3.3-3.

The numerical values described above are required to construct F, P and Q in Eq. (3.2-2). The specific elements of F, P and Q which must be assigned are:

$P_{33}(0)$ - the initial IMU error covariance matrix

$P_{33}(1)$ - the IMU turn-off turn-on instability error covariance matrix

Q_{33} - the process noise covariance matrix

TABLE 3.3-2
IMU TRUTH MODEL DATA BASE FOR CALIBRATED ERRORS

T-0042

Error Source Name and Group Number	Standard Deviation			Data Source
	Units	At Beginning of Hangar Cal	Turn-off Turn-on Instabilities	
2. Gyro Bias Drifts	sec/sec	0.035	0.016	Ref. 1
3. Gyro Mass Unbalances:				
Input Axis Acceleration	sec/sec/g	0.3	0.015	Ref. 1
Spin Axis Acceleration	sec/sec/g	0.02	0.005	Ref. 22
Output Axis Acceleration	sec/sec/g	0.025	0.01	Ref. 22
4. Gyro Torquer Scale Factors	ppm	400	100	Ref. 1
5. Gyro Misalignments	sec	120	15	Ref. 1
6. Accel. Biases - Low Gain:				
X,Y	ug	100	50	Ref. 1
Z	ug	200	50	Ref. 1
7. Accel. Scale Factors - Low Gain	ppm	200	100	Ref. 22
8. Accel. Biases - High Gain:				
X,Y	ug	100	50	Ref. 1
Z	ug	200	50	Ref. 1
9. Accel. Scale Factors - High Gain	ppm	200	100	Ref. 22
10. Accel. Scale Factor Asymmetries	ppm	200	0	Ref. 22
11. Accel. Nonorthogonalities	sec	60	10	Ref. 1
12. Accel. and Gyro Misalignments	sec	60	10	Ref. 1
13. Resolver Offsets	sec	200	20	Ref. 22
Gimbal Nonorthogonalities	sec	60	0	Ref. 22

F_{33} - the IMU truth model error dynamics matrix

R_{11} - the measurement error covariance matrix

Elements of P_{33} , Q_{33} and F_{33} are normally chosen together to define random processes with desired properties. For instance, a first-order markov process (exponentially correlated random process) is modeled with a specified rms value, σ_i , and correlation time, τ_i . In this case the relevant truth model matrix elements are:

$$P_{33_{ii}} = \sigma_i^2 \quad (3.3-1)$$

TABLE 3.3-3
IMU TRUTH MODEL DATA BASE FOR NONCALIBRATED ERRORS

T-0043

Error Source Name	Units	Standard Deviation	Data Source
14. Gyro Anisoelectricities:			
Input-Input Anisoel. Drift	$\widehat{\text{sec}}/\text{sec}/\text{g}^2$	0.005	Ref. 22
Spin-Spin Anisoel. Drift	$\widehat{\text{sec}}/\text{sec}/\text{g}^2$	0.005	Ref. 22
Input-Spin Anisoel. Drift	$\widehat{\text{sec}}/\text{sec}/\text{g}^2$	0.025	Ref. 22
Output-Spin Anisoel. Drift	$\widehat{\text{sec}}/\text{sec}/\text{g}^2$	0.025	Ref. 22
Input-Output Anisoel. Drift	$\widehat{\text{sec}}/\text{sec}/\text{g}^2$	0.005	Ref. 22
15. Gyro Output Axis Mass Unbalances	$\widehat{\text{sec}}/\text{sec}/\text{g}$	0.005	Ref. 22
16. Gyro Heading Sensitive Drift	$\widehat{\text{sec}}/\text{sec}$	0.005 (2)	Ref. 22
17. Gyro Thermal Transient Drift	$\widehat{\text{sec}}/\text{sec}$	$0.0064 e^{-t/600}$ (1)	Ref. 22
18. Accel. Nonlinearities:			
2 nd Order	$\mu\text{g}/\text{g}^2$	15	Ref. 22
Product Nonlinearity	$\mu\text{g}/\text{g}^2$	10	Ref. 22
19. Accel. Nonlinearities - 3 rd Order	$\mu\text{g}/\text{g}^3$	5	Ref. 22
20. Accel. Attitude Sensitive Biases	μg	10 (2)	Ref. 1
21. Accel. Attitude Sensitive Scale Factors	ppm	15 (2)	Ref. 1
22. Outer Roll Offset and Misalignments	$\widehat{\text{sec}}$	200	Ref. 1
23. Resolver Harmonics:			
1 st Harmonic	$\widehat{\text{sec}}$	7.6 (2)	Ref. 22
8 th Harmonic	$\widehat{\text{sec}}$	19.0 (2)	Ref. 22
9 th Harmonic	$\widehat{\text{sec}}$	4.2 (2)	Ref. 22
16 th Harmonic	$\widehat{\text{sec}}$	20.0	Ref. 22
24. Gyro Randomness	$\widehat{\text{sec}}/\text{sec}^{3/2}$	0.0001	See text
25. Accel. Output Noise	μg	5	Ref. 22
Velocity Quantization - Low Gain	$\text{ft}/\text{sec}^{3/2}$	0.0003	See text
Velocity Quantization - High Gain	$\text{ft}/\text{sec}^{3/2}$	0.00003	See text
26. Resolver Output Noise	$\widehat{\text{sec}}$	12	See text
Resolver Quantization	$\widehat{\text{sec}}$	5.8	See text
27. Vehicle Motions		See text	See text

(1) t = seconds after completing the 30 second digital torquing following a platform slow.

(2) Standard deviation of maximum amplitude.

$$F_{33_{ii}} = -1/\tau_i \quad (3.3-2)$$

$$Q_{33_{ii}} = 2\sigma_i^2/\tau_i \quad (3.3-3)$$

A constant error source can be considered a special case of the above with $\tau_i = \infty$ and $F_{33_{ii}} = Q_{33_{ii}} = 0$.

The gyro randomness error assumes a random walk model with a growth rate of $32 \times 10^{-6} (\text{deg/hr})^2/\text{hr}$. This variance corresponds to a standard deviation of $0.0001 \text{ sec/sec}^{3/2}$ as given in Table 3.3-3.

The velocity quantization error with the accelerometers operating in the low gain mode is determined as follows:

$$\text{One } \Delta V \text{ pulse} = 0.0343 \text{ fps} \quad (3.3-4)$$

Assuming that each ΔV pulse count has a random error selected from a uniform distribution ranging from -0.0172 fps to $+0.0172 \text{ fps}$, and one such error is introduced every 0.32 sec computational cycle*, the error variance is

$$Q_{33_{ii}} = (0.0343)^2/12/0.32 \quad (3.3-5)$$

$$= 0.0003 (\text{fps})^2/\text{sec} \quad (3.3-6)$$

The quantization level for the resolvers is 20 sec . Because dithering rates are applied to all axes along which successive resolver measurements are made, this quantization error may be represented as an uncorrelated measurement noise of

$$R_{11_{ii}} = (20)^2/12 = 33.3 (\text{sec})^2 \quad (3.3-7)$$

The vehicle motions model was specified in detail in Ref. 1. The equivalent state space representation of this effect is

*NASA is presently considering a longer computational cycle. If a change is made, the quantization models must be changed accordingly.

$$\begin{bmatrix} \underline{x}_w \\ \underline{x}_v \end{bmatrix} = \begin{bmatrix} A & | & O \\ \hline & & \\ B & | & C \end{bmatrix} \begin{bmatrix} \underline{x}_w \\ \underline{x}_v \end{bmatrix} + \begin{bmatrix} K \\ \hline O \end{bmatrix} [\underline{N}] \quad (3.3-8)$$

where

$$\underline{x}_w = \begin{bmatrix} \text{North wind velocity} \\ \text{West wind velocity} \\ \text{West wind acceleration} \end{bmatrix}$$

$$\underline{x}_v = \begin{bmatrix} \text{North IMU displacement} \\ \text{North IMU velocity} \\ \text{West IMU displacement} \\ \text{West IMU velocity} \end{bmatrix}$$

N is a white, gaussian random process and A, B, C and K are defined in Ref. 1.

In the OFT launch configuration, the vertical IMU velocity is caused mainly by the vehicle sway motion. Assuming that this motion is primarily along the vehicle yaw direction, then the vertical IMU velocity can be modeled as being proportional to the corresponding horizontal motion. The IMU velocity then becomes a measurement error source for the LSF filter since the filter uses successive velocity measurements to derive IMU accelerations and acceleration rates.

3.4 PARTIAL ERROR BUDGET FOR CALIBRATION AND ALIGNMENT

The covariance analysis program for the IMU cal/align software was developed and checked out during this contract period; however, generation of a detailed error budget is part

of a planned future effort. During the program checkout process, error budget contributions for a number of specific error groups were computed. The purpose for these runs was twofold: (1) to illustrate the type of results which can be obtained via covariance analysis, and (2) to improve understanding of the relative importance of certain major error sources. An example of the results obtained is presented in this section.

Detailed error budgets showing the rms contribution to all hangar and preflight calibrated parameters from two groups of error sources - second-order accelerometer nonlinearities and resolver harmonics - were generated at the end of each cal/align sequence. Tables 3.4-1 and 3.4-2 summarize the results from the hangar calibration and the preflight calibration, respectively; where the former includes Hangar Coarse Alignment, Hangar Cal A and Hangar Cal B, and the latter Preflight Coarse Alignment and Preflight Cal A. Each entry in these tables represents the rms contribution of the error source group indicated at the top to the calibrated parameters specified in the left-hand column. As a comparison, the contribution from all error source groups combined, as obtained from the monte carlo simulations reported in Ref. 1, are also shown.

As is apparent from Tables 3.4-1 and 3.4-2, the second-order accelerometer nonlinearities are significant contributors to the calibration errors of accelerometer bias and scale factor asymmetries. This result was to be expected because the calibration algorithm cannot distinguish accelerometer quadratic nonlinearities from biases and scale factor asymmetries. These results also confirm the conclusions obtained from the monte carlo simulations

TABLE 3.4-1
HANGAR CALIBRATION ERROR BUDGET FOR
ERROR SOURCE GROUPS 18 AND 23

T-0405

CALIBRATED PARAMETERS	UNITS	GROUP 18	GROUP 23	ALL GROUPS*
Level Coarse Alignment	(sec	0.5	28.9	216.0
Azimuth Coarse Alignment	(sec	0.0	28.9	630.0
Gyro Bias Drifts	(sec/s	0.000	0.000	0.014
Gyro Mass Unbalance	(sec/s/g			
Input Axis		0.000	0.000	0.059
Spin Axis		0.000	0.000	0.020
Output Axis		0.000	0.000	0.007
Gyro Torquer Scale Factors	ppm	8.1	0.0	64.0
Gyro Misalignments	(sec	0.0	0.0	8.0
Accel. Biases-Low Gain	ug	18.2	0.0	33.0
Accel. Scale Factors-Low Gain	ppm	0.0	0.0	15.0
Accel. Biases-High Gain	ug	18.2	0.0	43.0
Accel. Scale Factors-High Gain	ppm	0.0	0.0	15.0
Accel. Scale Factor Asymmetries	ppm	29.6	0.0	59.0
Accel. Nonorthogonalities	(sec	0.0	0.0	2.0
Accel. and Gyro Misalignments	(sec	0.0	0.0	18.0
Resolver Offsets, Gimbal Nonorthogonalities	(sec	0.0	25.0	37.0

*Based on Monte Carlo simulations including all error groups reported in Ref. 1

TABLE 3.4-2
PREFLIGHT CALIBRATION ERROR BUDGET FOR
ERROR SOURCE GROUPS 18 AND 23

T-0406

CALIBRATED PARAMETERS	UNITS	GROUP 18	GROUP 23	ALL GROUPS*
Level Coarse Alignment	(sec	3.2	29.1	196.0
Azimuth Coarse Alignment	(sec	5.5	37.5	546.0
Gyro Bias Drift	(sec/s	0.000	0.000	0.009
Accel. Biases-Low Gain	ug	18.2	0.0	47.0
Accel. Scale Factors-Low Gain	ppm	0.0	0.0	11.0
Accel. Biases-High Gain	ug	18.2	0.0	52.0
Accel. Scale Factors-High Gain	ppm	0.0	0.0	13.0

*Based on Monte Carlo simulations using all error groups reported in Ref. 1

which indicated that supplemental errors, primarily accelerometer heading sensitivities and nonlinearities, are significant contributors.

Table 3.4-1 shows that resolver harmonics are a significant contributor to the resolver offset and gimbal nonorthogonality calibration errors. The monte carlo sensitivity studies in Ref. 1 also support this conclusion. Tables 3.4-1 and 3.4-2 also indicate that resolver harmonics contribute to both Hangar and Preflight Coarse Alignment errors, however, these contributions are not significant when compared to other error sources. Another result exhibited by the error budgets is that the calibration of the remaining IMU error parameters is insensitive to resolver harmonic errors.

Each of the two error source groups causes larger coarse alignment errors during the preflight phase than during the hangar phase. This is so because both error source groups propagate into other accelerometer and resolver errors during hangar calibration. These errors, in turn, degrade the Preflight Coarse Alignment accuracy. This does not imply, however, that preflight coarse alignment is less accurate than hangar coarse alignment.

4. ENTRY, PRELAND AND LANDING NAVIGATION

Previous TASC reports (Refs. 1 through 3) have evaluated entry, preland and landing navigation performance for a number of different hardware/software configurations as part of NASA's development program for the Space Shuttle navigation system. As a consequence of performance limitations encountered with the previous filter design, NASA has modified the baseline filter and the recommended filter parameter values in an attempt to improve navigation accuracy (Refs. 45 and 47 respectively). The objective of the current study is to generate performance projections for the revised filter for the OFT-1 mission in 1979. The level of detail provided in this analysis should be useful for inferring the error mechanisms which limit navigation system performance for the current mechanization and for evaluating the impact of proposed system modifications.

The trajectory and measurement schedule for the performance study are presented in Section 4.1 and the baseline filter design is reviewed in Section 4.2. Section 4.3 contains the truth model which defines the environment in which the navigation performance is evaluated. The results of the navigation performance analysis and performance sensitivity to the dominant error sources are discussed in Sections 4.4 and 4.5 respectively.

4.1 TRAJECTORY AND MEASUREMENT SCHEDULE

The reference trajectory for the entry, preland and landing phases is the nominal trajectory for the OFT-1 mission.

The OFT-1 mission entails a launch from Cape Kennedy into a 38 degree inclination orbit and a landing at Edwards Air Force Base. The approach path is straight except for a dog-leg maneuver when the Terminal Area Energy Management (TAEM) alignment cylinder is intercepted at an altitude of approximately 28,000 ft. Figure 4.1-1 shows the ground track for the last segment of the entry phase and for the landing phase. The total elapsed time between entry interface at 400,000 ft and touchdown is 1630 sec.

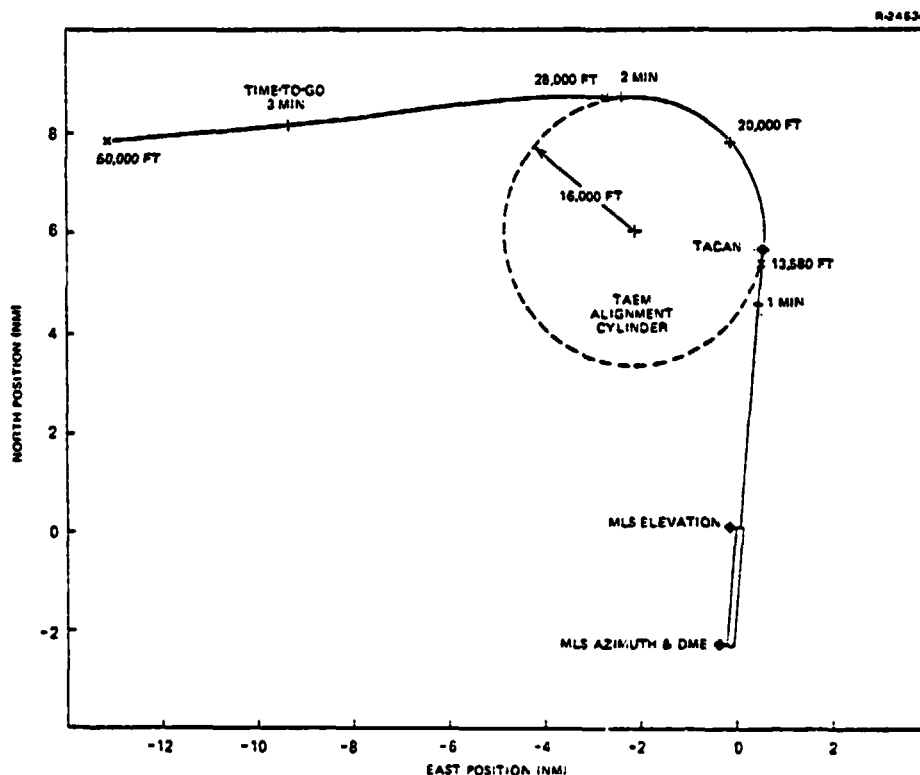


Figure 4.1-1 Approach and Landing Ground Track for OFT-1 Mission

The OFT-1 trajectory differs from previous trajectories used by TASC to evaluate the Shuttle entry and landing navigation systems in two important respects - it is low latitude rather than polar and the reentry flight path is much steeper. The low latitude approach will avoid the large

atmospheric density modeling errors associated with polar regions. Such modeling errors can significantly affect drag update accuracy. On the other hand, the steeper flight path angle will yield higher vehicle acceleration which, in turn, will make navigation system performance more sensitive to error sources such as IMU misalignments and accelerometer scale factor errors.

The measurement schedule assumed for the OFT-1 mission is indicated in Table 4.1-1. Processing of the first drag update measurement occurs at an altitude of 282,000 ft when the vehicle deceleration has reached approximately 0.025g. Acquisition of TACAN at 145,000 ft ends the entry navigation phase and signals the start of preland navigation. Drag update measurements are processed down to 100,000 ft; the baro altimeter is switched on at an altitude of 85,000 ft. MLS acquisition occurs at 20,000 ft when the Shuttle is on the TAEM alignment cylinder and the range-to-go is approximately 51,000 ft. Through the entry and preland navigation phases the measurements are processed at 3.84 sec intervals.

The switch to the landing navigation phase ($t=T_{SW}$) occurs at 13,500 ft (approximately 12,000 ft above the Shuttle touchdown point), at which time the update interval is reduced to 1.92 sec. Finally, at an altitude of approximately 100 ft above the runway (near the runway threshold), the MLS elevation measurement is replaced by radar altimeter measurements at an update interval of 0.16 sec.

The antenna locations for the radio navigation aids are given in Table 4.1-2. The TACAN antenna is located 34,320 ft short of the nominal touchdown point on the runway center line. Location of the TACAN antenna on the Shuttle approach path rather than at the far end of the runway (as

TABLE 4.1-1
KEY EVENTS FOR OFT-1 MISSION

T-0489

NAVIGATION PHASE	EVENT	ELAPSED TIME (sec)	TIME TO TOUCHDOWN (sec)	ALTITUDE ABOVE GEOID (ft)	RELATIVE VELOCITY (fps)	RANGE-TO-GO (ft)
ENTRY NAVIGATION PHASE	Entry Interface, T_0	0.0	1630.1	398,837.	24295.	19,600,000.
	First Drag Measurement, T_{DRAG}	188.2	1441.9	282,174.	24399.	15,400,000.
PRELAND NAVIGATION PHASE	First TACAN Measurement, T_{TACAN}	1052.2	577.9	144,780.	7391.	1,425,000.
	Last Drag Measurement	1248.0	382.1	100,263.	3446.	479,000.
	First Baro Altimeter Measurement, T_{BA}	1309.4	320.7	84,257.	2447.	282,000.
	First MLS Azimuth, Elevation, & DME Measurements, T_{MLS} (No TACAN Measurement) (No Baro Altimeter)	1536.0	94.1	20,370.	662.	51,000.
LANDING NAVIGATION PHASE	Reduce Filter Dimension, T_{SW} Switch from 3.84 sec Update Cycle to 1.92 sec Update Cycle	1562.9	67.2	13,580.	622.	35,000.
	First Radar Altimeter Measurement, T_{RA} (No MLS Elevation Measurement) Switch from 1.92 sec Update Cycle to 0.16 sec Update Cycle	1622.4	7.7	2,387.	382.	2,700.
	Touchdown	1630.1	0.0	2,293.	315.	0.

TABLE 4.1-2
SENSOR LOCATIONS WITH RESPECT TO TOUCHDOWN POINT

SENSOR	DOWNRANGE (ft)	CROSSRANGE (ft)
TACAN	34,320	0
MLS Elevation	850	300
MLS Azimuth and DME	13,800	300

had been assumed in Ref. 3) should yield improved geometry during the TAEM alignment maneuver. The MLS antennas are offset 300 ft from the center line, approximately where they had been located in previous TASC studies.

4.2 NAVIGATION FILTER

The navigation filter for the entry through landing phases is the baseline filter specified in Ref. 45*. Before T_{SW} the filter is a variable dimension Kalman filter with up to 12 states. After T_{SW} it is a 6 state complementary filter. A schedule of filter states is presented in Fig. 4.2-1.

Implementation of the filter covariance equations is detailed in Refs. 1 and 3. The data base for the filter includes an initial covariance matrix and parameter values associated with each of the navigation sensors, including both the correlated error states and the measurement noise. The initial covariance matrix at initiation of the deorbit burn was provided by NASA (Ref. 47) and assumes that the most recent navigation fix and IMU alignment were two hours

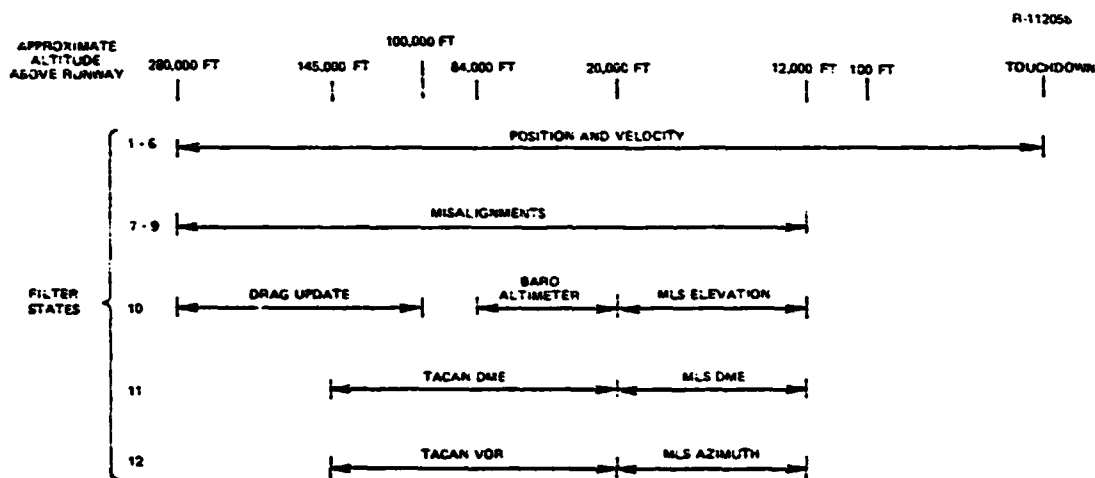


Figure 4.2-1 Schedule for Entry, Preland and Landing Phase Navigation Filter States

*The navigation filter has undergone a major redesign since this effort was completed. Navigation performance with the new filter will be evaluated in a subsequent report.

prior to deorbit. The covariance matrix is diagonal except for correlations between downrange and crossrange errors*. The remaining parameter values were also provided by NASA. The filter data base is summarized in Table 4.2-1.

Prior to the landing navigation phase the measurement matrices for all external navigation aids are of the form:

$$H_F = \begin{bmatrix} h_p & | & 0 & | & 0 & | & h_b \end{bmatrix} \quad (4.2-1)$$

where h_p is the 1x3 partial derivative of the measurement with respect to the nominal position and h_b is the partial

TABLE 4.2-1
FILTER STATE AND MEASUREMENT ERROR STATISTICS FOR
ENTRY AND PRELAND NAVIGATION FILTER

T-0267

Measurement	Correlated Error Filter State		Measurement Noise
	Standard Deviation	Correlation Time (sec)	Standard Deviation
Position	16,700 ft	∞	—
Velocity	18.7 fps	∞	—
Misalignments	4.4 mrad	∞	—
Drag-Altitude	9000 ft	120	5148 ft
Baro Altimeter	443 ft + 3.5% of altitude	60	60-750 ft (altitude dependent)
TACAN DME	524 ft	80	131 ft
TACAN VOR	29 mrad	20	14 mrad
MLS DME	80 ft	∞	26 ft
MLS Azimuth	0.96 mrad	∞	0.3 mrad
MLS Elevation	0.96 mrad	∞	0.3 mrad

*Downrange and radial navigation errors will be coupled due to the effect of orbital dynamics — a downrange velocity error at orbital perigee will generate a radial position error at orbital apogee, etc. The filter accounts for this effect by assuming -1 correlations between downrange velocity and vertical position and between downrange position and vertical velocity.

derivative with respect to the bias states. The drag update measurement is implemented as a pseudo-altitude measurement*. During landing navigation H_F is of the form:

$$H_F = \begin{bmatrix} h_p & 1 & 0 \end{bmatrix} \quad (4.2-2)$$

For all external navigation aids, the first three elements of H_F are identical to those of H_S in the truth model.

The gain computation algorithm in the Kalman filter mode (i.e., prior to T_{SW}) includes measurement underweighting in order to minimize the possibility of filter divergence:

$$K = PH^T \left[u_{70} HPH^T + R \right]^{-1} \quad (4.2-3)$$

where the measurement underweighting factor u_{70} is 1.2 when the rss (filter-indicated) position error is greater than 3280 ft and 1.0 otherwise. For the measurement schedule and filter parameter values used in this study, underweighting is switched off (u_{70} is set to unity) at approximately 49,000 ft.

In the complementary filter mode (i.e., after T_{SW}) the filter covariance is not computed and all gains are based upon pre-stored gain schedules. In this mode the MLS DME and radar altimeter gains are padloaded constants scaled by the update cycle, and the MLS azimuth and elevation gains are padloaded constants scaled by the update cycle and the range-to-go. The gains used for the study are summarized in Table 4.2-2 and are based on Ref. 45.

*In previous efforts the drag update measurement was implemented as a pseudo-drag measurement (Refs. 1 and 3). The measurement matrix H_F in that case included a partial derivative with respect to the nominal velocity, h_v , which was non-zero.

TABLE 4.2-2
LANDING NAVIGATION GAINS IN RUNWAY COORDINATES

T-0493

MEASUREMENT	POSITION GAINS*			VELOCITY GAINS*		
	R	DR	CR	R	DR	CR
MLS Azimuth	0	0	$0.2 R_{GO} \delta$	0	0	$0.02 R_{GO} \delta$
MLS Range	0	0.26	0	0	0.026	0
MLS Elevation	$0.1 R_{GO} \delta$	0	0	$0.01 R_{GO} \delta$	0	0
Radar Altimeter	1.56256	0	0	0	0	0

* R_{GO} is range-to-go. δ is measurement interval (1.92 sec for MLS measurements, 0.16 sec for the radar altimeter measurement).

The filter outlined above has been exercised over the trajectory and measurement schedule presented in Section 4.1. The time history of the filter-indicated performance between the deorbit burn and initiation of the landing phase is summarized in Table 4.2-3 in the form of rms values of position and velocity errors in the UVW coordinate frame (vertical, downrange, crossrange). The filter does not compute a performance measure (covariance) during the landing phase.

TABLE 4.2-3
FILTER-INDICATED PERFORMANCE

T-0494

EVENT	ELAPSED TIME (sec)	RMS POSITION ERROR (ft)			RMS VELOCITY ERROR (fps)		
		R	DR	CR	R	DR	CR
Initiation of Deorbit Burn	—	16700	16700	16700	18.7	18.7	18.7
Entry Interface	0.0	7016	35391	15942	28.6	6.7	19.7
First Drag Measurement	163.2	4633	36917	15628	29.9	3.8	19.9
	188.2 ⁺	3966	35639	15813	29.2	3.1	19.9
First Tacan Measurements	1029.1 ⁺	7959	27189	32753	35.9	34.9	79.8
	1052.2 ⁺	7847	12575	28088	25.5	26.0	73.7
First Baro Altimeter Measurement	1305.6 ⁺	6693	2275	4183	22.6	14.5	30.6
	1309.4 ⁺	3717	1553	4047	16.2	11.5	29.6
MLS Acquisition	1536.0 ⁻	828	964	459	10.7	8.4	5.6
	1536.0 ⁺	63	69	74	9.7	6.8	4.6
Initiation of Landing Navigation Phase	1562.9 ⁻	54	78	44	1.0	1.2	0.9

The filter-indicated performance down to the first TACAN measurement at 1052.2 sec is considerably worse than that determined in Ref. 3, primarily because the initial IMU misalignment and crossrange navigation uncertainties are much more severe than in the previous study. This pessimism relative to the previous study continues down to MLS acquisition because of larger uncertainties assumed for the TACAN and baro altimeter measurements. At the switch to landing navigation, the filter-indicated errors are approximately twice as large as those in Ref. 3.

4.3 ENTRY, PRELAND AND LANDING PHASE TRUTH MODEL

The "real world" environment in which the filter is evaluated is characterized by the truth model, i.e., a mathematical model of the various error sources which occur in the operational environment for the navigation system. The truth model for the entry phase is an extended version of the model first presented in Ref. 3. The truth model for the preland and landing phases is a modification of that detailed in Ref. 1.

4.3.1 Truth Model Definitions

The truth model for the entry phase consists of a total of 47 error states plus random errors associated with accelerometer quantization and the altitude pseudo-measurement. The error states are listed in Table 4.3-1 which groups them into four general categories:

- Filter states and measurement noises
- IMU-related states
- Gravity model errors
- Drag-related states

TABLE 4.3-1
ENTRY PHASE TRUTH MODEL STATES AND ERROR SOURCES

T-0495		
ERROR SOURCE	NUMBER OF STATES	NUMBER OF ERROR SOURCES
I. <u>FILTER STATES AND MEASUREMENT NOISES</u>		
1. Position Errors	3	3
Velocity Errors	3	3
Platform Misalignments	3	3
Correlated Measurement Errors		
Altitude	1	1
Uncorrelated Measurement Noise		
Altitude	—	1
INS Quantization Noise	—	3
II. <u>IMU ERRORS</u>		
Accelerometer		
2. Biases	3	3
3. Scale Factors	3	3
4. Asymmetries	3	3
5. Non-orthogonalities	3	3
Gyro		
7. Bias Drifts	3	3
8. Mass Unbalances	5	5
III. <u>GRAVITY MODEL ERRORS</u>		
6. Gravitational Deflections and Anomalies	3	3
IV. <u>NON-ESTIMATED, DRAG-RELATED STATES</u>		
21. Non-Standard Density		
1962 Standard Atmosphere Error	1	1
Time-Varying Bias	1	1
First-Order Markov	1	1
22. Non-Standard Wind		
Westerly (Time-Varying Bias)	1	1
Headwind (First-Order Markov)	1	1
Crosswind (Second-Order Markov)	2	2
Turbulence (First- and Second- Order Markovs)	5	5
23. Non-Standard Aerodynamics		
Time-Varying Bias	1	1
First-Order Markov	1	1
TOTALS	47	51

The principal differences between the entry phase truth model used in this study and that of Ref. 3 are improvements in the IMU error model and in the aerodynamics error model in the drag-related states. These changes are discussed in detail in Section 4.3.2 where the truth model data base is presented.

The truth model states and other error sources used to evaluate the Shuttle navigation system during the preland and landing phases are listed in Table 4.3-2, which also divides them into four categories:

- Filter states and measurement noises
- IMU-related states
- Gravity model errors
- External aid-related states

The last category includes the drag-related states of Table 4.3-1. In addition to the changes in the IMU and aerodynamics models cited above, the major modifications to the truth model for these phases involve a revision of the data base to reflect the best available sensor performance data, and the addition of radar altimeter terrain modeling errors for several additional runways.

4.3.2 Truth Model Data Base

This section presents the truth model data base for the entry through landing phases of the OFT-1 mission. A short discussion of the change to the aerodynamics error model is included.

Initial conditions at deorbit will be a function of the accuracy of the most recent navigation system update

TABLE 4.3-2
TRUTH MODEL STATES AND ERROR SOURCES FOR THE
PRELAND AND LANDING PHASES

T-0496		
ERROR SOURCE	NUMBER OF STATES	NUMBER OF ERROR SOURCES
I. FILTER STATES AND MEASUREMENT NOISES		
1. Position Errors	3	3
Velocity Errors	3	3
Platform Misalignments	3	3
Correlated Sensor Measurement Errors	7	7
Uncorrelated Measurement Noise		
Navigation Sensors	—	8
INS Quantization Noise	—	3
II. IMU ERRORS		
Accelerometer		
2. Biases	3	3
3. Scale Factors	3	3
4. Asymmetries	3	3
5. Non-orthogonalities	3	3
Gyro		
7. Bias Drifts	3	3
8. Mass Unbalances	5	5
III. GRAVITY MODEL ERRORS		
6. Gravitational Deflections and Anomalies	3	3
IV. NON-ESTIMATED, EXTERNAL AID-RELATED STATES		
10. TACAN Range Bias First-Order Markov	1	1
11. TACAN Range Scale Factor	1	1
12. Baro Altimeter Errors		
Bias	1	1
Scale Factor	1	1
First-Order Markov	1	1
Static Defect	1	1
13. MLS Scale Factor and Biases		
Range Bias	1	1
Range Scale Factor	1	1
Azimuth	1	1
Elevation	1	1
14. MLS Second-Order Markov		
Range	2	1
Azimuth	2	1
Elevation	2	1
15. Radar Altimeter Errors		
Bias	1	1
Terrain Modeling	1	1
Terrain Averaging	1	1
Antenna Pointing	1	1
Timing Delay	1	1
Receiver Noise	1	1
Fading	1	1
16. TACAN Survey Errors	6	6
17. MLS Survey Errors	6	6
19. TACAN Bearing Bias First-Order Markov	1	1
20. MLS Timing Bias	3	3
21, 22, 23 Drag-Related States (Table 4.3-1)	4	14
TOTALS	92	100

and of the subsequent open loop propagation. The initial covariance for the current study assumes an uploaded navigation fix and an IMU alignment via star tracker two hours prior to deorbit (Ref. 47). The resulting navigation errors at deorbit are primarily in-plane errors - 12,000 ft and 13 fps rss. The IMU misalignments are $285 \text{ } \widehat{\text{sec}}$ rms per axis, which accounts for both the star tracker errors and gyro drift during the two hour interval.

The IMU error model has been modified to be consistent with the IMU performance specification (Ref. 28). The IMU states are a subset of those defined for the IMU calibration and alignment analysis in Ref. 1. Gyro anisotropies, accelerometer nonlinearities, etc. have been ignored in this study because of their negligible effect on navigation errors (Refs. 1 and 3). Table 4.3-3 presents the truth model data base for the IMU-related error sources.

The major change to the drag-related error models is an improvement in the aerodynamics error model to reflect the relationship between drag coefficient errors and Shuttle

TABLE 4.3-3
TRUTH MODEL DATA BASE
FOR IMU-RELATED ERROR SOURCES

T-0499		
ERROR SOURCE	STANDARD DEVIATION	DATA SOURCE
1. INS Quantization Error	1.0 cm/sec	Ref. 28
2. Accelerometer Biases	50 μ g	Ref. 28
3. Accelerometer Scale Factors	100 ppm	Ref. 28
4. Accelerometer Asymmetries	100 ppm	Ref. 28
5. Accelerometer Nonorthogonalities	15 $\widehat{\text{sec}}$	Ref. 28
7. Gyro Bias Drifts	0.035 deg/hr	Ref. 28
8. Gyro Mass Unbalances	0.025 deg/hr/g	Ref. 28

control surface deflections. The C_D variation (Group 23), previously modeled as a stationary markov process, has been modeled as the markov process plus a time-varying bias term. This bias term is determined as a function of relative velocity, flight-path angle and control surface deflections.

The drag coefficient computational model used in the filter is a quadratic function of the computed angle of attack $\alpha_c(t)$:

$$C_{D_c}(\alpha_c) = C_0 + C_1\alpha_c + C_2\alpha_c^2 \quad (4.3-1)$$

where C_0 , C_1 and C_2 are constants. Aerodynamic data presented in Ref. 46 gives the true drag coefficient by:

$$\begin{aligned} C_D(\alpha, M, \delta_{BF}, \delta_{SB}, \delta_E) = & C_{D_{untr}}(\alpha, M, \delta_{BF}, \delta_{SB}, \delta_E) + \Delta C_{D_{BF}}(\alpha, M, \delta_{BF}) \\ & + \Delta C_{D_{SB}}(\alpha, M, \delta_{SB}) + \Delta C_{D_E}(\alpha, M, \delta_E) \end{aligned} \quad (4.3-2)$$

where

$\alpha(t)$ is the angle of attack,

$M(t)$ is the Mach number, and

$C_{D_{untr}}$ is the untrimmed drag coefficient,

$\Delta C_{D_{BF}}$, $\Delta C_{D_{SB}}$ and ΔC_{D_E} are the increments of the drag coefficient due to the body flap, speed brake and elevon settings, respectively,

$\delta_{BF}(t)$, $\delta_{SB}(t)$ and $\delta_E(t)$ are the body flap, speed brake and elevon deflections, respectively.

With the assumption that the error in $\alpha_c(t)$ is a negligible contributor to the error in $C_{D_c}(\alpha_c)$, the deviation of C_{D_c} from the true C_D for the OFT-1 mission is presented in Fig. 4.3-1.

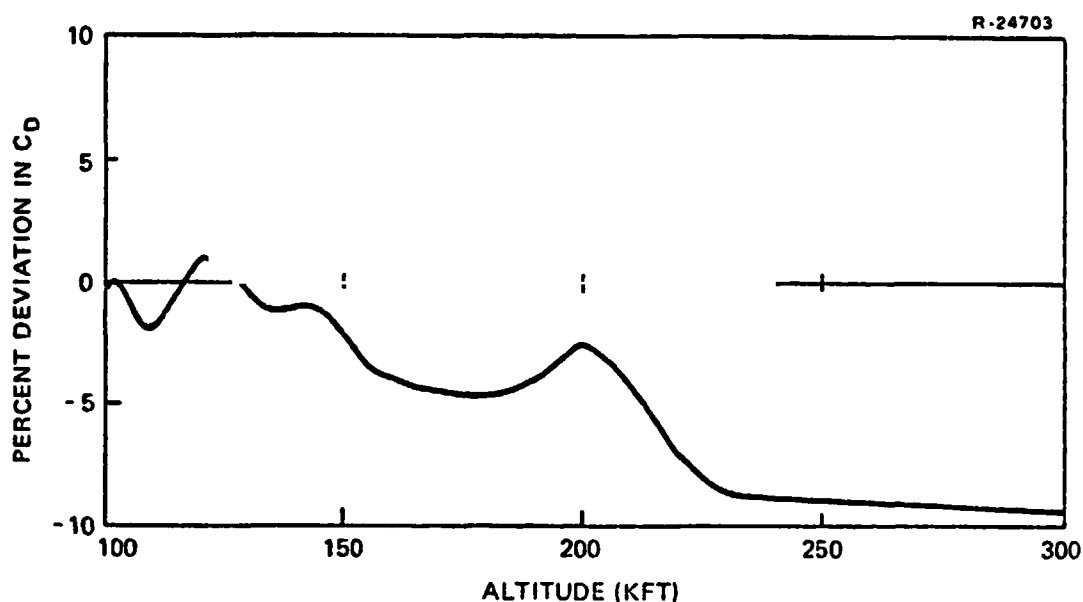


Figure 4.3-1 Deviation of Navigation Filter C_D
Model From True C_D

The greater deviations observed at high altitudes are a function of the poorer accuracy of C_{Dc} for the larger angles of attack used in the upper atmosphere. The range of this modeling error is 1.1% to -9.5%.

The Group 21 time-varying density bias which exhibits both latitude- and season-dependence, is shown in Figs. 4.3-2a and 4.3-2b respectively as percent deviations from the 1962 Standard Atmosphere. Dashed lines on the profiles denote the mean density deviations corresponding to the altitude-latitude profile for the OFT-1 mission. Because of the low inclination for OFT-1, this error is smaller at high altitudes than it would be for higher inclination orbits such as reference mission 3B (see Ref. 3). The remaining drag-related errors utilize the same data base presented in Ref. 3. Table 4.3-4 summarizes the parameter ranges for the drag-related error models (Group 1, Groups 21 through 23).

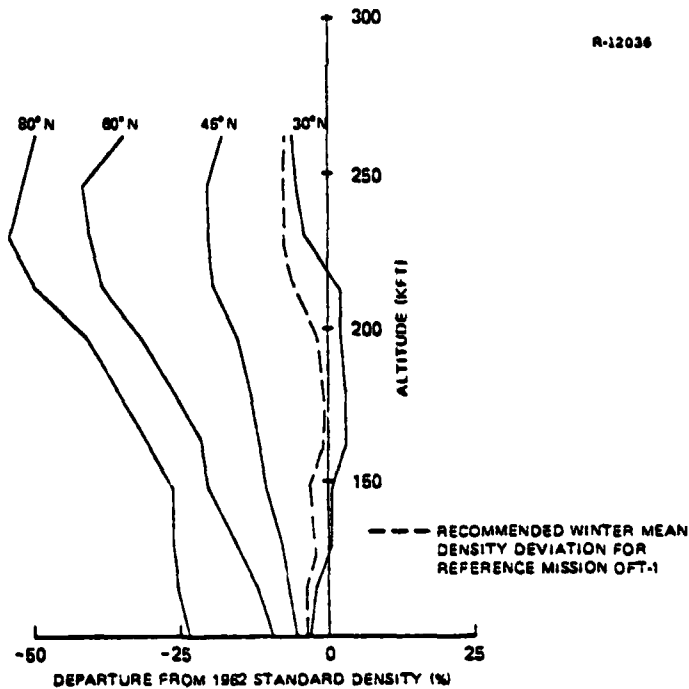


Figure 4.3-2a Time-Varying Density Bias for December - January Given as Percent Departure From 1962 Standard Atmosphere (Ref. 53)

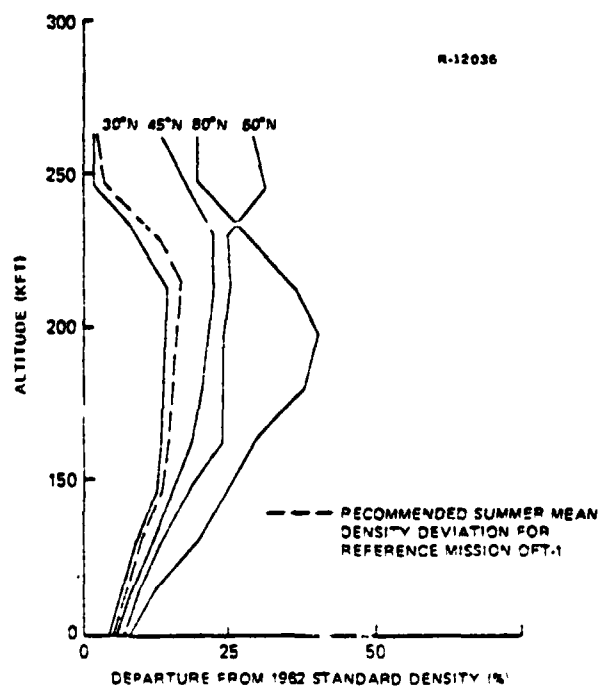


Figure 4.3-2b Time-Varying Density Bias for June - July Given as Percent Departure From 1962 Standard Atmosphere (Ref. 53)

TABLE 4.3-4
TRUTH MODEL DATA BASE
FOR DRAG-RELATED ERROR SOURCES

T-0497

ERROR SOURCE	STANDARD DEVIATION	CORRELATION TIME (Distance)	DATA SOURCE
1. Uncorrelated Altitude Pseudo-Measurement Noise	1250 ft	—	Ref. 3
21. Non-Standard Density 1962 Standard Atmosphere Error	0 - 21%	—	Ref. 3
Time-Varying Bias	0 - 17%	—	Fig. 4.3-2
First-Order Markov	2 - 6%	(14 - 270 nm)	Ref. 3
22. Non-Standard Wind			
Westerly (Time-Varying Bias)	0 - 295 fps	—	Ref. 3
Headwind (First-Order Markov)	40 - 110 fps	(270 nm)	Ref. 3
Crosswind (Second-Order Markov)	40 - 110 fps	(270 nm)	Ref. 3
Turbulence (First- and Second-Order Markovs)	13 fps	(1750 ft)	Ref. 3
23. C_D Variations			
Time-Varying Bias	0 - 9.5%	—	Fig. 4.3-1
First-Order Markov	5%	100 sec	Ref. 3

A detailed discussion of the radar altimeter error model can be found in Ref. 1. Terrain modeling errors for runways at Andersen Air Force Base, Guam, and Hickam Air Force Base, Hawaii, have been added to the radar altimeter-related truth model data base. Both of these locations are secondary landing sites for the Space Shuttle. Figure 4.3-3 shows the terrain modeling errors for both the north and south runways at Andersen, and for runways 8 and 26 at Hickam.

The truth model data base for the external aid-related error sources of Group 1 and Groups 10 through 20 is presented in Table 4.3-5. Although the state definitions are the same as developed in Refs. 1 and 3, many of the data base values have been revised to reflect more recent sensor performance data. The table contains applicable references for the data values selected.

The gravity model errors (Group 6), which have a negligible effect on system performance, have been ignored in this study.

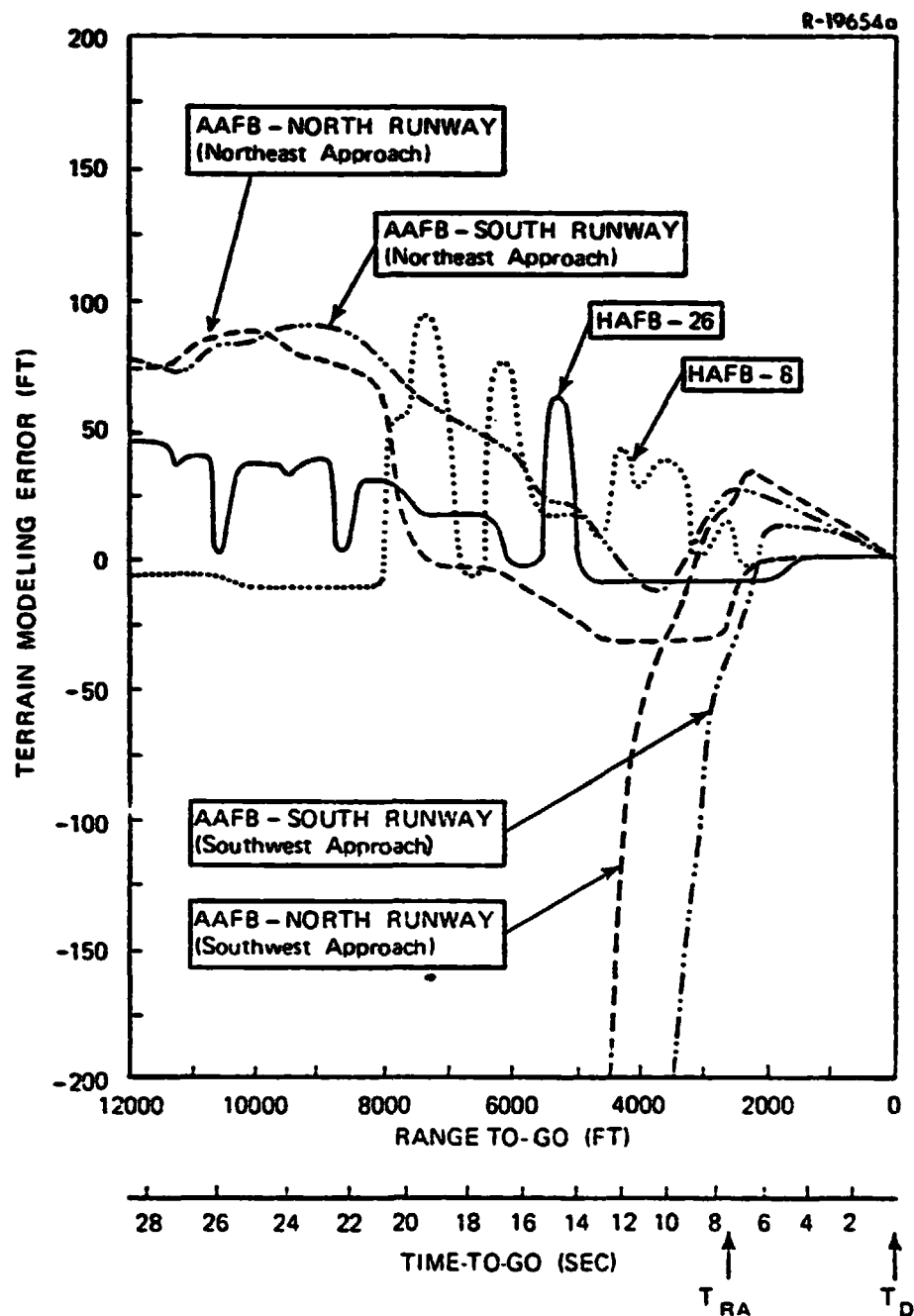


Figure 4.3-3 Terrain Modeling Error for Approach Paths to Secondary Space Shuttle Landing Sites

TABLE 4.3-5
TRUTH MODEL DATA BASE FOR EXTERNAL
AID-RELATED ERROR SOURCES

T-0498

ERROR SOURCE	STANDARD DEVIATION	TIME CONSTANT	DATA SOURCE
1. Uncorrelated Measurement Noise			
TACAN Range	100 ft	—	Ref. 49
TACAN Bearing	12 mrad	—	Refs. 49,35
Baro Altimeter	$0.24 e^{h/24170}$ ft	—	Ref. 33
MLS Azimuth	0.2 mrad	—	Ref. 34
MLS Elevation	0.1 mrad	—	Ref. 34
MLS Range	40 ft	—	Refs. 34,35
Radar Altimeter	0.9 ft	—	Ref. 1
10. TACAN Range Bias First-Order Markov	385 ft	300 sec	Ref. 49
11. TACAN Range Scale Factor	100 ppm	∞	Ref. 49
12. Baro Altimeter Errors			
Bias	100 ft	∞	Ref. 2
Scale Factor	3% of alt	∞	Ref. 2
Static Defect	1.52×10^{-4} ft/ft ² /sec ²	∞	Ref. 2
First-Order Markov	20 ft	100 sec	Ref. 2
13. MLS Scale Factor and Biases			
Range Bias	60 ft	∞	Ref. 34
Range Scale Factor	400 ppm	∞	Ref. 34
Azimuth	0.6 mrad	∞	Ref. 34
Elevation	0.4 mrad	∞	Ref. 34
14. MLS Second-Order Markovs			
Range	40 ft	4 sec	Refs. 34,35
Azimuth	0.3 mrad	4 sec	Ref. 34
Elevation	0.3 mrad	4 sec	Ref. 34
15. Radar Altimeter Errors			
Bias	1 ft	—	—
Terrain Modeling	< 150 ft*	—	Ref. 1
Terrain Averaging	< 25 ft*	—	Ref. 1
Antenna Pointing	< 7 ft*	—	Ref. 1
Timing Delay	< 0.5 ft*	—	Ref. 1
Receiver Noise	negligible	0.5 sec	Ref. 1
Fading	< 0.3 ft*	0.5 sec	Ref. 1
16. TACAN Survey Errors	1 ft	∞	—
17. MLS Survey Errors	1 ft	∞	—
19. TACAN Bearing Bias First-Order Markov	12 mrad	2×10^4 ft/V _R	Refs. 49,35
20. MLS Timing Bias	50 msec	∞	—

*Absolute range rather than standard deviation.

4.4 ENTRY, PRELAND AND LANDING NAVIGATION PERFORMANCE

This section presents detailed performance results for the Space Shuttle entry, preland and landing navigation system. Overall performance curves, showing the time histories of position and velocity errors due to all error sources combined, are given. "Baseline Error Budget" tables show the contributions of individual error sources, or small groups of error sources, at specific times, to position and velocity errors. These detailed error budgets have been computed at five significant time points:

- The end of the entry navigation phase ($t = T_{TACAN}$, Alt. = 145,000 ft)
- The initiation of MLS measurement processing ($t = T_{MLS}$, Alt. = 20,000 ft)
- The initiation of the landing navigation phase ($t = T_{SW}$, Alt. = 12,000 ft above the runway)
- The initiation of radar altimeter measurement processing ($t = T_{RA}$, Alt. = 100 ft above the runway)
- Touchdown ($t = T_D$).

Section 4.4.1 presents the results from entry down to 20,000 ft and Section 4.4.2 presents the results for altitudes below 20,000 ft.

4.4.1 Navigation System Performance: Entry to 20,000 ft

Figures 4.4-1a and 4.4.1b present overall performance curves for the entry phase and the initial portion of the preland phase of the OFT-1 mission. The curves show rms position and velocity errors due to the combined effects of

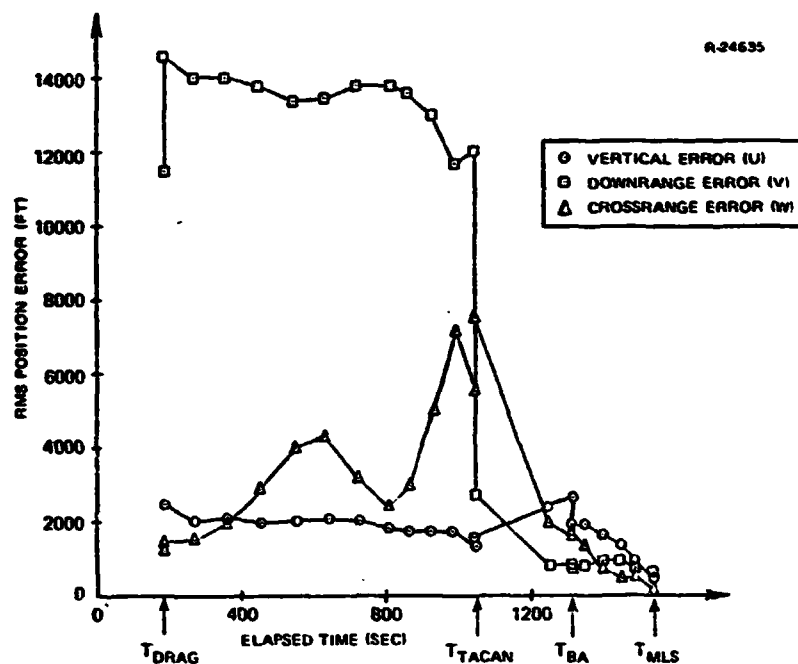


Figure 4.4-1a Overall Performance Down to 20,000 ft: Position

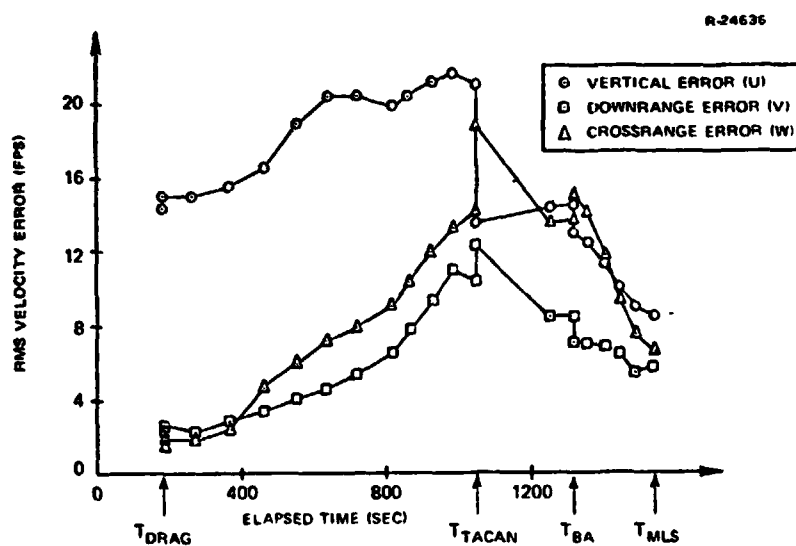


Figure 4.4-1b Overall Performance Down to 20,000 ft: Velocity

all error source groups in the truth model. They were generated by root-sum-squaring individual error source contributions at specified intervals (as tabulated in Appendix C).

The initial covariance for the entry filter is quite pessimistic relative to the truth model errors and this pessimism is reflected in the overall performance curves. The filter-indicated downrange error at T_{DRAG} is 35,600 ft rms vs 11,400 ft rms for the truth model. As a consequence, the filter overweights the first drag update measurement to yield a net increase in the downrange position error. A similar pessimism pervades crossrange position uncertainty and all three components of velocity, but the altitude pseudo-measurement does not contain sufficient information to attempt to improve these estimates.

After the initial transients, the drag update filter does an effective job of limiting downrange and radial position errors. The growth in the velocity errors (and in the crossrange position error) is attributable primarily to the large IMU misalignments, although the errors are not nearly as large as anticipated by the filter. The increase in the velocity errors at T_{TACAN} is disconcerting, but again it is attributable to the pessimistic filter-indicated performance. (At T_{TACAN} , the filter-indicated rms crossrange velocity error is 80 fps vs a truth model uncertainty of 14 fps.) Following T_{TACAN} , the navigation errors exhibit a general decreasing trend. At T_{BA} vertical position and velocity errors show sharp declines, reflecting the acquisition of the baro altimeter measurement. The processing of TACAN bearing measurements accounts for the large steady decrease in crossrange errors between T_{TACAN} and T_{MLS} .

To illustrate the effect that the drag update measurements have on the vertical position error, several truth

model runs without this "external aid" were made. Just prior to TACAN acquisition the total vertical position error for this no measurement case is approximately 4700 ft as compared to the 1436 ft observed when the drag measurements are employed. Clearly then, the processing of the drag altitude pseudo-measurements distinctly reduces vertical position errors.

System error covariances have been computed for each group of error sources down to the 20,000 ft altitude of the reference trajectory. Detailed error budgets showing rms position and velocity errors were generated at the end of the entry phase ($t = T_{\text{TACAN}}$, Alt. = 145,000 ft) and at 20,000 ft. Each entry in the error budgets is the rms contribution of the error source or sources indicated in the left-hand column. The entries in each column are root-sum-squared to obtain the total projected performance of the navigation filter. These performance values are compared with the Space Shuttle landing specifications (from Ref. 43) at the bottom of the error budget at 20,000 ft*. To focus attention to the major contributors in each column, every number whose magnitude is greater than 20% of the rms total for that column has been circled.

Table 4.4-1 presents the baseline error budget for the entry filter. The major contributors to navigation errors at 145,000 ft are:

- The initial condition errors (Group 1)
- The altitude pseudo-measurement noise (Group 1)
- The non-standard atmospheric density modeling error (Group 21)

*These landing specifications are guidelines, not inviolable requirements. The vertical velocity specification, in particular, may ultimately be relaxed.

TABLE 4.4-1
BASELINE ERROR BUDGET FOR THE ENTRY NAVIGATION PHASE

T-0501

ERROR SOURCE	VALUE	RMS NAVIGATION ERROR AT 145,000 ft					
		POSITION (ft)			VELOCITY (fps)		
		R	DR	CR	R	DR	CR
I. <u>FILTER STATES AND MEASUREMENT NOISE</u>							
Initial Condition Errors	Ref. 47	153.	10490.	3618.	16.57	2.78	2.00
Positions and Velocities	285 sec	635.	674.	2412.	5.63	5.03	13.50
Misalignments							
Uncorrelated Measurement Noise							
Altitude	1250 ft	476.	697.	306.	2.01	0.70	0.36
INS Quantization Noise	0.0328 fps	27.	160.	132.	0.55	0.47	0.13
II. <u>INU-RELATED STATES</u>							
Accelerometer Errors							
2. Biases	50 ug	320.	1906.	1633.	5.31	5.47	1.22
3. Scale Factors	100 ppm	6.	161.	53.	0.53	0.87	0.29
4. Asymmetries	100 ppm	45.	206.	80.	0.41	0.95	0.38
5. Nonorthogonalities	15 sec	31.	58.	19.	0.42	0.04	0.02
Gyro Errors							
7. Bias Drifts	0.035°/hr	105.	257.	428.	1.32	1.29	2.51
8. Mass Unbalances	0.025°/hr/g	6.	23.	25.	0.12	0.14	0.20
IV. <u>DRAG-RELATED STATES</u>							
21. Non-Standard Density							
1962 Standard Atmosphere	4-Term (<9%)	613.	4905.	2772.	6.46	5.50	1.25
Modeling Error	Ref. 3						
Time-Varying Bias	Winter (<8%)	142.	117.	246.	0.52	0.43	0.46
	Fig. 4.3-2a						
First-Order Markov	(<6%) Ref.3	177.	500.	303.	0.72	0.55	0.33
22. Non-Standard Wind							
Westerly	Winter	259.	9.	4.	0.72	0.20	0.04
	(<295 fps)						
	Ref. 3						
Crosswind	(<110 fps)	84.	89.	55.	0.28	0.12	0.06
Headwind	Ref. 3						
23. Non-Standard Aerodynamics							
Time-Varying Bias	(<9.5%)	865.	67.	796.	2.37	1.76	2.41
	Fig. 4.3-1						
First-Order Markov	5% of C _D	208.	438.	278.	0.77	0.51	0.31
Total Projected Performance		1436.	11805.	5516.	19.76	10.06	14.21

Except for vertical position and crossrange velocity, which are dominated by drag-related errors and initial misalignments respectively, each of the navigation errors is attributable to both initial condition and drag-related errors. This relative balance between initial conditions and drag-related errors suggests that the filter combines the altitude pseudo-measurements with inertial information in an effective

manner. However, filter parameter and gain variation studies would be required to prove this hypothesis.

The large error contributions of initial position and velocity uncertainties can be explained via a mechanism which couples these initial errors to the navigation errors at 145,000 ft (and later) through platform misalignments. The filter responds to the large initial position and velocity uncertainties by adjusting the misalignment estimates to account for a portion of these errors – thus, in effect, introducing an initial position- and velocity-generated misalignment. (This behavior can be observed in the appropriate table – Group 1 – in Appendix C by noting the immediate increase in platform tilt errors following the first drag update at $t = T_{\text{DRAG}}$.) In turn, the misalignments propagate via the system dynamics directly into position and velocity errors.

Of the IMU-related sources, only the accelerometer bias errors contribute significantly to vertical and down-range velocity errors. The minor role of IMU error sources in this study vis-a-vis Ref. 3 can be attributed to a difference in assumed initial conditions. In Ref. 3 the navigation system had been operating in the pure inertial mode since launch. Hence, the majority of the navigation errors at deorbit were directly attributable to IMU error sources. By contrast, the present study assumes a navigation fix and IMU alignment two hours prior to deorbit. This eliminates all IMU contributions to deorbit navigation errors except those which can accrue (accelerometer bias, gyro bias drift) during the ensuing two hour orbital coast.

Table 4.4-2 lists the contributions of alternative error source models (e.g., season-dependent atmospheric density error models for the summer instead of the winter profile).

TABLE 4.4-2
ALTERNATIVE CONTRIBUTIONS FOR THE ENTRY NAVIGATION PHASE

T-0502

ERROR SOURCE	VALUE	RMS NAVIGATION ERROR AT 145,000 ft					
		POSITION (ft)			VELOCITY (fps)		
		R	DR	CR	R	DR	CR
21. Non-Standard Density							
1962 Standard Atmosphere Modeling Error	1-Term(<21%) Ref. 3	3813.	2830.	3076.	7.54	2.00	5.26
Time-Varying Bias	Summer(<16%) Fig. 4.3-2b	938.	572.	77.	2.04	0.65	0.95
22. Non-Standard Wind							
Westerly	Summer (<200 fps) Ref. 3	137.	129.	41.	0.25	0.02	0.06

The 1-term density modeling error is seen to be potentially a much greater contributor to vertical position error than the 4-term model because of the larger uncertainties (20% vs 5%) associated with the 1-term atmospheric density model near 145,000 ft. For the filter evaluated in this study, the vertical position error would more than triple with the 1-term model. This performance sensitivity underscores the need for an accurate onboard atmospheric density model for drag updating.

Table 4.4-3 presents the baseline error budget for the navigation filter at 20,000 ft. The major contributors to navigation errors are:

- The initial condition errors (Group 1)
- The TACAN range bias error (Group 10)
- The TACAN bearing bias error (Group 19)
- The baro altimeter bias, scale factor and static defect errors (Group 12).

TABLE 4.4-3
BASELINE ERROR BUDGET AT 20,000 FT

T-0503

1-0303

ERROR SOURCE	VALUE	RMS NAVIGATION ERROR AT 20,000 ft					
		POSITION (ft)			VELOCITY (fps)		
		R	DR	CR	R	DR	CR
I. FILTER STATES AND MEASUREMENT NOISE							
Initial Conditions	Ref. 47	179.6	431.5	90.2	5.28	3.86	4.51
Positions and Velocities	285 sec	55.3	49.9	64.7	3.88	2.23	3.70
Misalignments							
Uncorrelated Measurement Noise							
TACAN Range	100 ft	132.2	110.5	33.6	0.99	0.63	0.30
TACAN Bearing	12 mrad	68.3	122.9	83.5	0.45	0.54	0.60
Baro Altimeter	0.24 e ^b /24018 ft	0.3	0.2	0.1	0.00	0.00	0.00
INS Quantization Noise	0.0328 fps	5.8	9.4	1.9	0.21	0.14	0.12
II. INU-RELATED STATES							
Accelerometer							
2. Biases	50 μ g	75.8	127.9	20.0	1.92	1.78	0.86
3. Scale Factors	100 ppm	23.8	52.5	10.3	0.35	0.67	0.46
4. Asymmetries	100 ppm	25.7	56.4	10.8	0.26	0.76	0.45
5. Nonorthogonalities	15 sec	8.0	21.6	2.7	0.26	0.40	0.17
Gyro							
7. Bias Drifts	0.035°/hr	15.7	20.9	13.0	0.95	0.65	0.82
8. Mass Unbalances	0.025°/hr/g	2.9	5.4	1.9	0.17	0.16	0.13
IV. EXTERNAL AID-RELATED STATES							
10. TACAN Range Bias	385 ft	244.1	365.1	114.1	2.57	2.54	2.72
11. TACAN Range Scale Factor	100 ppm	7.0	9.8	0.1	0.22	0.32	0.01
12. Baro Altimeter Errors							
Bias	100 ft						
Scale Factor	3%	319.9	284.0	59.1	4.00	0.91	0.44
Static Defect	1.52 $\times 10^{-4}$ ft/ft ² /sec ²						
First-Order Markov	20 ft	10.0	8.0	3.1	0.08	0.05	0.03
16. TACAN Survey Errors	1 ft	0.7	1.0	1.0	0.01	0.00	0.01
19. TACAN Bearing Bias	12 mrad	142.0	184.4	192.1	1.16	1.07	1.16
1., 21., 22., 23. Drag-Related Errors	Table 4.4-1	6.5	16.6	5.7	0.60	0.31	0.29
Total Projected Performance		497.1	698.4	273.4	8.57	5.83	6.73
Touchdown Specifications		3.0	80.0	4.7	0.20	3.00	2.00

Note that the large initial condition errors continue to be major contributors to the velocity errors. The TACAN range and bearing bias errors are principal contributors to all components of position error, and the range bias is also a contributor to all components of the velocity error. The baro altimeter errors contribute significantly to position errors and to the vertical velocity error. Additionally, TACAN range and TACAN bearing measurement noises show large effects in the vertical and crossrange position errors, respectively. Accelerometer bias errors continue to propagate into significant vertical and downrange velocity errors.

The Shuttle is approximately midway through its TAEM alignment maneuver at 20,000 ft. TACAN range and bearing information collected prior to the initiation of the maneuver becomes crossrange and downrange information, respectively, when the Shuttle is at or beyond the 20,000 ft mark because of the right angle turn. This accounts for the contribution of the TACAN range bias to crossrange errors, etc. The large contributions of the TACAN range bias to vertical channel errors, and the baro altimeter errors to downrange channel errors can be attributed to the high correlations which exist between the vertical and downrange channels (at deorbit, vertical and downrange errors are perfectly correlated).

Appendix C contains detailed computer printouts of all error contribution time histories corresponding to Tables 4.4-1 through 4.4-3.

4.4.2 Navigation System Performance: 20,000 ft to Touchdown

Figures 4.4-2a and 4.4-2b present overall performance curves from 20,000 ft to touchdown. At T_{MLS} there are large decreases in all three error components, reflecting the high accuracy of the MLS measurements as compared to TACAN and baro altimeter measurements. Subsequent to T_{MLS} the position errors become essentially the navigation accuracy of MLS. The initial radar altimeter measurement results in an increase in vertical position error due to the large terrain modeling error for Vandenberg AFB, as was also observed in the Ref. 1 study.

All components of the velocity error decrease with MLS measurement processing until the switch to the complementary filter at T_{SW} . The downrange velocity error

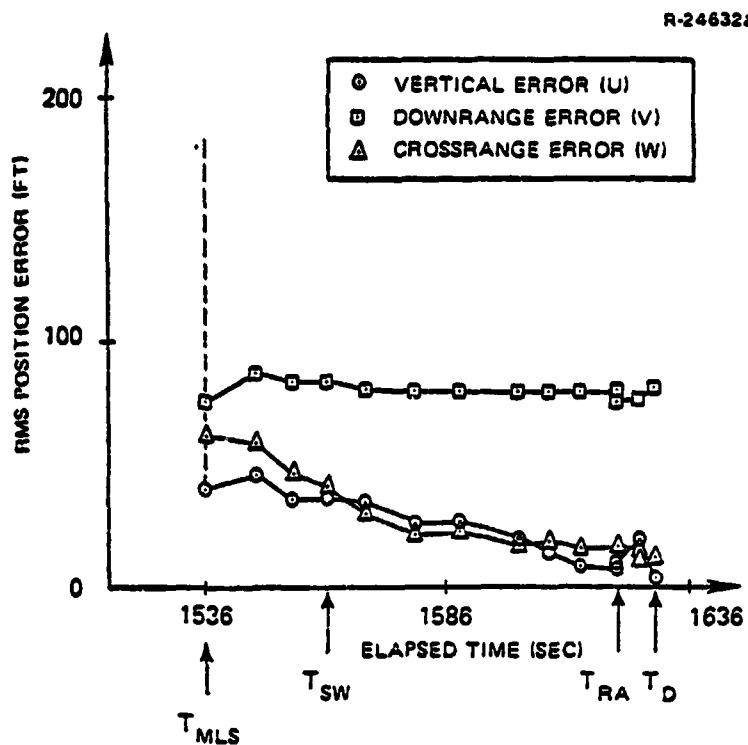


Figure 4.4-2a Overall Performance from 20,000 ft to Touchdown: Position

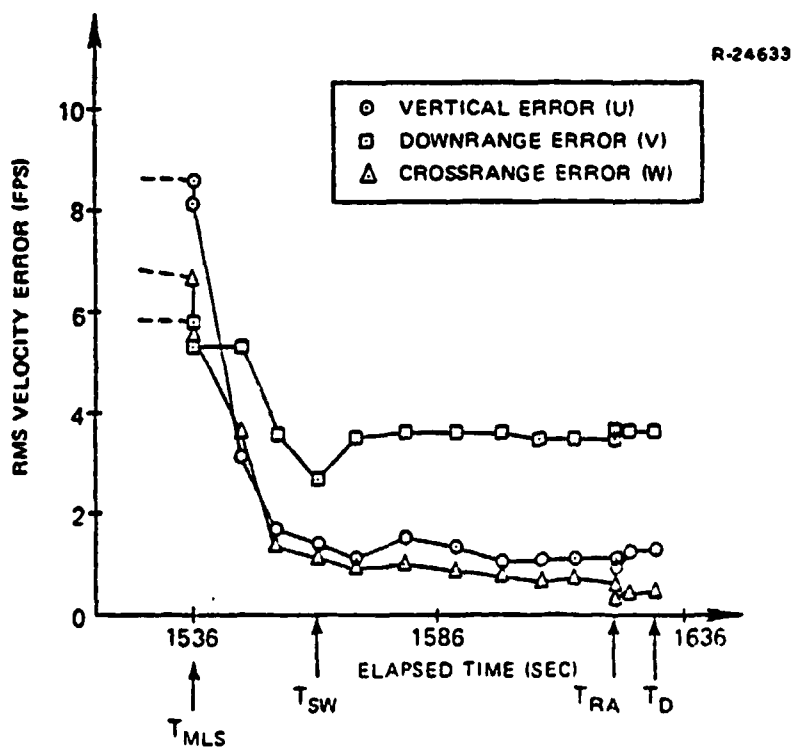


Figure 4.4-2b Overall Performance from 20,000 ft to Touchdown: Velocity

REPRODUCIBILITY OF THE
ORIGINAL PAGE IS POOR

increases after T_{SW} due to the effects of the MLS range second-order markov error. The unstable growth in vertical velocity error at T_{RA} observed in Ref. 1 does not occur here since the vertical channel is not coupled with the downrange or crossrange channels via the MLS gains and since there are no vertical velocity updates after T_{RA} (see Table 4.2-2). Hence neither MLS range errors nor the increase in the vertical position error due to the terrain modeling error drive the velocity errors up. Subsequent to T_{RA} there is a slight increase in the vertical velocity component due to IMU misalignments.

Table 4.4-4 is the baseline error budget at T_{SW} . The major contributors to navigation errors are:

- The MLS azimuth and DME measurement noises (Group 1)
- The MLS scale factors and biases (Group 13)
- The MLS second-order markovs (Group 14)
- The MLS timing biases (Group 20).

The significance of MLS measurements to the filter is clearly evident by the fact that nearly all the major contributors are MLS-related. The MLS azimuth error sources dominate both position and velocity crossrange errors, as do the MLS range error sources in the downrange channel. The steepness of the descent path, approximately a 20-24 deg glide slope, causes the downrange error sources (MLS range errors) to contribute large vertical channel errors. These MLS range-related error sources along with MLS elevation-related errors dominate the vertical channel errors.

The MLS second-order markov errors (Group 14) show particularly large effects on the velocity errors. These

THE ANALYTIC SCIENCES CORPORATION

TABLE 4.4-4
BASELINE ERROR BUDGET AT T_{SW}

T-0504

ERROR SOURCE		VALUE	RMS NAVIGATION ERROR AT 13,580 ft					
			POSITION (ft)			VELOCITY (fps)		
			R	DR	CR	R	DR	CR
I. FILTER STATES AND MEASUREMENT NOISE								
Initial Conditions								
Positions and Velocities		Ref. 47	1.2	0.6	1.3	0.09	0.34	0.19
Misalignments		285 sec	2.8	4.8	7.4	0.18	0.18	0.27
Uncorrelated Measurement Noise								
TACAN Range		100 ft	0.5	0.7	0.4	0.00	0.01	0.01
TACAN Bearing		12 mrad	0.3	1.3	1.4	0.01	0.01	0.02
Baro Altimeter		0.24 e ^h /24170 ft	0.0	0.0	0.0	0.00	0.00	0.00
MLS Azimuth		0.2 mrad	1.0	3.8	8.0	0.03	0.03	0.45
MLS Elevation		0.1 mrad	2.9	0.7	0.2	0.18	0.05	0.01
MLS DME		40 ft	11.6	25.7	2.7	0.64	1.76	0.08
INS Quantization Noise		0.0328 fps	0.1	0.1	0.2	0.01	0.01	0.01
II. IMU-RELATED STATES								
Accelerometer								
2. Biases		50 ug	6.8	1.7	3.1	0.05	0.07	0.15
3. Scale Factors		100 ppm	0.1	0.2	0.5	0.03	0.05	0.01
4. Asymmetries		100 ppm	0.2	0.2	0.6	0.03	0.05	0.02
5. Nonorthogonalities		15 sec	0.2	0.3	0.7	0.04	0.01	0.03
Gyro								
7. Bias Drifts		0.035°/hr	0.8	1.4	1.9	0.08	0.05	0.08
8. Mass Unbalances		0.025°/hr/g	0.2	0.3	0.4	0.02	0.01	0.02
IV. EXTERNAL AID-RELATED STATES								
10. TACAN Range Bias		385 ft	5.5	8.6	7.3	0.10	0.05	0.17
11. TACAN Range Scale Factor		100 ppm	0.2	0.4	0.6	0.02	0.00	0.01
12. Baro Altimeter Errors								
Bias		100 ft						
Scale Factor		3% of alt.						
Static Defect		1.52 x 10 ⁻⁴ ft/ft ² /sec ²	0.7	7.5	4.5	0.38	0.13	0.05
First-Order Markov		20 ft	0.0	0.0	0.0	0.00	0.00	0.00
13. MLS Scale Factor and Biases								
Range Bias		60 ft	18.2	55.1	0.1	0.05	0.04	0.13
Range Scale Factor		400 ppm	5.6	17.3	0.1	0.10	0.21	0.06
Azimuth Bias		0.6 mrad	0.3	0.8	25.7	0.06	0.08	6.30
Elevation Bias		0.4 mrad	13.5	3.6	0.4	0.23	0.09	0.02
14. MLS Second-Order Markovs								
Range		40 ft	16.6	38.4	3.2	0.90	2.12	0.09
Azimuth		0.3 mrad	2.0	6.5	16.1	0.06	0.05	0.87
Elevation		0.3 mrad	13.1	3.0	1.0	0.78	0.24	0.04
17. MLS Survey Errors		1 ft	1.0	0.2	1.0	0.00	0.00	0.00
19. TACAN Bearing Bias		12 mrad	0.5	2.8	2.3	0.02	0.03	0.03
20. MLS Timing Bias								
Range		50 msec	9.9	29.2	0.0	0.03	0.10	0.06
Azimuth		50 msec	0.9	1.2	4.3	0.05	0.05	0.65
Elevation		50 msec	2.0	0.5	0.1	0.03	0.02	0.00
Total Projected Performance			37.0	81.4	37.9	1.46	2.81	1.30
Touchdown Specifications			3.0	80.0	4.7	0.20	3.00	2.00

error sources are primarily due to multipath effects, but little data on the magnitudes or frequency characteristics for multipath is available. Such large velocity error contributions due to multipath effects suggest that an improved error model based on more extensive test data is necessary to accurately assess landing navigation performance.

The IMU misalignments, which have been major contributors all through the higher altitudes, are lesser contributors at T_{SW} . The baro altimeter continues to be a major contributor to vertical velocity, and the TACAN range bias still makes considerable contributions to position errors.

Several error sources found in the past (Ref. 1) to be minor contributors to navigation errors at this and lower altitudes have been ignored in Table 4.4-4 and all subsequent baseline error budgets. These include the drag-related errors and the TACAN survey errors.

Table 4.4-5 presents the baseline error budget at 100 ft above the runway touchdown point, just prior to the first radar altimeter measurement. The major error contributors are:

- The initial conditions (Group 1)
- MLS errors and measurement noises (Groups 1, 13, 14 and 20)
- Baro altimeter errors (Group 12).

After T_{SW} , with the suboptimal gain structure of the complementary filter, the misalignment terms experience a marked increase in importance. The initial position and velocity errors show an increased error contribution after T_{SW} through their coupling with the misalignments via the

THE ANALYTIC SCIENCES CORPORATION

TABLE 4.4-5
BASELINE ERROR BUDGET AT 100 FT ABOVE RUNWAY

T-0505

ERROR SOURCE	VALUE	RMS NAVIGATION ERROR AT 100 ft					
		POSITION (ft)			VELOCITY (fps)		
		R	DR	CR	R	DR	CR
I. <u>FILTER STATES AND MEASUREMENT NOISE</u>							
Initial Conditions							
Positions and Velocities	Ref. 47	(3.5)	2.3	1.0	(0.34)	0.36	(0.32)
Misalignments	285 sec	(2.5)	5.2	(2.6)	(0.31)	0.25	(0.22)
Uncorrelated Measurement Noise							
TACAN Range	100 ft	0.0	0.7	0.2	0.01	0.00	0.01
TACAN Bearing	12 mrad	0.0	1.4	0.5	0.01	0.00	0.01
Baro Altimeter	h/24170	0.0	0.0	0.0	0.00	0.00	0.00
MLS Azimuth	0.24 e ft	0.1	4.2	2.4	0.04	0.01	(0.19)
MLS Elevation	0.1 mrad	0.4	0.2	0.1	0.04	0.01	0.00
MLS DME	40 ft	(1.8)	(25.1)	1.0	0.20	(1.97)	0.04
INS Quantization Noise	0.0328 fps	0.3	0.2	0.1	0.03	0.03	0.01
II. <u>IMU-RELATED STATES</u>							
Accelerometer							
2. Biases	50 ug	1.2	1.7	1.3	0.12	0.12	0.09
3. Scale Factors	100 ppm	0.4	0.1	0.4	0.05	0.06	0.03
4. Asymmetries	100 ppm	0.4	0.3	0.4	0.05	0.06	0.03
5. Nonorthogonalities	15 sec	0.2	0.5	0.3	0.03	0.00	0.02
Gyro							
7. Bias Drifts	0.035°/hr	0.9	1.7	0.6	0.10	0.08	0.07
8. Mass Unbalances	0.025°/hr/g	0.1	0.4	0.1	0.02	0.01	0.02
IV. <u>EXTERNAL-AID RELATED STATES</u>							
10. TACAN Range Bias	385 ft	0.3	10.2	(2.8)	0.15	0.04	0.08
11. TACAN Range Scale Factor	100 ppm	0.1	0.6	0.3	0.02	0.01	0.00
12. Baro Altimeter Errors							
Bias	100 ft						
Scale Factor	3% of alt.	(4.1)	10.3	1.6	(0.52)	0.39	0.04
Static Defect	1.52 x 10 ⁻⁴ ft/ft ² /sec ²						
20 ft		0.0	0.0	0.0	0.00	0.00	0.00
13. First-Order Markov							
MLS Scale Factor and Biases							
Range Bias	60 ft	0.8	(57.7)	1.3	(0.48)	0.03	0.02
Range Scale Factor	400 ppm	0.5	5.2	0.2	0.08	0.18	0.00
Azimuth Bias	0.6 mrad	0.1	0.7	(8.7)	0.03	0.01	(0.27)
Elevation Bias	0.4 mrad	1.1	0.2	0.1	0.20	0.03	0.00
14. MLS Second-Order Markovs							
Range	40 ft	(3.8)	(42.4)	1.3	(0.41)	(2.96)	0.06
Azimuth	0.3 mrad	0.2	7.3	(6.1)	0.08	0.02	(0.45)
Elevation	0.3 mrad	(2.5)	0.7	0.4	(0.23)	0.05	0.01
17. MLS Survey Errors	1 ft	1.0	0.0	1.0	0.01	0.00	0.00
19. TACAN Bearing Bias	12 mrad	0.1	3.2	0.9	0.02	0.00	0.02
20. MLS Timing Bias							
range	50 msec	0.5	(19.1)	0.5	0.20	0.31	0.00
Azimuth	50 msec	0.1	2.0	0.9	(0.04)	0.01	0.00
Elevation	50 msec	1.1	0.0	0.0	(0.31)	0.03	0.00
Total Projected Performance		8.2	80.5	12.2	1.11	3.63	0.70
Touchdown Specifications		3.0	80.0	4.7	0.20	3.00	2.00

mechanism described in Section 4.4.1. The dominant velocity error contributors continue to be the MLS second-order markov errors. In particular, the 40 ft error of the range second-order markov couples directly into velocity errors.

The MLS range and azimuth measurement noises and range and azimuth biases affect the downrange and crossrange error components about as expected. Even though the downrange velocity error grows following T_{SW} , the suboptimal filter appears to select reasonable MLS gains in the downrange and crossrange channels. In the vertical channel, however, the baro altimeter errors contribute at least as much as the MLS errors. In addition, MLS range errors remain important contributors to vertical velocity even though the final approach following the flare maneuver is made with a low (1-3 deg) glide slope. This behavior suggests that the complementary filter underweights the MLS elevation measurement.

The baseline error budget at touchdown is given in Table 4.4-6. The error in vertical position slightly exceeds the touchdown specification - with nearly all of the vertical position error due to the terrain modeling error for Vandenberg's runway 30 (other landing sites are discussed later). The downrange position error is nominally equal to the touchdown specification, and the crossrange position error is approximately twice the specification - both totals primarily due to MLS error sources. The MLS biases and second-order markovs are again the dominant error sources in the downrange and crossrange channels.

The vertical velocity error exceeds the touchdown specification; however, it is significantly smaller than that observed in Ref. 1. Since the radar altimeter measurement is

TABLE 4.4-6
BASELINE ERROR BUDGET — TOUCHDOWN

T-0506

ERROR SOURCE	VALUE	RMS NAVIGATION ERROR AT TOUCHDOWN					
		POSITION (ft)			VELOCITY (fps)		
		R	DR	CR	R	DR	CR
I. Initial Conditions							
Positions and Velocities	Ref. 47	0.1	2.2	1.1	0.58	0.37	0.33
Misalignments	285 sec	0.0	5.2	(2.1)	(0.48)	0.26	(0.22)
Uncorrelated Noise							
Radar Altimeter	0.9 ft	0.3	0.0	0.0	0.00	0.00	0.00
MLS Azimuth	0.2 mrad	0.0	4.2	2.0	0.04	0.01	0.02
MLS Elevation	0.1 mrad	0.0	0.2	0.1	0.04	0.01	0.00
MLS DME	40 ft	0.0	(25.1)	0.9	0.21	(1.97)	0.00
RSS for Other External Navigation Aids		0.0	1.6	0.5	0.05	0.03	0.02
II. INU-Related States	Table 4.4-5	0.0	2.5	1.4	(0.29)	0.17	0.12
IV. External Aid-Related States							
13. MLS Scale Factor and Biases							
Azimuth Bias	0.6 mrad	0.0	0.7	(7.2)	0.03	0.01	(0.24)
Elevation Bias	0.4 mrad	0.0	0.2	0.1	0.21	0.02	0.00
Range Bias	60 ft	0.0	(57.6)	1.4	(0.48)	0.01	0.03
Range Scale Factor	400 ppm	0.0	4.2	0.3	0.09	0.16	0.00
14. MLS Second-Order Markov							
Azimuth	0.3 mrad	0.0	7.3	(5.3)	0.09	0.02	(0.39)
Elevation	0.3 mrad	0.0	0.7	0.4	0.02	0.04	0.01
Range	40 ft	0.0	(44.4)	1.2	(0.43)	(3.07)	0.06
15. Radar Altimeter Errors							
Bias	1 ft	(1.0)	0.0	0.0	0.00	0.00	0.00
Terrain Modeling Error (VAFB-30)	Ref. 1	(3.7)	0.0	0.0	0.00	0.00	0.00
All Instrument and Other Errors	Ref. 1	0.0	0.0	0.0	0.00	0.00	0.00
10.-12., 17.-20. RMS for Other External Navigation Aids	Table 4.4-5	0.1	(22.2)	(3.0)	(0.88)	0.59	0.09
Total Projected Performance		3.8	80.6	10.3	1.42	3.73	0.65
Touchdown Specifications		3.0	80.0	4.7	0.20	3.00	2.00

not used to update vertical velocity, and MLS does not update the vertical channel after the MLS elevation measurement is lost, the vertical velocity errors show a slight increasing trend after T_{RA} . On the other hand, these same factors prevent the excessive increase in vertical velocity error after T_{RA} as observed in Ref. 1. That is to say, the large vertical position error due to terrain modeling errors at T_{RA} does not propagate into large velocity errors in any channel.

The downrange velocity error exceeds the touchdown specification slightly. The dominant error source is the MLS range second-order markov, which again underlines the need for a better understanding of the frequency and magnitude of this error source and may warrant an investigation of techniques for minimizing its effects. The crossrange velocity is within the touchdown specification. The major contributors to this error are the MLS azimuth bias and second-order markov, and the initial conditions.

The terrain modeling error included in Table 4.4-6 is for runway 30 at Vandenberg AFB. The contributions of the terrain modeling errors to vertical position errors for the other primary landing sites and for the secondary sites at Andersen AFB and Hickam AFB are presented in Table 4.4-7. Only Vandenberg's runway 30 and Andersen's North runway (southwest approach) yield vertical position errors at touchdown which exceed the runway specification.

TABLE 4.4-7
CONTRIBUTION OF TERRAIN MODELING ERROR
TO VERTICAL POSITION ERROR AT TOUCHDOWN

T-0535

LANDING SITE	RMS VERTICAL POSITION ERROR AT TOUCHDOWN (ft)	LANDING SITE	RMS VERTICAL POSITION ERROR AT TOUCHDOWN (ft)
<u>Edwards AFB</u>		<u>Andersen AFB</u>	
Runway: 4	0.4	North Runway:	
17	0.0	NE Approach	0.5
22	0.0	SW Approach	3.1
35	0.9	South Runway:	
<u>Kennedy Space Center</u>		NE Approach	2.6
Runway: 15	1.0	SW Approach	2.0
33	0.0		
<u>Vandenberg AFB</u>		<u>Hickam AFB</u>	
Runway: 12	2.1	Runway: 8	0.0
30	3.7	26	0.0

Appendix D contains detailed computer printouts of all error contribution time histories corresponding to Tables 4.4-4 through 4.4-7. Of note are the large misalignments observed in the tables for Group 1 (initial positions and velocities, and misalignments), Group 2 (accelerometer biases), Group 7 (gyro bias drifts) and Group 12 (baro altimeter bias, scale factor and static defect). These errors are transients due to the filter's attempt to estimate platform misalignments based on a combination of MLS measurements and the assumed correlations between the misalignments and velocity errors at 20,000 ft. In order to demonstrate that these errors are in fact transients, a partial error budget was generated using a 12 state Kalman filter down to the runway threshold. The filter substantially reduced the misalignments between the baseline T_{SW} (alt=12,000 ft) and the runway threshold. Elimination of some of the filter difficulties discussed in Section 4.4.1, such as an overly pessimistic filter covariance above 20,000 ft, should improve the filter-predicted correlations between velocity errors and misalignments and thus reduce the transients.

In summary, the navigation filter performs reasonably well down to touchdown. The transition from a Kalman to a complementary filter is made without significant transients in the estimates, and the fixed MLS and radar altimeter gains maintain reasonable navigation accuracy. The only significant departure from the touchdown specification is in vertical velocity, although downrange velocity and all three components of position are also out-of-spec. There is evidence to suggest that the velocity estimates at touchdown and the vertical position performance prior to the first radar altimeter measurement could be improved with a more judicious choice of complementary filter gains, but it is doubtful that the vertical velocity specification could be met.

4.5 ENTRY, PRELAND AND LANDING SENSITIVITY ANALYSIS

This section contains several curves indicating the sensitivity of navigation system performance to variations in truth model error source statistics (while holding filter parameters fixed) for the entry, preland and landing navigation phases. These "fixed filter" sensitivity curves illustrate the effect of an unknown variation in the rms value of an error source or group of error sources.

The baseline error budget for the entry navigation phase, Table 4.4-1, indicates that the initial condition errors dominate the vertical and crossrange velocity errors. Figure 4.5-1 presents vertical velocity error sensitivity at 145,000 ft to initial position and velocity errors; Fig. 4.5-2, the crossrange velocity error sensitivity to initial misalignment errors. An increase in the initial condition errors in either case results in substantial increases in the velocity errors — a factor of two worsening of initial condition errors would result in at least a 67% increase in the vertical velocity error and a 100% increase in crossrange velocity error. Halving the initial position and velocity uncertainty would yield only a 29% improvement in vertical velocity error. However, similarly reducing the initial misalignment uncertainty (to 140 $\widehat{\text{sec}}$) would yield a nearly 40% improvement in the crossrange velocity.

At 20,000 ft the vertical velocity channel is dominated by initial condition errors and the baro altimeter bias, scale factor and static defect errors. The sensitivity of this error to the baro altimeter errors is presented in Fig. 4.5-3. Because of the presence of other major error sources, the effects of varying the baro altimeter uncertainties are not as dramatic as observed for the initial

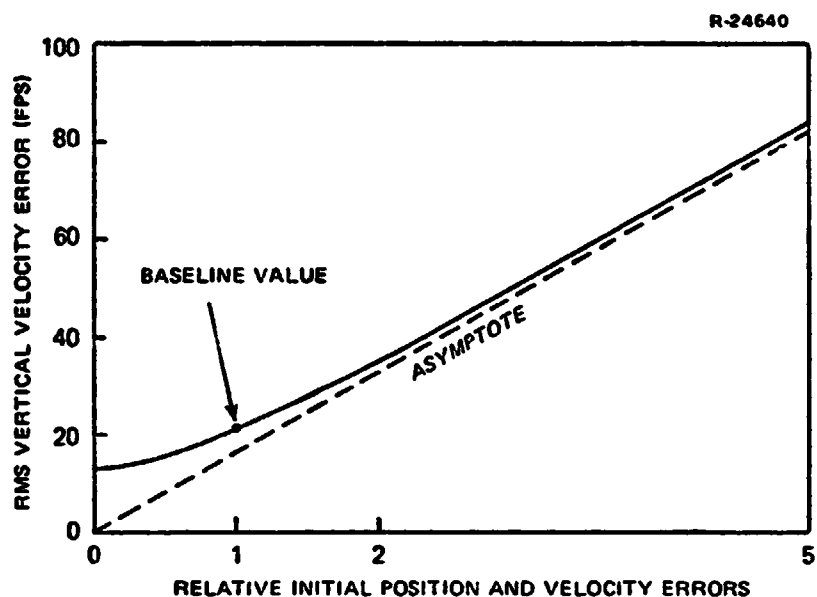


Figure 4.5-1 RMS Vertical Velocity Error Sensitivity at 145,000 ft to Initial Position and Velocity Errors

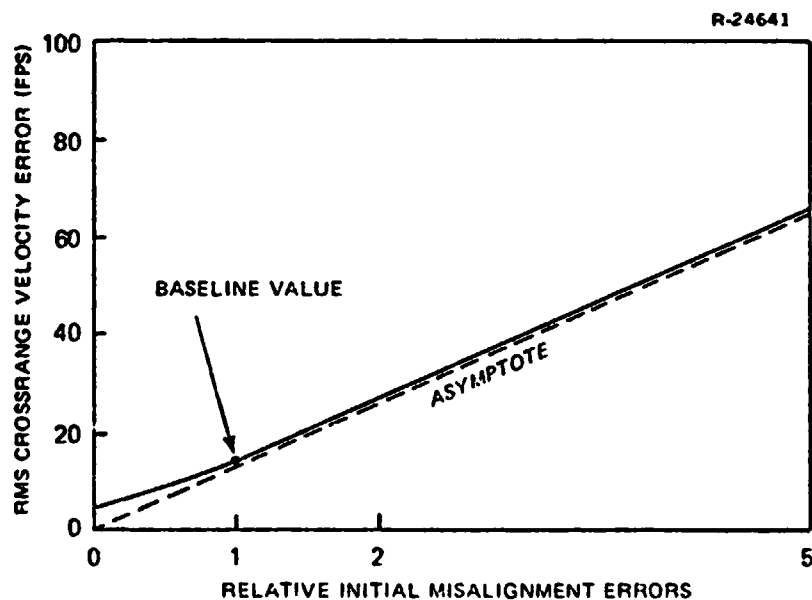


Figure 4.5-2 RMS Crossrange Velocity Error Sensitivity at 145,000 ft to Initial Misalignment Errors

condition errors in Figs. 4.5-1 and 4.5-2. Since the initial conditions errors contribute about as much as the baro altimeter uncertainties to vertical velocity at 20,000 ft, the sensitivity curves for these error sources would be quite similar.

Major error sources at T_{RA} , 100 ft above the touchdown point, are the MLS-related errors. The sensitivity of the vertical velocity error to the MLS range bias uncertainty is shown in Fig. 4.5-4. Again, because of other error sources of equal importance, the vertical velocity error is seen to be basically insensitive to changes in this error source. A sensitivity curve for the baro altimeter uncertainties, also a major contributor to the vertical velocity error at T_{RA} , would be very similar to Fig. 4.5-4.

In contrast to the vertical velocity error, the downrange velocity error at T_{RA} is dominated by a single error source - the MLS range second-order markov error. The sensitivity curve in Fig. 4.5-5 reveals that doubling the markov uncertainty would result in a 77% increase in downrange velocity error; while a markov error of zero would yield nearly a 50% improvement in the velocity error.

The final sensitivity curve, Fig. 4.5-6, presents the sensitivity of crossrange position error at touchdown to the MLS azimuth bias error, and indicates the appropriate touchdown specification. It is clear that even if the MLS bias error were zero, the touchdown specification still would not be met. This arises because the MLS azimuth second-order markov error contribution is itself larger than the specification. Therefore to meet this specification both MLS azimuth errors must be significantly reduced.

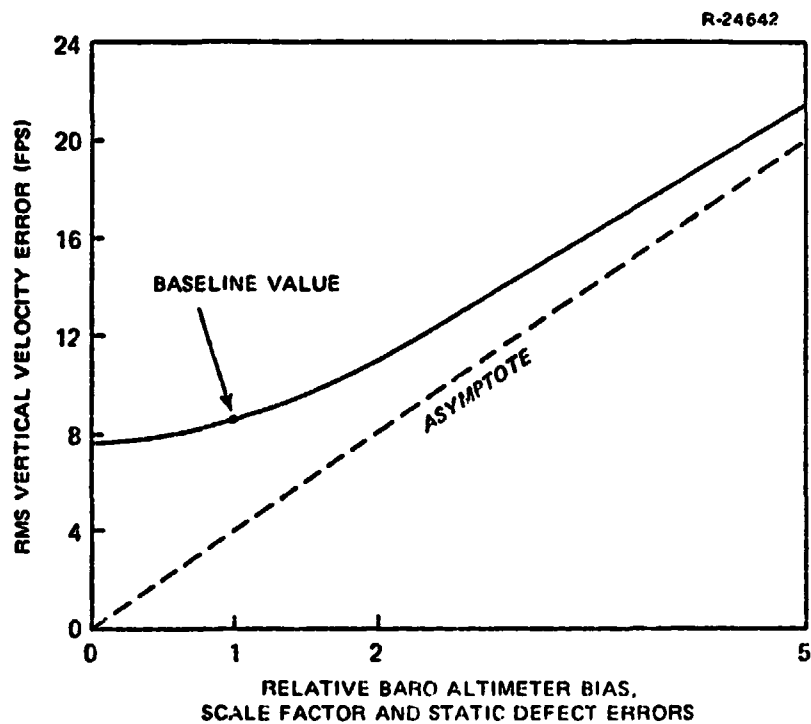


Figure 4.5-3 RMS Vertical Velocity Error Sensitivity at 20,000 ft to Baro Altimeter Bias, Scale Factor and Static Defect Errors

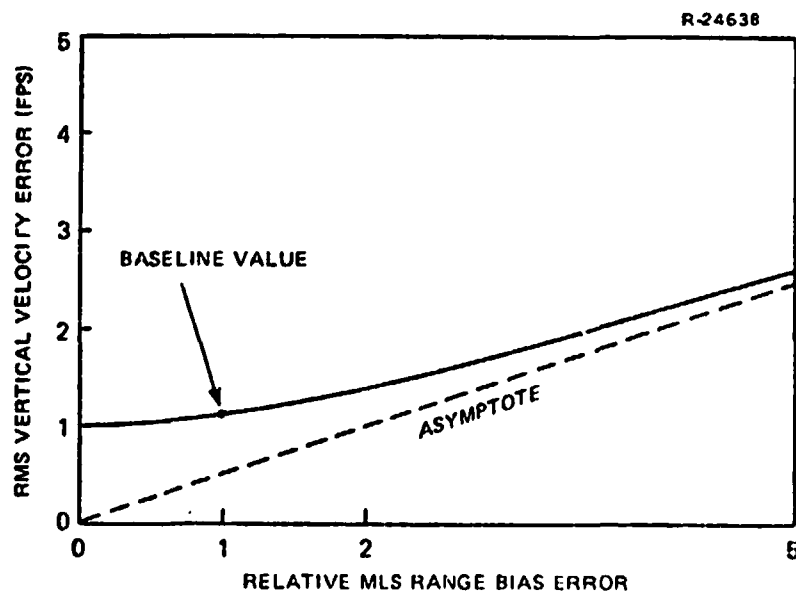


Figure 4.5-4 RMS Vertical Velocity Error Sensitivity at 100 ft to MLS Range Bias Error

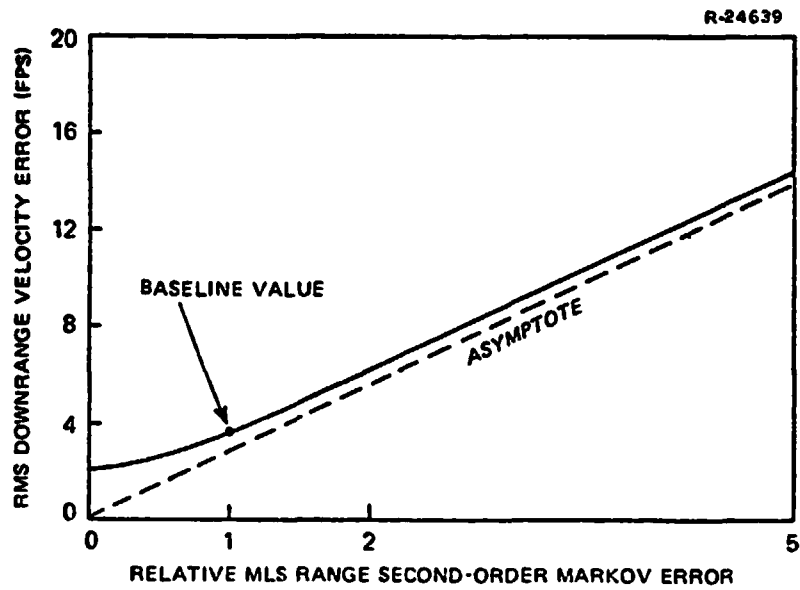


Figure 4.5-5 RMS Downrange Velocity Error Sensitivity at 100 ft to MLS Range Second-Order Markov Error

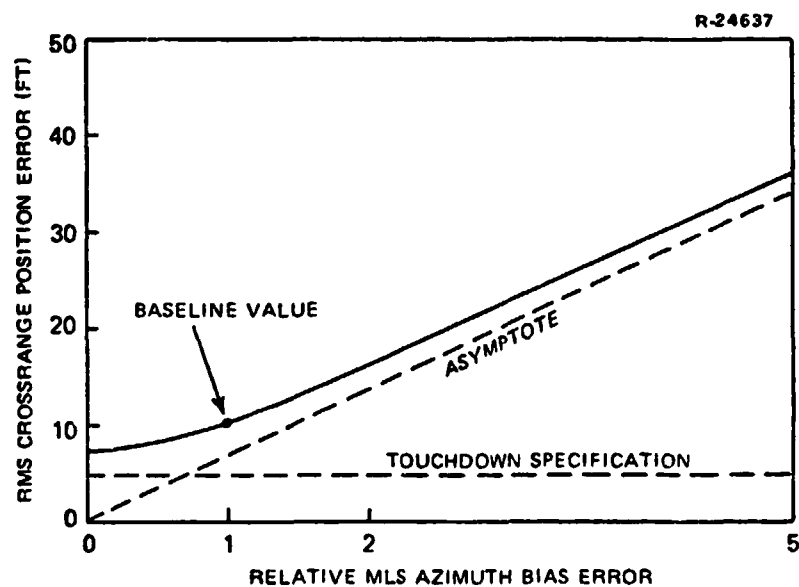


Figure 4.5-6 RMS Crossrange Position Error Sensitivity at Touchdown to MLS Azimuth Bias Error

5.

SUMMARY AND CONCLUSIONS

A detailed analysis of Space Shuttle navigation has been presented. The study encompassed navigation performance during each of the major mission phases - from prelaunch IMU calibration and alignment, through ascent and orbital operations, to entry and landing. The ascent and orbital operations studies evaluated the potential effectiveness of GPS-aided navigation in the 1984+ time frame; the remaining studies considered navigation performance for the OFT-1 mission in 1979. In each instance, the analytical techniques and navigation error models used for the study were described. Detailed navigation error budgets were generated for nominal mission profiles and performance sensitivity to the dominant error sources was evaluated. A summary of the most significant findings of the study is presented in the following subsections.

5.1 ASCENT AND ORBITAL NAVIGATION

The objective of the ascent navigation study was to provide NASA with an assessment of potential navigation accuracy in the operational GPS (1984+) time frame. The Shuttle was assumed to be equipped with a multichannel X-receiver capable of processing the high accuracy (P-code) satellite transmissions. An 11-state navigation filter was designed and a candidate measurement sequence was defined. The measurement sequence provided GPS measurement updates to the navigation state vector at a low update rate - range and range-rate measurements from one GPS satellite every

THE ANALYTIC SCIENCES CORPORATION

6 sec. This update rate is significantly below the capability of the GPS receiver, but was selected to minimize the computational burden on the Space Shuttle computer. No significant performance improvement would be anticipated by adopting a higher update rate.

The results of the ascent study are presented in Table 5-1. Relative to pure inertial navigation, GPS-aiding can provide a factor of 100 improvement in position estimation at orbit insertion and a factor of 30 improvement in velocity estimation. Furthermore, GPS measurements can be used to align the IMU during ascent. Although IMU errors are the major contributors to the remaining misalignment uncertainty, the error budget upon which Table 5-1 was based clearly indicates that the navigation performance is completely dominated by GPS-related errors. This dominance of GPS-related error sources implies that navigation performance is insensitive to an increase in the magnitude of any other error source as long as GPS is available.

TABLE 5-1
EFFECT OF GPS IN REDUCING ORBIT INSERTION ERRORS

T-0269a

IMPLEMENTATION	RMS POSITION ERRORS (ft)			RMS VELOCITY ERRORS (fps)			RMS MISALIGNMENT ERRORS (sec)		
	DR	CR	R	DR	CR	R	DR	CR	R
Pure Inertial Navigation*	2280	2730	1864	5.2	7.6	7.4	64	62	61
GPS-Aided Navigation	7	9	16	0.1	0.1	0.2	25	13	15

*Errors at midpoint of final Orbital Maneuvering System (OMS) insertion burn, 142 sec prior to insertion.

An important conclusion to be drawn from the ascent navigation study is that, when GPS-aiding is used, ascent navigation accuracy is not sensitive to the quality of the IMU or to how accurately the IMU is calibrated and aligned. The role of the IMU is to provide an inertial reference with short term stability so that GPS measurements taken at different times can be "tied together" to generate an accurate navigation estimate. This requirement could be met by the Space Shuttle IMU without an extensive prelaunch calibration and alignment.

The present baseline for operational Space Shuttle missions specifies the Tracking and Data Relay Satellite System (TDRSS) as the principal navigation aid for orbit determination. Table 5-2 compares orbit determination accuracy for TDRSS with the results of the GPS-aided orbital navigation study. The table clearly implies that GPS can provide significantly better navigation accuracy than TDRSS from shorter measurement sequences. Although the GPS results were based on a 2 min measurement sequence, comparable accuracy could be obtained with only a few seconds of data if the navigation filter were optimized. These

TABLE 5-2
PROJECTED ORBIT DETERMINATION ACCURACIES
FOR TDRSS AND GPS

NAVIGATION AID	LENGTH OF MEASUREMENT SEQUENCE (min)	RSS POSITION ERRORS (ft)	RSS VELOCITY ERRORS (fps)
TDRSS	5	~200 *	Not Specified
GPS	2	20	0.2

*Data interpretation subject to qualification discussed in Section 2.7.

performance results, coupled with the operational advantage that GPS does not require ground processing and subsequent uploading of the navigation solution, clearly favor GPS as the more desirable orbital navigation aid.

5.2 PRELAUNCH CALIBRATION AND ALIGNMENT

The prelaunch calibration and alignment study was a continuation of the performance phase of the IMU Software Verification and Validation Program initially reported in Ref. 1. The emphasis was on development of a covariance analysis simulation for the OFT software. This program will be used to generate a detailed cal/align error budget in a subsequent study.

5.3 ENTRY, PRELAND AND LANDING NAVIGATION

The principal finding of the entry, preland and landing navigation study is that the navigation filter as described in Ref. 45 incorporates measurements from the navigation aids into the navigation solution in a reasonably effective manner, particularly after the transition to landing navigation at 12,000 ft. Previous studies by TASC (Ref. 1) had uncovered a tendency for the velocity estimates generated by the filter to diverge following the switch to the complementary mode ($t = T_{SW}$) because of a dynamic coupling between the vertical and downrange estimates. The filter presented in Ref. 45 was modified by NASA to eliminate this coupling. As shown in Fig. 5-1, downrange and vertical velocity errors increase somewhat during the landing phase, but the overall result is stable velocity estimation performance.

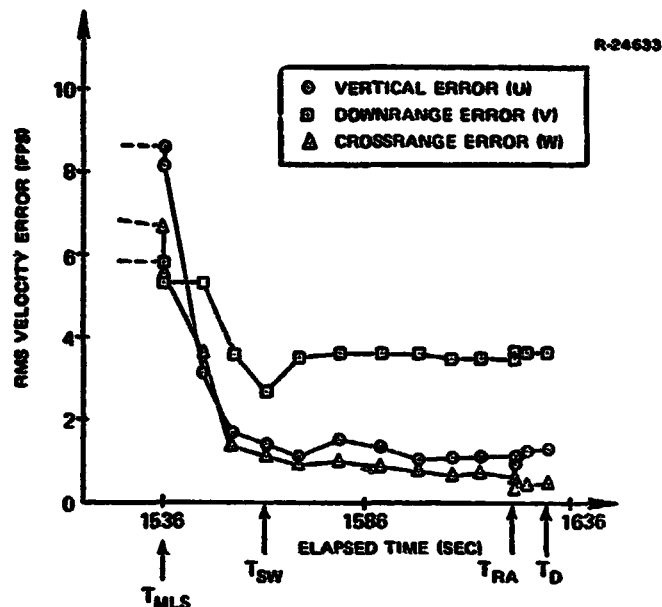


Figure 5-1 Velocity Performance During Landing —
Complementary Mode Begins at T_{SW}

The results of this and previous TASC studies suggest that the basic navigation filter design has the potential for achieving near-specification performance at touchdown, however, careful attention must be given to filter parameter and gain selection in order to attain this level of performance. The candidate entry and preland parameter values provided by NASA are quite pessimistic and result in a number of major navigation performance anomalies, e.g., a sudden increase in navigation errors following TACAN acquisition. Similarly, although the landing filter prevents velocity estimation divergence, there is considerable evidence to suggest that appropriately selected gains could improve velocity estimation accuracy during landing. A thorough parameter tradeoff study could result in an improvement in entry, preland and landing navigation performance over that predicted in this study.

If subsequent analysis shows that satisfactory navigation performance cannot be attained with the present

THE ANALYTIC SCIENCES CORPORATION

filter/navigation system combination, an alternative would be to replace the navigation aids used prior to MLS acquisition with GPS. GPS-aiding during entry and preland could potentially yield improved navigation performance with a simpler navigation filter. A quantitative evaluation of this alternative will be completed by TASC during the next contract period.

APPENDIX A
ANALYTIC EVALUATION OF TWO MECHANIZATIONS
OF THE DRAG UPDATE FILTER

The drag update filter used in the Space Shuttle entry navigation system during blackout employs a type of pseudo-measurement in order to improve the on-board estimate of position and velocity. To date, an atmospheric drag pseudo-measurement has been assumed for the filter; however, the alternative of using an altitude pseudo-measurement exists. The Kalman filter used in the computer navigation program requires the definition of a measurement matrix H_F for the pseudo-measurement. Additionally, if the performance of the drag update filter is to be evaluated using a "truth model," the measurement matrix H_S for the truth model must also be defined. Two schemes for finding H_S , one employing drag pseudo-measurements and the other employing altitude pseudo-measurements, are described and compared in this appendix.

A.1 DESCRIPTION OF MECHANIZATIONS

The atmospheric drag pseudo-measurement $q_m(t)$ is defined to be a drag acceleration measurement constructed from the IMU accelerometer outputs. The expected (i.e., predicted) drag acceleration $q_p(t)$ is computed from the current estimate of position and velocity, a nominal atmospheric density model and estimates of the Shuttle's aerodynamic coefficients. The difference between $q_m(t)$ and $q_p(t)$ is the residual

$$\delta q_{S_q}(t) = q_m(t) - q_p(t) \quad (A.1-1)$$

which appears in the update equation for the truth model error state vector

$$\delta \underline{x}_S(t^+) = \delta \underline{x}_S(t^-) - K_{S_q}(t) \delta q_S(t) \quad (A.1-2)$$

where $\delta \underline{x}_S(t^-)$ is the estimation error prior to the update and $\delta \underline{x}_S(t^+)$ is the estimation error after the update. This mechanization is depicted in Fig. A.1-1.

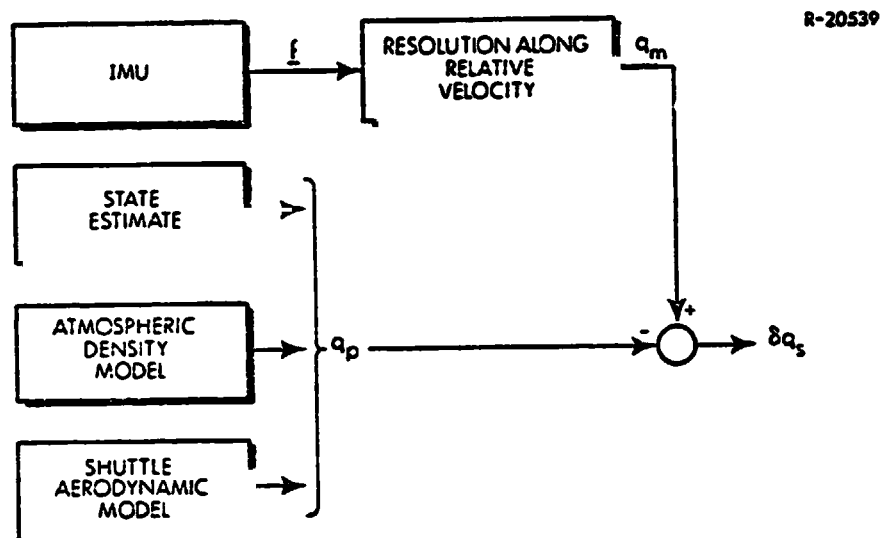


Figure A.1-1 Simplified Conceptual View* of Drag Pseudo-Measurement Mechanization

The matrices of first partial derivatives $H_{m_q}(t)$ and $H_{p_q}(t)$ relate $q_m(t)$ and $q_p(t)$, respectively, to the truth

*Figures A.1-1 and A.1-2 are intended to merely indicate conceptually what functional blocks are involved in generating the pseudo-measurements versus the predicted values. These figures in no way attempt to present the detailed steps necessary to develop any of the variables.

model state vector. The measurement matrix for the truth model is then defined by

$$H_{S_q}(t) = H_{p_q}(t) - H_{m_q}(t) \quad (A.1-3)$$

An alternative approach employing altitude pseudo-measurements $h_m(t)$ and expected altitude $h_p(t)$ can be used to generate the truth model measurement matrix. In this scheme the measured altitude is computed from IMU accelerometer outputs, current position and velocity estimates, a nominal atmospheric density model and estimates of the Shuttle's aerodynamic coefficients; while the expected altitude is interpreted from the current estimate of Shuttle position. Similar to Eqs. (A.1-1) and (A.1-2) the residual and error update equations are

$$\delta h_S(t) = h_m(t) - h_p(t) \quad (A.1-4)$$

$$\delta \underline{x}_S(t^+) = \delta \underline{x}_S(t^-) - K_{S_h}(t) \delta h_S(t) \quad (A.1-5)$$

Figure A.1-2 depicts this scheme.

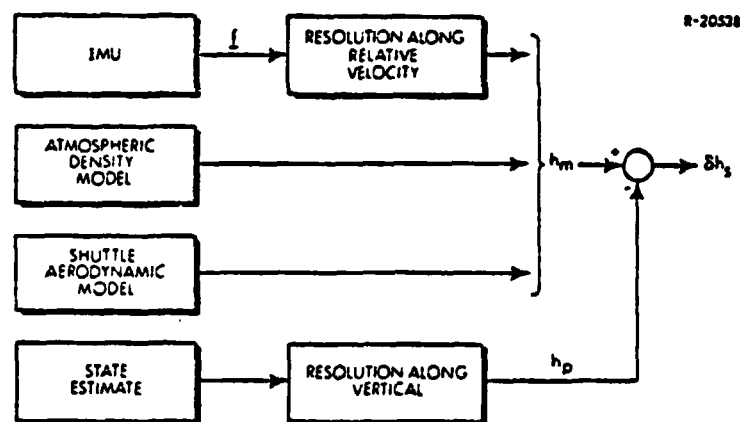


Figure A.1-2 Simplified Conceptual View of Altitude Pseudo-Measurement Mechanization

$H_{m_h}(t)$ and $H_{p_h}(t)$ relate $h_m(t)$ and $h_p(t)$, respectively, to the truth model state vector, and $H_{S_h}(t)$ is the truth model measurement matrix given by

$$H_{S_h}(t) = H_{p_h}(t) - H_{m_h}(t) \quad (A.1-6)$$

This appendix presents a comparison of these schemes, and answers the question of whether or not the system error sources have the same effect on the performance for both mechanizations. Table A.1-1 lists the truth model states used in evaluating the drag update filter.

TABLE A.1-1
DRAG UPDATE TRUTH MODEL STATES

Error Source Names	State
I. ESTIMATED STATES AND UNCORRELATED NOISES	
Group 1.	
Position Errors	1-3
Velocity Errors	4-6
Platform Misalignments	7-9
Accelerometer 'Biases' (First-Order Markovs)	10-12
Correlated Measurement Error (First Order Markov)	
Drag	13
II. NON-ESTIMATED, IMU-RELATED STATES	
Group 2. Accelerometer True Biases	14-16
Group 3. Accelerometer Scale Factor Errors	17-19
Group 4. Accelerometer Misalignments	20-25
Group 5. Accelerometer Nonlinearities	26-28
Group 6. Gravitational Deflections and Anomalies	29-31
Group 7. Gyro True Bias Drifts	32-34
Group 8. Gyro Mass Unbalances	35-40
Group 9. Gyro Anisoelasticities	41-43
III. NON-ESTIMATED, DRAG RELATED STATES	
Group 21. Non-Standard Density	
1962 Standard Atmosphere Error	44
Time-Varying Bias	45
First-Order Markov	46
Group 22. Non-Standard Wind	
Westerly (Time-Varying Bias)	47
Headwind (First-Order Markov)	48
Crosswind (Second-Order Markov)	49-50
Turbulence (First- and Second-Order Markovs)	51-55
Group 23. Non-Standard Aerodynamics	
First-Order Markov	56

A.2 DRAG MEASUREMENT MECHANIZATION

This section is essentially an outline of Appendix C of Ref. 2, in which the truth model measurement matrix for the drag acceleration pseudo-measurement case is developed. The text here presents only the highlights of that development. Detailed derivations and definitions can be found in the noted appendix.

The drag acceleration pseudo-measurement extracted from the accelerometer outputs is

$$q_m(t) = |\underline{i}_{VR_c}(t) \cdot \underline{f}_c(t)| \quad (A.2-1)$$

where $\underline{i}_{VR_c}(t)$ is a unit vector in the direction of the computed relative velocity and $\underline{f}_c(t)$ is the measured specific force. The difference between the true drag acceleration and that measured is

$$\delta q_m(t) = q(t) - q_m(t) \quad (A.2-2)$$

Combining Eqs. (A.2-1) and (A.2-2) the perturbation $\delta q_m(t)$ can be defined by

$$\delta q_m(t) = \delta \underline{i}_{VR}(t) \cdot \underline{f}(t) + \underline{i}_{VR}(t) \cdot \delta \underline{f}(t) \quad (A.2-3)$$

where

$$\begin{aligned} \delta \underline{i}_{VR}(t) &= \underline{i}_{VR}(t) - \underline{i}_{VR_c}(t) \\ \delta \underline{f}(t) &= \underline{f}(t) - \underline{f}_c(t) \end{aligned}$$

and $\underline{i}_{VR}(t)$ is a unit vector in the direction of the true relative velocity and $\underline{f}(t)$ is the true specific force. The error $\delta \underline{f}(t)$ in measured acceleration can be attributed to the standard IMU acceleration error sources defined in the

drag update truth model, namely, platform misalignments (Group 1) and accelerometer errors (Groups 2 through 5). Thus, the quantity $\underline{i}_{VR}(t) \cdot \delta \underline{f}(t)$ in Eq. (A.2-3) introduces terms in $H_{mq}(t)$ relating to truth model states 7-9 and 14-28. The remaining term in Eq. (A.2-3) is given by

$$\delta \underline{i}_{VR}(t) \cdot \underline{f}(t) = -\underline{F}_L(t)(\underline{\Omega}_E \times \delta \underline{r}(t)) + \underline{F}_L(t) \delta \underline{v}(t) - \underline{F}_L(t) \underline{V}_w(t) \quad (A.2-4)$$

where

$$\underline{F}_L(t) = \frac{\underline{f}^T(t)}{|\underline{V}_c(t) - \underline{\Omega}_E \times \underline{R}_c(t)|} - \frac{\underline{f}^T \underline{i}_{VR_c}(t) \underline{i}_{VR_c}^T(t)}{|\underline{V}_c(t) - \underline{\Omega}_E \times \underline{R}_c(t)|} \quad (A.2-5)$$

$\underline{\Omega}_E$ is the earth rate, $\underline{V}_w(t)$ is the atmospheric wind and $\underline{R}_c(t)$ and $\underline{V}_c(t)$ are the computed position and velocity vectors, respectively. Adding in these terms, relating to position, velocity and non-standard wind error states, completes $H_{mq}(t)$

$$H_{mq}(t) = \begin{bmatrix} \text{position errors} & \text{velocity errors} & \text{platform misalignments} & & \\ \underline{-F}_L(\underline{\Omega}_E \times) & \underline{F}_L & \underline{i}_{VR}^T T_{I/P} F_P & 0 & \\ 3 & 6 & 9 & 13 & \\ \text{accelerometer biases} & \text{accelerometer scale factor errors} & & & \\ \underline{i}_{VR}^T T_{I/P} & \underline{i}_{VR}^T T_{I/P} F_4 & & & \\ 16 & 19 & & & \\ \text{accelerometer misalignments} & \text{accelerometer nonlinearities} & \text{winds} & & \\ \underline{i}_{VR}^T T_{I/P} F_4 & \underline{i}_{VR}^T T_{I/P} F_5 & 0 & \underline{-F}_L & 0 & 0 \\ 25 & 28 & 46 & 55 & & \end{bmatrix} \quad (A.2-6)$$

where $T_{I/P}$ is the transformation matrix from platform to inertial reference coordinates; and F_p, F_3, F_4, F_5 are matrices whose elements are the components of the specific force $\underline{f}(t)$ coordinatized in platform coordinates.

The computation of $H_{S_q}(t)$ requires that $H_{p_q}(t)$ also be determined; the equation for $\delta q_p(t)$ must therefore be found. The expected drag acceleration is

$$q_p(t) = \frac{1}{2} C_{D_c}(t) \frac{A}{m} \rho_c(t) V_{R_c}^2(t) \quad (A.2-7)$$

where $C_{D_c}(t)$ is the computed drag coefficient for the Space Shuttle, A is its cross-sectional area, and m is its mass. $\rho_c(t)$ and $V_{R_c}(t)$ are the computed atmospheric density and computed relative velocity, respectively. The difference between the true drag and that computed is

$$\delta q_p(t) = q(t) - q_p(t) \quad (A.2-8)$$

From Eqs. (A.2-7) and (A.2-8) the relationship defining the perturbation $\delta q_p(t)$ is

$$\begin{aligned} \delta q_p(t) = & \frac{1}{2} \delta C_D(t) \frac{A}{m} \rho(t) V_R^2(t) + \frac{1}{2} C_D(t) \frac{A}{m} \delta \rho(t) V_R^2(t) \\ & + C_D(t) \frac{A}{m} \rho(t) \underline{V}_R(t) \cdot \delta \underline{V}_R(t) \end{aligned} \quad (A.2-9)$$

which can be written in terms of the true drag as

$$q_p(t) = q(t) \left\{ \frac{\delta C_D(t)}{C_D(t)} + \frac{\delta \rho(t)}{\rho(t)} + \frac{2 \underline{V}_R(t) \cdot \delta \underline{V}_R(t)}{V_R^2(t)} \right\} \quad (A.2-10)$$

where

$$\delta\rho(t) = \rho(t) - \rho_c(t)$$

$$\delta C_D(t) = C_D(t) - C_{D_c}(t)$$

$$\delta \underline{V}_R(t) = \underline{V}_R(t) - \underline{V}_{R_c}(t) = \delta \underline{v}(t) - \underline{\Omega}_E \times \delta \underline{r}(t) - \underline{V}_w(t) \quad (A.2-11)$$

Considering the drag coefficient term in Eq. (A.2-10), $\delta C_D(t)$ can be approximated by

$$\delta C_D(t) = C_{D_f}(\alpha, M, t) \quad (A.2-12)$$

where $C_{D_f}(\alpha, M, t)$ is the difference between the true Space Shuttle drag coefficient and that predicted by the drag coefficient computational model. Assuming that the drag correlated error and the non-standard aerodynamics errors are defined as percent deviations from their nominal values, the terms of $H_{p_q}(t)$ corresponding to error states 13 (drag correlated measurement error of Group 1) and 56 (Group 23) can easily be written. The $\delta\rho(t)/\rho(t)$ term in Eq. (A.2-10) is considered by first making the assumptions that the atmospheric density model from which $\rho_c(t)$ is computed is a simple exponential function of computed altitude $h_c(t)$

$$\rho_c(h_c) = \rho_0 e^{-\frac{h_c(t)}{h_{sc}}} \quad (A.2-13)$$

and that the true atmospheric density satisfies

$$\rho(R) = \rho_0 e^{-\frac{h(t)}{h_{sc}}} + \rho_f(R) \quad (A.2-14)$$

where $h(t)$ is the true altitude, ρ_o and h_{sc} are constants and $\rho_f(R)$ is the difference between the true atmospheric density and that predicted by the atmospheric density computational model. A first order expansion for $\delta\rho(t)$ yields

$$\delta\rho(R) \approx -\rho_c(t) \frac{\underline{i}_R(t) \cdot \delta\underline{r}(t)}{h_{sc}} + \rho_f(R) \quad (A.2-15)$$

where $\underline{i}_R(t)$ is the unit vector along $\underline{R}(t)$. The dependence of the error in expected drag $\delta q_p(t)$ on position and non-standard density errors is evident from Eqs. (A.2-15) and (A.2-10). The position error related terms in $H_{pq}(t)$ follow directly from the first term on the right hand side of Eq. (A.2-15). With the assumption that the non-standard density errors are defined as percent deviations from their nominal values, the terms in $H_{pq}(t)$ related to the Group 21 error states follow from the $\rho_f(R)$ quantity in Eq. (A.2-15) and from Eq. (A.2-10). Substituting Eq. (A.2-11) into the last term in Eq. (A.2-10) completes the derivation of $H_{pq}(t)$, adding terms related to the position, velocity and non-standard wind error states.

$$H_{pq}(t) = q(t) \left[\begin{array}{c|c|c|c|c|c|c} \text{position errors} & \text{velocity errors} & & \text{drag correlated error} & & & \\ \hline -\frac{\underline{i}_R^T}{h_{sc}} - \frac{2\underline{i}_{VR}^T (\underline{\Omega}_E \times)}{V_R} & \frac{2\underline{i}_{VR}^T}{V_R} & 0 & 1 & 0 & & \\ \hline & & & & & & \\ \hline \text{non-standard density error model} & \text{non-standard wind} & & \text{non-standard aerodynamics errors} & & & \\ \hline 1 & 1 & 1 & -\frac{2\underline{i}_{VR}^T}{V_R} & 0 & 1 & \\ \hline & & & & & & \end{array} \right] \quad (A.2-16)$$

A.3 ALTITUDE MEASUREMENT MECHANIZATION

Consider the following pair of equations in which the non-standard density error model term $\rho_f(R)$ has been ignored.

$$\rho(t) = \rho_o e^{-\frac{h(t)}{h_{sc}}} \quad (A.3-1)$$

$$q(t) = |\underline{i}_{VR}(t) \cdot \underline{f}(t)| = \frac{1}{2} C_D(t) \frac{A}{m} \rho(t) V_R^2(t) \quad (A.3-2)$$

where all variables have been previously defined. Equations (A.3-1) and (A.3-2) represent the situation in which altitude and velocity are known precisely, the accelerometers are perfect and the computational models for the drag coefficient and atmospheric density are exact. Solving for $h(t)$ yields the altitude pseudo-measurement equation

$$h(t) = h_{sc} \log \frac{\frac{1}{2} C_D(t) \frac{A}{m} \rho_o V_R^2(t)}{q(t)} \quad (A.3-3)$$

from which the relationship for $\delta h_p(t)$ can be easily established

$$\delta h_p(t) = h_{sc} \left\{ \frac{\delta C_D(t)}{C_D(t)} + \frac{2 \underline{i}_{VR}(t) \cdot \delta \underline{V}_R(t)}{V_R(t)} - \frac{\delta q(t)}{q(t)} \right\} \quad (A.3-4)$$

The first two terms on the right hand side of Eq. (A.3-4) also appear in Eq. (A.2-10), and so affect $H_{mh}(t)$ as they affect $H_{pq}(t)$. That is to say, these terms introduce into $H_{mh}(t)$ terms related to the position and velocity, non-standard wind, non-standard aerodynamics and drag correlated error states. The last term in Eq. (A.3-4) can be considered by first noting that $q(t) = |\underline{i}_{VR}(t) \cdot \underline{f}(t)|$.

Then $\delta q(t)$ is given by Eq. (A.2-3), which equation completely determined $H_{mq}(t)$. Thus, $\delta q(t)$ inserts into $H_{mh}(t)$ all the terms in $H_{mq}(t)$.

The final item of concern in developing $H_{mh}(t)$ is to now consider a non-standard density error model term in Eq. (A.3-1), namely

$$\rho(R) = \rho_o e^{-\frac{h(t)}{h_{sc}}} + \rho_f(R) \quad (A.3-5)$$

where again, as before, $\rho_f(R)$ is the difference between the true atmospheric density and that predicted by the atmospheric density computational model. Eq. (A.2-15) gives $\delta\rho(R)$ as a function of $\delta h_m(t)$

$$\delta\rho(R) \approx -\rho_c(t) \frac{\delta h_m(t)}{h_{sc}} + \rho_f(R) \quad (A.3-6)$$

where $\delta h(t)$ has been substituted in for $i_R(t) \cdot \delta r(t)$. This equation can be solved for $\delta h_m(t)$,

$$\delta h_m(t) \approx -h_{sc} \frac{\delta\rho(R)}{\rho_c(t)} + h_{sc} \frac{\rho_f(R)}{\rho_c(t)} \quad (A.3-7)$$

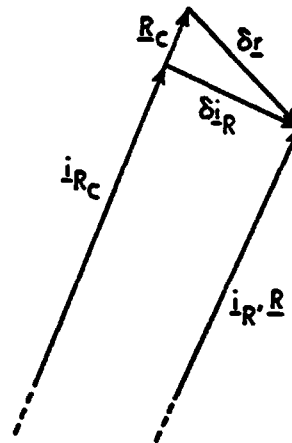
The $\rho_f(R)/\rho_c(t)$ term in Eq. (A.3-7) indicates the effect of the non-standard density error model on $\delta h_m(t)$. Note that this effect is the same as that exhibited by $\rho_f(R)$ on $\delta q_p(t)$ (from Eqs. (A.2-15) and (A.2-10)) in deriving $H_{pq}(t)$. Therefore the matrix $H_{mh}(t)$ is completely established.

$$\begin{aligned}
 H_{m_h}(t) = h_{sc} \left[\begin{array}{c} \text{position errors} \\ - \frac{2i_{VR}^T (\Omega_E \times)}{V_R} + \frac{F_L (\Omega_E \times)}{q} \\ \text{velocity errors} \\ \frac{2i_{VR}^T}{V_R} - \frac{F_L}{q} \\ \text{platform misalignments} \\ \frac{i_{VR}^T T_{I/P} F_P}{q} \\ \text{drag correlated error} \\ 0 \quad 1 \\ \text{accelerometer biases} \\ - \frac{i_{VR}^T T_{I/P}}{q} \\ \text{accelerometer scale factor errors} \\ - \frac{i_{VR}^T T_{I/P} F_3}{q} \\ \text{accelerometer misalignments} \\ - \frac{i_{VR}^T T_{I/P} F_4}{q} \\ \text{accelerometer nonlinearities} \\ - \frac{i_{VR}^T T_{I/P} F_5}{q} \\ \text{non-standard density error model} \\ 0 \quad 1 \quad 1 \quad 1 \\ \text{non-standard wind} \\ - \frac{2i_{VR}^T}{V_R} + \frac{F_L}{q} \quad 0 \\ \text{non-standard aerodynamics errors} \\ 1 \end{array} \right] \quad (A.3-8)
 \end{aligned}$$

To determine $H_{S_h}(t)$, the matrix of first partials $H_{p_h}(t)$ must also be developed. The altitude measurement, taken from the current estimate of Shuttle position, is given by

$$h_p(t) = h_c(t) = \underline{i}_{R_c}(t) \cdot \underline{R}_c(t) \quad (A.3-9)$$

where $\underline{i}_{R_c}(t)$ is a unit vector in the direction of computed position and $\underline{R}_c(t)$ is the computed position vector. The perturbation in the expected altitude $\delta h_p(t)$ can be determined by considering small perturbations about the nominal values in Eq. (A.3-9). These perturbations are illustrated in Fig. A.3-1.



R-20537

Figure A.3-1 Definition of Perturbations in Position Vector and Unit Relative Position Vector

The difference between the true altitude and that predicted is

$$\begin{aligned}\delta h_p(t) &= h(t) - h_c(t) \\ &= \underline{i}_R(t) \cdot \underline{R}(t) - \underline{i}_{R_c}(t) \cdot \underline{R}_c(t)\end{aligned}\quad (\text{A.3-10})$$

Using the definitions

$$\begin{aligned}\delta \underline{i}_R(t) &= \underline{i}_R(t) - \underline{i}_{R_c}(t) \\ \delta \underline{r}(t) &= \underline{R}(t) - \underline{R}_c(t)\end{aligned}$$

in Eq. (A.3-10) yields

$$\delta h_p(t) = \underline{i}_R(t) \cdot \underline{R}(t) - [\underline{i}_R(t) - \delta \underline{i}_R(t)] \cdot [\underline{R}(t) - \delta \underline{r}(t)]\quad (\text{A.3-11})$$

$\delta \underline{i}_R(t)$ and $\underline{R}(t)$ are perpendicular, so $\delta \underline{i}_R(t) \cdot \underline{R}(t) = 0$. To first order, an expansion of the last term in Eq. (A.3-11) yields

$$\delta \underline{h}_p(t) = \underline{i}_R(t) \cdot \delta \underline{r}(t) \quad (A.3-12)$$

The measurement matrix $H_{p_h}(t)$ is simply

$$H_{p_h}(t) = \begin{bmatrix} \underbrace{\text{position errors}}_{\substack{\mathbf{i}^T \\ \mathbf{-R}}} & \vdots & 0 \end{bmatrix} \quad (\text{A.3-13})$$

A.4 COMPARISON OF MECHANIZATIONS

The truth model measurement matrix using the drag measurement scheme is defined by

$$H_{S_q}(t) = H_{p_q}(t) - H_{m_q}(t) \quad (A.4-1)$$

which from Eqs. (A.2-16) and (A.2-6) is

$$H_{S_q}(t) = q(t) \left[-\frac{i_R^T}{h_{sc}} - \frac{2i_{VR}^T(\Omega_E x)}{V_R} + \frac{F_L(\Omega_E x)}{q} \right]_3 - \frac{2i_{VR}^T}{V_R} - \frac{F_L}{q} \Big|_6$$
$$\left[-\frac{i_{VR}^T T_{I/P} F_P}{q} \right]_9 \quad 0 \quad 1 \quad \left[-\frac{i_{VR}^T T_{I/P}}{q} \right]_{16}$$
$$\left[-\frac{i_{VR}^T T_{I/P} F_3}{q} \right]_{19} - \left[\frac{i_{VR}^T T_{I/P} F_4}{q} \right]_{25} - \left[\frac{i_{VR}^T T_{I/P} F_5}{q} \right]_{28}$$
$$\left[0 \quad 1 \quad 1 \quad 1 \quad -\frac{2i_{VR}^T}{V_R} + \frac{F_L}{q} \quad 0 \quad 1 \right]_{43 \quad 46 \quad 55 \quad 56} \quad (A.4-2)$$

If the truth model measurement matrix associated with the altitude measurement mechanization is similarly defined, i.e.,

$$H_{S_h}(t) = H_{p_h}(t) - H_{m_h}(t) \quad (A.4-3)$$

then Eqs. (A.3-13) and (A.3-8) yield

$$H_{S_h}(t) = -h_{sc} \left[\begin{array}{c|c|c|c} \frac{i_R^T}{h_{sc}} - \frac{2i_{VR}^T(\Omega_E x)}{V_R} + \frac{F_L(\Omega_E x)}{q} & \frac{2i_{VR}}{V_R} - \frac{F_L}{q} & & \\ \hline - \frac{i_{VR}^T T_{I/P} F_P}{q} & 0 & 1 & - \frac{i_{VR}^T T_{I/P}}{q} \\ \hline - \frac{i_{VR}^T T_{I/P} F_3}{q} & - \frac{i_{VR}^T T_{I/P} F_4}{q} & - \frac{i_{VR}^T T_{I/P} F_5}{q} & \\ \hline 0 & 1 & 1 & 1 \\ \hline \end{array} \right] \begin{array}{c} 3 \\ 9 \\ 19 \\ 43 \\ 46 \\ 55 \\ 56 \end{array} \quad \begin{array}{c} 6 \\ 16 \\ 28 \end{array} \quad (A.4-4)$$

Now, in the absence of measurement noise the following two equations hold:

$$\delta q_S(t) = H_{S_q}(t) \delta \hat{x}(t) \quad (A.4-5)$$

$$\delta h_S(t) = H_{S_h}(t) \delta \hat{x}(t) \quad (A.4-6)$$

where $\delta \hat{x}(t)$ has been previously defined to be the estimate of the truth model state vector. In order to examine the effects of employing drag acceleration measurements versus altitude measurement the relationship between $\delta q_S(t)$ and

$\delta h_S(t)$ must be determined and then used to establish the proper relationship between $H_{S_q}(t)$ and $H_{S_h}(t)$. From Eq. (A.3-3) the relationship between $\delta h_S(t)$ and $\delta q_S(t)$ is easily derived

$$\delta h_S(t) = - \frac{h_{sc}}{q(t)} \delta q(t) \quad (A.4-7)$$

Substituting Eq. (A.4-5) into Eq. (A.4-7) gives

$$\delta h_S(t) = - \frac{h_{sc}}{q(t)} H_{S_q}(t) \delta \hat{x}(t) \quad (A.4-8)$$

from which it is clear from Eq. (3.4-6) that if

$$H_{S_h}(t) = - \frac{h_{sc}}{q(t)} H_{S_q}(t) \quad (A.4-9)$$

then the effects of employing drag acceleration measurements are no different than the effects of using altitude measurements. It is easily seen that Eqs. (A.4-2) and (A.4-4) satisfy the relationship of Eq. (A.4-9). Thus, to first order, the two mechanizations presented here yield the same effect in the performance evaluation of the drag update filter.

APPENDIX B
TRUTH MODEL DETAILS FOR THE
CAL/ALIGN COVARIANCE ANALYSIS

An error covariance simulation of the IMU calibration and alignment procedure consists basically of two operations: (1) propagation of IMU errors during a ground mode sequence, including least squares fit (LSF) estimation sequences and time delays for thermal stabilization, and (2) updates of IMU errors before and/or after an error propagation, including setting the initial platform misalignment after a platform slewing, torquing out platform tilts, storing LSF estimates for later use and updating IMU error compensation terms. This appendix contains some of the details required for defining the IMU error propagations and updates. Section B.1 gives an explicit derivation of Coarse Alignment linearized error equations and Section B.2 contains an analysis of the platform misalignments at the end of a platform repositioning operation.

B.1 COARSE ALIGNMENT LINEAR ERROR ANALYSIS

To implement the Coarse Alignment sequence of the covariance simulation program, it is necessary to express each measurement or computation performed during that sequence in terms of the IMU errors via a linear relationship. This linear relationship is then used to generate an update matrix as needed for Eqs. (3.2-5) and (3.2-6).

THE ANALYTIC SCIENCES CORPORATION ---

Coarse Alignment starts with a platform position given by caged gimbals. To keep the subsequent analysis simple assume, without loss of generality, that the initial platform orientation is such that the mechanical gimbal angles are zero. The first step then is to measure the gimbal angles:

$$\begin{aligned}\phi_m &= \phi_t + \text{ORE} \\ \theta_m &= \theta_t + \text{PE} \\ \psi_m &= \psi_t + \text{AZE} \\ \alpha_m &= \alpha_t + \text{IRE}\end{aligned}\tag{B.1-1}$$

where

$\phi_m, \theta_m, \psi_m, \alpha_m$ are the measured outer roll, pitch, azimuth and inner roll gimbal angles,
 $\phi_t = \theta_t = \psi_t = \alpha_t = 0$ are the mechanical gimbal angles,
 ORE, PE, AZE, IRE are errors incurred in measuring the corresponding gimbal angles (resolver offsets, resolver harmonic errors, resolver randomness and quantization, etc.)

The measured angles are then used to compute a transformation from navigation base to platform, $T_{P/B}$

$$T_{P/B} = \begin{bmatrix} \cos \psi_m & -\sin \psi_m & 0 \\ \sin \psi_m & \cos \psi_m & 0 \\ 0 & 0 & 1 \end{bmatrix} \begin{bmatrix} 1 & 0 & 0 \\ 0 & 1 & -\alpha_m \\ 0 & \alpha_m & 1 \end{bmatrix} \begin{bmatrix} \cos \theta_m & 0 & \sin \theta_m \\ 0 & 1 & 0 \\ -\sin \theta_m & 0 & \cos \theta_m \end{bmatrix} \begin{bmatrix} 1 & 0 & 0 \\ 0 & \cos \phi_m & -\sin \phi_m \\ 0 & \sin \phi_m & \cos \phi_m \end{bmatrix}\tag{B.1-2}$$

Since the measured angles ϕ_m , θ_m , α_m , and ψ_m are all small, $T_{P/B}$ becomes

$$T_{P/B} = I + \begin{pmatrix} \text{ORE} + \text{IRE} \\ \text{PE} \\ \text{AZE} \end{pmatrix} \times \quad (\text{B.1-3})$$

where

$$\begin{pmatrix} x_1 \\ x_2 \\ x_3 \end{pmatrix} \times = \begin{bmatrix} 0 & -x_3 & x_2 \\ x_3 & 0 & -x_1 \\ -x_2 & x_1 & 0 \end{bmatrix} \quad (\text{B.1-4})$$

To determine the error in $T_{P/B}$ first define the navigation base axes corresponding to a perfect IMU. Let these axes be represented by the subindex 0 (see Section A.3 of Ref. 1) and defined as follows:

x_0 = outer roll axis

y_0 = perpendicular to x_0 and in the plane of the outer roll gimbal when the mechanical angle of this gimbal is zero.

$z_0 = x_0 \times y_0$

With these definitions TNBP can now be written as

$$T_{P/B} = T_{P/O} T_{O/B}^{(1)} \quad (\text{B.1-5})$$

$$= \left[I + \begin{pmatrix} 0 \\ a \\ b-DP \end{pmatrix} \times \right] \left[I + \psi_G^0 \times \right] \quad (\text{B.1-6})$$

(1) When the mechanical gimbal angles are zero then $T_{P/B}$ is a function of the three small gimbal nonorthogonalities only.

where

ψ_G^O = Misalignment error of $T_{P/B}$, expressed in "O" coordinates

a = Azimuth gimbal nonorthogonality

b = Pitch gimbal nonorthogonality

DP = Outer roll gimbal nonorthogonality calibration error

Substituting Eq. (B.1-3) into Eq. (B.1-6) and solving for ψ_G results in

$$\psi_G^O = \begin{pmatrix} \text{ORE} + \text{IRE} \\ \text{PE} - a \\ \text{AZE} - b + \text{DP} \end{pmatrix} \quad (\text{B.1-7})$$

The next step in Coarse Alignment is to estimate the transformation from reference to platform, $T_{P/L}$, via a least squares fit to accelerometer data. Let $T_{P/LCA}$ be the actual transformation matrix generated, then

$$T_{P/LCA} = T_{P/L} T_{L/LCA} = T_{P/L} (I + \psi_{CA}^L x) \quad (\text{B.1-8})$$

where ψ_{CA}^L are the misalignment errors of $T_{L/LCA}$, expressed in reference (level) coordinates, and $T_{P/L}$ is the true transformation at the beginning of Coarse Alignment.

$T_{P/LCA}$ and $T_{P/B}$ are now combined to give the transformation from navigation base to reference, TNBR:

$$\text{TNBR} = T_{P/LCA}^T T_{P/B} \quad (\text{B.1-9})$$

Now, if the error in TNBR is represented by the misalignment vector $\psi_{\text{NBR}}^{\text{L}}$, then TNBR can also be expressed in terms of the transformation from outer roll coordinates to reference, $T_{\text{L/O}}$:

$$\text{TNBR} = \left[\text{I} - \psi_{\text{NBR}}^{\text{L}} \right] T_{\text{L/O}} \quad (\text{B.1-10})$$

Combining Eqs. (B.1-5) to (B.1-10) to eliminate $T_{\text{P/B}}$, $T_{\text{P/LCA}}$ and TNBR one obtains

$$\left[\text{I} - \psi_{\text{NBR}}^{\text{L}} \right] = \left[\text{I} - \psi_{\text{CA}}^{\text{L}} \right] T_{\text{L/P}} T_{\text{P/O}} \left[\text{I} + \psi_{\text{G}}^{\text{O}} \right] T_{\text{O/L}} \quad (\text{B.1-11})$$

or

$$\psi_{\text{NBR}}^{\text{L}} = \psi_{\text{CA}}^{\text{L}} - T_{\text{L/O}} \psi_{\text{G}}^{\text{O}} \quad (\text{B.1-12})$$

where $\psi_{\text{CA}}^{\text{L}}$ is defined below.

In Eq. (B.1-12) $\psi_{\text{NBR}}^{\text{L}}$ represents the error incurred in estimating the transformation from navigation base axes to reference axes, $\psi_{\text{G}}^{\text{O}}$ is a function of IMU errors as defined by Eq. (B.1-7), and $\psi_{\text{CA}}^{\text{L}}$ represents the error in estimating the transformation from reference to platform. The latter is related to the LSF filter output errors as follows

$$\psi_{\text{CA}}^{\text{L}} = \begin{pmatrix} \delta \theta_{2/\text{G}}^{\text{L}} \\ -\delta \theta_{1/\text{G}}^{\text{L}} \\ -\delta \theta_{1/\Omega_{\text{N}}}^{\text{L}} \end{pmatrix} \quad (\text{B.1-13})$$

where

$\delta\theta_1^L$ is the LSF estimation error of the north acceleration

$\delta\theta_2^L$ is the LSF estimation error of the west acceleration

$\delta\dot{\theta}_1^L$ is the LSF estimation error of the north acceleration rate

G is the local gravity acceleration

Ω_N is the north component of the earth's rotation

At the end of Coarse Alignment the misalignments ψ_{NBR}^L are stored in certain dummy states and saved for subsequent use. These misalignments would be used, for instance, when simulating a platform repositioning operation. The right hand side of Eq. (B.1-12) is a linear combination of several IMU errors, and this relationship will be used to generate the storage matrix (as required in Eqs. (3.2-5) and (3.2-6)).

B.2 PLATFORM REPOSITIONING LINEAR ERROR ANALYSIS

When completing a platform repositioning operation, the final platform position is such that the relationship

$$T_{P/B} = TRD \cdot TNBR \quad (B.2-1)$$

is satisfied, where

$T_{P/B}$ = transformation from navigation base to platform computed from measured gimbal angles (see Eq. B.1-2)

TRD = desired transformation from reference to platform,

TNBR = transformation from navigation base to reference determined during Coarse Alignment.

When Eq. (B.2-1) is satisfied, then the gimbal angles for a perfect gimbal train would be ϕ_t , θ_t , and ψ_t . The transformation from outer roll axes (see definition in Section B.1) to platform axes is therefore

$$T_{P/O} = T_{\psi_t} T_{\theta_t} T_{\phi_t} \quad (B.2-2)$$

or

$$T_{P/O} = \begin{bmatrix} \cos \psi_t & -\sin \psi_t & 0 \\ \sin \psi_t & \cos \psi_t & 0 \\ 0 & 0 & 1 \end{bmatrix} \begin{bmatrix} \cos \theta_t & 0 & \sin \theta_t \\ 0 & 1 & 0 \\ -\sin \theta_t & 0 & \cos \theta_t \end{bmatrix} \begin{bmatrix} 1 & 0 & 0 \\ 0 & \cos \phi_t & -\sin \phi_t \\ 0 & \sin \phi_t & \cos \phi_t \end{bmatrix} \quad (B.2-3)$$

and the measured gimbal angles corresponding to the imperfect gimbal train are related to the ideal gimbal angles as follows:

$$\begin{pmatrix} \alpha_m \\ \phi_m \\ \theta_m \\ \psi_m \end{pmatrix} = \begin{pmatrix} 0 \\ \phi_t \\ \theta_t \\ \psi_t \end{pmatrix} + \begin{pmatrix} \text{IRE} \\ \text{ORE} + \text{DP} \tan \theta_t \\ \text{PE-a} \\ \text{AZE} - b + \text{DP}/\cos \theta_t \end{pmatrix} \quad (B.2-4)$$

where

IRE, ORE, PE, AZE are the inner roll, outer roll, pitch, and azimuth resolver errors - including resolver offsets, resolver harmonics and resolver measurement errors and quantization,

a, b, DP are the azimuth, pitch, and outer roll gimbal nonorthogonality errors.

The measured gimbal angles are then used to compute the transformation from navigation base to platform, resulting in

$$T_{P/B} = T_{\psi_t} \left[I + \alpha^6 x \right] T_{\epsilon_t} T_{\phi_t} \left[I + \beta^0 x \right] \quad (B.2-5)$$

or

$$T_{P/B} = T_{P/O} T_{O/L} \left[I + (\alpha^L + \beta^L) x \right] T_{L/O} \quad (B.2-6)$$

where

$$\alpha^L = T_{L/P} T_{\psi_t} \alpha^6 \quad (B.2-7)$$

$$\beta^L = T_{L/O} \beta^0 \quad (B.2-8)$$

$$\alpha^6 = \begin{pmatrix} IRE \\ PE - a \\ AZE - b + DP/\cos \epsilon_t \end{pmatrix} \quad (B.2-9)$$

$$\beta^0 = \begin{pmatrix} ORE + DP \tan \epsilon_t \\ 0 \\ 0 \end{pmatrix} \quad (B.2-10)$$

Now solving Eq. (B.2-1) for the desired platform orientation, TRD, and subsequently substituting Eqs. (B.2-5) and (B.1-10) into the result yields

$$A = T_{P/B} T_{NBR}^T \quad (B.2-11)$$

$$= T_{P/L} \left[I + (\alpha^L + \beta^L) x \right] T_{L/O} T_{O/L} \left[I + \psi_{NBR}^L x \right] \quad (B.2-12)$$

In Eq. (B.2-12), TRD and $T_{P/L}$ are the desired and the resulting transformation matrices from reference to platform, respectively. Therefore, the initial platform misalignment resulting from a cluster repositioning is

$$\psi_{CR}^L = \alpha^L + \beta^L + \psi_{NBR}^R \quad (B.2-13)$$

or, after substituting Eqs. (B.1-12), (B.1-7), (B.2-9), and (B.2-10)

$$\psi_{CR}^L = T_{L/P}^T \psi_t \begin{pmatrix} IRE \\ PE - a \\ AZE - b + DP/\cos \theta_t \end{pmatrix} - T_{L/O} \begin{pmatrix} IRE - DP \tan \theta_t \\ PE - a \\ AZE - b + DP \end{pmatrix} + \psi_{CA}^L \quad (B.2-14)$$

Note that when $\psi_t = \theta_t = \phi = 0$ then the error in repositioning the platform is exactly equal to the error in estimating the transformation from reference to platform during Coarse Alignment, which is what one would expect.

In the covariance simulation program a platform repositioning can therefore be simulated by an instantaneous change in platform orientation followed by an assignment of initial platform misalignments according to Eq. (B.2-14).

APPENDIX C
ERROR CONTRIBUTION TIME HISTORIES:
DEORBIT TO 20,000 FT

This appendix presents the time histories associated with the error budget results summarized in Section 4.4.1. The data is presented in tabular form with each table indicating the rms errors in position and velocity, and the rms value of the platform alignment estimates, in both the R (runway) and V (relative velocity) coordinate frames which result from a specific error source or group of errors.

The time points in each table begin at deorbit burn and are printed at appropriate time intervals down to MLS acquisition. Time points are also included just before and after each external navigation aid is activated. Thus there are two rows of data for each of the following times (see Table 4.1-1):

$$T_{\text{DRAG}} = 1375.19 \text{ sec}$$

$$T_{\text{TACAN}} = 2239.19 \text{ sec}$$

$$T_{\text{BA}} = 2496.47 \text{ sec}$$

The final row in each table presents the rms errors just prior to the first MLS measurements at an altitude of 20,000 ft:

$$T_{\text{MLS}} = 2723.03 \text{ sec}$$

In addition, the rms value of each of states 10 through 12 is given at 20,000 ft. The magnitudes and mathematical

THE ANALYTIC SCIENCES CORPORATION

description of the error sources are given in Section 4.3.

Units are in feet, fps, and radians.

GROUP 1: INITIAL CONDITION ERRORS POSITIONS AND VELOCITIES

TIME	POSITION ESTIMATE R	POSITION ESTIMATE D	ERROR C	VELOCITY ESTIMATE R	VELOCITY ESTIMATE D	ERROR C	PLATFORM TILT R	PLATFORM TILT D	ESTIMATE D	ERROR C
20.55	9.593E+03	8.466E+02	6.000E+03	6.625E+00	1.492E+00	9.743E+00	1.000E-10	1.000E-10	1.000E-10	1.000E-10
7.75.19	7.424E+03	8.285E+02	8.757E+03	1.019E+01	1.275E+00	9.446E+00	1.000E-10	1.000E-10	1.000E-10	1.000E-10
7.16.19	7.161E+03	8.279E+02	8.226E+03	9.981E+00	1.260E+00	9.374E+00	1.000E-10	1.000E-10	1.000E-10	1.000E-10
6.53.51	6.709E+03	8.252E+02	8.559E+03	1.031E+01	1.265E+00	9.374E+00	1.000E-10	1.000E-10	1.000E-10	1.000E-10
6.51.81	6.182E+03	8.271E+02	8.862E+03	1.074E+01	1.265E+00	9.374E+00	1.000E-10	1.000E-10	1.000E-10	1.000E-10
5.56.46	5.564E+03	8.317E+02	9.125E+03	1.074E+01	1.265E+00	9.374E+00	1.000E-10	1.000E-10	1.000E-10	1.000E-10
4.89.47	4.890E+03	8.340E+02	9.453E+03	1.133E+01	1.415E+00	7.874E+00	1.000E-10	1.000E-10	1.000E-10	1.000E-10
4.16.79	4.155E+03	8.313E+02	9.871E+03	1.234E+01	1.508E+00	7.764E+00	1.000E-10	1.000E-10	1.000E-10	1.000E-10
3.51.11	3.415E+03	8.313E+02	1.079E+04	1.441E+01	1.605E+00	7.475E+00	1.000E-10	1.000E-10	1.000E-10	1.000E-10
2.67.43	2.678E+03	8.305E+02	1.067E+04	1.525E+01	1.651E+00	6.645E+00	1.000E-10	1.000E-10	1.000E-10	1.000E-10
2.54.87	2.177E+03	8.323E+02	1.087E+04	1.574E+01	1.702E+00	5.645E+00	1.000E-10	1.000E-10	1.000E-10	1.000E-10
1.16.31	1.704E+03	8.371E+02	1.100E+04	1.624E+01	1.765E+00	4.875E+00	1.000E-10	1.000E-10	1.000E-10	1.000E-10
1.27.0E	1.270E+03	8.435E+02	1.105E+04	1.654E+01	1.765E+00	4.875E+00	1.000E-10	1.000E-10	1.000E-10	1.000E-10
0.84.5E	0.845E+02	8.492E+02	1.105E+04	1.654E+01	1.810E+00	3.703E+00	1.000E-10	1.000E-10	1.000E-10	1.000E-10
3.39.19	7.714E+02	5.782E+02	1.876E+03	8.646E+01	1.810E+00	3.462E+00	1.000E-10	1.000E-10	1.000E-10	1.000E-10
35.03	1.289E+03	1.186E+03	5.294E+02	8.951E+00	1.477E+00	8.215E+00	1.000E-10	1.000E-10	1.000E-10	1.000E-10
6.96.47	1.699E+03	1.012E+03	7.266E+02	5.332E+00	7.225E+00	5.703E+00	1.000E-10	1.000E-10	1.000E-10	1.000E-10
4.42.55	5.599E+02	1.248E+03	4.666E+02	6.718E+00	7.295E+00	5.372E+00	1.000E-10	1.000E-10	1.000E-10	1.000E-10
4.42.55	4.666E+02	8.021E+02	3.584E+02	7.012E+00	9.076E+00	4.312E+00	1.000E-10	1.000E-10	1.000E-10	1.000E-10
4.61.6E	4.616E+02	4.329E+02	3.685E+02	7.045E+00	8.840E+00	2.827E+00	1.000E-10	1.000E-10	1.000E-10	1.000E-10
4.42.3E	4.423E+02	2.174E+02	4.136E+02	6.693E+00	7.124E+00	2.241E+00	1.000E-10	1.000E-10	1.000E-10	1.000E-10
4.00.3E	4.003E+02	2.285E+02	4.641E+02	5.946E+00	5.609E+00	1.841E+00	1.000E-10	1.000E-10	1.000E-10	1.000E-10
3.34.71	3.347E+02	2.600E+02	5.246E+02	5.284E+00	5.037E+00	1.474E+00	1.000E-10	1.000E-10	1.000E-10	1.000E-10
3.30.79	3.307E+02	2.600E+02	5.246E+02	5.284E+00	5.037E+00	1.474E+00	1.000E-10	1.000E-10	1.000E-10	1.000E-10
3.30.79	3.307E+02	2.600E+02	5.246E+02	5.284E+00	5.037E+00	1.474E+00	1.000E-10	1.000E-10	1.000E-10	1.000E-10
3.30.79	3.307E+02	2.600E+02	5.246E+02	5.284E+00	5.037E+00	1.474E+00	1.000E-10	1.000E-10	1.000E-10	1.000E-10

TIME	U	V	W	U	V	W	U	V	W
20.55	1.036E+03	1.125E+04	1.039E+03	1.181E+01	1.126E+00	1.040E+00	1.000E-10	1.000E-10	1.000E-10
27.55	1.220E+03	1.142E+04	7.453E+02	1.347E+01	1.091E-01	1.025E+00	1.000E-05	1.000E-05	1.000E-05
37.55	1.035E+04	1.086E+04	7.499E+02	1.387E+01	9.971E-01	1.029E+00	1.162E-05	1.162E-05	1.162E-05
43.51	9.127E+02	1.084E+04	7.828E+02	1.344E+01	1.050E+00	1.039E+00	1.991E-05	1.991E-05	1.991E-05
47.51	1.047E+03	1.077E+04	2.178E+03	1.344E+01	1.511E+00	1.070E+00	2.014E-05	2.014E-05	2.014E-05
50.15	1.179E+03	1.046E+04	2.056E+03	1.365E+01	2.090E+00	1.117E+00	3.914E-05	3.914E-05	3.914E-05
52.47	1.179E+03	1.046E+04	2.056E+03	1.365E+01	2.090E+00	1.117E+00	5.120E-05	5.120E-05	5.120E-05
54.15	1.045E+03	1.019E+04	2.257E+03	1.512E+01	3.212E+00	1.203E+00	7.251E-05	7.251E-05	7.251E-05
56.79	1.045E+03	1.019E+04	2.257E+03	1.512E+01	3.212E+00	1.203E+00	9.069E-05	9.069E-05	9.069E-05
59.43	8.430E+02	1.080E+04	2.550E+02	1.592E+01	3.307E+00	1.620E+00	7.069E-05	7.069E-05	7.069E-05
63.43	7.157E+02	1.090E+04	2.550E+02	1.592E+01	3.307E+00	1.620E+00	7.580E-05	7.580E-05	7.580E-05
65.11	5.900E+02	1.101E+04	1.420E+03	1.621E+01	2.852E+00	2.251E+00	7.580E-05	7.580E-05	7.580E-05
67.54	4.527E+02	1.069E+04	3.119E+03	1.648E+01	2.744E+00	2.294E+00	7.445E-05	7.445E-05	7.445E-05
70.31	3.001E+02	1.043E+04	3.159E+03	1.668E+01	2.765E+00	2.182E+00	7.100E-05	7.100E-05	7.100E-05
73.19	1.525E+02	1.049E+03	3.618E+03	1.657E+01	2.762E+00	1.995E+00	6.740E-05	6.740E-05	6.740E-05
75.19	6.401E+02	1.042E+03	3.170E+02	8.447E+00	3.409E+00	2.874E+00	7.402E-05	7.402E-05	7.402E-05
77.03	1.249E+02	1.042E+03	1.201E+02	5.962E+00	3.379E+00	2.745E+00	7.402E-05	7.402E-05	7.402E-05
79.47	1.595E+02	1.575E+02	1.210E+03	5.330E+00	3.055E+00	8.531E+00	1.075E-04	1.075E-04	1.075E-04
82.47	4.453E+02	2.504E+02	1.325E+02	6.719E+00	1.649E+00	9.780E+00	1.249E-04	1.249E-04	1.249E-04
84.55	4.453E+02	1.635E+02	8.630E+02	7.041E+00	1.497E+00	9.780E+00	1.653E-04	1.653E-04	1.653E-04
86.61	4.603E+02	2.837E+02	4.939E+02	6.690E+00	1.487E+00	7.322E+00	1.822E-04	1.822E-04	1.822E-04
88.71	4.414E+02	3.690E+02	2.881E+02	5.690E+00	1.364E+00	5.747E+00	1.987E-04	1.987E-04	1.987E-04
90.79	3.999E+02	4.151E+02	3.092E+02	5.279E+00	1.137E+00	4.150E+00	6.709E-04	6.709E-04	6.709E-04
93.03	1.796E+02	4.315E+02	9.021E+01	5.279E+00	3.858E+00	4.150E+00	9.089E-04	9.089E-04	9.089E-04

ADDITIONAL STATE ESTIMATES AT 20,000 FY (10 TO NF)
1.835E+02 9.807E+01 4.076E-03

REPRODUCIBILITY OF THE
ORIGINAL PAGE IS POOR

GROUP 1 INITIAL CONDITION ERRORS MISALIGNMENTS									
TIME	POSITION R	ESTIMATE D	ERROR C	VELOCITY R	ESTIMATE D	ERROR C	PLATFORM R	TILT D	ESTIMATE C
120.55	1.000E-10	1.000E-10	1.000E-10	1.000E-10	1.000E-10	1.000E-10	1.379E-03	1.379E-03	1.379E-03
1375.19	1.734E+02	4.658E+02	1.041E+03	6.095E-01	1.637E-01	1.483E+00	1.379E-03	1.379E-03	1.379E-03
1375.19	4.630E+02	4.630E+02	4.010E+02	3.047E-01	1.637E-01	1.483E+00	1.379E-03	1.379E-03	1.379E-03
1463.51	5.479E+02	4.515E+02	4.089E+02	7.735E-01	5.723E-01	1.197E+00	1.379E-03	1.379E-03	1.379E-03
1551.83	5.520E+02	4.830E+02	4.993E+02	4.830E+00	3.740E+00	2.354E+00	1.379E-03	1.379E-03	1.379E-03
1640.15	5.635E+02	5.566E+02	7.046E+02	3.201E+00	5.566E+00	2.354E+00	1.379E-03	1.379E-03	1.379E-03
1728.47	5.710E+02	9.305E+02	7.776E+02	4.667E+00	5.566E+00	2.354E+00	1.379E-03	1.379E-03	1.379E-03
1816.79	5.834E+02	1.400E+03	9.602E+02	4.481E+00	6.932E+00	7.125E+00	1.379E-03	1.379E-03	1.379E-03
1905.11	5.934E+02	1.400E+03	5.402E+02	4.571E+00	8.117E+00	1.125E+00	1.379E-03	1.379E-03	1.379E-03
1993.43	6.180E+02	1.584E+03	3.924E+02	4.817E+00	9.505E+00	2.101E+00	1.379E-03	1.379E-03	1.379E-03
2054.47	6.346E+02	1.807E+03	3.924E+02	5.189E+00	1.135E+01	3.508E+00	1.379E-03	1.379E-03	1.379E-03
2116.31	6.491E+02	1.807E+03	3.924E+02	5.609E+00	1.330E+01	3.508E+00	1.379E-03	1.379E-03	1.379E-03
2177.75	6.685E+02	2.086E+03	5.658E+02	5.622E+00	1.405E+01	2.976E+00	1.379E-03	1.379E-03	1.379E-03
2239.19	6.850E+02	1.720E+03	1.720E+02	5.115E+00	1.268E+01	2.976E+00	1.379E-03	1.379E-03	1.379E-03
2300.63	8.520E+02	1.640E+02	1.074E+02	7.361E+00	7.862E+00	3.239E+00	1.379E-03	1.379E-03	1.379E-03
2435.03	1.020E+03	1.434E+02	3.067E+02	7.233E+00	7.862E+00	3.239E+00	1.379E-03	1.379E-03	1.379E-03
2496.47	3.233E+02	1.830E+02	1.409E+02	5.901E+00	6.541E+00	3.173E+00	1.379E-03	1.379E-03	1.379E-03
2542.55	2.043E+02	2.043E+02	1.331E+02	5.715E+00	6.000E+00	3.193E+00	1.379E-03	1.379E-03	1.379E-03
2588.63	2.613E+02	1.806E+02	1.690E+02	5.435E+00	5.332E+00	3.432E+00	1.379E-03	1.379E-03	1.379E-03
2634.71	2.256E+02	1.263E+02	1.909E+02	4.975E+00	4.582E+00	3.613E+00	1.379E-03	1.379E-03	1.379E-03
2680.79	1.544E+02	6.690E+01	1.709E+02	4.400E+00	3.908E+00	3.583E+00	1.379E-03	1.379E-03	1.379E-03
2723.03	5.524E+01	6.763E+01	4.593E+01	3.888E+00	2.908E+00	3.137E+00	1.379E-03	1.379E-03	1.379E-03
TIME	U	V	W	U	V	W	U	V	W
120.55	1.000E-10	1.000E-10	1.000E-10	1.000E-10	1.000E-10	1.000E-10	1.379E-03	1.379E-03	1.379E-03
1375.19	7.390E+02	7.512E+02	4.748E+02	1.465E+00	1.552E-01	1.547E-01	1.379E-03	1.379E-03	1.379E-03
1375.19	6.250E+02	2.109E+02	4.748E+02	1.000E+00	5.701E-01	1.454E-01	1.379E-03	1.379E-03	1.379E-03
1463.51	6.421E+02	2.221E+02	4.697E+02	1.315E+00	4.650E-01	1.943E+00	1.379E-03	1.379E-03	1.379E-03
1551.83	6.995E+02	2.761E+02	4.711E+02	2.013E+00	1.040E-01	3.641E+00	1.379E-03	1.379E-03	1.379E-03
1640.15	7.633E+02	2.621E+02	5.165E+02	5.080E+00	1.040E+00	5.414E+00	1.379E-03	1.379E-03	1.379E-03
1728.47	7.945E+02	6.065E+02	6.270E+02	5.080E+00	1.658E+00	6.146E+00	1.379E-03	1.379E-03	1.379E-03
1816.79	7.744E+02	7.060E+02	8.363E+02	4.515E+00	1.576E+00	6.146E+00	1.379E-03	1.379E-03	1.379E-03
1905.11	7.257E+02	6.610E+02	1.103E+03	4.515E+00	1.728E+00	6.146E+00	1.379E-03	1.379E-03	1.379E-03
1993.43	6.771E+02	4.610E+02	1.394E+03	4.363E+00	1.959E+00	6.146E+00	1.379E-03	1.379E-03	1.379E-03
2054.47	6.511E+02	2.176E+02	1.606E+03	4.515E+00	2.435E+00	6.146E+00	1.379E-03	1.379E-03	1.379E-03
2116.31	6.269E+02	2.463E+02	1.814E+03	5.306E+00	3.538E+00	9.017E+00	1.379E-03	1.379E-03	1.379E-03
2177.75	6.345E+02	7.249E+02	1.998E+03	5.306E+00	5.722E+00	1.240E+01	1.379E-03	1.379E-03	1.379E-03
2239.19	6.434E+02	6.741E+02	2.412E+03	5.913E+00	5.022E+00	1.240E+01	1.379E-03	1.379E-03	1.379E-03
2293.03	8.487E+02	4.304E+02	1.668E+03	5.913E+00	4.781E+00	1.240E+01	1.379E-03	1.379E-03	1.379E-03
2435.03	1.016E+03	3.163E+02	1.668E+03	7.185E+00	3.466E+00	6.220E+00	1.379E-03	1.379E-03	1.379E-03
2496.47	3.219E+02	1.012E+02	1.512E+02	5.875E+00	3.466E+00	6.220E+00	1.379E-03	1.379E-03	1.379E-03
2542.55	2.472E+02	1.414E+02	2.002E+02	5.875E+00	3.466E+00	6.220E+00	1.379E-03	1.379E-03	1.379E-03
2588.63	2.606E+02	1.850E+02	2.002E+02	5.875E+00	3.466E+00	6.220E+00	1.379E-03	1.379E-03	1.379E-03
2634.71	2.250E+02	2.021E+02	1.685E+02	5.422E+00	3.954E+00	5.586E+00	1.379E-03	1.379E-03	1.379E-03
2680.79	1.563E+02	2.021E+02	1.685E+02	4.966E+00	4.005E+00	4.182E+00	1.379E-03	1.379E-03	1.379E-03
2723.03	5.530E+01	4.987E+01	6.474E+01	3.888E+00	2.908E+00	3.695E+00	1.379E-03	1.379E-03	1.379E-03

ADDITIONAL STATE ESTIMATES AT 20.000 FT (10 TO NF)
4.749E+01 5.722E+00 2.846E-03

THE ANALYTIC SCIENCES CORPORATION

GROUP 1 PSEUDO-ALTITUDE MEASUREMENT NOISE (MULTIPLY BY 0.25)

TIME	POSITION ESTIMATE ERROR R	VELOCITY ESTIMATE ERROR R	PLATFORM TILT ESTIMATE ERROR R	PLATFORM TILT ESTIMATE ERROR C	VELOCITY ESTIMATE ERROR C	PLATFORM TILT ESTIMATE ERROR C
120.55	1.000E-10	1.000E-10	1.000E-10	1.000E-10	1.000E-10	1.000E-10
1375.19	1.238E-05	1.377E-05	1.213E-08	1.075E-07	1.000E-10	1.000E-10
1375.19	2.613E+03	3.811E+03	3.668E-01	2.550E+00	1.000E-10	1.000E-10
1463.51	1.731E+01	1.741E+00	2.065E-01	1.235E+00	1.471E-04	3.976E-04
1551.81	1.539E+03	1.584E+00	3.062E-01	1.393E+00	9.503E-05	2.807E-04
1551.81	1.611E+03	3.071E+00	3.959E-01	2.390E+00	8.738E-05	5.946E-04
1728.47	1.668E+03	2.252E+03	4.191E-01	3.390E+00	5.751E-05	6.722E-04
1816.79	1.600E+03	2.540E+02	5.738E-01	1.260E+00	6.475E-05	1.456E-04
1905.11	1.600E+03	2.540E+02	7.153E-01	1.260E+00	7.339E-05	5.139E-04
1993.43	1.611E+03	2.937E+00	7.337E-01	1.271E-01	7.190E-05	4.347E-04
2074.87	1.611E+03	7.337E+00	6.550E-01	1.250E+00	6.454E-05	3.932E-04
2116.75	1.631E+03	8.181E+00	7.184E-01	2.019E+00	5.681E-05	3.675E-04
2177.75	1.782E+03	8.422E+00	9.331E-01	2.504E+00	5.977E-05	3.928E-04
2210.19	1.796E+03	8.228E+00	1.060E+00	2.806E+00	5.977E-05	3.928E-04
2239.19	1.553E+03	5.822E+00	1.181E+00	1.395E+00	5.120E-05	3.043E-04
2435.03	2.487E+02	5.033E+00	1.181E+00	1.395E+00	1.281E-04	2.818E-04
2435.03	2.487E+02	2.398E+00	2.335E+00	1.240E+00	1.247E-04	2.818E-04
2496.47	3.020E+02	3.293E+00	1.500E+00	5.730E-01	8.209E-05	2.633E-04
2496.47	1.781E+02	2.242E+00	1.532E+00	4.750E-01	7.505E-05	2.633E-04
2552.55	1.191E+02	2.242E+00	1.532E+00	4.750E-01	6.575E-05	2.633E-04
2552.55	8.715E+01	3.290E+01	1.532E+00	5.203E-01	5.575E-05	2.633E-04
2634.71	1.191E+01	1.247E+00	1.052E+00	5.203E-01	5.575E-05	2.633E-04
2634.71	4.342E+01	1.555E+00	9.021E-01	5.137E-01	5.575E-05	2.633E-04
2680.79	4.342E+01	1.555E+00	9.021E-01	5.137E-01	5.575E-05	2.633E-04
2723.03	2.103E+01	1.376E+00	9.531E-01	5.045E-01	5.575E-05	2.633E-04
2723.03	4.652E+01	1.376E+00	9.531E-01	5.045E-01	5.575E-05	2.633E-04
120.55	1.000E-10	1.000E-10	1.000E-10	1.000E-10	1.000E-10	1.000E-10
1375.19	5.447E-05	1.000E-10	1.000E-10	1.000E-10	1.000E-10	1.000E-10
1375.19	4.603E+03	1.064E+00	1.064E+00	1.115E-08	1.000E-10	1.000E-10
1463.51	2.276E+02	1.668E+00	3.777E-01	2.665E-01	1.476E-05	1.320E-04
1551.81	3.164E+02	2.002E+00	3.705E-01	2.003E-01	3.443E-05	1.320E-04
1551.81	7.394E+02	3.810E+00	7.059E-01	2.003E-01	4.143E-05	1.320E-04
1728.47	2.500E+03	6.440E+00	1.017E+00	3.531E-01	4.273E-05	1.190E-04
1728.47	2.500E+03	7.059E+00	6.217E-01	4.069E-01	4.273E-05	1.190E-04
1816.79	2.635E+03	7.059E+00	6.217E-01	4.069E-01	4.273E-05	1.190E-04
1816.79	1.734E+03	7.059E+00	6.217E-01	4.069E-01	4.273E-05	1.190E-04
1905.11	1.734E+03	7.059E+00	6.217E-01	4.069E-01	4.273E-05	1.190E-04
1905.11	1.734E+03	7.059E+00	6.217E-01	4.069E-01	4.273E-05	1.190E-04
2074.87	1.800E+03	7.059E+00	6.217E-01	4.069E-01	4.273E-05	1.190E-04
2074.87	1.800E+03	7.059E+00	6.217E-01	4.069E-01	4.273E-05	1.190E-04
2116.75	1.800E+03	7.059E+00	6.217E-01	4.069E-01	4.273E-05	1.190E-04
2116.75	1.800E+03	7.059E+00	6.217E-01	4.069E-01	4.273E-05	1.190E-04
2177.75	1.800E+03	7.059E+00	6.217E-01	4.069E-01	4.273E-05	1.190E-04
2177.75	1.800E+03	7.059E+00	6.217E-01	4.069E-01	4.273E-05	1.190E-04
2239.19	1.800E+03	7.059E+00	6.217E-01	4.069E-01	4.273E-05	1.190E-04
2239.19	1.800E+03	7.059E+00	6.217E-01	4.069E-01	4.273E-05	1.190E-04
2435.03	1.800E+03	7.059E+00	6.217E-01	4.069E-01	4.273E-05	1.190E-04
2435.03	1.800E+03	7.059E+00	6.217E-01	4.069E-01	4.273E-05	1.190E-04
2496.47	2.045E+02	3.045E+02	1.532E+00	1.532E+00	1.532E+00	1.532E+00
2496.47	2.045E+02	3.045E+02	1.532E+00	1.532E+00	1.532E+00	1.532E+00
2552.55	2.045E+02	3.045E+02	1.532E+00	1.532E+00	1.532E+00	1.532E+00
2552.55	2.045E+02	3.045E+02	1.532E+00	1.532E+00	1.532E+00	1.532E+00
2598.63	2.045E+02	3.045E+02	1.532E+00	1.532E+00	1.532E+00	1.532E+00
2598.63	2.045E+02	3.045E+02	1.532E+00	1.532E+00	1.532E+00	1.532E+00
2634.71	2.045E+02	3.045E+02	1.532E+00	1.532E+00	1.532E+00	1.532E+00
2634.71	2.045E+02	3.045E+02	1.532E+00	1.532E+00	1.532E+00	1.532E+00
2680.79	2.045E+02	3.045E+02	1.532E+00	1.532E+00	1.532E+00	1.532E+00
2680.79	2.045E+02	3.045E+02	1.532E+00	1.532E+00	1.532E+00	1.532E+00
2723.03	2.045E+02	3.045E+02	1.532E+00	1.532E+00	1.532E+00	1.532E+00
2723.03	2.045E+02	3.045E+02	1.532E+00	1.532E+00	1.532E+00	1.532E+00

ADDITIONAL STATE ESTIMATES AT 20,000 FT (10 TO NF)
2.263E+01 1.864E+01 4.645E-04

GROUP 1 TACAN BEARING MEASUREMENT NOISE

TIME	POSITION R	ESTIMATE D	ERROR C	VELOCITY R	ESTIMATE D	ERROR C	PLATFORM R	TILT D	ESTIMATE D	ERROR C
2239.19	1.000E-10	1.000E-10	1.000E-10	1.000E-10	1.000E-10	1.000E-10	1.000E-10	1.000E-10	1.000E-10	1.000E-10
2239.19	2.717E+01	5.000E+03	4.000E+03	2.000E+02	1.000E+01	5.000E+01	5.700E+04	1.420E-05	4.310E-05	4.310E-05
2435.03	2.441E+02	3.000E+02	5.000E+02	6.000E+01	1.220E+00	3.200E+02	1.220E-05	1.220E-05	7.650E-05	7.650E-05
2496.47	2.433E+02	5.232E+02	2.240E+01	3.240E+01	2.230E+00	9.000E+01	1.410E-05	1.130E-05	1.400E-04	1.400E-04
2496.47	7.314E+01	4.000E+02	4.000E+02	7.670E+01	2.000E+00	2.500E+01	2.210E-05	1.700E-05	1.590E-04	1.590E-04
2542.55	2.367E+01	5.436E+02	4.600E+01	1.320E+00	2.000E+00	2.100E+01	1.510E-05	3.220E-06	2.050E-04	2.050E-04
2588.63	3.070E+01	4.600E+02	2.317E+01	1.167E+00	2.570E+00	6.000E+01	1.000E-05	5.520E-06	1.620E-04	1.620E-04
2614.71	3.000E+01	3.217E+02	3.700E+01	0.000E+00	2.000E+00	1.310E+01	1.290E-05	8.150E-06	1.170E-04	1.170E-04
2680.79	5.105E+01	1.613E+02	0.274E+01	6.710E+01	1.361E+00	2.000E+01	1.550E-05	1.380E-05	9.670E-05	9.670E-05
2723.03	6.022E+01	8.691E+01	1.206E+02	4.462E+01	6.610E-01	4.600E+01	3.170E-05	1.500E-05	6.780E-05	6.780E-05
TIME	U	V	W	U	V	W	U	V	W	W
2239.19	1.000E-10	1.000E-10	1.000E-10	1.000E-10	1.000E-10	1.000E-10	1.000E-10	1.000E-10	1.000E-10	1.000E-10
2239.19	2.255E+01	1.103E+03	4.076E+03	1.242E+01	3.610E+00	9.420E+00	5.730E+04	8.480E-05	8.520E-06	8.520E-06
2435.03	2.422E+02	1.770E+01	3.000E+02	6.277E+01	1.600E+02	1.220E+00	1.220E-05	7.650E-05	1.290E-05	1.290E-05
2496.47	2.410E+02	1.743E+02	4.947E+02	3.353E+01	7.341E-01	2.110E+00	1.400E-05	1.300E-04	6.170E-05	6.170E-05
2496.47	7.200E+01	1.230E+02	4.722E+02	7.710E+01	5.210E-01	2.030E+00	2.360E-05	1.400E-04	5.550E-05	5.550E-05
2542.55	2.394E+01	4.740E+01	5.385E+02	1.327E+00	4.820E-01	2.810E+00	1.620E-05	1.900E-04	5.120E-05	5.120E-05
2588.63	3.917E+01	7.970E+01	4.594E+02	1.171E+00	4.641E-01	2.536E+00	9.770E-05	1.590E-04	3.570E-05	3.570E-05
2634.71	3.507E+01	8.842E+01	3.116E+02	8.849E+01	4.921E-01	1.973E+00	1.263E-05	1.140E-04	2.900E-05	2.900E-05
2680.79	5.103E+01	1.043E+02	1.483E+02	6.730E+01	5.100E-01	1.293E+00	1.551E-05	9.260E-05	3.100E-05	3.100E-05
2723.03	6.020E+01	1.220E+02	8.349E+01	4.467E+01	5.416E-01	6.026E+01	3.170E-05	5.940E-05	3.590E-05	3.590E-05

ADDITIONAL STATE ESTIMATES AT 20.000 FT (10 TO NF)
6.404E+01 1.223E+01 1.799E-03

GROUP 2 ACCELEROMETER BIASES

TIME	POSITION ESTIMATE ERROR R	VELOCITY ESTIMATE V	PLATFOM TILT ESTIMATE ERROR D	W	U	V	W	U	V	W
120.55	0.000E+00	0.000E+00	0.000E+00	0.000E+00	0.000E+00	0.000E+00	0.000E+00	0.000E+00	0.000E+00	0.000E+00
1375.19	1.173E+03	1.046E+03	1.340E+03	1.340E+03	1.340E+03	1.340E+03	1.340E+03	1.340E+03	1.340E+03	1.340E+03
1375.19	1.793E+03	1.046E+03	1.340E+03	1.340E+03	1.340E+03	1.340E+03	1.340E+03	1.340E+03	1.340E+03	1.340E+03
1463.51	1.089E+03	1.116E+03	1.340E+03	1.340E+03	1.340E+03	1.340E+03	1.340E+03	1.340E+03	1.340E+03	1.340E+03
1551.83	1.943E+03	1.178E+03	1.340E+03	1.340E+03	1.340E+03	1.340E+03	1.340E+03	1.340E+03	1.340E+03	1.340E+03
1640.15	1.814E+03	1.241E+03	1.340E+03	1.340E+03	1.340E+03	1.340E+03	1.340E+03	1.340E+03	1.340E+03	1.340E+03
1720.47	1.624E+03	1.329E+03	1.340E+03	1.340E+03	1.340E+03	1.340E+03	1.340E+03	1.340E+03	1.340E+03	1.340E+03
1816.79	1.493E+03	1.309E+03	1.340E+03	1.340E+03	1.340E+03	1.340E+03	1.340E+03	1.340E+03	1.340E+03	1.340E+03
1903.43	1.167E+03	1.412E+03	1.340E+03	1.340E+03	1.340E+03	1.340E+03	1.340E+03	1.340E+03	1.340E+03	1.340E+03
2054.87	9.400E+02	1.464E+03	1.340E+03	1.340E+03	1.340E+03	1.340E+03	1.340E+03	1.340E+03	1.340E+03	1.340E+03
2110.31	6.363E+02	1.541E+03	1.340E+03	1.340E+03	1.340E+03	1.340E+03	1.340E+03	1.340E+03	1.340E+03	1.340E+03
2179.19	3.627E+02	1.562E+03	1.340E+03	1.340E+03	1.340E+03	1.340E+03	1.340E+03	1.340E+03	1.340E+03	1.340E+03
2239.49	3.645E+02	1.502E+03	1.340E+03	1.340E+03	1.340E+03	1.340E+03	1.340E+03	1.340E+03	1.340E+03	1.340E+03
2315.03	7.560E+02	1.135E+03	1.340E+03	1.340E+03	1.340E+03	1.340E+03	1.340E+03	1.340E+03	1.340E+03	1.340E+03
2406.47	1.176E+03	4.237E+02	1.340E+03	1.340E+03	1.340E+03	1.340E+03	1.340E+03	1.340E+03	1.340E+03	1.340E+03
2492.55	3.153E+02	5.700E+02	1.340E+03	1.340E+03	1.340E+03	1.340E+03	1.340E+03	1.340E+03	1.340E+03	1.340E+03
2584.01	3.327E+02	1.427E+02	1.340E+03	1.340E+03	1.340E+03	1.340E+03	1.340E+03	1.340E+03	1.340E+03	1.340E+03
2640.79	2.201E+02	1.339E+02	1.340E+03	1.340E+03	1.340E+03	1.340E+03	1.340E+03	1.340E+03	1.340E+03	1.340E+03
2723.03	7.575E+01	1.004E+02	1.340E+03	1.340E+03	1.340E+03	1.340E+03	1.340E+03	1.340E+03	1.340E+03	1.340E+03

ADDITIONAL STATE ESTIMATES AT 20.000 FT (15 TO NF)

1.671E+01 1.508E-03

THE ANALYTIC SCIENCES CORPORATION

GROUP 5 ACCELEROMETER NONORTHOGONALITIES

TIME	POSITION P	ESTIMATE D	ERROR C	VELOCITY R	ESTIMATE D	PROP C	PLATFORM R	TILT D	ESTIMATE D	ERROR C
120.55	0.000E+00	1.000E+00	0.000E+00	0.000E+00	0.000E+00	0.000E+00	0.000E+00	0.000E+00	0.000E+00	0.000E+00
1375.19	1.120E+01	1.755E+01	1.413E+01	1.348E+02	1.407E+03	2.072E+02	0.000E+00	0.000E+00	0.000E+00	0.000E+00
1375.19	1.740E+01	4.901E+01	9.510E+00	7.771E+03	5.314E+04	2.111E+02	4.724E+07	1.977E+06	2.000E+00	0.000E+00
1403.51	1.920E+01	1.247E+02	9.373E+00	2.774E+02	7.379E+04	2.111E+02	7.317E+07	1.986E+06	2.000E+00	0.000E+00
1551.83	1.705E+01	1.250E+00	9.779E+00	9.872E+02	1.200E+03	1.529E+02	8.946E+06	2.607E+06	3.924E+07	3.924E+07
1640.15	1.518E+01	1.404E+00	1.031E+01	1.652E+01	2.049E+03	1.319E+02	1.019E+06	3.433E+06	4.397E+07	4.397E+07
1728.47	1.394E+01	1.775E+00	7.909E+00	2.941E+01	3.063E+03	2.347E+02	1.072E+06	4.578E+06	4.469E+07	4.469E+07
1816.79	1.612E+01	2.272E+00	7.640E+00	3.020E+01	4.208E+03	3.424E+02	1.066E+06	6.284E+06	4.224E+07	4.224E+07
1905.11	2.017E+01	3.044E+00	1.212E+01	3.020E+01	6.253E+03	4.387E+02	1.075E+06	8.364E+06	4.010E+07	4.010E+07
1993.43	2.454E+01	3.820E+00	2.060E+01	3.020E+01	8.067E+03	4.387E+02	1.164E+06	1.044E+07	3.959E+07	3.959E+07
2054.37	2.754E+01	4.015E+00	2.875E+01	3.442E+01	1.000E+04	4.387E+02	1.259E+06	1.183E+07	4.421E+07	4.421E+07
2116.31	3.017E+01	3.470E+00	3.834E+01	3.742E+01	1.241E+04	7.701E+02	1.338E+06	1.318E+07	5.755E+07	5.755E+07
2177.75	3.291E+01	1.709E+00	4.847E+01	4.055E+01	1.254E+04	9.069E+02	1.343E+06	1.443E+07	7.765E+07	7.765E+07
2239.19	3.529E+01	9.704E+01	5.807E+01	4.171E+01	1.294E+04	6.779E+02	1.318E+06	1.500E+07	7.610E+07	7.610E+07
2300.53	3.724E+01	2.515E+00	1.151E+01	4.502E+01	1.251E+04	4.322E+02	1.420E+06	1.587E+07	8.566E+07	8.566E+07
2435.13	3.123E+01	4.337E+01	7.846E+01	4.815E+01	2.500E+04	1.436E+01	1.067E+06	1.898E+07	7.809E+06	7.809E+06
2496.47	1.244E+01	3.750E+01	1.022E+01	3.926E+01	3.716E+01	1.624E+01	8.857E+05	2.044E+05	1.649E+05	1.649E+05
2502.47	1.244E+01	3.750E+01	1.022E+01	3.926E+01	3.716E+01	1.624E+01	8.857E+05	2.044E+05	1.649E+05	1.649E+05
2562.55	1.582E+01	2.270E+01	1.316E+01	3.741E+01	3.830E+01	1.707E+01	1.177E+05	2.082E+05	1.881E+05	1.881E+05
2588.63	1.815E+01	5.810E+00	1.865E+01	3.741E+01	3.830E+01	1.707E+01	1.177E+05	2.082E+05	1.881E+05	1.881E+05
2634.71	1.844E+01	8.613E+00	2.705E+01	3.741E+01	3.830E+01	1.707E+01	1.177E+05	2.082E+05	1.881E+05	1.881E+05
2680.79	7.942E+00	1.055E+01	1.418E+01	2.579E+01	3.570E+01	2.448E+01	1.651E+05	1.809E+05	2.892E+05	2.892E+05
2721.03	7.942E+00	1.055E+01	1.418E+01	2.579E+01	3.570E+01	2.448E+01	1.651E+05	1.809E+05	2.892E+05	2.892E+05
120.55	0.000E+00	0.000E+00	0.000E+00	0.000E+00	0.000E+00	0.000E+00	0.000E+00	0.000E+00	0.000E+00	0.000E+00
1375.19	1.417E+01	1.302E+01	5.630E+01	2.875E+02	1.322E+03	0.000E+00	0.000E+00	0.000E+00	0.000E+00	0.000E+00
1375.19	1.373E+01	1.400E+01	3.320E+01	1.916E+02	1.150E+03	0.000E+00	0.000E+00	0.000E+00	0.000E+00	0.000E+00
1403.51	1.400E+01	1.504E+01	3.020E+01	2.494E+02	2.263E+03	0.000E+00	0.000E+00	0.000E+00	0.000E+00	0.000E+00
1551.83	1.522E+01	1.337E+00	1.337E+00	7.213E+02	5.412E+03	2.263E+03	4.416E+07	9.780E+06	2.560E+06	2.560E+06
1640.15	1.400E+01	1.290E+00	3.020E+01	2.214E+02	1.172E+03	2.853E+02	7.657E+07	1.973E+06	4.222E+06	4.222E+06
1728.47	1.421E+01	9.420E+00	3.020E+01	2.697E+02	1.172E+03	2.853E+02	7.657E+07	1.973E+06	4.222E+06	4.222E+06
1816.79	1.534E+01	4.220E+00	4.220E+00	2.847E+02	1.172E+03	2.853E+02	7.657E+07	1.973E+06	4.222E+06	4.222E+06
1905.11	1.534E+01	4.220E+00	4.220E+00	2.847E+02	1.172E+03	2.853E+02	7.657E+07	1.973E+06	4.222E+06	4.222E+06
1993.43	2.321E+01	2.427E+01	5.290E+01	3.600E+02	8.432E+03	2.104E+02	1.043E+06	8.257E+06	1.042E+06	1.042E+06
2054.37	2.321E+01	2.427E+01	5.290E+01	3.600E+02	8.432E+03	2.104E+02	1.043E+06	8.257E+06	1.042E+06	1.042E+06
2116.31	2.577E+01	3.021E+01	6.041E+01	4.076E+02	1.160E+04	1.636E+02	1.252E+06	3.142E+06	1.282E+06	1.282E+06
2177.75	2.577E+01	3.021E+01	6.041E+01	4.076E+02	1.160E+04	1.636E+02	1.252E+06	3.142E+06	1.282E+06	1.282E+06
2239.19	2.577E+01	3.021E+01	6.041E+01	4.076E+02	1.160E+04	1.636E+02	1.252E+06	3.142E+06	1.282E+06	1.282E+06
2300.53	3.123E+01	1.324E+01	1.044E+01	4.504E+02	2.172E+04	3.151E+02	1.293E+06	5.866E+06	1.321E+06	1.321E+06
2435.13	2.710E+01	4.240E+00	4.240E+00	4.504E+02	2.172E+04	3.151E+02	1.293E+06	5.866E+06	1.321E+06	1.321E+06
2496.47	3.113E+01	6.700E+00	3.020E+01	4.024E+02	1.290E+04	2.561E+02	1.396E+06	9.600E+06	1.537E+06	1.537E+06
2502.47	3.113E+01	6.700E+00	3.020E+01	4.024E+02	1.290E+04	2.561E+02	1.396E+06	9.600E+06	1.537E+06	1.537E+06
2562.55	1.230E+01	5.000E+00	2.450E+01	3.020E+01	3.944E+03	3.944E+03	1.004E+05	2.195E+05	1.537E+05	1.537E+05
2588.63	1.230E+01	5.000E+00	2.450E+01	3.020E+01	3.944E+03	3.944E+03	1.004E+05	2.195E+05	1.537E+05	1.537E+05
2634.71	1.811E+01	1.042E+01	4.236E+01	3.750E+01	1.502E+04	4.244E+01	1.168E+05	2.244E+05	1.727E+05	1.727E+05
2680.79	1.811E+01	1.042E+01	4.236E+01	3.750E+01	1.502E+04	4.244E+01	1.168E+05	2.244E+05	1.727E+05	1.727E+05
2721.03	7.942E+00	2.175E+01	8.036E+00	2.440E+01	3.378E+01	3.378E+01	1.197E+05	3.804E+05	1.664E+05	1.664E+05
2721.03	7.942E+00	2.175E+01	8.036E+00	2.440E+01	3.378E+01	3.378E+01	1.197E+05	3.804E+05	1.664E+05	1.664E+05

ADDITIONAL STATE ESTIMATES AT 20.000 FT (10 TO NF)
7.988E+00 5.285E+00 2.991E-04

GROUP 7 GYRO IAS DRIFTS									
TIME	POSITION ESTIMATE R	ESTIMATE ERROR C	VELOCITY ESTIMATE D	ESTIMATE ERROR C	PLATFORM TILT ESTIMATE R	TILT ESTIMATE D	ESTIMATE ERROR C		
120.55	0.000E+00	0.000E+00	0.000E+00	0.000E+00	0.000E+00	0.000E+00	0.000E+00	0.000E+00	0.000E+00
1375.19	3.741E+00	7.210E+01	1.501E+02	1.045E+02	0.127E-04	0.127E-04	0.127E-04	0.127E-04	0.127E-04
1463.5	1.167E+01	5.782E+00	8.931E+02	8.705E+02	2.117E-04	2.117E-04	2.117E-04	2.117E-04	2.117E-04
1551.83	1.695E+01	1.420E+01	7.850E+01	3.200E+01	2.200E-04	2.200E-04	2.200E-04	2.200E-04	2.200E-04
1640.15	4.040E+01	3.422E+01	5.243E+01	9.364E+01	2.249E-04	2.249E-04	2.249E-04	2.249E-04	2.249E-04
1728.47	5.502E+01	6.824E+01	7.694E+01	9.364E+01	2.249E-04	2.249E-04	2.249E-04	2.249E-04	2.249E-04
1816.79	8.486E+01	1.150E+02	4.197E+01	1.123E+00	2.249E-04	2.249E-04	2.249E-04	2.249E-04	2.249E-04
1905.11	8.250E+01	1.414E+02	9.662E+01	1.440E+00	2.249E-04	2.249E-04	2.249E-04	2.249E-04	2.249E-04
1993.41	9.199E+01	2.553E+02	1.041E+00	1.721E+00	2.249E-04	2.249E-04	2.249E-04	2.249E-04	2.249E-04
2054.87	1.017E+02	3.053E+02	1.041E+00	2.062E+00	2.249E-04	2.249E-04	2.249E-04	2.249E-04	2.249E-04
2116.31	1.111E+02	3.662E+02	1.041E+00	2.062E+00	2.249E-04	2.249E-04	2.249E-04	2.249E-04	2.249E-04
2177.75	1.214E+02	4.385E+02	1.378E+00	2.447E+00	2.249E-04	2.249E-04	2.249E-04	2.249E-04	2.249E-04
2239.19	1.167E+02	3.123E+02	1.552E+00	2.410E+00	2.249E-04	2.249E-04	2.249E-04	2.249E-04	2.249E-04
2299.19	2.251E+02	6.573E+01	1.043E+00	1.409E+00	2.249E-04	2.249E-04	2.249E-04	2.249E-04	2.249E-04
2496.47	2.915E+02	4.339E+01	2.047E+00	1.299E+00	2.249E-04	2.249E-04	2.249E-04	2.249E-04	2.249E-04
2496.47	7.206E+01	8.112E+01	1.610E+00	1.183E+00	2.249E-04	2.249E-04	2.249E-04	2.249E-04	2.249E-04
2542.55	3.583E+01	5.351E+01	1.525E+00	1.046E+00	2.249E-04	2.249E-04	2.249E-04	2.249E-04	2.249E-04
2588.63	7.110E+01	5.325E+01	1.428E+00	9.805E+01	2.249E-04	2.249E-04	2.249E-04	2.249E-04	2.249E-04
2634.71	7.120E+01	5.861E+01	1.282E+00	8.708E+01	2.249E-04	2.249E-04	2.249E-04	2.249E-04	2.249E-04
2680.79	5.257E+01	5.498E+01	1.109E+00	6.898E+01	2.249E-04	2.249E-04	2.249E-04	2.249E-04	2.249E-04
2723.03	1.573E+01	1.839E+01	9.471E+01	5.744E+01	2.249E-04	2.249E-04	2.249E-04	2.249E-04	2.249E-04
TIME	U	V	W	U	V	W	U	V	W
120.55	0.000E+00	0.000E+00	0.000E+00	0.000E+00	0.000E+00	0.000E+00	0.000E+00	0.000E+00	0.000E+00
1375.19	1.256E+01	1.214E+01	8.071E+00	3.149E+02	7.612E-03	1.045E+02	0.127E-04	0.127E-04	0.127E-04
1463.5	1.199E+01	4.970E+00	8.031E+00	8.931E+02	3.135E-02	3.200E+01	2.117E-04	2.117E-04	2.117E-04
1551.83	3.492E+01	4.911E+00	1.393E+01	3.274E+01	2.955E-02	8.705E+02	2.200E-04	2.200E-04	2.200E-04
1640.15	5.232E+01	2.975E+01	6.500E+01	8.541E+01	2.088E-01	9.364E+01	2.249E-04	2.249E-04	2.249E-04
1728.47	6.525E+01	4.013E+01	1.102E+02	9.214E+01	2.745E-01	1.091E+00	2.249E-04	2.249E-04	2.249E-04
1816.79	7.267E+01	3.151E+01	1.608E+02	8.605E+01	3.457E-01	1.175E+00	2.249E-04	2.249E-04	2.249E-04
1905.11	7.836E+01	2.717E+01	2.149E+02	8.825E+01	5.515E-01	1.473E+00	2.249E-04	2.249E-04	2.249E-04
1993.41	8.278E+01	6.754E+01	2.550E+02	9.577E+01	7.480E-01	1.733E+00	2.249E-04	2.249E-04	2.249E-04
2054.87	8.651E+01	1.349E+02	2.969E+02	1.081E+00	1.010E+00	2.074E+00	2.249E-04	2.249E-04	2.249E-04
2116.31	9.533E+01	2.195E+02	3.402E+02	1.220E+00	1.401E+00	2.370E+00	2.249E-04	2.249E-04	2.249E-04
2177.75	1.051E+02	2.568E+02	4.271E+02	1.315E+00	1.282E+00	2.511E+00	2.249E-04	2.249E-04	2.249E-04
2239.19	1.133E+02	9.392E+01	3.031E+02	1.481E+00	1.324E+00	2.511E+00	2.249E-04	2.249E-04	2.249E-04
2299.19	2.243E+02	6.369E+01	6.708E+01	1.945E+00	1.324E+00	2.511E+00	2.249E-04	2.249E-04	2.249E-04
2496.47	2.904E+02	8.298E+01	9.229E+01	2.032E+00	1.388E+00	1.133E+00	2.249E-04	2.249E-04	2.249E-04
2496.47	9.261E+01	3.193E+01	9.210E+01	1.600E+00	1.064E+00	1.133E+00	2.249E-04	2.249E-04	2.249E-04
2542.55	7.576E+01	3.731E+01	5.907E+01	1.519E+00	1.064E+00	1.064E+00	2.249E-04	2.249E-04	2.249E-04
2588.63	8.084E+01	5.273E+01	3.715E+01	1.424E+00	1.064E+00	1.064E+00	2.249E-04	2.249E-04	2.249E-04
2634.71	7.204E+01	5.887E+01	2.459E+01	1.280E+00	1.064E+00	1.064E+00	2.249E-04	2.249E-04	2.249E-04
2680.79	5.252E+01	5.221E+01	2.593E+01	1.108E+00	1.064E+00	1.064E+00	2.249E-04	2.249E-04	2.249E-04
2723.03	1.574E+01	2.091E+01	1.299E+01	9.472E+01	6.455E-01	8.705E+02	2.249E-04	2.249E-04	2.249E-04

ADDITIONAL STATE ESTIMATES AT 20.000 FT (10 TO NF)
1.362E+01 2.078E+00 7.394E-04

GROUP B GYRO MASS UNBALANCES

TIME	POSITION ESTIMATE ERROR R	GYRO MASS UNBALANCES R	VELOCITY ESTIMATE ERROR D	PLATFORM TILT ESTIMATE ERROR C	PLATFORM TILT ESTIMATE ERROR D	PLATFORM TILT ESTIMATE ERROR C
120.55	0.000E+00	0.000E+00	0.000E+00	0.000E+00	0.000E+00	0.000E+00
1375.19	4.936E-02	2.948E-01	8.873E-05	3.385E-04	1.643E-06	6.302E-07
1375.19	1.472E-01	1.794E-01	7.002E-05	3.385E-04	1.643E-06	6.302E-07
1463.51	1.732E-01	1.130E-01	6.483E-04	1.643E-03	2.202E-06	1.258E-06
1551.83	1.771E-01	1.153E-01	2.655E-03	1.643E-03	4.353E-06	1.258E-06
1640.15	2.030E-01	1.991E-01	9.484E-03	5.440E-02	8.334E-06	8.334E-06
1728.47	6.030E-01	4.937E-01	3.204E-02	3.602E-02	1.230E-05	1.372E-05
1816.79	1.212E+00	3.245E+00	4.733E-02	3.602E-02	1.230E-05	1.372E-05
1905.11	1.957E+00	5.490E+00	5.805E-02	1.835E-02	1.835E-05	1.835E-05
1993.43	2.887E+00	8.150E+00	5.169E-02	4.808E-02	2.230E-05	2.230E-05
2081.75	3.692E+00	1.074E+01	6.623E-02	7.320E-02	2.110E-05	2.110E-05
2170.07	4.712E+00	1.427E+01	1.133E-01	1.000E-01	2.400E-05	2.400E-05
2258.39	5.918E+00	1.906E+01	1.976E-01	1.235E-01	2.772E-05	2.772E-05
2346.71	7.405E+00	2.504E+01	1.310E-01	1.163E-01	3.433E-05	3.433E-05
2435.03	8.984E+00	3.234E+01	2.002E-01	1.524E-01	3.433E-05	3.433E-05
2523.35	1.615E+01	4.234E+01	1.393E-01	1.524E-01	4.353E-05	4.353E-05
2611.67	2.025E+01	5.444E+01	1.333E-01	1.524E-01	4.353E-05	4.353E-05
2700.00	1.622E+01	7.842E+01	1.263E-01	1.663E-01	4.353E-05	4.353E-05
2788.32	9.991E+00	7.842E+01	1.263E-01	1.663E-01	4.353E-05	4.353E-05
2876.64	1.350E+01	7.842E+01	1.263E-01	1.663E-01	4.353E-05	4.353E-05
2964.96	1.350E+01	7.842E+01	1.263E-01	1.663E-01	4.353E-05	4.353E-05
3053.28	3.396E+00	1.088E+01	1.046E-01	1.813E-01	5.000E-05	5.000E-05
3141.60	1.020E+01	1.133E+01	9.123E-02	1.989E-01	5.000E-05	5.000E-05
3229.92	3.361E+00	4.620E+00	8.123E-02	1.899E-01	5.000E-05	5.000E-05

TIME	U	V	W	U	V	W
120.55	0.000E+00	0.000E+00	0.000E+00	0.000E+00	0.000E+00	0.000E+00
1375.19	2.185E-01	0.000E+00	0.000E+00	0.000E+00	0.000E+00	0.000E+00
1375.19	1.832E-01	0.000E+00	0.000E+00	0.000E+00	0.000E+00	0.000E+00
1463.51	3.228E-01	0.000E+00	0.000E+00	0.000E+00	0.000E+00	0.000E+00
1551.83	7.464E-01	0.000E+00	0.000E+00	0.000E+00	0.000E+00	0.000E+00
1640.15	1.301E+00	0.000E+00	0.000E+00	0.000E+00	0.000E+00	0.000E+00
1728.47	1.762E+00	0.000E+00	0.000E+00	0.000E+00	0.000E+00	0.000E+00
1816.79	2.263E+00	0.000E+00	0.000E+00	0.000E+00	0.000E+00	0.000E+00
1905.11	2.740E+00	0.000E+00	0.000E+00	0.000E+00	0.000E+00	0.000E+00
1993.43	3.465E+00	0.000E+00	0.000E+00	0.000E+00	0.000E+00	0.000E+00
2081.75	4.431E+00	0.000E+00	0.000E+00	0.000E+00	0.000E+00	0.000E+00
2170.07	5.834E+00	0.000E+00	0.000E+00	0.000E+00	0.000E+00	0.000E+00
2258.39	6.680E+00	0.000E+00	0.000E+00	0.000E+00	0.000E+00	0.000E+00
2346.71	8.011E+01	0.000E+00	0.000E+00	0.000E+00	0.000E+00	0.000E+00
2435.03	2.513E+01	0.000E+00	0.000E+00	0.000E+00	0.000E+00	0.000E+00
2523.35	1.301E+01	0.000E+00	0.000E+00	0.000E+00	0.000E+00	0.000E+00
2611.67	1.192E+01	0.000E+00	0.000E+00	0.000E+00	0.000E+00	0.000E+00
2700.00	1.346E+01	0.000E+00	0.000E+00	0.000E+00	0.000E+00	0.000E+00
2788.32	1.010E+01	0.000E+00	0.000E+00	0.000E+00	0.000E+00	0.000E+00
2876.64	2.941E+00	0.000E+00	0.000E+00	0.000E+00	0.000E+00	0.000E+00

ADDITIONAL STATE ESTIMATES AT 20.000 FT (10 TO NF)
2.588E+00 9.857E-01 1.557E-04

THE ANALYTIC SCIENCES CORPORATION

GROUP 10 TACAN RANGE BIAS									
TIME	POSITION ESTIMATE ERROR			VELOCITY ESTIMATE ERROR			PLATFORM TILT ESTIMATE ERROR		
	R	D	C	R	D	C	R	D	C
2239.19	1.000E-10	1.000E-10	1.000E-10	1.000E-10	1.000E-10	1.000E-10	1.000E-10	1.000E-10	1.000E-10
2239.19	4.317E+00	4.296E+00	3.220E+02	3.173E-01	1.088E-02	1.800E-01	2.491E-07	2.422E-06	1.014E-06
2435.03	5.223E+02	1.308E+03	3.850E+02	3.836E+00	6.483E+00	1.852E+00	1.333E-04	6.150E-05	5.142E-04
2496.47	1.244E+03	1.014E+03	5.006E+02	6.076E+00	6.837E+00	2.282E+00	1.349E-04	9.542E-05	5.845E-04
2496.47	4.165E+02	1.022E+03	4.005E+02	4.169E+00	7.756E+00	1.870E+00	1.402E-04	5.422E-05	5.711E-04
2542.55	3.206E+02	6.742E+02	4.008E+02	3.530E+00	6.540E+00	1.855E+00	1.675E-04	4.793E-05	4.646E-04
2588.63	3.118E+02	7.093E+02	4.245E+02	3.264E+00	5.245E+00	1.895E+00	1.757E-04	4.844E-05	4.079E-04
2634.71	2.740E+02	1.555E+02	4.432E+02	3.054E+00	4.610E+00	1.877E+00	1.852E-04	5.420E-05	3.649E-04
2680.79	2.281E+02	1.904E+02	4.230E+02	2.735E+00	3.574E+00	1.731E+00	1.852E-04	5.420E-05	3.649E-04
2723.03	2.442E+02	3.234E+02	2.042E+02	2.567E+00	3.469E+00	1.364E+00	1.782E-04	6.308E-05	3.125E-04
TIME	POSITION ESTIMATE ERROR			VELOCITY ESTIMATE ERROR			PLATFORM TILT ESTIMATE ERROR		
	R	D	C	R	D	C	R	D	C
2239.19	1.000E-10	1.000E-10	1.000E-10	1.000E-10	1.000E-10	1.000E-10	1.000E-10	1.000E-10	1.000E-10
2239.19	1.819E+01	3.072E+02	9.496E-01	3.039E-01	1.959E-01	4.965E-02	1.000E-10	1.000E-10	1.000E-10
2435.03	5.225E+02	3.712E+02	1.312E+03	3.846E+00	1.839E+00	6.481E+00	2.335E-07	2.365E-07	2.621E-06
2496.47	1.280E+03	5.323E+02	1.003E+03	6.073E+00	1.832E+00	6.481E+00	1.344E-04	5.149E-04	4.957E-05
2496.47	4.160E+02	4.545E+02	1.001E+03	4.180E+00	2.253E+00	7.403E+00	1.332E-04	5.704E-04	1.557E-04
2542.55	3.200E+02	4.294E+02	6.567E+02	3.535E+00	2.265E+00	6.403E+00	1.413E-04	5.443E-04	1.800E-04
2588.63	3.112E+02	4.346E+02	2.956E+02	3.266E+00	2.052E+00	5.231E+00	1.608E-04	4.517E-04	1.176E-04
2634.71	2.737E+02	4.371E+02	1.725E+02	3.053E+00	1.964E+00	4.378E+00	1.744E-04	3.912E-04	9.586E-05
2680.79	2.280E+02	3.896E+02	2.519E+02	2.736E+00	1.725E+00	3.575E+00	1.888E-04	3.982E-04	1.025E-04
2723.03	2.441E+02	3.651E+02	1.141E+02	2.569E+00	2.543E+00	2.724E+00	1.840E-04	3.114E-04	1.025E-04
ADDITIONAL STATE ESTIMATES AT 20.000 FT (10 TO NF)									
	2.262E+02	6.314E+01	3.245E-03						

GROUP 11 TACAN RANGE SCALE FACTOR

TIME	POSITION R	ESTIMATE D	TACAN RANGE SCALE FACTOR C	VELOCITY R	ESTIMATE D	ERROR C	PLATFORM TILT N	ESTIMATE D	ERROR C
2239.19	0.000E+00	0.000E+00	0.000E+00	0.000E+00	0.000E+00	0.000E+00	0.000E+00	0.000E+00	0.000E+00
2239.19	1.661E+00	1.661E+00	1.230E+02	1.230E+02	1.230E+02	1.230E+02	1.230E+02	1.230E+02	1.230E+02
2435.03	5.223E+01	6.873E+00	1.077E+01	1.077E+01	1.077E+01	1.077E+01	1.077E+01	1.077E+01	1.077E+01
2496.47	1.266E+01	1.075E+01	2.756E+01	2.756E+01	2.756E+01	2.756E+01	2.756E+01	2.756E+01	2.756E+01
2496.47	4.663E+00	9.072E+00	2.973E+01	2.973E+01	2.973E+01	2.973E+01	2.973E+01	2.973E+01	2.973E+01
2542.55	1.662E+01	8.906E+00	1.296E+01	1.296E+01	1.296E+01	1.296E+01	1.296E+01	1.296E+01	1.296E+01
2548.63	2.397E+01	6.118E+00	1.305E+00	1.305E+00	1.305E+00	1.305E+00	1.305E+00	1.305E+00	1.305E+00
2634.71	2.420E+01	2.792E+00	1.078E+01	1.078E+01	1.078E+01	1.078E+01	1.078E+01	1.078E+01	1.078E+01
2680.79	1.947E+01	3.876E+00	1.539E+01	1.539E+01	1.539E+01	1.539E+01	1.539E+01	1.539E+01	1.539E+01
2723.03	6.963E+00	6.613E+00	7.276E+00	7.276E+00	7.276E+00	7.276E+00	7.276E+00	7.276E+00	7.276E+00
TIME	U	V	W	U	V	W	U	V	W
2239.19	0.000E+00	0.000E+00	0.000E+00	0.000E+00	0.000E+00	0.000E+00	0.000E+00	0.000E+00	0.000E+00
2239.19	6.000E+00	1.187E+02	3.653E+01	1.187E+01	1.187E+01	1.187E+01	1.187E+01	1.187E+01	1.187E+01
2435.03	5.095E+01	2.204E+01	1.952E+01	1.718E+01	1.718E+01	1.718E+01	1.718E+01	1.718E+01	1.718E+01
2496.47	1.297E+01	2.476E+01	1.869E+01	4.112E+01	4.112E+01	4.112E+01	4.112E+01	4.112E+01	4.112E+01
2542.55	1.671E+01	1.033E+01	1.173E+01	4.504E+01	4.504E+01	4.504E+01	4.504E+01	4.504E+01	4.504E+01
2548.63	2.395E+01	2.558E+00	5.177E+00	4.504E+01	4.504E+01	4.504E+01	4.504E+01	4.504E+01	4.504E+01
2634.71	2.417E+01	1.117E+01	8.023E+01	4.035E+01	4.035E+01	4.035E+01	4.035E+01	4.035E+01	4.035E+01
2680.79	1.946E+01	1.445E+01	6.613E+00	3.140E+01	3.140E+01	3.140E+01	3.140E+01	3.140E+01	3.140E+01
2723.03	6.967E+00	9.829E+00	1.254E+01	3.200E+01	3.200E+01	3.200E+01	3.200E+01	3.200E+01	3.200E+01

ADDITIONAL STATE ESTIMATES AT 20.000 FT (10 TO NP)
5.698E+00 2.233E+00 1.462E-04

GROUP 12 HARD ALTIMETER BIAS, SCALE FACTOR, AND STATIC EFFECT

TIME	POSITION ESTIMATE ERROR			VELOCITY ESTIMATE ERROR			PLATFORM TILT ESTIMATE ERROR		
	U	V	W	U	V	W	U	V	W
2496.47	0.000E+00	0.000E+00	0.000E+00	0.000E+00	0.000E+00	0.000E+00	0.000E+00	0.000E+00	0.000E+00
2496.47	1.836E+03	4.079E+02	4.409E+02	4.409E+00	3.045E+00	2.159E+00	1.708E-04	1.196E-04	2.077E-05
2542.55	1.950E+03	2.079E+02	6.809E+02	4.142E+00	4.512E+00	2.467E+00	2.042E-04	1.340E-04	1.180E-04
2588.63	1.622E+03	1.208E+02	7.338E+02	2.198E+00	4.481E+00	2.746E+00	1.276E-04	1.452E-04	3.302E-04
2634.71	1.216E+03	3.913E+01	7.028E+02	7.066E+00	3.404E+00	2.114E+00	4.368E-05	1.657E-04	5.497E-04
2680.79	8.109E+02	2.255E+02	5.540E+02	2.255E+00	1.599E+00	1.059E+00	1.493E-04	1.851E-04	6.872E-04
2723.03	3.107E+02	2.369E+02	1.678E+02	3.099E+00	3.889E-01	9.329E-01	3.047E-04	1.809E-04	7.208E-04
TIME	U	V	W	U	V	W	U	V	W
2496.47	0.000E+00	0.000E+00	0.000E+00	0.000E+00	0.000E+00	0.000E+00	0.000E+00	0.000E+00	0.000E+00
2496.47	1.829E+03	5.779E+02	2.304E+02	4.454E+00	3.113E+00	2.127E+00	1.714E-04	5.687E-05	1.017E-04
2542.55	1.950E+03	7.263E+02	5.022E+01	4.118E+00	3.900E+00	3.702E+00	2.074E-04	8.739E-05	1.592E-04
2588.63	1.618E+03	7.515E+02	5.211E+01	2.179E+00	3.549E+00	3.899E+00	1.283E-04	3.067E-04	2.054E-04
2634.71	1.234E+03	6.918E+02	1.478E+02	7.980E+00	2.687E+00	2.974E+00	4.402E-05	5.107E-04	2.622E-04
2680.79	8.184E+02	5.057E+02	3.220E+02	2.254E+00	1.313E+00	1.393E+00	1.501E-04	6.417E-04	3.075E-04
2723.03	3.199E+02	2.840E+02	5.913E+01	3.996E+00	9.100E-01	4.383E-01	3.047E-04	6.506E-04	3.590E-04

ADDITIONAL STATE ESTIMATES AT 20.000 FT (10 TO NF)
2.969E+02 8.937E+01 2.293E-03

THE ANALYTIC SCIENCES CORPORATION

GROUP 12 HARD ALTITUDE FIRST-ORDER MARKOV

TIME	POSITION ESTIMATE ERROR R	POSITION ESTIMATE ERROR D	VELOCITY ESTIMATE ERROR R	VELOCITY ESTIMATE ERROR D	PLATFORM TILT ESTIMATE ERROR R	PLATFORM TILT ESTIMATE ERROR D	PLATFORM TILT ESTIMATE ERROR C
2496.47	1.000E-10	1.000E-10	1.000E-10	1.000E-10	1.000E-10	1.000E-10	1.000E-10
2496.47	1.366E+01	3.074E+00	3.344E-02	2.273E-02	1.270E-06	8.622E-07	1.545E-07
2542.55	1.509E+01	2.417E+00	4.179E-02	1.527E-02	1.972E-06	9.961E-07	3.333E-06
2542.55	1.447E+01	2.544E+00	4.882E-02	1.772E-02	2.405E-06	1.078E-06	5.342E-06
2634.71	1.453E+01	2.770E+00	5.934E-02	2.624E-02	3.405E-06	1.238E-06	6.496E-06
2680.79	1.403E+01	5.552E+00	7.198E-02	3.024E-02	4.104E-06	1.534E-06	8.425E-06
2723.03	1.000E+01	7.674E+00	8.136E-02	5.403E-02	3.935E-06	1.840E-06	3.657E-06
TIME	U	V	W	V	U	V	W
2496.47	1.070E-10	1.000E-10	1.000E-10	1.000E-10	1.000E-10	1.000E-10	1.000E-10
2496.47	1.361E+01	4.298E+00	1.714E+00	2.331E-02	1.275E-06	4.231E-07	7.567E-07
2542.55	1.500E+01	5.473E+00	2.273E+00	3.010E-02	2.306E-06	3.184E-06	1.363E-06
2542.55	1.444E+01	6.342E+00	3.086E+00	3.132E-02	2.610E-06	5.138E-06	1.778E-06
2634.71	1.448E+01	7.338E+00	3.920E+00	3.381E-02	3.420E-06	6.587E-06	2.274E-06
2680.79	1.402E+01	7.214E+00	7.198E-02	3.081E-02	4.113E-06	8.047E-06	2.916E-06
2723.03	1.001E+01	7.965E+00	8.141E-02	5.323E-02	3.983E-06	8.253E-06	5.341E-06

ADDITIONAL STATE ESTIMATES AT 20.000 FT (10 TO NF)
9.530E+00 2.565E+00 2.446E-05

GROUP 16 TACAN SURVEY ERRORS (MULTIPLY BY 0.1)

TIME	POSITION R	ESTIMATE D	ERROR C	VELOCITY V	ESTIMATE D	ERROR C	PLATFORM U	GILT D	ESTIMATE D	ERROR C
2239.19	0.030E+00	0.000E+00	0.000E+00	0.000E+00	0.000E+00	0.000E+00	0.000E+00	0.000E+00	0.000E+00	0.000E+00
2239.19	1.132E-01	2.877E+00	8.349E+00	8.242E-03	5.688E-03	4.646E-03	1.259E-07	6.343E-07	3.595E-08	3.595E-08
2435.03	2.501E+00	7.574E+00	9.641E+00	8.631E-03	1.631E-02	6.122E-03	9.149E-07	2.781E-07	2.818E-07	2.818E-07
2406.47	4.253E+00	7.472E+00	9.501E+00	1.179E-02	1.693E-02	6.943E-03	9.377E-07	2.663E-07	1.504E-06	1.504E-06
2406.47	1.353E+00	7.018E+00	9.873E+00	8.749E-03	3.645E-02	9.049E-02	1.141E-06	3.834E-07	3.220E-06	3.220E-06
2642.55	1.537E+00	7.783E+00	1.027E+01	2.066E-02	2.896E-02	1.267E-02	1.392E-06	4.130E-07	3.961E-06	3.961E-06
2588.63	2.241E+00	9.135E+00	1.003E+01	3.066E-02	4.722E-02	1.653E-02	1.263E-06	4.564E-07	4.099E-06	4.099E-06
2638.71	3.087E+00	9.938E+00	1.091E+01	3.302E-02	4.722E-02	1.716E-02	1.019E-06	5.433E-07	5.243E-06	5.243E-06
2680.79	5.083E+00	1.052E+01	1.049E+01	4.506E-02	4.422E-02	2.043E-02	1.192E-06	1.138E-06	8.586E-06	8.586E-06
2723.03	6.879E+00	1.188E+01	7.633E+00	6.770E-02	6.162E-02	2.043E-02	1.192E-06	1.138E-06	8.586E-06	8.586E-06
TIME	U	V	W	U	V	W	U	V	W	
2239.19	0.000E+00	0.000E+00	0.000E+00	0.000E+00	0.000E+00	0.000E+00	0.000E+00	0.000E+00	0.000E+00	0.000E+00
2239.19	4.756E-01	8.035E+00	3.736E+00	7.894E-03	5.491E-03	5.466E-03	3.234E-07	4.823E-08	6.825E-08	6.825E-08
2435.03	2.605E+00	9.575E+00	7.486E+00	8.684E-03	6.562E-03	1.013E-02	9.157E-07	2.862E-07	2.671E-07	2.671E-07
2406.47	4.317E+00	9.897E+00	6.826E+00	1.183E-02	9.623E-03	1.553E-02	9.495E-07	1.396E-06	6.029E-07	6.029E-07
2406.47	1.419E+00	1.033E+01	6.747E+00	8.770E-03	1.324E-02	1.832E-02	1.154E-06	1.545E-06	6.507E-07	6.507E-07
2588.63	1.581E+00	1.045E+01	7.531E+00	2.082E-02	1.557E-02	3.524E-02	1.323E-06	3.114E-06	8.633E-07	8.633E-07
2638.71	2.021E+00	1.069E+01	9.176E+00	2.901E-02	1.740E-02	4.611E-02	1.324E-06	3.874E-06	9.135E-07	9.135E-07
2680.79	3.029E+00	1.066E+01	1.008E+01	3.307E-02	1.909E-02	4.586E-02	1.265E-06	4.308E-06	9.692E-07	9.692E-07
2723.03	5.083E+00	1.052E+01	1.049E+01	4.506E-02	1.999E-02	4.586E-02	1.020E-06	5.137E-06	1.348E-06	1.348E-06
	6.881E+00	9.687E+00	1.027E+01	6.775E-02	2.599E-02	6.317E-02	1.198E-06	7.017E-06	5.078E-06	5.078E-06

ADDITIONAL STATE ESTIMATES AT 20.000 FT (10 TO NF)
6.321E+00 2.187E+00 1.130E-04

GROUP 19 TACAN BEARING BIAS

TIME	POSITION ESTIMATE R	VELOCITY ESTIMATE R	PLATFORM TILT N	ESTIMATE D	ERROR C
2239.19	1.000E-10	1.000E-10	1.000E-10	1.000E-10	1.000E-10
2239.19	2.737E+01	2.046E+02	5.740E-04	1.420E-05	4.313E-05
2435.03	4.208E+02	1.272E+01	2.943E-05	2.257E-05	1.294E-04
2406.47	3.337E+02	5.307E+01	1.147E-05	1.517E-05	2.217E-04
2406.47	9.422E+01	1.103E+00	4.510E-05	2.096E-05	2.345E-04
2542.55	5.421E+01	7.391E+01	2.570E-05	5.027E-05	3.022E-04
2534.63	8.451E+01	4.254E+01	2.137E-05	1.201E-05	2.557E-04
2634.71	9.973E+01	4.718E+01	2.077E-05	1.942E-05	1.914E-04
2640.79	1.334E+02	2.261E+01	1.514E-05	2.548E-05	1.594E-04
2723.03	1.419E+02	1.153E+02	3.414E-05	1.190E-04	1.406E-04
TIME	U	V	U	V	M
2239.19	1.000E-10	1.000E-10	1.000E-10	1.000E-10	1.000E-10
2239.19	2.255E+01	1.143E+01	5.734E-04	1.420E-05	4.313E-05
2435.03	4.174E+02	3.157E+01	2.721E-05	2.257E-05	1.294E-04
2406.47	3.304E+02	2.628E+02	3.194E-05	2.257E-05	2.217E-04
2406.47	9.650E+01	1.924E+02	4.191E-05	2.096E-05	2.345E-04
2542.55	5.487E+01	1.312E+02	2.990E-05	5.027E-05	3.022E-04
2534.63	8.421E+01	1.263E+02	2.169E-05	1.201E-05	2.557E-04
2634.71	1.022E+02	1.263E+02	2.099E-05	1.942E-05	1.594E-04
2640.79	1.335E+02	1.149E+02	2.099E-05	2.548E-05	1.406E-04
2723.03	1.420E+02	1.844E+02	3.433E-05	1.190E-04	1.406E-04

ADDITIONAL STATE ESTIMATES AT 20.000 FT (10 TO NF)
1.307E+02 3.940E+01 1.850E-03

GROUP 21 TIME-VARYING DENSITY DEVIATIONS WINTER PROFILE

TIME	POSITION R	ESTIMATE D	ERROR C	VELOCITY R	ESTIMATE D	ERROR C	PLATFORM TILT R	ESTIMATE D	ERROR C
1375.19	0.000E+00	0.000E+00	0.000E+00	0.000E+00	0.000E+00	0.000E+00	0.000E+00	0.000E+00	0.000E+00
1375.51	9.090E+01	8.120E+00	1.343E+02	6.210E-02	1.276E-02	8.805E-02	5.116E-06	1.323E-05	2.166E-06
1463.51	1.816E+02	2.010E+01	3.226E+02	2.080E-01	4.276E-02	1.895E-01	1.571E-05	4.264E-05	6.707E-06
1551.81	1.930E+02	2.047E+01	3.329E+02	3.400E-01	7.940E-02	2.345E-01	1.983E-05	5.633E-05	8.437E-06
1640.15	4.930E+01	2.133E+01	3.341E+02	2.296E-01	1.340E-01	3.746E-01	2.451E-05	8.478E-05	1.043E-05
1729.47	1.747E+01	1.471E+00	3.678E+02	7.604E-01	1.654E-01	3.465E-01	2.325E-05	6.770E-05	9.818E-06
1816.79	3.354E+01	2.094E+01	3.437E+02	8.359E-01	2.387E-01	2.365E-01	2.355E-05	5.738E-05	9.512E-06
1905.11	3.255E+01	5.412E+01	3.401E+02	6.369E-01	2.995E-01	3.465E-02	2.545E-05	3.582E-05	8.558E-06
1993.41	4.177E+01	8.767E+01	2.931E+02	5.318E-01	3.710E-01	6.170E-02	2.702E-05	3.792E-05	8.558E-06
2084.87	6.753E+01	1.122E+02	2.491E+02	5.574E-01	4.226E-01	1.500E-01	2.726E-05	2.021E-05	7.768E-06
2177.75	8.231E+01	1.390E+02	2.491E+02	5.372E-01	4.827E-01	1.500E-01	2.760E-05	1.637E-05	7.107E-06
2239.19	1.224E+02	1.715E+02	2.437E+02	6.228E-01	5.449E-01	2.341E-01	1.754E-05	1.574E-05	6.977E-06
2337.19	1.302E+02	1.989E+02	1.970E+02	5.461E-01	5.661E-01	2.341E-01	2.755E-05	1.474E-05	6.518E-06
2435.03	1.269E+02	1.393E+02	3.258E+02	5.461E-01	4.429E-01	1.351E-01	2.091E-05	1.515E-05	7.188E-06
2496.47	1.712E+02	4.684E+01	2.714E+01	3.899E-01	2.514E-01	1.422E-01	7.005E-06	1.374E-05	8.143E-06
2542.55	1.152E+02	4.211E+01	3.110E+01	2.382E-01	3.404E-01	1.412E-01	6.024E-06	1.092E-05	1.463E-05
2588.61	4.124E+01	1.840E+01	9.360E+00	7.847E-03	2.309E-01	3.515E-02	1.672E-06	5.111E-06	1.902E-05
2630.79	1.418E+00	1.374E+01	4.372E+00	6.259E-03	1.693E-01	1.908E-03	4.803E-06	3.825E-06	1.623E-05
2680.79	8.313E+00	4.372E+00	4.372E+00	6.457E-02	1.107E-01	1.908E-03	4.803E-06	3.825E-06	1.623E-05
2723.03	4.403E+00	3.335E+00	3.415E+00	6.454E-02	6.735E-02	5.251E-03	5.589E-06	3.673E-06	1.156E-05
	1.628E-01	7.577E-01	1.954E+00	6.197E-02	4.055E-02	1.212E-02	5.589E-06	3.473E-06	1.156E-05
	4.223E-01	2.552E-01	2.552E-01	5.684E-02	2.512E-02	2.012E-02	5.263E-06	3.089E-06	9.114E-06
TIME	U	V	W	U	V	W	U	V	W
1375.19	0.000E+00	0.000E+00	0.000E+00	0.000E+00	0.000E+00	0.000E+00	0.000E+00	0.000E+00	0.000E+00
1375.51	2.041E+01	1.602E+02	3.429E+00	1.066E-01	2.111E-02	9.275E-02	1.655E-06	4.593E-06	1.428E-05
1463.51	5.872E+01	3.694E+02	1.970E+01	2.822E-01	2.194E-02	3.158E-02	1.455E-06	1.452E-05	4.312E-05
1551.81	1.076E+02	3.120E+02	7.556E+01	4.227E-01	1.745E-02	6.132E-02	9.775E-06	2.112E-05	5.547E-05
1640.15	1.238E+02	3.337E+02	9.455E+01	7.549E-01	6.425E-02	1.035E-01	1.431E-05	3.415E-05	8.692E-05
1729.47	1.510E+02	3.457E+02	7.930E+01	8.373E-01	7.490E-02	1.609E-01	1.899E-05	3.526E-05	5.071E-05
1816.79	1.146E+02	2.644E+02	3.806E+00	1.755E-01	3.367E-02	3.933E-01	2.331E-05	2.094E-05	2.941E-05
1905.11	9.311E+01	2.633E+02	8.035E+01	4.972E-01	1.449E-01	3.933E-01	2.574E-05	1.330E-05	2.051E-05
2054.87	1.050E+02	2.522E+02	1.429E+02	5.195E-01	2.443E-01	4.160E-01	9.682E-06	9.682E-06	1.872E-05
2177.75	1.073E+02	1.899E+02	2.014E+02	5.028E-01	3.402E-01	4.190E-01	5.493E-06	5.493E-06	1.872E-05
2239.19	1.413E+02	1.282E+02	2.596E+02	5.242E-01	4.875E-01	3.744E-01	8.449E-07	8.449E-07	1.872E-05
2337.19	1.270E+02	2.062E+01	1.406E+02	5.242E-01	4.337E-01	4.583E-01	4.110E-06	4.110E-06	1.872E-05
2435.03	1.704E+02	3.282E+01	1.406E+02	3.610E-01	2.901E-01	3.744E-01	7.925E-06	7.925E-06	1.872E-05
2496.47	1.347E+02	4.545E+01	2.876E+01	3.855E-01	1.605E-01	3.744E-01	1.385E-05	1.385E-05	1.872E-05
2542.55	1.412E+01	1.577E+01	1.422E+01	6.601E-03	1.121E-01	2.049E-01	1.911E-06	1.911E-06	1.872E-05
2588.61	8.279E+00	5.877E+00	7.121E+00	6.301E-02	4.669E-02	1.618E-01	1.773E-05	1.773E-05	1.872E-05
2630.79	4.390E+00	3.975E+00	2.600E+00	6.460E-02	6.858E-03	1.083E-01	1.521E-05	1.521E-05	6.751E-06
2680.79	1.623E+00	2.061E+00	3.889E-01	6.199E-02	4.582E-03	6.715E-02	1.294E-05	1.294E-05	6.751E-06
2723.03	1.832E-01	1.010E-01	4.828E-01	5.685E-02	3.182E-02	4.626E-03	9.773E-06	9.773E-06	3.947E-06

ADDITIONAL STATE ESTIMATES AT 20.000 FT (10 TO NF)
3.898E+02 1.341E-01 2.309E-05

GROUP 21 TIME-VARYING DENSITY DEVIATIONS SUMMER PROFILE

ADDITIONAL STATE ESTIMATES AT 20,000 FT (10 TO NF)
2.311E+00 1.546E+00 6.470E-05

THE ANALYTIC SCIENCES CORPORATION

GROUP 21 1962 STANDARD ATMOSPHERE MODFLING FROM 4-TERM MODEL

TIME	POSITION R	ESTIMATE D	ERROR C	VELOCITY R	ESTIMATE D	ERROR C	PLATFORM R	TYLT D	ESTIMATE D	ERROR C
1375.19	0.000E+00	0.000E+00	0.000E+00	0.000E+00	0.000E+00	0.000E+00	0.000E+00	0.000E+00	0.000E+00	0.000E+00
1375.19	4.820E+03	4.305E+02	7.122E+03	3.294E+00	6.747E-01	4.704E+00	2.712E-04	7.34E-04	1.18E-04	1.18E-04
1463.51	4.498E+03	2.101E+02	7.115E+03	4.374E+00	7.443E-01	3.265E+00	1.521E-04	2.398E-04	2.659E-05	2.659E-05
1551.83	4.212E+03	9.206E+01	7.497E+03	5.621E+00	5.707E-01	3.265E+00	1.151E-04	2.398E-04	2.333E-05	2.333E-05
1640.15	3.712E+03	1.619E+02	7.777E+03	6.743E+00	1.215E+00	2.381E+00	1.130E-04	3.598E-04	2.017E-05	2.017E-05
1728.47	2.849E+03	1.043E+02	8.025E+03	9.671E+00	1.507E+00	1.744E+00	1.170E-04	3.280E-04	1.112E-04	1.112E-04
1816.79	2.028E+03	2.467E+02	8.193E+03	1.033E+01	1.482E+00	5.269E-01	1.403E-04	1.474E-04	6.432E-05	6.432E-05
1905.11	1.258E+03	4.246E+02	8.148E+03	8.434E+00	2.208E+00	3.516E+00	1.429E-04	1.392E-04	1.413E-06	1.413E-06
1993.43	1.044E+03	6.724E+02	7.420E+03	8.634E+00	2.403E+00	4.322E+00	1.397E-04	5.158E-05	8.966E-06	8.966E-06
2054.87	5.534E+02	8.021E+02	6.740E+03	8.475E+00	2.760E+00	4.322E+00	9.482E-05	5.640E-05	3.189E-05	3.189E-05
2117.75	2.502E+02	1.073E+03	6.380E+03	6.798E+00	2.835E+00	1.749E+00	4.449E-05	3.326E-05	6.459E-05	6.459E-05
2239.19	2.458E+02	7.432E+02	9.425E+02	2.115E+00	1.844E+00	5.088E-01	6.554E-05	3.577E-05	9.449E-05	9.449E-05
2335.03	3.295E+02	6.667E+01	8.449E+02	8.040E-01	3.771E-01	2.351E-01	7.715E-05	3.577E-05	1.112E-04	1.112E-04
2436.47	3.333E+02	5.809E+01	5.362E+01	1.145E-01	2.241E-01	8.507E-02	7.993E-05	3.577E-05	1.112E-04	1.112E-04
2496.47	1.050E+02	1.074E+02	3.220E+01	3.339E-01	1.126E-01	1.531E-01	7.085E-05	3.577E-05	1.112E-04	1.112E-04
2542.55	6.048E+01	4.916E+00	2.353E+01	4.481E-01	1.443E-01	1.935E-01	6.983E-05	3.234E-05	8.738E-05	8.738E-05
2588.63	3.517E+01	4.115E+00	1.779E+01	4.728E-01	1.443E-01	1.935E-01	6.983E-05	3.234E-05	8.738E-05	8.738E-05
2634.71	2.057E+01	3.050E+00	1.283E+01	4.728E-01	1.443E-01	1.935E-01	6.983E-05	3.234E-05	8.738E-05	8.738E-05
2680.79	1.007E+01	6.050E+00	4.279E+00	4.728E-01	1.443E-01	1.935E-01	6.983E-05	3.234E-05	8.738E-05	8.738E-05
2723.03	2.011E+00	3.050E+00	4.279E+00	4.728E-01	1.443E-01	1.935E-01	6.983E-05	3.234E-05	8.738E-05	8.738E-05
1375.19	0.000E+00	0.000E+00	0.000E+00	0.000E+00	0.000E+00	0.000E+00	0.000E+00	0.000E+00	0.000E+00	0.000E+00
1375.19	1.401E+03	8.494E+03	1.818E+02	0.000E+00	1.112E+00	4.916E-01	9.000E+00	2.435E-04	4.214E-04	4.214E-04
1463.51	7.952E+02	8.341E+03	1.595E+02	5.652E+00	2.827E-01	5.404E-01	7.257E-05	1.270E-04	2.066E-04	2.066E-04
1551.83	4.304E+03	8.504E+03	1.371E+03	6.530E+00	1.890E-01	1.096E+00	7.010E-05	1.035E-04	3.337E-04	3.337E-04
1640.15	2.372E+02	8.504E+03	2.154E+03	7.243E+00	7.011E-01	1.635E+00	9.072E-04	1.035E-04	3.337E-04	3.337E-04
1728.47	3.935E+02	8.243E+03	2.154E+03	8.859E+00	1.305E+00	2.678E+00	1.079E-04	1.035E-04	3.337E-04	3.337E-04
1816.79	6.410E+02	8.144E+03	1.033E+03	9.833E+00	2.425E+00	2.678E+00	1.079E-04	1.035E-04	3.337E-04	3.337E-04
1905.11	7.954E+02	7.504E+03	1.033E+03	8.000E+00	3.550E+00	2.678E+00	1.079E-04	1.035E-04	3.337E-04	3.337E-04
1993.43	3.461E+02	7.034E+03	1.564E+02	8.000E+00	5.441E+00	2.678E+00	1.079E-04	1.035E-04	3.337E-04	3.337E-04
2054.87	5.017E+02	6.366E+03	2.040E+02	8.000E+00	5.441E+00	2.678E+00	1.079E-04	1.035E-04	3.337E-04	3.337E-04
2117.75	7.254E+02	5.150E+03	3.255E+02	8.000E+00	5.441E+00	2.678E+00	1.079E-04	1.035E-04	3.337E-04	3.337E-04
2239.19	8.142E+02	4.905E+03	2.722E+02	6.537E+00	5.958E+00	1.843E+00	1.079E-04	1.035E-04	3.337E-04	3.337E-04
2335.03	3.061E+02	6.489E+02	9.973E+01	2.019E+00	5.115E-01	1.096E+00	9.072E-04	1.035E-04	3.337E-04	3.337E-04
2436.47	3.280E+02	8.606E+01	6.872E+01	7.977E-01	4.450E-02	1.096E+00	9.072E-04	1.035E-04	3.337E-04	3.337E-04
2496.47	1.427E+02	8.606E+01	1.194E+01	2.347E-01	3.245E-02	1.096E+00	9.072E-04	1.035E-04	3.337E-04	3.337E-04
2542.55	5.225E+01	1.731E+01	6.199E+01	1.142E-01	3.245E-02	1.096E+00	9.072E-04	1.035E-04	3.337E-04	3.337E-04
2588.63	3.225E+01	1.055E+01	2.382E+01	1.142E-01	3.245E-02	1.096E+00	9.072E-04	1.035E-04	3.337E-04	3.337E-04
2634.71	2.052E+01	1.861E+01	7.337E+00	4.443E-01	1.355E-01	1.935E-01	6.983E-05	3.234E-05	8.738E-05	8.738E-05
2680.79	1.006E+01	1.207E+01	5.337E+00	4.728E-01	1.443E-01	1.935E-01	6.983E-05	3.234E-05	8.738E-05	8.738E-05
2723.03	2.016E+00	7.633E+00	1.916E+00	4.728E-01	1.443E-01	1.935E-01	6.983E-05	3.234E-05	8.738E-05	8.738E-05

ADDITIONAL STATE ESTIMATES AT 20,000 FT (10 TO NF)
3.566E+00 1.711E+00 8.923E-05

THE ANALYTIC SCIENCES CORPORATION

GROUP 21 1962 STANDARD ATMOSPHERE MODELING ERROR 1-TERM MODEL

TIME	POSITION D	ESTIMATE ERROR C	VELOCITY R	ESTIMATE ERROR U	PLATITUDE R	TILT D	ESTIMATE ERROR C
1375.19	0.000E+00	0.000E+00	0.000E+00	0.000E+00	0.000E+00	0.000E+00	0.000E+00
1375.51	4.57E+03	6.74E+03	3.22E+00	6.12E-01	2.57E-04	6.95E-04	1.08E-04
1463.51	4.07E+03	6.57E+03	4.07E+00	7.41E-01	1.78E-04	6.95E-04	1.08E-04
1551.51	3.43E+03	6.30E+03	5.04E+00	1.11E-01	2.02E-04	5.94E-04	7.51E-05
1640.15	2.80E+03	7.00E+03	7.00E+00	1.44E+00	2.05E-04	6.13E-04	7.09E-05
1728.47	2.01E+03	6.20E+03	1.03E+01	1.03E+01	2.05E-04	6.13E-04	7.09E-05
1816.79	1.23E+03	7.54E+03	7.54E+03	8.52E+00	2.05E-04	6.13E-04	7.09E-05
1905.11	1.05E+03	6.36E+03	1.05E+03	2.59E+00	2.05E-04	6.13E-04	7.09E-05
1993.43	1.57E+03	5.66E+03	3.65E+03	3.89E+00	2.05E-04	6.13E-04	7.09E-05
2081.75	2.09E+03	4.82E+03	7.31E-01	4.31E+00	2.05E-04	6.13E-04	7.09E-05
2170.07	1.57E+03	4.82E+03	1.90E+00	5.01E+00	2.05E-04	6.13E-04	7.09E-05
2258.39	1.04E+03	3.54E+03	5.67E+00	5.42E+00	2.05E-04	6.13E-04	7.09E-05
2346.71	4.04E+03	3.54E+03	7.46E+00	5.67E+00	2.05E-04	6.13E-04	7.09E-05
2435.03	1.57E+03	6.30E+03	9.85E+00	4.26E+00	2.05E-04	6.13E-04	7.09E-05
2523.35	1.57E+03	1.75E+02	1.75E+02	1.75E+02	2.05E-04	6.13E-04	7.09E-05
2611.67	3.37E+02	4.80E+02	1.07E+00	6.64E+00	2.05E-04	6.13E-04	7.09E-05
2700.00	6.71E+01	1.04E+02	1.87E+00	3.00E+00	2.05E-04	6.13E-04	7.09E-05
2788.32	2.30E+00	7.64E+01	1.20E+00	2.09E+00	2.05E-04	6.13E-04	7.09E-05
2876.64	6.38E+00	1.09E+01	7.50E+01	1.05E+00	2.05E-04	6.13E-04	7.09E-05
2964.96	5.95E+00	3.57E+00	4.74E-01	5.15E-01	2.05E-04	6.13E-04	7.09E-05
3053.28	1.28E+01	4.02E+00	3.01E-01	3.37E-01	2.05E-04	6.13E-04	7.09E-05
3141.60	0.00E+00	0.00E+00	0.00E+00	0.00E+00	0.00E+00	0.00E+00	0.00E+00
3229.92	0.00E+00	0.00E+00	0.00E+00	0.00E+00	0.00E+00	0.00E+00	0.00E+00
3318.24	0.00E+00	0.00E+00	0.00E+00	0.00E+00	0.00E+00	0.00E+00	0.00E+00
3406.56	0.00E+00	0.00E+00	0.00E+00	0.00E+00	0.00E+00	0.00E+00	0.00E+00
3494.88	0.00E+00	0.00E+00	0.00E+00	0.00E+00	0.00E+00	0.00E+00	0.00E+00
3583.20	0.00E+00	0.00E+00	0.00E+00	0.00E+00	0.00E+00	0.00E+00	0.00E+00
3671.52	0.00E+00	0.00E+00	0.00E+00	0.00E+00	0.00E+00	0.00E+00	0.00E+00
3759.84	0.00E+00	0.00E+00	0.00E+00	0.00E+00	0.00E+00	0.00E+00	0.00E+00
3848.16	0.00E+00	0.00E+00	0.00E+00	0.00E+00	0.00E+00	0.00E+00	0.00E+00
3936.48	0.00E+00	0.00E+00	0.00E+00	0.00E+00	0.00E+00	0.00E+00	0.00E+00
4024.80	0.00E+00	0.00E+00	0.00E+00	0.00E+00	0.00E+00	0.00E+00	0.00E+00
4113.12	0.00E+00	0.00E+00	0.00E+00	0.00E+00	0.00E+00	0.00E+00	0.00E+00
4201.44	0.00E+00	0.00E+00	0.00E+00	0.00E+00	0.00E+00	0.00E+00	0.00E+00
4289.76	0.00E+00	0.00E+00	0.00E+00	0.00E+00	0.00E+00	0.00E+00	0.00E+00
4378.08	0.00E+00	0.00E+00	0.00E+00	0.00E+00	0.00E+00	0.00E+00	0.00E+00
4466.40	0.00E+00	0.00E+00	0.00E+00	0.00E+00	0.00E+00	0.00E+00	0.00E+00
4554.72	0.00E+00	0.00E+00	0.00E+00	0.00E+00	0.00E+00	0.00E+00	0.00E+00
4643.04	0.00E+00	0.00E+00	0.00E+00	0.00E+00	0.00E+00	0.00E+00	0.00E+00
4731.36	0.00E+00	0.00E+00	0.00E+00	0.00E+00	0.00E+00	0.00E+00	0.00E+00
4819.68	0.00E+00	0.00E+00	0.00E+00	0.00E+00	0.00E+00	0.00E+00	0.00E+00
4908.00	0.00E+00	0.00E+00	0.00E+00	0.00E+00	0.00E+00	0.00E+00	0.00E+00
4996.32	0.00E+00	0.00E+00	0.00E+00	0.00E+00	0.00E+00	0.00E+00	0.00E+00
5084.64	0.00E+00	0.00E+00	0.00E+00	0.00E+00	0.00E+00	0.00E+00	0.00E+00
5172.96	0.00E+00	0.00E+00	0.00E+00	0.00E+00	0.00E+00	0.00E+00	0.00E+00
5261.28	0.00E+00	0.00E+00	0.00E+00	0.00E+00	0.00E+00	0.00E+00	0.00E+00
5349.60	0.00E+00	0.00E+00	0.00E+00	0.00E+00	0.00E+00	0.00E+00	0.00E+00
5437.92	0.00E+00	0.00E+00	0.00E+00	0.00E+00	0.00E+00	0.00E+00	0.00E+00
5526.24	0.00E+00	0.00E+00	0.00E+00	0.00E+00	0.00E+00	0.00E+00	0.00E+00
5614.56	0.00E+00	0.00E+00	0.00E+00	0.00E+00	0.00E+00	0.00E+00	0.00E+00
5702.88	0.00E+00	0.00E+00	0.00E+00	0.00E+00	0.00E+00	0.00E+00	0.00E+00
5791.20	0.00E+00	0.00E+00	0.00E+00	0.00E+00	0.00E+00	0.00E+00	0.00E+00
5879.52	0.00E+00	0.00E+00	0.00E+00	0.00E+00	0.00E+00	0.00E+00	0.00E+00
5967.84	0.00E+00	0.00E+00	0.00E+00	0.00E+00	0.00E+00	0.00E+00	0.00E+00
6056.16	0.00E+00	0.00E+00	0.00E+00	0.00E+00	0.00E+00	0.00E+00	0.00E+00
6144.48	0.00E+00	0.00E+00	0.00E+00	0.00E+00	0.00E+00	0.00E+00	0.00E+00
6232.80	0.00E+00	0.00E+00	0.00E+00	0.00E+00	0.00E+00	0.00E+00	0.00E+00
6321.12	0.00E+00	0.00E+00	0.00E+00	0.00E+00	0.00E+00	0.00E+00	0.00E+00
6409.44	0.00E+00	0.00E+00	0.00E+00	0.00E+00	0.00E+00	0.00E+00	0.00E+00
6497.76	0.00E+00	0.00E+00	0.00E+00	0.00E+00	0.00E+00	0.00E+00	0.00E+00
6586.08	0.00E+00	0.00E+00	0.00E+00	0.00E+00	0.00E+00	0.00E+00	0.00E+00
6674.40	0.00E+00	0.00E+00	0.00E+00	0.00E+00	0.00E+00	0.00E+00	0.00E+00
6762.72	0.00E+00	0.00E+00	0.00E+00	0.00E+00	0.00E+00	0.00E+00	0.00E+00
6851.04	0.00E+00	0.00E+00	0.00E+00	0.00E+00	0.00E+00	0.00E+00	0.00E+00
6939.36	0.00E+00	0.00E+00	0.00E+00	0.00E+00	0.00E+00	0.00E+00	0.00E+00
7027.68	0.00E+00	0.00E+00	0.00E+00	0.00E+00	0.00E+00	0.00E+00	0.00E+00
7116.00	0.00E+00	0.00E+00	0.00E+00	0.00E+00	0.00E+00	0.00E+00	0.00E+00
7204.32	0.00E+00	0.00E+00	0.00E+00	0.00E+00	0.00E+00	0.00E+00	0.00E+00
7292.64	0.00E+00	0.00E+00	0.00E+00	0.00E+00	0.00E+00	0.00E+00	0.00E+00
7380.96	0.00E+00	0.00E+00	0.00E+00	0.00E+00	0.00E+00	0.00E+00	0.00E+00
7469.28	0.00E+00	0.00E+00	0.00E+00	0.00E+00	0.00E+00	0.00E+00	0.00E+00
7557.60	0.00E+00	0.00E+00	0.00E+00	0.00E+00	0.00E+00	0.00E+00	0.00E+00
7645.92	0.00E+00	0.00E+00	0.00E+00	0.00E+00	0.00E+00	0.00E+00	0.00E+00
7734.24	0.00E+00	0.00E+00	0.00E+00	0.00E+00	0.00E+00	0.00E+00	0.00E+00
7822.56	0.00E+00	0.00E+00	0.00E+00	0.00E+00	0.00E+00	0.00E+00	0.00E+00
7910.88	0.00E+00	0.00E+00	0.00E+00	0.00E+00	0.00E+00	0.00E+00	0.00E+00
8000.00	0.00E+00	0.00E+00	0.00E+00	0.00E+00	0.00E+00	0.00E+00	0.00E+00

ADDITIONAL STATE ESTIMATES AT 20,000 FT (10 TO NF)
1.095E+01 3.173E+00 2.855E-04

[illegible]

ADDITIONAL STATE ESTIMATES AT 20.00C FT (10 TO NF)
5.936E-01 3.856E-01 1.931E-05

ADDITIONAL STATE ESTIMATES AT 20.00C FT (10 TO NF)
5.936E-01 3.856E-01 1.931E-05

GROUP 22 WESTERLOO WINDS WINTER PROFILE

TIME	POSITION R	ESTIMATE O	ERROR C	VELOCITY R	ESTIMATE O	ERROR C	PLATFORM R	TILT D	ESTIMATE O	ERROR C
1375.19	0.000E+00	0.000E+00	0.000E+00	0.000E+00	0.000E+00	0.000E+00	0.000E+00	0.000E+00	0.000E+00	0.000E+00
1375.19	8.131E-01	7.264E-01	1.202E-01	5.509E-01	1.742E-01	7.931E-01	4.571E-07	1.230E-06	1.935E-07	1.935E-07
1463.51	1.044E-01	1.160E-01	1.782E-01	1.131E-02	2.308E-03	1.011E-02	6.905E-07	3.892E-06	2.881E-07	2.881E-07
1551.83	6.746E-00	1.275E+00	1.742E-01	1.742E-01	4.369E-03	1.308E-02	1.122E-06	3.520E-06	5.036E-07	5.036E-07
1640.15	7.761E+00	3.074E+00	1.391E-01	5.385E-02	1.042E-02	4.008E-02	2.159E-06	1.030E-05	9.571E-07	9.571E-07
1728.47	2.014E+01	2.835E+00	1.849E-01	1.114E-01	1.713E-02	6.415E-02	2.345E-06	1.317E-05	1.032E-06	1.032E-06
1816.79	4.167E+01	2.442E+00	2.944E-01	1.869E-01	2.274E-02	7.411E-02	2.279E-06	1.709E-05	9.302E-07	9.302E-07
1905.11	6.287E+01	6.619E-01	3.710E-01	2.336E-01	2.645E-02	4.281E-02	2.192E-06	1.811E-05	8.721E-07	8.721E-07
1993.43	9.602E+01	2.395E-01	4.214E-01	3.164E-01	2.876E-02	6.225E-02	1.993E-06	2.024E-05	7.241E-07	7.241E-07
2054.87	1.652E+02	1.158E+00	9.017E-01	5.973E-01	2.103E-02	8.595E-02	8.113E-07	2.976E-05	1.711E-06	1.711E-06
2116.31	1.852E+02	2.325E+00	6.623E-01	5.973E-01	2.645E-02	1.303E-01	1.147E-06	2.684E-05	1.231E-06	1.231E-06
2177.75	2.476E+02	7.698E+00	7.910E-01	7.913E-01	3.128E-02	1.077E-01	1.077E-06	2.968E-05	1.733E-06	1.733E-06
2239.19	2.578E+02	4.765E-01	2.819E-01	7.315E-01	2.157E-02	1.408E-01	8.141E-07	2.555E-05	9.611E-07	9.611E-07
2239.19	2.508E+02	1.357E+00	9.591E-01	6.725E-01	2.365E-02	1.205E-01	8.608E-07	2.501E-05	1.275E-06	1.275E-06
2435.03	2.797E+02	9.151E-01	4.141E-01	5.812E-01	4.966E-02	2.023E-01	1.422E-05	1.925E-05	1.961E-05	1.961E-05
2496.47	2.119E+02	8.238E-01	4.556E-01	3.182E-01	7.010E-01	1.995E-01	1.381E-05	1.444E-05	3.524E-05	3.524E-05
2496.47	6.430E+01	4.506E-01	1.150E-01	4.253E-02	4.652E-01	3.301E-02	7.272E-07	5.320E-06	3.712E-05	3.712E-05
2542.55	1.999E+01	3.141E-01	5.126E-00	1.348E-01	3.045E-01	2.335E-03	2.348E-06	3.383E-06	3.265E-05	3.265E-05
2588.63	1.095E+01	1.095E+01	5.357E+00	1.190E-01	2.055E-01	2.435E-03	2.945E-06	3.218E-06	2.409E-05	2.409E-05
2634.71	5.547E+00	6.642E+00	4.360E+00	1.031E-01	1.167E-01	2.461E-03	3.431E-06	3.013E-06	1.841E-05	1.841E-05
2680.79	1.815E+00	1.851E+00	2.440E+00	8.986E-02	6.559E-02	9.164E-03	3.788E-06	2.617E-06	1.452E-05	1.452E-05
2723.03	6.275E-01	1.316E+00	2.001E-01	7.720E-02	4.119E-02	1.623E-02	3.356E-06	1.993E-06	1.059E-05	1.059E-05

TIME	U	V	W	U	V	W	U	V	W
1375.19	0.000E+00	0.000E+00	0.000E+00	0.000E+00	0.000E+00	0.000E+00	0.000E+00	0.000E+00	0.000E+00
1375.51	2.360E+00	1.435E+01	3.068E-01	9.537E-03	1.898E-03	8.296E-04	1.483E-07	4.109E-07	1.260E-06
1463.51	2.600E+00	2.042E+01	8.051E-01	1.522E-02	1.015E-03	1.671E-03	2.890E-07	6.299E-07	1.913E-06
1551.83	3.515E+00	1.820E+01	2.612E+00	2.413E-02	1.185E-03	3.325E-03	5.375E-07	1.253E-06	3.475E-06
1640.15	1.315E+01	8.178E+00	6.847E+00	7.092E-02	1.004E-02	6.780E-03	1.155E-06	3.503E-06	9.903E-06
1728.47	2.502E+01	8.240E+00	5.537E+00	1.277E-01	2.006E-02	1.055E-02	1.603E-06	5.200E-06	1.224E-05
1816.79	4.842E+01	1.373E+01	6.084E+00	2.012E-01	2.006E-02	1.344E-02	2.603E-06	6.355E-06	1.593E-05
1905.11	7.013E+01	2.023E+01	2.638E+00	3.362E-01	1.020E-01	3.523E-02	2.382E-06	4.733E-06	1.748E-05
1993.43	1.022E+02	2.347E+01	2.813E+00	6.417E-01	6.417E-01	4.164E-02	2.500E-06	1.838E-06	2.013E-05
2054.87	1.774E+02	6.315E+01	1.363E+01	5.552E-01	1.744E-01	2.103E-02	1.514E-06	1.306E-06	2.975E-05
2116.31	1.916E+02	4.028E+01	1.913E+01	5.770E-01	2.032E-01	1.446E-02	1.703E-06	6.021E-06	2.616E-05
2177.75	2.516E+02	4.490E+01	3.585E+01	7.685E-01	6.855E-01	8.611E-02	1.341E-06	1.174E-05	2.730E-05
2239.19	2.592E+02	9.270E+00	4.272E+00	6.623E-01	6.988E-01	3.571E-02	6.893E-06	2.425E-05	2.425E-05
2319.19	2.425E+02	2.534E+01	8.072E+00	6.623E-01	6.988E-01	3.571E-02	6.893E-06	2.425E-05	2.425E-05
2435.03	2.763E+02	5.100E+01	9.092E+01	3.132E-01	2.346E-01	4.900E-01	9.325E-07	1.911E-05	1.996E-05
2496.47	2.100E+02	7.376E+01	6.159E+01	3.132E-01	2.346E-01	4.900E-01	1.397E-05	2.934E-05	1.996E-05
2542.55	6.399E+01	2.706E+01	3.833E+01	4.456E-02	1.697E-01	4.253E-01	2.778E-07	3.304E-05	1.771E-05
2588.63	1.090E+01	1.260E+01	2.930E+01	1.395E-01	8.059E-02	3.243E-01	2.645E-06	3.092E-05	1.108E-05
2634.71	5.548E+00	5.508E+00	1.560E+01	1.193E-01	4.097E-02	2.013E-01	3.100E-06	2.343E-05	7.788E-06
2680.79	1.809E+00	2.746E+00	5.734E+00	1.032E-01	1.843E-02	1.152E-01	1.800E-06	1.800E-05	6.386E-06
2723.03	6.288E-01	7.500E-01	1.009E-01	8.992E-02	2.860E-03	6.611E-02	3.795E-06	1.380E-05	5.227E-06
				7.723E-02	3.991E-02	1.902E-02	3.357E-06	9.109E-06	5.755E-06

ADDITIONAL STATE ESTIMATES AT 20.000 FT (10 TO NF)
3.024E-01 3.054E-01 3.081E-05

THE ANALYTIC SCIENCES CORPORATION

GROUP 22 WESTERLY WINDS SUMMER PROFILE

TIME	POSITION N	ESTIMATE D	ERROR C	VELOCITY R	ESTIMATE D	LENGTH C	WIND ONM N	WIND TILT D	ESTIMATE D	EMHUR C
1375.19	0.000E+00	0.000E+00	0.000E+00	0.000E+00	0.000E+00	0.000E+00	0.000E+00	0.000E+00	0.000E+00	0.000E+00
1375.51	2.317E+01	1.200E+00	3.100E+01	1.530E-02	3.440E-03	2.180E-02	0.000E+00	0.000E+00	0.000E+00	0.000E+00
1463.51	3.099E+01	6.400E+00	4.700E+01	1.530E-02	4.050E-03	2.180E-02	0.000E+00	0.000E+00	0.000E+00	0.000E+00
1551.83	3.534E+01	1.300E+00	5.260E+01	3.610E-02	6.000E-03	1.100E-02	0.000E+00	0.000E+00	0.000E+00	0.000E+00
1640.15	5.762E+01	6.650E+00	5.630E+01	1.610E-02	1.510E-02	4.080E-02	0.000E+00	0.000E+00	0.000E+00	0.000E+00
1728.47	7.100E+01	7.150E+00	3.890E+01	2.320E-01	1.510E-02	4.080E-02	0.000E+00	0.000E+00	0.000E+00	0.000E+00
1816.79	1.003E+02	3.870E+00	3.890E+01	2.320E-01	1.510E-02	4.080E-02	0.000E+00	0.000E+00	0.000E+00	0.000E+00
1905.11	1.160E+02	5.010E+00	4.050E+01	2.320E-01	1.510E-02	4.080E-02	0.000E+00	0.000E+00	0.000E+00	0.000E+00
1993.43	1.317E+02	2.060E+00	3.230E+01	3.610E-01	4.730E-02	2.470E-02	0.000E+00	0.000E+00	0.000E+00	0.000E+00
2081.75	1.470E+02	1.300E+00	7.200E+01	3.610E-01	5.740E-02	2.470E-02	0.000E+00	0.000E+00	0.000E+00	0.000E+00
2170.07	1.540E+02	4.000E+00	9.110E+01	3.210E-01	6.140E-02	2.470E-02	0.000E+00	0.000E+00	0.000E+00	0.000E+00
2258.39	1.650E+02	5.910E+00	1.250E+02	2.490E-01	6.200E-02	1.070E-02	0.000E+00	0.000E+00	0.000E+00	0.000E+00
2346.71	1.760E+02	8.050E+00	1.470E+01	3.610E-01	7.200E-02	1.070E-02	0.000E+00	0.000E+00	0.000E+00	0.000E+00
2435.03	1.870E+02	5.470E+00	2.430E+01	3.610E-01	7.200E-02	1.070E-02	0.000E+00	0.000E+00	0.000E+00	0.000E+00
2523.35	1.980E+02	4.910E+00	2.670E+01	2.130E-01	4.730E-02	1.070E-02	0.000E+00	0.000E+00	0.000E+00	0.000E+00
2611.67	2.090E+02	2.690E+00	6.700E+00	2.130E-01	4.730E-02	1.070E-02	0.000E+00	0.000E+00	0.000E+00	0.000E+00
2700.00	2.200E+02	1.400E+00	3.030E+00	4.170E-02	1.240E-01	9.130E-03	0.000E+00	0.000E+00	0.000E+00	0.000E+00
2788.32	2.310E+02	3.840E+00	2.400E+00	3.060E-02	3.540E-02	2.130E-02	0.000E+00	0.000E+00	0.000E+00	0.000E+00
2876.64	2.420E+02	1.040E+00	1.110E+01	2.690E-02	2.360E-02	2.130E-02	0.000E+00	0.000E+00	0.000E+00	0.000E+00

TIME	U	V	W	U	V	W	U	V	W	U	V	W
1375.19	0.000E+00	0.000E+00	0.000E+00	0.000E+00	0.000E+00	0.000E+00	0.000E+00	0.000E+00	0.000E+00	0.000E+00	0.000E+00	0.000E+00
1375.51	6.490E+00	3.940E+01	8.430E+01	0.000E+00	0.000E+00	0.000E+00	0.000E+00	0.000E+00	0.000E+00	0.000E+00	0.000E+00	0.000E+00
1463.51	4.280E+00	5.610E+01	4.110E+01	3.640E-02	1.490E-02	2.090E-03	0.000E+00	0.000E+00	0.000E+00	0.000E+00	0.000E+00	0.000E+00
1551.83	1.840E+00	6.320E+01	2.650E+00	5.300E-02	2.020E-02	3.000E-03	0.000E+00	0.000E+00	0.000E+00	0.000E+00	0.000E+00	0.000E+00
1640.15	2.260E+01	8.200E+01	6.420E+00	1.400E+01	4.500E-02	1.000E-02	0.000E+00	0.000E+00	0.000E+00	0.000E+00	0.000E+00	0.000E+00
1728.47	4.460E+01	7.850E+01	1.400E+01	1.420E+01	5.200E-02	1.000E-02	0.000E+00	0.000E+00	0.000E+00	0.000E+00	0.000E+00	0.000E+00
1816.79	9.306E+01	6.740E+01	1.300E+01	2.550E+01	5.200E-02	1.000E-02	0.000E+00	0.000E+00	0.000E+00	0.000E+00	0.000E+00	0.000E+00
1905.11	1.036E+02	6.220E+01	1.060E+01	2.630E+01	5.200E-02	1.000E-02	0.000E+00	0.000E+00	0.000E+00	0.000E+00	0.000E+00	0.000E+00
1993.43	1.205E+02	7.020E+01	6.100E+00	2.700E+01	5.200E-02	1.000E-02	0.000E+00	0.000E+00	0.000E+00	0.000E+00	0.000E+00	0.000E+00
2081.75	1.560E+02	5.700E+01	1.220E+00	3.700E+01	5.200E-02	1.000E-02	0.000E+00	0.000E+00	0.000E+00	0.000E+00	0.000E+00	0.000E+00
2170.07	1.490E+02	8.070E+01	1.790E+01	3.180E+01	5.200E-02	1.000E-02	0.000E+00	0.000E+00	0.000E+00	0.000E+00	0.000E+00	0.000E+00
2258.39	1.360E+02	1.290E+02	4.020E+01	3.180E+01	5.200E-02	1.000E-02	0.000E+00	0.000E+00	0.000E+00	0.000E+00	0.000E+00	0.000E+00
2346.71	1.380E+02	1.270E+02	1.020E+01	3.180E+01	5.200E-02	1.000E-02	0.000E+00	0.000E+00	0.000E+00	0.000E+00	0.000E+00	0.000E+00
2435.03	1.640E+02	3.000E+01	5.680E+01	2.630E+01	5.200E-02	1.000E-02	0.000E+00	0.000E+00	0.000E+00	0.000E+00	0.000E+00	0.000E+00
2523.35	1.250E+02	4.370E+01	3.680E+01	2.100E+01	5.200E-02	1.000E-02	0.000E+00	0.000E+00	0.000E+00	0.000E+00	0.000E+00	0.000E+00
2611.67	3.790E+01	1.600E+01	2.300E+01	2.100E+01	5.200E-02	1.000E-02	0.000E+00	0.000E+00	0.000E+00	0.000E+00	0.000E+00	0.000E+00
2700.00	1.200E+01	7.460E+00	1.730E+01	5.440E-02	3.210E-02	1.000E-02	0.000E+00	0.000E+00	0.000E+00	0.000E+00	0.000E+00	0.000E+00
2788.32	6.770E+00	5.070E+00	9.240E+00	4.200E-02	3.210E-02	1.000E-02	0.000E+00	0.000E+00	0.000E+00	0.000E+00	0.000E+00	0.000E+00
2876.64	3.440E+00	3.160E+00	3.370E+00	3.450E-02	1.800E-02	1.000E-02	0.000E+00	0.000E+00	0.000E+00	0.000E+00	0.000E+00	0.000E+00
2964.96	1.050E+00	1.320E+00	8.190E+00	3.060E-02	1.800E-02	1.000E-02	0.000E+00	0.000E+00	0.000E+00	0.000E+00	0.000E+00	0.000E+00
3053.28	3.740E+01	1.950E+01	6.910E+01	2.690E-02	1.800E-02	1.000E-02	0.000E+00	0.000E+00	0.000E+00	0.000E+00	0.000E+00	0.000E+00

ADDITIONAL STATE ESTIMATES AT 20.000 FT (10 TO NP)
2.500E-01 3.100E-01 1.740E-05

THE ANALYTIC SCIENCES CORPORATION

GROUP 22 CROSSWIND AND HEADWIND									
TIME	POSITION ESTIMATE ERROR			VELOCITY ESTIMATE ERROR			PLATFORM TILT ESTIMATE ERROR		
	U	V	W	U	V	W	U	V	W
1375.19	1.000E-10	1.000E-10	1.000E-10	1.000E-10	1.000E-10	1.000E-10	1.000E-10	1.000E-10	1.000E-10
1375.19	4.000E+00	4.000E+00	4.000E+00	4.000E+00	4.000E+00	4.000E+00	4.000E+00	4.000E+00	4.000E+00
1407.51	6.000E+00	6.000E+00	6.000E+00	6.000E+00	6.000E+00	6.000E+00	6.000E+00	6.000E+00	6.000E+00
1507.83	5.000E+00	5.000E+00	5.000E+00	5.000E+00	5.000E+00	5.000E+00	5.000E+00	5.000E+00	5.000E+00
1608.15	5.000E+00	5.000E+00	5.000E+00	5.000E+00	5.000E+00	5.000E+00	5.000E+00	5.000E+00	5.000E+00
1723.47	4.000E+00	4.000E+00	4.000E+00	4.000E+00	4.000E+00	4.000E+00	4.000E+00	4.000E+00	4.000E+00
1816.79	4.000E+00	4.000E+00	4.000E+00	4.000E+00	4.000E+00	4.000E+00	4.000E+00	4.000E+00	4.000E+00
1933.43	4.000E+00	4.000E+00	4.000E+00	4.000E+00	4.000E+00	4.000E+00	4.000E+00	4.000E+00	4.000E+00
2033.47	4.000E+00	4.000E+00	4.000E+00	4.000E+00	4.000E+00	4.000E+00	4.000E+00	4.000E+00	4.000E+00
2116.31	4.000E+00	4.000E+00	4.000E+00	4.000E+00	4.000E+00	4.000E+00	4.000E+00	4.000E+00	4.000E+00
2230.19	4.000E+00	4.000E+00	4.000E+00	4.000E+00	4.000E+00	4.000E+00	4.000E+00	4.000E+00	4.000E+00
2230.19	4.000E+00	4.000E+00	4.000E+00	4.000E+00	4.000E+00	4.000E+00	4.000E+00	4.000E+00	4.000E+00
2430.03	4.000E+00	4.000E+00	4.000E+00	4.000E+00	4.000E+00	4.000E+00	4.000E+00	4.000E+00	4.000E+00
2400.47	4.000E+00	4.000E+00	4.000E+00	4.000E+00	4.000E+00	4.000E+00	4.000E+00	4.000E+00	4.000E+00
2500.47	4.000E+00	4.000E+00	4.000E+00	4.000E+00	4.000E+00	4.000E+00	4.000E+00	4.000E+00	4.000E+00
2550.43	4.000E+00	4.000E+00	4.000E+00	4.000E+00	4.000E+00	4.000E+00	4.000E+00	4.000E+00	4.000E+00
2610.71	4.000E+00	4.000E+00	4.000E+00	4.000E+00	4.000E+00	4.000E+00	4.000E+00	4.000E+00	4.000E+00
2640.79	4.000E+00	4.000E+00	4.000E+00	4.000E+00	4.000E+00	4.000E+00	4.000E+00	4.000E+00	4.000E+00
2723.03	4.000E+00	4.000E+00	4.000E+00	4.000E+00	4.000E+00	4.000E+00	4.000E+00	4.000E+00	4.000E+00
1375.19	1.000E-10	1.000E-10	1.000E-10	1.000E-10	1.000E-10	1.000E-10	1.000E-10	1.000E-10	1.000E-10
1375.19	1.000E+00	1.000E+00	1.000E+00	1.000E+00	1.000E+00	1.000E+00	1.000E+00	1.000E+00	1.000E+00
1407.51	1.000E+00	1.000E+00	1.000E+00	1.000E+00	1.000E+00	1.000E+00	1.000E+00	1.000E+00	1.000E+00
1507.83	1.000E+00	1.000E+00	1.000E+00	1.000E+00	1.000E+00	1.000E+00	1.000E+00	1.000E+00	1.000E+00
1608.15	1.000E+00	1.000E+00	1.000E+00	1.000E+00	1.000E+00	1.000E+00	1.000E+00	1.000E+00	1.000E+00
1723.47	1.000E+00	1.000E+00	1.000E+00	1.000E+00	1.000E+00	1.000E+00	1.000E+00	1.000E+00	1.000E+00
1816.79	1.000E+00	1.000E+00	1.000E+00	1.000E+00	1.000E+00	1.000E+00	1.000E+00	1.000E+00	1.000E+00
1933.43	1.000E+00	1.000E+00	1.000E+00	1.000E+00	1.000E+00	1.000E+00	1.000E+00	1.000E+00	1.000E+00
2033.47	1.000E+00	1.000E+00	1.000E+00	1.000E+00	1.000E+00	1.000E+00	1.000E+00	1.000E+00	1.000E+00
2116.31	1.000E+00	1.000E+00	1.000E+00	1.000E+00	1.000E+00	1.000E+00	1.000E+00	1.000E+00	1.000E+00
2230.19	1.000E+00	1.000E+00	1.000E+00	1.000E+00	1.000E+00	1.000E+00	1.000E+00	1.000E+00	1.000E+00
2230.19	1.000E+00	1.000E+00	1.000E+00	1.000E+00	1.000E+00	1.000E+00	1.000E+00	1.000E+00	1.000E+00
2430.03	1.000E+00	1.000E+00	1.000E+00	1.000E+00	1.000E+00	1.000E+00	1.000E+00	1.000E+00	1.000E+00
2400.47	1.000E+00	1.000E+00	1.000E+00	1.000E+00	1.000E+00	1.000E+00	1.000E+00	1.000E+00	1.000E+00
2500.47	1.000E+00	1.000E+00	1.000E+00	1.000E+00	1.000E+00	1.000E+00	1.000E+00	1.000E+00	1.000E+00
2550.43	1.000E+00	1.000E+00	1.000E+00	1.000E+00	1.000E+00	1.000E+00	1.000E+00	1.000E+00	1.000E+00
2610.71	1.000E+00	1.000E+00	1.000E+00	1.000E+00	1.000E+00	1.000E+00	1.000E+00	1.000E+00	1.000E+00
2640.79	1.000E+00	1.000E+00	1.000E+00	1.000E+00	1.000E+00	1.000E+00	1.000E+00	1.000E+00	1.000E+00
2723.03	1.000E+00	1.000E+00	1.000E+00	1.000E+00	1.000E+00	1.000E+00	1.000E+00	1.000E+00	1.000E+00

ADDITIONAL STATE ESTIMATES AT 20.00 FT (10 TO NF)
1.000E-01 1.000E-01 1.000E-01 1.000E-01 1.000E-01 1.000E-01 1.000E-01 1.000E-01 1.000E-01 1.000E-01

GROUP 23 DRAG COEFFICIENT VARIATIONS (FIRST-ORDER MARKOV)

TIME	POSITION ESTIMATE ERROR R	VELOCITY ESTIMATE ERROR H	VELOCITY ESTIMATE ERROR D	PLATFORM TILT ESTIMATE ERROR C	PLATFORM TILT ESTIMATE ERROR D	PLATFORM TILT ESTIMATE ERROR C
1375.10	1.000E-10	1.000E-10	1.000E-10	1.000E-10	1.000E-10	1.000E-10
1375.19	2.400E+01	1.816E-01	3.772E-02	2.622E-01	4.089E-05	5.401E-06
1463.51	3.414E+02	3.691E+01	6.733E-02	2.957E-01	1.512E-05	5.401E-06
1551.83	1.533E+01	4.626E-01	8.793E-02	3.810E-01	4.394E-05	6.086E-06
1640.15	2.865E+02	6.042E+02	1.204E-01	3.127E-01	1.709E-05	6.841E-06
1728.47	1.849E+01	7.627E-01	1.539E-01	3.040E-01	5.829E-05	6.955E-06
1816.79	3.332E+01	9.172E-01	1.887E-01	2.712E-01	6.227E-05	5.877E-06
1905.11	5.070E+01	3.907E-01	2.230E-01	1.313E-01	1.930E-05	5.858E-06
1993.43	7.287E+01	6.681E-01	3.020E-01	1.767E-01	3.843E-05	5.525E-06
2081.75	9.000E+02	5.703E+02	3.387E-01	3.197E-01	1.925E-05	6.086E-06
2170.07	2.012E+02	1.093E+02	3.761E-01	3.913E-01	1.937E-05	6.222E-06
2258.39	2.047E+02	1.541E+02	3.910E-01	3.930E-01	1.940E-05	7.222E-06
2346.71	1.964E+02	4.972E+01	3.925E-01	1.754E-01	2.039E-05	7.510E-06
2435.03	1.800E+02	5.550E+01	3.252E-01	1.479E-01	1.303E-05	2.522E-05
2496.47	1.355E+02	4.823E+01	4.071E-01	1.407E-01	9.891E-06	2.409E-05
2542.55	4.114E+01	2.307E+01	2.820E-01	3.936E-02	4.753E-06	2.409E-05
2588.63	1.375E+01	9.221E+00	1.220E-01	1.631E-02	3.904E-06	2.234E-05
2634.71	4.285E+00	4.018E+00	1.220E-01	1.822E-02	3.840E-06	1.629E-05
2680.79	1.830E+00	3.127E+00	6.904E-02	1.970E-02	7.505E-06	1.357E-05
2723.03	6.435E-01	1.344E+00	2.459E-02	2.602E-02	3.217E-06	1.069E-05
1375.10	1.000E-10	1.000E-10	1.000E-10	1.000E-10	1.000E-10	1.000E-10
1375.19	7.807E+01	4.735E+02	1.014E+01	2.741E-02	1.357E-05	4.163E-05
1463.51	6.668E+01	6.434E+02	1.697E+01	4.447E-02	1.339E-05	4.163E-05
1551.83	5.019E+01	6.539E+02	5.440E-01	6.624E-02	1.622E-05	4.134E-05
1640.15	7.959E+01	6.522E+02	6.977E-01	1.023E-01	2.348E-05	5.411E-05
1728.47	1.075E+02	6.428E+02	1.647E+02	1.566E-01	2.506E-05	5.411E-05
1816.79	1.715E+02	6.303E+02	1.602E+02	2.704E-01	2.390E-05	5.473E-05
1905.11	1.824E+02	6.063E+02	1.431E+02	2.921E-01	1.521E-05	5.473E-05
1993.43	2.390E+02	5.771E+02	1.424E+02	2.919E-01	9.930E-06	3.814E-05
2081.75	2.038E+02	5.115E+02	9.522E-01	2.858E-01	7.974E-06	3.814E-05
2170.07	2.371E+02	3.385E+02	8.331E-01	2.917E-01	9.046E-06	2.829E-05
2258.39	2.093E+02	4.344E+02	7.721E-01	3.152E-01	8.993E-06	2.829E-05
2346.71	1.955E+02	6.523E+01	1.221E+02	3.559E-01	8.993E-06	2.829E-05
2435.03	1.791E+02	3.359E+01	5.513E+01	3.250E-01	2.507E-06	1.317E-05
2496.47	1.357E+02	4.551E+01	3.662E+01	3.451E-01	2.043E-05	1.617E-05
2542.55	4.095E+01	1.599E+01	2.514E+01	2.619E-01	2.043E-05	1.617E-05
2588.63	1.369E+00	1.885E+00	9.563E-02	1.968E-01	2.091E-05	6.653E-06
2634.71	7.985E+00	5.314E+00	2.466E-02	1.191E-01	1.788E-05	7.196E-06
2680.79	4.274E+00	3.575E+00	3.755E-02	6.745E-02	1.536E-05	6.924E-06
2723.03	1.828E+00	2.068E+00	7.366E-02	4.015E-02	1.272E-05	5.142E-06
2723.03	6.446E-01	1.357E+00	3.050E-02	1.869E-02	9.910E-06	5.142E-06

ADDITIONAL STATE ESTIMATES AT 20.000 FT (10 TO NF)

6.599E-01 3.606E-01 2.497E-05

APPENDIX D
ERROR CONTRIBUTION TIME HISTORIES:
20,000 FT TO TOUCHDOWN

This appendix presents the time histories associated with the error budget results summarized in Section 4.4.2. The data is presented in tabular form with each table indicating the rms errors in position and velocity, and the rms value of the platform alignment estimates, in both the R (runway) and V (relative velocity) coordinate frames, which result from a specific error source or group of errors.

The time points in each table begin at MLS acquisition and are printed at appropriate time intervals thereafter. Time points are also included just before and after processing of the first radar altimeter measurement. Thus there are two rows of data for each of the following times (see Table 4.1-1):

$$T_{\text{MLS}} = 2723.03 \text{ sec}$$

$$T_{\text{RA}} = 2809.43 \text{ sec}$$

A single row of each table corresponds to the initiation of the landing phase:

$$T_{\text{SW}} = 2749.91 \text{ sec}$$

The magnitudes and mathematical description of the error sources are given in Section 4.3. Units are in feet, fps, and radians.

D-2

185

D-3

GROUP 1 TACAN RANGE MEASUREMENT NT NT NT

D-5

GROUP 1 RAO ALTITUDE MEASUREMENT NOISE

TIME	POSITION ESTIMATE ERROR R	VELOCITY ESTIMATE ERROR R	PLATFORM TILT ESTIMATE ERROR R	PLATFORM TILT ESTIMATE ERROR C
2721.03	3.102E-01	4.724E-03	2.331E-07	1.225E-07
2723.03	1.512E-03	3.689E-03	2.390E-07	1.182E-07
2725.03	1.270E-03	2.944E-04	1.040E-08	6.437E-09
2727.03	1.277E-04	4.784E-05	7.215E-09	2.270E-09
2729.01	1.111E-04	3.194E-05	6.798E-09	2.235E-09
2731.09	9.513E-04	1.114E-05	6.798E-09	2.235E-09
2733.19	8.873E-04	8.154E-06	6.797E-09	2.235E-09
2735.79	9.267E-04	1.125E-05	6.797E-09	2.235E-09
2737.79	8.443E-04	1.066E-04	6.797E-09	2.235E-09
2739.07	6.329E-04	1.094E-05	6.796E-09	2.235E-09
2741.79	4.724E-03	1.094E-05	6.796E-09	2.235E-09
2743.79	2.122E-05	2.640E-05	6.795E-09	2.235E-09
2745.79	2.545E-05	2.435E-05	6.795E-09	2.235E-09
2747.79	1.747E-03	2.466E-05	6.794E-09	2.235E-09
2749.79	1.745E-03	2.466E-05	6.794E-09	2.235E-09
2751.79	1.745E-03	2.466E-05	6.794E-09	2.235E-09
2753.79	1.745E-03	2.466E-05	6.794E-09	2.235E-09
2755.79	1.745E-03	2.466E-05	6.794E-09	2.235E-09
2757.79	1.745E-03	2.466E-05	6.794E-09	2.235E-09
2759.79	1.745E-03	2.466E-05	6.794E-09	2.235E-09
2761.79	1.745E-03	2.466E-05	6.794E-09	2.235E-09
2763.79	1.745E-03	2.466E-05	6.794E-09	2.235E-09
2765.79	1.745E-03	2.466E-05	6.794E-09	2.235E-09
2767.79	1.745E-03	2.466E-05	6.794E-09	2.235E-09
2769.79	1.745E-03	2.466E-05	6.794E-09	2.235E-09
2771.79	1.745E-03	2.466E-05	6.794E-09	2.235E-09
2773.79	1.745E-03	2.466E-05	6.794E-09	2.235E-09
2775.79	1.745E-03	2.466E-05	6.794E-09	2.235E-09
2777.79	1.745E-03	2.466E-05	6.794E-09	2.235E-09
2779.79	1.745E-03	2.466E-05	6.794E-09	2.235E-09
2781.79	1.745E-03	2.466E-05	6.794E-09	2.235E-09
2783.79	1.745E-03	2.466E-05	6.794E-09	2.235E-09
2785.79	1.745E-03	2.466E-05	6.794E-09	2.235E-09
2787.79	1.745E-03	2.466E-05	6.794E-09	2.235E-09
2789.79	1.745E-03	2.466E-05	6.794E-09	2.235E-09
2791.79	1.745E-03	2.466E-05	6.794E-09	2.235E-09
2793.79	1.745E-03	2.466E-05	6.794E-09	2.235E-09
2795.79	1.745E-03	2.466E-05	6.794E-09	2.235E-09
2797.79	1.745E-03	2.466E-05	6.794E-09	2.235E-09
2799.79	1.745E-03	2.466E-05	6.794E-09	2.235E-09
2801.79	1.745E-03	2.466E-05	6.794E-09	2.235E-09
2803.79	1.745E-03	2.466E-05	6.794E-09	2.235E-09
2805.79	1.745E-03	2.466E-05	6.794E-09	2.235E-09
2807.79	1.745E-03	2.466E-05	6.794E-09	2.235E-09
2809.79	1.745E-03	2.466E-05	6.794E-09	2.235E-09
2811.79	1.745E-03	2.466E-05	6.794E-09	2.235E-09
2813.79	1.745E-03	2.466E-05	6.794E-09	2.235E-09
2815.79	1.745E-03	2.466E-05	6.794E-09	2.235E-09
2817.79	1.745E-03	2.466E-05	6.794E-09	2.235E-09

GROUP 1 ML5 AZIMUTH MEASUREMENT NOISE

TIME	POSITION ESTIMATE ERROR			VELOCITY ESTIMATE ERROR			PLATFORM TILT ESTIMATE ERROR		
	R	D	C	R	D	C	R	D	C
2723.03	1.000E-10	1.000E-10	1.000E-10	1.000E-10	1.000E-10	1.000E-10	1.000E-10	1.000E-10	1.000E-10
2723.03	2.834E-01	6.455E-01	1.201E+01	5.686E-02	2.847E-02	4.451E-02	2.221E-06	1.699E-06	9.390E-06
2723.03	4.411E-01	1.865E+00	1.389E+01	3.076E-01	1.461E-01	9.541E-01	1.820E-04	5.112E-05	9.618E-05
2742.23	1.013E+00	2.636E+00	9.537E+00	4.072E-02	4.411E-02	5.995E-01	1.102E-04	2.955E-05	3.017E-05
2749.91	1.036E+00	3.891E+00	7.966E+00	2.478E-02	1.895E-02	4.542E-01	8.942E-05	2.311E-05	3.091E-05
2757.50	9.554E-01	4.103E+00	5.697E+00	1.493E-02	1.543E-02	4.542E-01	8.942E-05	2.311E-05	3.091E-05
2767.19	1.044E+00	4.134E+00	4.439E+00	6.750E-03	9.512E-03	3.402E-01	8.939E-05	2.312E-05	3.092E-05
2776.79	9.945E-01	4.133E+00	3.900E+00	4.440E-03	9.211E-03	3.240E-01	8.939E-05	2.312E-05	3.092E-05
2786.19	7.934E-01	4.166E+00	3.347E+00	2.101E-02	9.211E-03	2.486E-01	8.939E-05	2.312E-05	3.092E-05
2794.07	4.973E-01	4.207E+00	2.900E+00	3.413E-02	9.211E-03	2.486E-01	8.939E-05	2.312E-05	3.092E-05
2801.75	1.430E-01	4.213E+00	2.459E+00	4.399E-02	9.211E-03	2.111E-01	8.939E-05	2.312E-05	3.092E-05
2809.43	1.118E-01	4.213E+00	2.459E+00	4.015E-02	1.059E-02	1.865E-01	8.939E-05	2.312E-05	3.092E-05
2809.43	8.217E-02	4.237E+00	2.059E+00	4.015E-02	8.866E-03	1.781E-01	8.939E-05	2.312E-05	3.092E-05
2811.35	1.675E-02	4.237E+00	1.969E+00	4.182E-02	9.590E-03	1.709E-01	8.939E-05	2.312E-05	3.092E-05
2813.27	1.681E-02	4.236E+00	1.883E+00	4.280E-02	9.590E-03	1.636E-01	8.939E-05	2.312E-05	3.092E-05
2815.19	1.692E-02	4.235E+00	1.800E+00	4.377E-02	8.816E-03	1.565E-01	8.939E-05	2.312E-05	3.092E-05
2817.11	1.026E-02	4.240E+00	2.016E+00	4.477E-02	1.021E-02	1.565E-01	8.939E-05	2.312E-05	3.092E-05
TIME	POSITION ESTIMATE ERROR			VELOCITY ESTIMATE ERROR			PLATFORM TILT ESTIMATE ERROR		
	R	D	C	R	D	C	R	D	C
2723.03	1.000E-10	1.000E-10	1.000E-10	1.000E-10	1.000E-10	1.000E-10	1.000E-10	1.000E-10	1.000E-10
2723.03	2.834E-01	6.455E-01	1.201E+01	5.686E-02	2.847E-02	4.451E-02	2.221E-06	1.699E-06	9.390E-06
2723.03	4.411E-01	1.865E+00	1.389E+01	3.076E-01	1.461E-01	9.541E-01	1.820E-04	5.112E-05	9.618E-05
2742.23	1.007E+00	2.636E+00	9.537E+00	4.072E-02	4.411E-02	5.995E-01	1.102E-04	2.955E-05	3.017E-05
2749.91	1.036E+00	3.891E+00	7.966E+00	2.478E-02	1.895E-02	4.542E-01	8.942E-05	2.311E-05	3.091E-05
2757.50	9.554E-01	4.103E+00	5.697E+00	1.493E-02	1.543E-02	4.542E-01	8.942E-05	2.311E-05	3.091E-05
2767.19	1.044E+00	4.134E+00	4.439E+00	6.750E-03	9.512E-03	3.402E-01	8.939E-05	2.312E-05	3.092E-05
2776.79	9.945E-01	4.133E+00	3.900E+00	4.440E-03	9.211E-03	3.240E-01	8.939E-05	2.312E-05	3.092E-05
2786.19	7.934E-01	4.166E+00	3.347E+00	2.101E-02	9.211E-03	2.486E-01	8.939E-05	2.312E-05	3.092E-05
2794.07	4.973E-01	4.207E+00	2.900E+00	3.413E-02	9.211E-03	2.486E-01	8.939E-05	2.312E-05	3.092E-05
2801.75	1.430E-01	4.213E+00	2.459E+00	4.399E-02	9.211E-03	2.111E-01	8.939E-05	2.312E-05	3.092E-05
2809.43	1.118E-01	4.213E+00	2.459E+00	4.015E-02	1.059E-02	1.865E-01	8.939E-05	2.312E-05	3.092E-05
2809.43	8.217E-02	4.237E+00	2.059E+00	4.015E-02	8.866E-03	1.781E-01	8.939E-05	2.312E-05	3.092E-05
2811.35	1.675E-02	4.237E+00	1.969E+00	4.182E-02	9.590E-03	1.709E-01	8.939E-05	2.312E-05	3.092E-05
2813.27	1.681E-02	4.236E+00	1.883E+00	4.280E-02	9.590E-03	1.636E-01	8.939E-05	2.312E-05	3.092E-05
2815.19	1.692E-02	4.235E+00	1.800E+00	4.377E-02	8.816E-03	1.565E-01	8.939E-05	2.312E-05	3.092E-05
2817.11	1.026E-02	4.240E+00	2.016E+00	4.477E-02	1.021E-02	1.565E-01	8.939E-05	2.312E-05	3.092E-05
TIME	POSITION ESTIMATE ERROR			VELOCITY ESTIMATE ERROR			PLATFORM TILT ESTIMATE ERROR		
	R	D	C	R	D	C	R	D	C
2723.03	1.000E-10	1.000E-10	1.000E-10	1.000E-10	1.000E-10	1.000E-10	1.000E-10	1.000E-10	1.000E-10
2723.03	2.834E-01	6.455E-01	1.201E+01	5.686E-02	2.847E-02	4.451E-02	2.221E-06	1.699E-06	9.390E-06
2723.03	4.411E-01	1.865E+00	1.389E+01	3.076E-01	1.461E-01	9.541E-01	1.820E-04	5.112E-05	9.618E-05
2742.23	1.007E+00	2.636E+00	9.537E+00	4.072E-02	4.411E-02	5.995E-01	1.102E-04	2.955E-05	3.017E-05
2749.91	1.036E+00	3.891E+00	7.966E+00	2.478E-02	1.895E-02	4.542E-01	8.942E-05	2.311E-05	3.091E-05
2757.50	9.554E-01	4.103E+00	5.697E+00	1.493E-02	1.543E-02	4.542E-01	8.942E-05	2.311E-05	3.091E-05
2767.19	1.044E+00	4.134E+00	4.439E+00	6.750E-03	9.512E-03	3.402E-01	8.939E-05	2.312E-05	3.092E-05
2776.79	9.945E-01	4.133E+00	3.900E+00	4.440E-03	9.211E-03	3.240E-01	8.939E-05	2.312E-05	3.092E-05
2786.19	7.934E-01	4.166E+00	3.347E+00	2.101E-02	9.211E-03	2.486E-01	8.939E-05	2.312E-05	3.092E-05
2794.07	4.973E-01	4.207E+00	2.900E+00	3.413E-02	9.211E-03	2.486E-01	8.939E-05	2.312E-05	3.092E-05
2801.75	1.430E-01	4.213E+00	2.459E+00	4.399E-02	9.211E-03	2.111E-01	8.939E-05	2.312E-05	3.092E-05
2809.43	1.118E-01	4.213E+00	2.459E+00	4.015E-02	1.059E-02	1.865E-01	8.939E-05	2.312E-05	3.092E-05
2809.43	8.217E-02	4.237E+00	2.059E+00	4.015E-02	8.866E-03	1.781E-01	8.939E-05	2.312E-05	3.092E-05
2811.35	1.675E-02	4.237E+00	1.969E+00	4.182E-02	9.590E-03	1.709E-01	8.939E-05	2.312E-05	3.092E-05
2813.27	1.681E-02	4.236E+00	1.883E+00	4.280E-02	9.590E-03	1.636E-01	8.939E-05	2.312E-05	3.092E-05
2815.19	1.692E-02	4.235E+00	1.800E+00	4.377E-02	8.816E-03	1.565E-01	8.939E-05	2.312E-05	3.092E-05
2817.11	1.026E-02	4.240E+00	2.016E+00	4.477E-02	1.021E-02	1.565E-01	8.939E-05	2.312E-05	3.092E-05

GROUP 1 MSL ELEVATION MEASUREMENT NOISE

TIME	POSITION ESTIMATE ERROR R	VELOCITY ESTIMATE ERROR R	VELOCITY ESTIMATE ERROR D	PLATFORM TILT ESTIMATE ERROR C	PLATFORM TILT ESTIMATE ERROR D	PLATFORM TILT ESTIMATE ERROR C
2723.03	1.000E-10	1.000E-10	1.000E-10	1.000E-10	1.000E-10	1.000E-10
2723.03	4.016E+00	2.934E-02	1.265E-02	1.774E-01	2.943E-07	2.635E-06
2734.55	6.926E+00	7.914E-01	2.834E-01	1.547E-01	2.164E-04	1.102E-04
2742.23	3.127E+00	2.756E-01	8.148E-02	1.814E-02	5.955E-06	3.610E-05
2749.91	2.924E+00	1.756E-01	5.499E-02	7.322E-01	1.959E-06	2.775E-05
2757.59	2.299E+00	1.171E-01	2.725E-02	6.809E-04	3.746E-06	2.775E-05
2767.12	1.229E+00	1.443E-01	4.143E-02	1.988E-03	4.519E-06	2.775E-05
2776.79	1.017E+00	1.029E-01	2.514E-02	3.375E-03	4.530E-06	2.775E-05
2786.12	8.035E-01	6.535E-02	1.179E-02	3.493E-03	3.895E-06	2.775E-05
2794.07	6.035E-01	5.354E-02	1.077E-02	3.410E-03	4.549E-06	2.775E-05
2801.75	4.534E-01	4.495E-02	1.018E-02	3.289E-03	3.887E-06	2.775E-05
2809.43	4.034E-01	3.721E-02	1.054E-02	2.835E-03	4.567E-06	2.776E-05
2809.43	2.261E-03	3.721E-02	8.577E-03	2.777E-03	4.567E-06	2.776E-05
2811.35	2.197E-03	3.835E-02	9.147E-03	2.602E-03	3.959E-06	2.776E-05
2813.27	2.075E-03	3.904E-02	8.648E-03	2.488E-03	4.571E-06	2.776E-05
2815.19	2.052E-03	3.973E-02	8.180E-03	2.378E-03	3.853E-06	2.776E-05
2817.11	4.472E-03	4.046E-02	9.595E-03	2.118E-03	3.850E-06	2.776E-05
TIME	U	V	W	U	V	W
2723.03	1.000E-10	1.000E-10	1.000E-10	1.000E-10	1.000E-10	1.000E-10
2723.03	4.016E+00	2.934E-02	1.265E-02	4.764E-07	1.933E-06	1.841E-06
2734.55	6.926E+00	7.914E-01	2.834E-01	3.597E-05	5.759E-05	9.642E-05
2742.23	3.127E+00	2.756E-01	8.148E-02	5.784E-06	9.852E-06	3.523E-05
2749.91	2.924E+00	1.756E-01	5.499E-02	3.943E-06	3.655E-06	2.782E-05
2757.59	2.299E+00	1.171E-01	2.725E-02	3.230E-06	4.104E-06	2.782E-05
2767.12	1.229E+00	1.443E-01	4.143E-02	3.913E-06	4.271E-06	2.779E-05
2776.79	1.017E+00	1.029E-01	2.514E-02	3.897E-06	4.512E-06	2.776E-05
2786.12	8.035E-01	6.535E-02	1.179E-02	3.880E-06	4.639E-06	2.774E-05
2794.07	6.035E-01	5.354E-02	1.077E-02	3.867E-06	4.609E-06	2.775E-05
2801.75	4.534E-01	4.495E-02	1.018E-02	3.853E-06	4.585E-06	2.776E-05
2809.43	4.034E-01	3.721E-02	1.054E-02	3.840E-06	4.585E-06	2.776E-05
2809.43	2.261E-03	3.721E-02	8.577E-03	3.840E-06	4.585E-06	2.776E-05
2811.35	2.197E-03	3.835E-02	9.147E-03	3.840E-06	4.585E-06	2.776E-05
2813.27	2.075E-03	3.904E-02	8.648E-03	3.840E-06	4.585E-06	2.776E-05
2815.19	2.052E-03	3.973E-02	8.180E-03	3.840E-06	4.585E-06	2.776E-05
2817.11	4.472E-03	4.046E-02	9.595E-03	3.840E-06	4.585E-06	2.776E-05

[illegible]

GROUP 1: RADAR ALTIMETER MEASUREMENT NOISE

TIME	POSITION R	ESTIMATE D	ERROR C	VFLOCI R	ESTIMATE D	ERROR C	PROP C	U	PLATFORM R	TILT D	ESTIMATE D	ERROR C
2809.43	1.000E-10	1.000E-10	1.000E-10	1.000E-10	1.000E-10	1.000E-10	1.000E-10	1.000E-10	1.000E-10	1.000E-10	1.000E-10	1.000E-10
2809.43	2.250E-01	4.730E-04	2.447E-05	7.525E-09	5.049E-05	1.000E-10	1.000E-10	1.000E-10	1.000E-10	1.000E-10	1.000E-10	1.000E-10
2809.43	3.400E-01	5.036E-04	2.233E-05	1.213E-08	5.630E-05	1.000E-10	1.000E-10	1.000E-10	1.000E-10	1.000E-10	1.000E-10	1.000E-10
2811.37	3.400E-01	5.036E-04	3.924E-05	1.254E-08	5.630E-05	1.000E-10	1.000E-10	1.000E-10	1.000E-10	1.000E-10	1.000E-10	1.000E-10
2815.19	3.400E-01	3.774E-04	6.168E-05	2.493E-06	2.146E-05	1.000E-10	1.000E-10	1.000E-10	1.000E-10	1.000E-10	1.000E-10	1.000E-10
2817.11	3.400E-01	4.049E-04	1.939E-04	2.493E-06	2.063E-05	2.219E-05	2.219E-05	2.219E-05	1.000E-10	1.000E-10	1.000E-10	1.000E-10
2830.43	1.000E-10	1.000E-10	1.000E-10	1.000E-10	1.000E-10	1.000E-10	1.000E-10	1.000E-10	1.000E-10	1.000E-10	1.000E-10	1.000E-10
2830.43	2.250E-01	2.104E-04	3.733E-05	1.473E-07	5.049E-05	1.000E-10	1.000E-10	1.000E-10	1.000E-10	1.000E-10	1.000E-10	1.000E-10
2830.43	3.400E-01	3.400E-04	7.916E-05	1.310E-06	5.630E-05	1.000E-10	1.000E-10	1.000E-10	1.000E-10	1.000E-10	1.000E-10	1.000E-10
2811.37	3.400E-01	9.200E-04	1.062E-04	2.034E-06	3.989E-05	1.000E-10	1.000E-10	1.000E-10	1.000E-10	1.000E-10	1.000E-10	1.000E-10
2815.19	3.400E-01	1.046E-03	1.339E-04	2.539E-06	2.146E-05	1.000E-10	1.000E-10	1.000E-10	1.000E-10	1.000E-10	1.000E-10	1.000E-10
2817.11	3.400E-01	1.162E-03	2.728E-04	2.984E-06	2.063E-05	2.219E-05	2.219E-05	2.219E-05	1.000E-10	1.000E-10	1.000E-10	1.000E-10

GROUP 1 QUANTIZATION ERROR

TIME	POSITION R	ESTIMATE D	ERROR C	VELOCITY R	ESTIMATE D	ERROR C	PLATFORM R	TILT D	ESTIMATE D	ERROR C
27272.03	5.150E+00	7.501E+00	5.590E+00	2.144E+01	1.953E+01	1.441E+01	3.447E+05	5.866E+05	5.254E+05	-
27272.04	5.160E+00	7.513E+00	6.588E+00	2.039E+01	1.895E+01	1.441E+01	3.543E+05	5.826E+05	5.254E+05	-
27272.05	6.104E+00	1.621E+01	2.037E+01	1.862E+02	4.035E+02	4.035E+02	5.131E+05	6.578E+05	8.214E+05	-
27272.06	6.105E+00	1.621E+01	2.037E+01	1.862E+02	4.035E+02	4.035E+02	5.622E+05	6.730E+05	8.277E+05	-
27272.07	6.107E+00	2.244E+01	2.239E+01	2.314E+02	4.777E+02	5.490E+02	5.646E+05	6.770E+05	8.277E+05	-
27272.08	1.624E+01	2.244E+01	2.239E+01	2.444E+02	1.666E+02	3.000E+02	5.646E+05	6.770E+05	8.277E+05	-
27272.09	1.624E+01	2.244E+01	2.239E+01	1.959E+02	1.376E+02	3.000E+02	5.630E+05	6.747E+05	8.277E+05	-
27272.10	1.624E+01	1.931E+01	1.780E+01	1.770E+02	1.133E+02	4.000E+02	5.630E+05	6.747E+05	8.277E+05	-
27272.11	1.974E+01	1.874E+01	1.510E+01	1.170E+02	1.325E+02	4.000E+02	5.630E+05	6.752E+05	8.278E+05	-
27272.12	1.847E+01	1.847E+01	1.124E+01	2.738E+02	1.804E+02	5.000E+02	5.623E+05	6.755E+05	8.279E+05	-
27272.13	1.847E+01	1.847E+01	1.124E+01	2.738E+02	1.804E+02	5.000E+02	5.623E+05	6.755E+05	8.279E+05	-
27272.14	2.590E+01	2.713E+01	8.745E+02	2.910E+02	2.100E+02	7.000E+02	5.620E+05	6.757E+05	8.279E+05	-
27272.15	2.600E+01	1.962E+01	8.27E+02	2.910E+02	2.100E+02	7.000E+02	5.619E+05	6.758E+05	8.280E+05	-
27272.16	2.821E+03	2.915E+03	7.945E+02	3.592E+02	2.393E+02	8.000E+02	5.619E+05	6.758E+05	8.280E+05	-
27272.17	3.124E+03	2.911E+03	7.349E+02	3.592E+02	2.393E+02	8.000E+02	5.617E+05	6.759E+05	8.280E+05	-
27272.18	3.124E+03	2.911E+03	6.826E+02	4.673E+02	2.683E+02	9.000E+02	5.616E+05	6.759E+05	8.280E+05	-
27272.19	4.040E+03	2.942E+03	6.826E+02	4.673E+02	2.683E+02	9.000E+02	5.616E+05	6.759E+05	8.280E+05	-

[illegible]

GROUP 2 ACCELEROMETER BIASES

TIME	POSITION R	ESTIMATE D	ACCELEROMETER ERROR C	VELOCITY R	ESTIMATE D	VELOCITY ERROR C	PLATFORM R	TILT D	ESTIMATE C	ERROR C
2723.03	7.850E+00	1.137E+02	9.795E+01	1.250E+00	1.400E+00	1.942E+00	6.100E+04	4.212E-04	5.900E-04	5.900E-04
2723.03	1.140E+00	1.512E+00	1.466E+00	1.384E+00	1.027E+01	1.660E+01	6.131E-04	4.212E-04	5.900E-04	5.900E-04
2734.55	1.302E+00	1.749E+00	2.222E+00	1.023E-01	2.265E-01	2.500E-01	4.237E-04	3.920E-04	4.017E-04	4.017E-04
2742.23	7.060E-01	1.871E+00	2.669E+00	3.382E-02	5.868E-02	7.840E-02	3.730E-04	3.730E-04	4.017E-04	4.017E-04
2749.59	1.214E+00	1.797E+00	3.025E+00	4.796E-01	7.684E-02	1.477E-02	3.240E-04	3.730E-04	4.017E-04	4.017E-04
2757.59	1.614E+00	1.807E+00	3.367E+00	1.128E-01	6.035E-02	4.622E-02	3.240E-04	3.730E-04	4.017E-04	4.017E-04
2767.19	1.329E+00	1.699E+00	2.767E+00	1.024E-02	6.505E-02	7.220E-02	3.240E-04	3.730E-04	4.017E-04	4.017E-04
2766.39	1.490E+00	1.774E+00	2.286E+00	8.156E-02	6.362E-02	8.095E-02	3.240E-04	3.730E-04	4.017E-04	4.017E-04
2794.07	9.529E-01	1.826E+00	1.938E+00	8.809E-02	6.458E-02	8.672E-02	3.240E-04	3.730E-04	4.017E-04	4.017E-04
2801.75	1.207E+00	1.838E+00	1.586E+00	1.140E-01	6.735E-02	9.432E-02	3.240E-04	3.730E-04	4.017E-04	4.017E-04
2809.43	6.762E-01	1.726E+00	1.304E+00	1.238E-01	1.211E-01	8.966E-02	3.240E-04	3.730E-04	4.017E-04	4.017E-04
2811.35	9.877E-03	1.817E+00	1.336E+00	1.540E-01	1.001E-01	7.700E-02	3.240E-04	3.730E-04	4.017E-04	4.017E-04
2813.27	1.010E-02	1.802E+00	1.240E+00	1.717E-01	1.147E-01	7.980E-02	3.240E-04	3.730E-04	4.017E-04	4.017E-04
2815.19	1.100E-02	1.793E+00	1.192E+00	1.881E-01	1.085E-01	7.200E-02	3.240E-04	3.730E-04	4.017E-04	4.017E-04
2817.11	2.250E-02	1.699E+00	1.145E+00	2.049E-01	1.286E-01	6.110E-02	3.240E-04	3.730E-04	4.017E-04	4.017E-04
TIME	U	V	W	U	V	W	U	V	W	
2723.03	7.850E+00	1.495E+02	9.067E+01	1.250E+00	2.340E+00	7.130E+00	6.100E+04	4.212E-04	5.900E-04	5.900E-04
2723.03	1.139E+00	2.099E+00	3.073E+00	1.384E+00	1.810E+00	2.370E+00	6.131E-04	4.212E-04	5.900E-04	5.900E-04
2734.55	1.202E+00	2.596E+00	3.762E+00	1.023E-01	4.499E+00	6.810E+00	4.237E-04	3.920E-04	4.017E-04	4.017E-04
2742.23	7.060E-01	2.140E+00	3.073E+00	3.382E-02	6.794E+00	1.477E+00	3.240E-04	3.730E-04	4.017E-04	4.017E-04
2749.59	1.214E+00	1.768E+00	3.381E+00	4.806E-02	7.027E+00	2.440E+00	3.240E-04	3.730E-04	4.017E-04	4.017E-04
2757.59	1.329E+00	1.674E+00	3.281E+00	1.129E-01	6.471E+00	2.222E+00	3.240E-04	3.730E-04	4.017E-04	4.017E-04
2767.19	1.329E+00	1.674E+00	3.281E+00	1.024E-02	6.471E+00	2.222E+00	3.240E-04	3.730E-04	4.017E-04	4.017E-04
2766.39	1.490E+00	1.714E+00	2.769E+00	8.156E-02	6.362E+00	2.222E+00	3.240E-04	3.730E-04	4.017E-04	4.017E-04
2794.07	9.529E-01	1.832E+00	2.281E+00	8.809E-02	6.458E+00	2.222E+00	3.240E-04	3.730E-04	4.017E-04	4.017E-04
2801.75	6.762E-01	1.832E+00	1.586E+00	1.140E-01	6.735E+00	2.222E+00	3.240E-04	3.730E-04	4.017E-04	4.017E-04
2809.43	9.877E-03	1.813E+00	1.336E+00	1.540E-01	7.027E+00	2.222E+00	3.240E-04	3.730E-04	4.017E-04	4.017E-04
2811.35	1.010E-02	1.813E+00	1.240E+00	1.717E-01	7.027E+00	2.222E+00	3.240E-04	3.730E-04	4.017E-04	4.017E-04
2813.27	1.100E-02	1.796E+00	1.192E+00	1.881E-01	7.027E+00	2.222E+00	3.240E-04	3.730E-04	4.017E-04	4.017E-04
2815.19	2.250E-02	1.699E+00	1.145E+00	2.049E-01	7.027E+00	2.222E+00	3.240E-04	3.730E-04	4.017E-04	4.017E-04
2817.11	2.250E-02	1.699E+00	1.145E+00	2.049E-01	7.027E+00	2.222E+00	3.240E-04	3.730E-04	4.017E-04	4.017E-04

GROUP 3 ACCELEROMETER SCALE FACTORS

TIME	POSITION R	ESTIMATE D	ERROR C	VELOCITY R	ESTIMATE D	ERROR C	PLATFORM R	YILT D	ESTIMATE D	ERROR C
2723.01	7.407E+00	4.452E+01	3.735E+01	7.137E-01	4.791E-01	2.51E-01	2.31E-05	8.92E-05	5.75E-05	5.75E-05
2723.55	5.297E-01	6.929E+00	5.917E+00	5.648E-01	3.015E-01	1.140E-01	2.35E-05	9.18E-05	6.05E-05	6.05E-05
2724.23	8.168E-02	1.424E+00	1.017E+00	1.109E-02	6.399E-02	3.530E-02	1.24E-05	9.70E-05	1.01E-04	1.01E-04
2724.91	1.207E-01	1.459E-01	3.182E-01	2.249E-02	5.325E-02	9.479E-03	2.80E-05	9.68E-05	1.10E-04	1.10E-04
2725.59	3.594E-01	1.614E-01	6.233E-01	4.141E-02	2.958E-02	2.021E-02	2.65E-05	9.68E-05	1.10E-04	1.10E-04
2726.27	3.703E-01	2.262E-01	4.847E-01	3.148E-02	2.392E-02	2.021E-02	2.65E-05	9.68E-05	1.10E-04	1.10E-04
2726.95	3.335E-01	1.991E-01	4.174E-01	2.859E-02	3.241E-02	1.774E-02	2.67E-05	9.70E-05	1.10E-04	1.10E-04
2727.63	3.010E-01	2.062E-01	3.684E-01	3.069E-02	3.735E-02	1.832E-02	2.67E-05	9.70E-05	1.10E-04	1.10E-04
2728.31	3.161E-01	1.915E-01	3.530E-01	4.094E-02	5.609E-02	3.568E-02	2.68E-05	9.71E-05	1.10E-04	1.10E-04
2728.99	3.300E-01	1.118E-01	3.685E-01	4.920E-02	5.589E-02	2.710E-02	2.68E-05	9.71E-05	1.10E-04	1.10E-04
2729.67	3.418E-01	1.832E-01	3.059E-01	4.921E-02	5.071E-02	3.112E-02	2.68E-05	9.71E-05	1.10E-04	1.10E-04
2730.35	3.773E-03	1.801E-01	3.020E-01	6.173E-02	4.883E-02	3.019E-02	2.68E-05	9.71E-05	1.10E-04	1.10E-04
2731.03	3.346E-03	1.822E-01	2.955E-01	7.567E-02	4.683E-02	3.019E-02	2.68E-05	9.71E-05	1.10E-04	1.10E-04
2731.71	8.336E-03	1.174E-01	3.452E-01	8.261E-02	5.530E-02	3.519E-02	2.68E-05	9.71E-05	1.10E-04	1.10E-04
TIME	U	V	M	U	V	M	U	V	M	
2723.01	7.352E+00	5.08E+01	2.137E+02	7.133E-01	4.997E-01	1.679E-01	2.23E-05	9.20E-05	4.4E-05	4.4E-05
2723.55	5.297E-01	9.099E+00	5.207E-01	5.646E-01	2.917E-01	1.380E-01	2.35E-05	1.09E-05	5.91E-05	5.91E-05
2724.23	8.168E-02	1.073E+00	5.207E-01	1.106E-02	2.156E-02	7.224E-02	2.35E-05	1.09E-05	5.91E-05	5.91E-05
2724.91	1.207E-01	1.008E-01	4.521E-01	2.249E-02	5.295E-02	2.099E-02	2.35E-05	1.09E-05	5.91E-05	5.91E-05
2725.59	3.594E-01	1.590E-01	6.561E-01	4.141E-02	2.958E-02	2.099E-02	2.35E-05	1.09E-05	5.91E-05	5.91E-05
2726.27	3.703E-01	2.215E-01	6.561E-01	3.141E-02	3.392E-02	2.099E-02	2.35E-05	1.09E-05	5.91E-05	5.91E-05
2726.95	3.335E-01	2.067E-01	4.849E-01	2.854E-02	3.236E-02	1.777E-02	2.35E-05	1.09E-05	5.91E-05	5.91E-05
2727.63	3.010E-01	2.004E-01	4.173E-01	3.064E-02	3.487E-02	1.837E-02	2.35E-05	1.09E-05	5.91E-05	5.91E-05
2728.31	3.161E-01	2.073E-01	3.681E-01	4.074E-02	3.729E-02	1.837E-02	2.35E-05	1.09E-05	5.91E-05	5.91E-05
2728.99	3.300E-01	1.925E-01	3.329E-01	4.929E-02	5.600E-02	2.369E-02	2.35E-05	1.09E-05	5.91E-05	5.91E-05
2729.67	3.418E-01	1.831E-01	3.058E-01	4.929E-02	5.061E-02	2.369E-02	2.35E-05	1.09E-05	5.91E-05	5.91E-05
2730.35	3.773E-03	1.801E-01	3.020E-01	6.181E-02	4.580E-02	2.369E-02	2.35E-05	1.09E-05	5.91E-05	5.91E-05
2731.03	3.346E-03	1.822E-01	2.955E-01	7.567E-02	4.670E-02	2.369E-02	2.35E-05	1.09E-05	5.91E-05	5.91E-05
2731.71	8.336E-03	1.174E-01	3.452E-01	8.267E-02	5.610E-02	2.369E-02	2.35E-05	1.09E-05	5.91E-05	5.91E-05

GROUP 4 ACCELEROMETER ASYMMETRIES

TIME	POSITION ESTIMATE ERROR R	VELOCITY ESTIMATE ERROR R	PLATFORM YLT ESTIMATE ERROR R	VELOCITY ESTIMATE ERROR D	PLATFORM YLT ESTIMATE ERROR D	VELOCITY ESTIMATE ERROR C	PLATFORM YLT ESTIMATE ERROR C
2723.03	7.624E+00	4.778E+01	4.027E+01	5.232E+01	3.492E+01	2.802E+01	3.129E+05
2723.03	5.661E-01	7.393E+01	6.379E+01	3.296E+01	3.492E+01	1.537E+01	5.129E+05
2723.03	9.868E-01	1.485E+00	1.192E+01	1.569E+01	3.492E+01	1.687E+01	5.129E+05
2742.23	1.390E-01	1.769E+01	4.600E+01	6.548E+01	3.492E+01	4.877E+01	1.174E+04
2749.91	1.520E-01	2.232E+01	6.067E+01	5.482E+01	3.492E+01	2.077E+01	1.174E+04
2757.59	3.422E-01	3.404E+01	7.690E+01	5.151E+01	3.492E+01	2.077E+01	1.174E+04
2767.19	3.715E-01	3.715E+01	7.712E+01	5.151E+01	3.492E+01	2.077E+01	1.174E+04
2776.79	3.911E-01	3.456E+01	6.114E+01	5.151E+01	3.492E+01	2.077E+01	1.174E+04
2786.39	3.486E-01	3.417E+01	5.193E+01	5.151E+01	3.492E+01	2.077E+01	1.174E+04
2794.07	3.198E-01	3.512E+01	4.965E+01	5.151E+01	3.492E+01	2.077E+01	1.174E+04
2801.75	2.448E-01	3.420E+01	3.965E+01	5.151E+01	3.492E+01	2.077E+01	1.174E+04
2809.43	2.448E-01	3.420E+01	3.965E+01	5.151E+01	3.492E+01	2.077E+01	1.174E+04
2811.35	4.302E-03	3.311E+01	3.472E+01	5.151E+01	3.492E+01	2.077E+01	1.174E+04
2813.27	4.376E-03	3.309E+01	3.380E+01	5.151E+01	3.492E+01	2.077E+01	1.174E+04
2815.19	4.376E-03	3.309E+01	3.380E+01	5.151E+01	3.492E+01	2.077E+01	1.174E+04
2817.11	8.147E-03	2.827E+01	3.756E+01	5.151E+01	3.492E+01	2.077E+01	1.174E+04
TIME	POSITION ESTIMATE ERROR U	VELOCITY ESTIMATE ERROR U	PLATFORM YLT ESTIMATE ERROR U	VELOCITY ESTIMATE ERROR V	PLATFORM YLT ESTIMATE ERROR V	VELOCITY ESTIMATE ERROR W	PLATFORM YLT ESTIMATE ERROR W
2723.03	7.575E+00	4.778E+01	4.027E+01	5.232E+01	3.492E+01	2.802E+01	3.129E+05
2723.03	5.653E-01	7.393E+01	6.379E+01	3.296E+01	3.492E+01	1.537E+01	5.129E+05
2742.23	1.388E-01	1.769E+01	4.557E+01	6.548E+01	3.492E+01	4.877E+01	1.174E+04
2749.91	1.519E-01	2.226E+01	6.071E+01	5.470E+01	3.492E+01	2.077E+01	1.174E+04
2757.59	3.425E-01	3.352E+01	7.150E+01	5.151E+01	3.492E+01	2.077E+01	1.174E+04
2767.19	3.906E-01	3.456E+01	6.117E+01	5.151E+01	3.492E+01	2.077E+01	1.174E+04
2776.79	3.481E-01	3.420E+01	5.193E+01	5.151E+01	3.492E+01	2.077E+01	1.174E+04
2786.39	3.073E-01	3.525E+01	4.965E+01	5.151E+01	3.492E+01	2.077E+01	1.174E+04
2801.75	3.351E-01	3.420E+01	3.965E+01	5.151E+01	3.492E+01	2.077E+01	1.174E+04
2809.43	4.347E-01	3.342E+01	3.472E+01	5.151E+01	3.492E+01	2.077E+01	1.174E+04
2811.35	3.033E-03	3.311E+01	3.472E+01	5.151E+01	3.492E+01	2.077E+01	1.174E+04
2813.27	3.033E-03	3.311E+01	3.472E+01	5.151E+01	3.492E+01	2.077E+01	1.174E+04
2815.19	4.385E-03	3.311E+01	3.472E+01	5.151E+01	3.492E+01	2.077E+01	1.174E+04
2817.11	8.566E-03	2.827E+01	3.756E+01	5.151E+01	3.492E+01	2.077E+01	1.174E+04

D-14

REPRODUCIBILITY OF THE
ORIGINAL PAGE IS POOR

GROUP 7 GYRO BIAS DRIFTS									
TIME	POSITION ESTIMATE ERROR			VELOCITY ESTIMATE ERROR			PLATFORM TILT ESTIMATE ERROR		
	R	D	C	R	D	C	R	D	C
2723.03	3.46E+00	2.00E+01	2.01E+01	6.12E-01	9.37E-01	9.36E-01	2.39E-04	2.13E-04	2.41E-04
2723.03	1.691E-01	3.21E-01	3.68E-01	6.15E-01	7.51E-01	8.09E-01	2.39E-04	2.13E-04	2.41E-04
2734.55	7.27E-01	1.85E+00	1.82E+00	1.02E-01	1.02E-01	1.02E-01	2.39E-04	2.13E-04	2.41E-04
2742.23	7.38E-01	1.45E+00	1.72E+00	6.57E-02	1.22E-02	1.22E-02	2.39E-04	2.13E-04	2.41E-04
2749.91	8.31E-01	1.40E+00	1.66E+00	6.57E-02	4.47E-02	8.07E-02	2.39E-04	2.13E-04	2.41E-04
2757.59	1.13E+00	1.09E+00	1.92E+00	8.53E-02	6.89E-02	2.58E-02	2.39E-04	2.13E-04	2.41E-04
2767.19	7.35E-01	1.53E+00	1.87E+00	5.44E-02	4.21E-02	3.12E-02	2.39E-04	2.13E-04	2.41E-04
2776.79	5.08E-01	1.53E+00	1.58E+00	4.46E-02	4.46E-02	4.46E-02	2.39E-04	2.13E-04	2.41E-04
2786.39	4.14E-01	1.55E+00	1.30E+00	6.24E-02	4.46E-02	5.52E-02	2.39E-04	2.13E-04	2.41E-04
2794.07	4.18E-01	1.56E+00	1.09E+00	7.54E-02	4.46E-02	4.46E-02	2.39E-04	2.13E-04	2.41E-04
2801.75	5.64E-01	1.58E+00	8.65E-01	9.41E-02	6.27E-02	7.14E-02	2.39E-04	2.13E-04	2.41E-04
2809.43	8.50E-01	1.70E+00	6.01E-01	1.02E-01	8.37E-02	6.51E-02	2.39E-04	2.13E-04	2.41E-04
2809.43	4.86E-01	1.60E+00	6.34E-01	1.02E-01	6.91E-02	6.51E-02	2.39E-04	2.13E-04	2.41E-04
2811.35	1.20E-02	1.61E+00	6.34E-01	1.35E-01	7.62E-02	6.51E-02	2.39E-04	2.13E-04	2.41E-04
2813.27	1.23E-02	1.61E+00	5.91E-01	1.35E-01	7.62E-02	6.51E-02	2.39E-04	2.13E-04	2.41E-04
2815.19	1.29E-02	1.61E+00	5.53E-01	1.46E-01	7.37E-02	6.37E-02	2.39E-04	2.13E-04	2.41E-04
2817.11	1.25E-02	1.71E+00	4.24E-01	1.58E-01	8.71E-02	7.15E-02	2.39E-04	2.13E-04	2.41E-04
TIME	U	V	M	U	V	M	U	V	M
2723.03	3.88E+00	3.59E+01	1.38E+01	1.27E-01	9.42E-01	7.87E-01	2.39E-04	2.13E-04	2.41E-04
2723.03	1.68E-01	3.12E-01	3.79E-01	6.58E-02	9.00E-01	7.87E-01	2.39E-04	2.13E-04	2.41E-04
2734.55	7.35E-01	1.55E+00	2.08E+00	9.93E-02	2.18E-01	3.02E-01	2.39E-04	2.13E-04	2.41E-04
2742.23	8.29E-01	1.63E+00	1.55E+00	6.57E-02	7.34E-01	2.97E-01	2.39E-04	2.13E-04	2.41E-04
2749.91	1.13E+00	1.35E+00	1.90E+00	8.18E-02	4.60E-01	2.58E-01	2.39E-04	2.13E-04	2.41E-04
2757.59	7.37E-01	1.67E+00	1.94E+00	8.54E-02	4.60E-01	2.58E-01	2.39E-04	2.13E-04	2.41E-04
2767.19	5.06E-01	1.54E+00	1.88E+00	6.61E-02	4.60E-01	2.58E-01	2.39E-04	2.13E-04	2.41E-04
2776.79	5.06E-01	1.54E+00	1.88E+00	6.61E-02	4.60E-01	2.58E-01	2.39E-04	2.13E-04	2.41E-04
2786.39	4.13E-01	1.54E+00	1.27E+00	6.25E-02	4.60E-01	2.58E-01	2.39E-04	2.13E-04	2.41E-04
2794.07	4.18E-01	1.54E+00	1.09E+00	7.08E-02	4.60E-01	2.58E-01	2.39E-04	2.13E-04	2.41E-04
2801.75	5.66E-01	1.58E+00	8.64E-01	9.42E-02	6.27E-01	7.14E-01	2.39E-04	2.13E-04	2.41E-04
2809.43	8.50E-01	1.70E+00	6.00E-01	1.02E-01	8.37E-02	6.51E-02	2.39E-04	2.13E-04	2.41E-04
2809.43	4.86E-01	1.60E+00	6.33E-01	1.02E-01	6.91E-02	6.51E-02	2.39E-04	2.13E-04	2.41E-04
2811.35	7.90E-03	1.61E+00	6.33E-01	1.35E-01	7.62E-02	6.51E-02	2.39E-04	2.13E-04	2.41E-04
2813.27	7.90E-03	1.61E+00	5.91E-01	1.35E-01	7.62E-02	6.51E-02	2.39E-04	2.13E-04	2.41E-04
2815.19	8.75E-03	1.61E+00	5.53E-01	1.46E-01	7.37E-02	6.37E-02	2.39E-04	2.13E-04	2.41E-04
2817.11	1.61E-02	1.71E+00	4.24E-01	1.58E-01	8.71E-02	7.15E-02	2.39E-04	2.13E-04	2.41E-04

GROUP B GYRO MASS UNBALANCES

TIME	POSITION ESTIMATE R	GYRO MASS UNBALANCES D	VELOCITY ESTIMATE R	VELOCITY ESTIMATE ERROR D	VELOCITY ESTIMATE ERROR C	PLATFORM TILT ESTIMATE ERROR R	PLATFORM TILT ESTIMATE ERROR D	PLATFORM TILT ESTIMATE ERROR C
2723.03	4.377E-01	3.944E+00	8.821E-02	1.473E-01	2.012E-01	5.379E-05	5.071E-05	3.570E-05
2723.03	3.681E-02	4.831E-01	9.916E-02	1.294E-01	1.849E-01	5.379E-05	5.071E-05	3.570E-05
2723.55	1.174E-01	2.850E-01	1.961E-02	2.970E-02	9.593E-02	5.379E-05	5.071E-05	3.570E-05
2729.21	1.169E-01	3.094E-01	1.275E-02	9.904E-03	3.170E-02	4.422E-05	5.062E-05	4.454E-05
2729.59	2.001E-01	3.586E-01	1.384E-02	1.137E-02	8.879E-03	4.422E-05	5.062E-05	4.454E-05
2737.19	1.173E-01	3.337E-01	9.107E-03	7.401E-03	9.479E-03	4.422E-05	5.062E-05	4.454E-05
2737.79	1.173E-01	3.413E-01	9.107E-03	6.768E-03	1.364E-02	4.422E-05	5.062E-05	4.454E-05
2738.07	8.739E-02	3.471E-01	1.042E-02	7.129E-03	1.507E-02	4.422E-05	5.062E-05	4.454E-05
2738.75	7.662E-02	3.509E-01	1.259E-02	7.839E-03	1.577E-02	4.422E-05	5.062E-05	4.454E-05
2801.75	8.057E-02	3.570E-01	1.660E-02	1.306E-02	2.188E-02	4.422E-05	5.062E-05	4.454E-05
2809.43	1.351E-01	3.598E-01	1.661E-02	1.078E-02	1.890E-02	4.422E-05	5.062E-05	4.454E-05
2809.43	7.099E-02	3.576E-01	1.982E-02	1.219E-02	2.047E-02	4.422E-05	5.062E-05	4.454E-05
2813.27	2.166E-03	3.577E-01	2.166E-02	1.186E-02	1.989E-02	4.422E-05	5.062E-05	4.454E-05
2815.19	2.207E-03	3.577E-01	2.343E-02	1.148E-02	1.925E-02	4.422E-05	5.062E-05	4.454E-05
2817.11	1.388E-03	3.577E-01	2.523E-02	1.357E-02	2.190E-02	4.422E-05	5.062E-05	4.454E-05
TIME	U	V	U	V	M	U	V	M
2723.03	4.035E-01	8.85E+00	8.821E-02	1.995E-01	1.496E-01	5.379E-05	4.851E-05	3.866E-05
2723.03	3.171E-01	7.831E-02	9.916E-02	1.539E-01	1.372E-01	5.379E-05	4.851E-05	3.866E-05
2723.55	1.184E-01	2.734E-01	1.961E-02	4.639E-02	1.948E-02	4.422E-05	5.062E-05	4.454E-05
2729.21	2.056E-01	3.616E-01	1.274E-02	3.975E-02	2.183E-02	4.422E-05	5.062E-05	4.454E-05
2729.59	2.577E-01	3.527E-01	1.384E-02	1.007E-02	3.120E-02	4.422E-05	5.062E-05	4.454E-05
2737.19	1.172E-01	3.353E-01	9.121E-03	1.134E-02	8.879E-03	4.422E-05	5.062E-05	4.454E-05
2737.79	8.075E-02	3.484E-01	9.107E-03	7.750E-03	1.364E-02	4.422E-05	5.062E-05	4.454E-05
2738.07	7.430E-02	3.516E-01	1.042E-02	7.090E-03	1.507E-02	4.422E-05	5.062E-05	4.454E-05
2738.75	8.075E-02	3.516E-01	1.259E-02	7.839E-03	1.577E-02	4.422E-05	5.062E-05	4.454E-05
2801.75	1.357E-01	3.546E-01	1.661E-02	1.078E-02	1.890E-02	4.422E-05	5.062E-05	4.454E-05
2809.43	1.357E-01	3.546E-01	1.661E-02	1.078E-02	1.890E-02	4.422E-05	5.062E-05	4.454E-05
2809.43	7.099E-02	3.570E-01	1.982E-02	1.219E-02	2.047E-02	4.422E-05	5.062E-05	4.454E-05
2813.27	1.175E-03	3.577E-01	2.166E-02	1.148E-02	1.989E-02	4.422E-05	5.062E-05	4.454E-05
2815.19	1.175E-03	3.577E-01	2.343E-02	1.148E-02	1.925E-02	4.422E-05	5.062E-05	4.454E-05
2817.11	2.166E-03	3.577E-01	2.523E-02	1.357E-02	2.190E-02	4.422E-05	5.062E-05	4.454E-05

D-17

GROUP 12 HAND ALTIMETER UTAS, SCALF FACTOR, AND STATIC EFFECT

TIME	POSITION R	ESTIMATE D	ERROR C	VELOCITY P	ESTIMATE D	ERROR C	PLATFORM R	TILT D	ESTIMATE D	ERROR C
2723.03	1.163E+02	3.500E+02	2.232E+02	3.031E+00	2.385E+00	1.443E+00	1.696E-04	3.123E-04	7.202E-04	
2723.03	1.998E+00	3.500E+02	2.232E+02	3.031E+00	4.157E+00	1.443E+00	1.444E-04	3.123E-04	7.202E-04	
2723.03	1.737E+00	1.737E+00	1.737E+00	4.525E-01	1.737E+00	6.254E-01	4.619E-04	4.619E-04	1.277E-03	
2723.03	1.685E+00	6.661E+00	1.737E+00	3.093E-01	1.244E-01	1.561E-01	4.664E-04	4.664E-04	1.277E-03	
2723.03	1.717E+00	7.681E+00	4.221E+00	3.883E-01	1.244E-01	5.771E-02	4.664E-04	4.664E-04	1.277E-03	
2723.03	1.762E+00	1.762E+00	4.378E+00	4.022E-01	1.444E-01	2.499E-02	4.664E-04	4.664E-04	1.277E-03	
2723.03	4.253E-01	9.793E+00	3.949E+00	2.111E-01	1.444E-01	4.299E-02	5.015E-04	4.664E-04	1.277E-03	
2723.03	4.117E-01	9.296E+00	3.371E+00	1.857E-01	1.857E-01	2.217E-02	5.015E-04	4.664E-04	1.277E-03	
2723.03	1.599E-01	9.296E+00	2.831E+00	3.852E-01	2.852E-01	1.444E-01	4.664E-04	4.664E-04	1.277E-03	
2723.03	9.296E+00	9.296E+00	2.831E+00	3.852E-01	2.852E-01	1.444E-01	4.664E-04	4.664E-04	1.277E-03	
2723.03	2.361E+00	1.022E+01	2.042E+00	5.155E-01	3.024E-01	4.112E-02	4.664E-04	4.664E-04	1.277E-03	
2723.03	4.381E+00	9.505E+00	1.605E+00	5.205E-01	3.264E-01	4.492E-02	4.664E-04	4.664E-04	1.277E-03	
2723.03	2.361E+00	9.505E+00	1.605E+00	5.205E-01	3.264E-01	4.492E-02	4.664E-04	4.664E-04	1.277E-03	
2723.03	7.105E-02	9.666E+00	1.487E+00	6.188E-01	3.664E-01	5.122E-02	4.664E-04	4.664E-04	1.277E-03	
2723.03	7.232E-02	9.666E+00	1.487E+00	6.188E-01	3.664E-01	5.122E-02	4.664E-04	4.664E-04	1.277E-03	
2723.03	7.569E-02	9.666E+00	1.487E+00	6.188E-01	3.664E-01	5.122E-02	4.664E-04	4.664E-04	1.277E-03	
2723.03	4.616E-02	1.041E+01	1.174E+00	1.831E-01	4.086E-01	5.532E-02	4.664E-04	4.664E-04	1.277E-03	
TIME	U	V	W	U	V	W	U	V	W	
2723.03	1.165E+02	4.120E+02	5.574E+01	3.031E+00	2.755E+00	4.055E+00	1.693E-04	7.029E-04	3.497E-04	
2723.03	1.994E+00	4.120E+02	5.574E+01	3.031E+00	4.581E+00	1.443E+00	1.490E-04	7.666E-04	3.497E-04	
2723.03	1.737E+00	2.221E+00	1.009E+00	4.511E-01	1.162E-01	1.009E+00	1.435E-04	8.662E-04	1.046E-03	
2723.03	1.671E+00	6.841E+00	3.055E+00	3.091E-01	1.197E-01	1.481E-01	4.273E-04	6.036E-04	1.196E-03	
2723.03	1.735E+00	7.509E+00	4.055E+00	3.815E-01	1.290E-01	1.533E-01	5.010E-04	4.313E-04	1.253E-03	
2723.03	2.159E+00	1.055E+01	4.055E+00	4.027E-01	1.393E-01	2.451E-02	5.010E-04	4.516E-04	1.246E-03	
2723.03	4.249E+00	9.794E+00	4.055E+00	2.130E-01	1.165E-01	2.097E-02	5.012E-04	4.593E-04	1.243E-03	
2723.03	3.904E+00	9.294E+00	3.371E+00	3.862E-01	1.895E-01	2.497E-02	4.994E-04	4.731E-04	1.238E-03	
2723.03	1.671E-01	9.294E+00	2.831E+00	2.962E-01	2.071E-01	1.546E-02	4.979E-04	4.757E-04	1.238E-03	
2723.03	2.390E+00	9.420E+00	2.034E+00	5.064E-01	2.074E-01	1.546E-02	4.979E-04	4.757E-04	1.238E-03	
2723.03	4.113E+00	1.027E+01	1.634E+00	5.221E-01	3.019E-01	1.267E-02	4.973E-04	4.745E-04	1.238E-03	
2723.03	2.013E+00	9.682E+00	1.587E+00	3.219E-01	3.224E-01	4.513E-02	4.967E-04	4.733E-04	1.238E-03	
2723.03	4.013E+00	9.682E+00	1.587E+00	3.219E-01	3.224E-01	4.513E-02	4.967E-04	4.733E-04	1.238E-03	
2723.03	4.144E+00	9.686E+00	1.385E+00	6.158E-01	3.645E-01	5.363E-02	4.965E-04	4.730E-04	1.240E-03	
2723.03	4.014E+00	9.691E+00	1.385E+00	6.158E-01	3.645E-01	5.363E-02	4.965E-04	4.730E-04	1.240E-03	
2723.03	8.025E-02	1.041E+01	1.185E+00	7.844E-01	4.055E-01	5.571E-02	4.961E-04	4.727E-04	1.240E-03	

THE ANALYTIC SCIENCES CORPORATION

GROUP 12 BARO ALTIMETER FIRST-ORDER MARKOV

TIME	POSITION R	ESTIMATE D	ERROR C	VELOCITY R	ESTIMATE D	ERROR C	PLATFORM R	TILT D	ESTIMATE D	ERROR C
2721.03	1.00E+01	7.677E+00	3.761E+00	8.137E-02	5.400E-02	2.343E-02	3.293E-06	1.841E-06	9.657E-06	9.657E-06
2723.03	4.824E-02	2.158E-02	1.024E-02	5.364E-02	1.629E-02	1.743E-02	3.652E-06	1.786E-06	8.072E-06	8.072E-06
2724.55	4.243E-02	2.413E-02	1.381E-02	4.337E-02	1.004E-02	5.616E-04	1.942E-07	1.300E-07	6.813E-07	6.813E-07
2727.23	3.497E-02	2.174E-02	2.549E-02	8.370E-04	2.380E-04	1.787E-04	4.930E-08	2.884E-08	1.684E-07	1.684E-07
2729.91	3.154E-02	2.200E-02	2.597E-02	6.458E-04	1.529E-04	5.972E-05	4.555E-08	2.619E-08	1.429E-07	1.429E-07
2737.59	2.665E-02	2.526E-02	2.541E-02	3.385E-04	2.215E-04	1.421E-05	4.552E-08	2.513E-08	1.429E-07	1.429E-07
2747.19	2.185E-02	2.713E-02	2.263E-02	3.344E-04	1.104E-04	2.202E-05	4.548E-08	2.513E-08	1.429E-07	1.429E-07
2756.79	1.645E-02	2.713E-02	1.959E-02	3.540E-04	1.140E-04	2.779E-05	4.548E-08	2.513E-08	1.429E-07	1.429E-07
2764.07	1.118E-02	2.962E-02	1.715E-02	5.116E-04	1.643E-04	2.779E-05	4.548E-08	2.513E-08	1.429E-07	1.429E-07
2767.19	5.687E-03	3.024E-02	1.425E-02	6.315E-04	1.629E-04	2.688E-05	4.539E-08	2.533E-08	1.429E-07	1.429E-07
2769.43	1.256E-02	3.045E-02	1.325E-02	6.432E-04	9.392E-05	2.488E-05	4.533E-08	2.533E-08	1.429E-07	1.429E-07
2769.43	5.502E-04	3.029E-02	1.326E-02	6.432E-04	7.564E-05	2.351E-05	4.533E-08	2.533E-08	1.429E-07	1.429E-07
2771.35	1.314E-04	3.027E-02	1.302E-02	6.516E-04	7.034E-05	2.313E-05	4.532E-08	2.533E-08	1.429E-07	1.429E-07
2771.35	1.314E-04	3.025E-02	1.293E-02	6.565E-04	6.112E-05	2.217E-05	4.531E-08	2.533E-08	1.429E-07	1.429E-07
2775.19	1.346E-04	3.022E-02	1.281E-02	6.611E-04	5.345E-05	2.137E-05	4.530E-08	2.533E-08	1.429E-07	1.429E-07
2775.19	1.346E-04	3.020E-02	1.271E-02	6.659E-04	6.052E-05	2.212E-05	4.530E-08	2.533E-08	1.429E-07	1.429E-07
TIME	U	V	W	U	V	W	U	V	W	
2721.03	1.001E+01	8.273E+00	2.117E+00	8.142E-02	5.571E-02	1.894E-02	3.983E-06	7.556E-06	6.291E-06	6.291E-06
2723.03	4.822E-02	1.810E-02	1.507E-02	5.364E-02	2.249E-02	2.343E-02	3.652E-06	1.786E-06	5.022E-06	5.022E-06
2724.55	4.240E-02	2.249E-02	7.913E-02	4.336E-02	0.414E-02	8.665E-04	1.942E-07	1.300E-07	5.942E-07	5.942E-07
2727.23	3.494E-02	2.140E-02	4.450E-02	8.362E-04	2.307E-04	1.787E-04	4.940E-08	2.884E-08	1.644E-07	1.644E-07
2729.91	3.160E-02	2.302E-02	2.132E-02	6.460E-04	1.527E-04	5.989E-05	4.540E-08	2.175E-08	1.435E-07	1.435E-07
2737.59	2.659E-02	2.533E-02	2.296E-02	3.386E-04	2.227E-04	1.770E-05	4.540E-08	2.175E-08	1.435E-07	1.435E-07
2747.19	2.179E-02	2.599E-02	2.114E-02	3.552E-04	1.184E-04	2.377E-05	4.542E-08	2.175E-08	1.435E-07	1.435E-07
2756.79	1.610E-02	2.719E-02	1.777E-02	5.122E-04	1.629E-04	2.791E-05	4.538E-08	2.175E-08	1.435E-07	1.435E-07
2764.07	1.110E-02	2.971E-02	1.620E-02	6.320E-04	1.612E-04	2.751E-05	4.534E-08	2.175E-08	1.435E-07	1.435E-07
2767.19	5.502E-04	3.025E-02	1.458E-02	6.464E-04	1.242E-04	2.443E-05	4.533E-08	2.175E-08	1.435E-07	1.435E-07
2769.43	1.162E-02	3.045E-02	1.331E-02	6.435E-04	9.201E-05	2.502E-05	4.532E-08	2.175E-08	1.435E-07	1.435E-07
2769.43	6.531E-04	3.029E-02	1.303E-02	6.435E-04	7.176E-05	2.373E-05	4.532E-08	2.175E-08	1.435E-07	1.435E-07
2771.35	1.317E-04	3.027E-02	1.308E-02	6.516E-04	6.844E-05	2.217E-05	4.532E-08	2.175E-08	1.435E-07	1.435E-07
2771.35	1.317E-04	3.025E-02	1.288E-02	6.566E-04	5.922E-05	2.212E-05	4.532E-08	2.175E-08	1.435E-07	1.435E-07
2775.19	1.348E-04	3.022E-02	1.280E-02	6.613E-04	5.155E-05	2.130E-05	4.532E-08	2.175E-08	1.435E-07	1.435E-07
2775.19	1.348E-04	3.020E-02	1.251E-02	6.661E-04	5.866E-05	2.216E-05	4.532E-08	2.175E-08	1.435E-07	1.435E-07

D-21

GROUP 13 ML'S RANGE: SCALE FACTOR

TIME	POSITION ESTIMATE ERROR R	VELOCITY ESTIMATE ERROR R	ESTIMATE ERROR D	PLATFORM TILT ESTIMATE ERROR R	ESTIMATE ERROR D	PLATFORM TILT ESTIMATE ERROR R	ESTIMATE ERROR D
2723.03	0.000E+00	0.000E+00	0.000E+00	0.000E+00	0.000E+00	0.000E+00	0.000E+00
2723.03	8.624E+00	2.343E+01	1.650E+03	0.000E+00	0.000E+00	0.000E+00	0.000E+00
2726.87	8.722E+00	2.343E+01	1.650E+03	0.000E+00	0.000E+00	0.000E+00	0.000E+00
2734.55	7.112E+00	2.343E+01	1.650E+03	0.000E+00	0.000E+00	0.000E+00	0.000E+00
2742.23	6.475E+00	1.910E+01	4.222E-01	0.000E+00	0.000E+00	0.000E+00	0.000E+00
2749.91	5.674E+00	1.723E+01	4.441E-01	0.000E+00	0.000E+00	0.000E+00	0.000E+00
2756.79	3.761E+00	1.325E+01	3.171E-01	0.000E+00	0.000E+00	0.000E+00	0.000E+00
2764.07	2.721E+00	1.131E+01	2.555E-01	0.000E+00	0.000E+00	0.000E+00	0.000E+00
2771.35	1.699E+00	9.475E+00	2.355E-01	0.000E+00	0.000E+00	0.000E+00	0.000E+00
2778.63	8.111E+03	8.025E+00	2.202E-01	0.000E+00	0.000E+00	0.000E+00	0.000E+00
2801.75	4.635E+01	5.264E+00	1.994E-01	0.000E+00	0.000E+00	0.000E+00	0.000E+00
2809.43	2.860E-01	5.236E+00	1.892E-01	0.000E+00	0.000E+00	0.000E+00	0.000E+00
2811.35	2.058E-02	4.939E+00	1.842E-01	0.000E+00	0.000E+00	0.000E+00	0.000E+00
2813.27	1.960E-02	4.656E+00	1.791E-01	0.000E+00	0.000E+00	0.000E+00	0.000E+00
2815.19	1.890E-02	4.387E+00	1.739E-01	0.000E+00	0.000E+00	0.000E+00	0.000E+00
2817.11	4.351E-03	4.080E+00	1.733E-01	0.000E+00	0.000E+00	0.000E+00	0.000E+00
2723.03	0.000E+00	0.000E+00	0.000E+00	0.000E+00	0.000E+00	0.000E+00	0.000E+00
2723.03	8.601E+00	1.910E+01	1.380E+03	0.000E+00	0.000E+00	0.000E+00	0.000E+00
2726.87	8.702E+00	2.343E+01	1.650E+03	0.000E+00	0.000E+00	0.000E+00	0.000E+00
2734.55	7.345E+00	1.999E+01	6.485E+00	0.000E+00	0.000E+00	0.000E+00	0.000E+00
2742.23	6.447E+00	1.825E+01	2.549E+00	0.000E+00	0.000E+00	0.000E+00	0.000E+00
2749.91	5.649E+00	1.725E+01	1.141E-01	0.000E+00	0.000E+00	0.000E+00	0.000E+00
2756.79	3.731E+00	1.325E+01	1.949E-01	0.000E+00	0.000E+00	0.000E+00	0.000E+00
2764.07	2.664E+00	1.131E+01	1.672E-01	0.000E+00	0.000E+00	0.000E+00	0.000E+00
2771.35	1.664E+00	9.475E+00	2.672E-01	0.000E+00	0.000E+00	0.000E+00	0.000E+00
2778.63	8.136E+02	8.025E+00	2.422E-01	0.000E+00	0.000E+00	0.000E+00	0.000E+00
2801.75	4.797E-01	5.236E+00	2.182E-01	0.000E+00	0.000E+00	0.000E+00	0.000E+00
2809.43	2.697E-01	5.236E+00	1.900E-01	0.000E+00	0.000E+00	0.000E+00	0.000E+00
2811.35	5.025E-03	4.939E+00	1.841E-01	0.000E+00	0.000E+00	0.000E+00	0.000E+00
2813.27	4.778E-03	4.656E+00	1.774E-01	0.000E+00	0.000E+00	0.000E+00	0.000E+00
2815.19	4.798E-03	4.387E+00	1.744E-01	0.000E+00	0.000E+00	0.000E+00	0.000E+00
2817.11	8.876E-03	4.080E+00	1.742E-01	0.000E+00	0.000E+00	0.000E+00	0.000E+00

GROUP 13 MSL ELEVATION BIAS

TIME	POSITION R	ESTIMATE D	ERROR C	VELOCITY ESTIMATE P	ERROR C	PLATFORM TILT R	ESTIMATE D	ERROR C	PLATFORM TILT R	ESTIMATE D	ERROR C
2723.03	0.00E+00	0.00E+00	0.00E+00	0.00E+00	0.00E+00	0.00E+00	0.00E+00	0.00E+00	0.00E+00	0.00E+00	0.00E+00
2723.07	1.967E+01	1.967E+00	1.967E+00	1.174E-01	1.174E-01	1.967E+00	1.174E-01	1.174E-01	1.967E+00	1.174E-01	1.174E-01
2723.08	2.712E+01	5.017E+00	2.668E-01	2.000E-01	2.000E-01	1.967E+00	2.000E-01	2.000E-01	1.967E+00	2.000E-01	2.000E-01
2723.51	1.714E+01	5.017E+00	2.668E-01	2.000E-01	2.000E-01	1.967E+00	2.000E-01	2.000E-01	1.967E+00	2.000E-01	2.000E-01
2724.23	1.531E+01	5.017E+00	2.668E-01	2.000E-01	2.000E-01	1.967E+00	2.000E-01	2.000E-01	1.967E+00	2.000E-01	2.000E-01
2724.91	1.352E+01	5.017E+00	2.668E-01	2.000E-01	2.000E-01	1.967E+00	2.000E-01	2.000E-01	1.967E+00	2.000E-01	2.000E-01
2727.19	7.457E+00	2.119E+00	2.000E-01	2.000E-01	2.000E-01	1.967E+00	2.000E-01	2.000E-01	1.967E+00	2.000E-01	2.000E-01
2727.79	5.484E+00	1.416E+00	2.000E-01	2.000E-01	2.000E-01	1.967E+00	2.000E-01	2.000E-01	1.967E+00	2.000E-01	2.000E-01
2728.39	3.906E+00	1.416E+00	2.000E-01	2.000E-01	2.000E-01	1.967E+00	2.000E-01	2.000E-01	1.967E+00	2.000E-01	2.000E-01
2729.27	2.478E+00	1.416E+00	2.000E-01	2.000E-01	2.000E-01	1.967E+00	2.000E-01	2.000E-01	1.967E+00	2.000E-01	2.000E-01
2807.175	1.062E+00	1.416E+00	2.000E-01	2.000E-01	2.000E-01	1.967E+00	2.000E-01	2.000E-01	1.967E+00	2.000E-01	2.000E-01
2807.943	5.92E-01	1.416E+00	2.000E-01	2.000E-01	2.000E-01	1.967E+00	2.000E-01	2.000E-01	1.967E+00	2.000E-01	2.000E-01
2809.43	1.034E-02	2.575E-01	1.378E-01	2.000E-01	2.000E-01	1.967E+00	2.000E-01	2.000E-01	1.967E+00	2.000E-01	2.000E-01
2811.35	1.034E-02	2.575E-01	1.378E-01	2.000E-01	2.000E-01	1.967E+00	2.000E-01	2.000E-01	1.967E+00	2.000E-01	2.000E-01
2813.27	1.034E-02	2.575E-01	1.378E-01	2.000E-01	2.000E-01	1.967E+00	2.000E-01	2.000E-01	1.967E+00	2.000E-01	2.000E-01
2815.19	1.034E-02	2.575E-01	1.378E-01	2.000E-01	2.000E-01	1.967E+00	2.000E-01	2.000E-01	1.967E+00	2.000E-01	2.000E-01
2817.11	2.106E-02	2.422E-01	1.174E-01	2.000E-01	2.000E-01	1.967E+00	2.000E-01	2.000E-01	1.967E+00	2.000E-01	2.000E-01
TIME	U	V	W	U	V	U	V	W	U	V	W
2723.03	0.00E+00	0.00E+00	0.00E+00	0.00E+00	0.00E+00	0.00E+00	0.00E+00	0.00E+00	0.00E+00	0.00E+00	0.00E+00
2723.07	1.047E+01	1.047E+00	1.047E+00	1.174E-01	1.174E-01	1.047E+00	1.174E-01	1.174E-01	1.047E+00	1.174E-01	1.174E-01
2723.08	2.012E+01	4.040E+00	1.047E+00	2.000E-01	2.000E-01	1.047E+00	2.000E-01	2.000E-01	1.047E+00	2.000E-01	2.000E-01
2723.51	1.531E+01	4.040E+00	1.047E+00	2.000E-01	2.000E-01	1.047E+00	2.000E-01	2.000E-01	1.047E+00	2.000E-01	2.000E-01
2724.23	1.352E+01	4.040E+00	1.047E+00	2.000E-01	2.000E-01	1.047E+00	2.000E-01	2.000E-01	1.047E+00	2.000E-01	2.000E-01
2724.91	7.457E+00	1.352E+01	2.000E-01	2.000E-01	2.000E-01	1.047E+00	2.000E-01	2.000E-01	1.047E+00	2.000E-01	2.000E-01
2727.19	5.484E+00	1.352E+01	2.000E-01	2.000E-01	2.000E-01	1.047E+00	2.000E-01	2.000E-01	1.047E+00	2.000E-01	2.000E-01
2727.79	3.906E+00	1.352E+01	2.000E-01	2.000E-01	2.000E-01	1.047E+00	2.000E-01	2.000E-01	1.047E+00	2.000E-01	2.000E-01
2728.39	2.478E+00	1.352E+01	2.000E-01	2.000E-01	2.000E-01	1.047E+00	2.000E-01	2.000E-01	1.047E+00	2.000E-01	2.000E-01
2807.175	1.062E+00	1.352E+01	2.000E-01	2.000E-01	2.000E-01	1.047E+00	2.000E-01	2.000E-01	1.047E+00	2.000E-01	2.000E-01
2807.943	5.92E-01	1.352E+01	2.000E-01	2.000E-01	2.000E-01	1.047E+00	2.000E-01	2.000E-01	1.047E+00	2.000E-01	2.000E-01
2809.43	1.034E-02	2.575E-01	1.378E-01	2.000E-01	2.000E-01	1.047E+00	2.000E-01	2.000E-01	1.047E+00	2.000E-01	2.000E-01
2811.35	1.034E-02	2.575E-01	1.378E-01	2.000E-01	2.000E-01	1.047E+00	2.000E-01	2.000E-01	1.047E+00	2.000E-01	2.000E-01
2813.27	1.034E-02	2.575E-01	1.378E-01	2.000E-01	2.000E-01	1.047E+00	2.000E-01	2.000E-01	1.047E+00	2.000E-01	2.000E-01
2815.19	1.034E-02	2.575E-01	1.378E-01	2.000E-01	2.000E-01	1.047E+00	2.000E-01	2.000E-01	1.047E+00	2.000E-01	2.000E-01
2817.11	2.106E-02	2.422E-01	1.174E-01	2.000E-01	2.000E-01	1.047E+00	2.000E-01	2.000E-01	1.047E+00	2.000E-01	2.000E-01

D-25

[illegible]

D-26

[illegible]

GROUP 15 RADAR ALTIMETER TERRAIN MODELING ERROR EAFB 4										
TIME	POSITION R	ESTIMATE D	ERROR C	VELOCITY R	ESTIMATE D	ERROR C	PLATFORM R	TILT D	ESTIMATE D	ERROR C
2909.47	0.00E+00	0.00E+00	0.00E+00	0.00E+00	0.00E+00	0.00E+00	0.00E+00	0.00E+00	0.00E+00	0.00E+00
2909.47	9.191E-01	2.014E-03	9.996E-05	3.072E-08	2.067E-04	2.009E-05	0.00E+00	0.00E+00	0.00E+00	0.00E+00
2910.17	5.734E-03	5.046E-03	2.307E-04	1.526E-05	5.473E-04	1.887E-04	0.00E+00	0.00E+00	0.00E+00	0.00E+00
2911.27	3.141E+00	4.046E-03	4.307E-04	1.187E-05	1.157E-04	6.187E-04	0.00E+00	0.00E+00	0.00E+00	0.00E+00
2911.79	1.584E+00	4.736E-03	4.805E-04	4.432E-05	2.482E-04	1.816E-05	0.00E+00	0.00E+00	0.00E+00	0.00E+00
2912.11	4.008E-01	5.167E-03	9.651E-04	5.013E-05	2.422E-04	4.953E-05	0.00E+00	0.00E+00	0.00E+00	0.00E+00
2912.43	0.00E+00	0.00E+00	0.00E+00	0.00E+00	0.00E+00	0.00E+00	0.00E+00	0.00E+00	0.00E+00	0.00E+00
2912.80	0.00E+00	0.00E+00	0.00E+00	0.00E+00	0.00E+00	0.00E+00	0.00E+00	0.00E+00	0.00E+00	0.00E+00
2913.13	9.007E-01	8.207E-04	1.524E-04	6.018E-07	2.066E-04	4.000E-05	0.00E+00	0.00E+00	0.00E+00	0.00E+00
2913.37	2.044E+00	1.734E-03	6.337E-04	1.696E-05	5.477E-04	1.287E-05	0.00E+00	0.00E+00	0.00E+00	0.00E+00
2913.70	1.554E+00	4.227E-03	5.607E-05	4.512E-05	2.422E-04	4.970E-05	0.00E+00	0.00E+00	0.00E+00	0.00E+00
2914.02	4.00E-01	2.827E-03	5.596E-04	5.092E-05	2.422E-04	4.970E-05	0.00E+00	0.00E+00	0.00E+00	0.00E+00
2914.35	0.00E+00	0.00E+00	0.00E+00	0.00E+00	0.00E+00	0.00E+00	0.00E+00	0.00E+00	0.00E+00	0.00E+00
2914.68	9.007E-01	8.207E-04	1.524E-04	6.018E-07	2.066E-04	4.000E-05	0.00E+00	0.00E+00	0.00E+00	0.00E+00
2915.01	2.044E+00	1.734E-03	6.337E-04	1.696E-05	5.477E-04	1.287E-05	0.00E+00	0.00E+00	0.00E+00	0.00E+00
2915.34	1.554E+00	4.227E-03	5.607E-05	4.512E-05	2.422E-04	4.970E-05	0.00E+00	0.00E+00	0.00E+00	0.00E+00
2915.67	4.00E-01	2.827E-03	5.596E-04	5.092E-05	2.422E-04	4.970E-05	0.00E+00	0.00E+00	0.00E+00	0.00E+00

	GROUP 15 RADAR ALTIMETER TERRAIN MODELING ERROR EAFB 17					
TIME	POSITION ESTIMATE ERROR C		VELOCITY ESTIMATE ERROR C		PLATFORM TILT ESTIMATE ERROR C	
	R	D	R	D	U	V
280943	0.00E+00	0.00E+00	0.00E+00	0.00E+00	0.00E+00	0.00E+00
280943	0.00E+00	0.00E+00	0.00E+00	0.00E+00	0.00E+00	0.00E+00
280943	0.00E+00	0.00E+00	0.00E+00	0.00E+00	0.00E+00	0.00E+00
281135	0.00E+00	0.00E+00	0.00E+00	0.00E+00	0.00E+00	0.00E+00
281135	0.00E+00	0.00E+00	0.00E+00	0.00E+00	0.00E+00	0.00E+00
281519	0.00E+00	0.00E+00	0.00E+00	0.00E+00	0.00E+00	0.00E+00
281519	0.00E+00	0.00E+00	0.00E+00	0.00E+00	0.00E+00	0.00E+00
281711	0.00E+00	0.00E+00	0.00E+00	0.00E+00	0.00E+00	0.00E+00
281711	0.00E+00	0.00E+00	0.00E+00	0.00E+00	0.00E+00	0.00E+00
TIME	U	V	W	U	V	W
280943	0.00E+00	0.00E+00	0.00E+00	0.00E+00	0.00E+00	0.00E+00
280943	0.00E+00	0.00E+00	0.00E+00	0.00E+00	0.00E+00	0.00E+00
281135	0.00E+00	0.00E+00	0.00E+00	0.00E+00	0.00E+00	0.00E+00
281135	0.00E+00	0.00E+00	0.00E+00	0.00E+00	0.00E+00	0.00E+00
281519	0.00E+00	0.00E+00	0.00E+00	0.00E+00	0.00E+00	0.00E+00
281519	0.00E+00	0.00E+00	0.00E+00	0.00E+00	0.00E+00	0.00E+00
281711	0.00E+00	0.00E+00	0.00E+00	0.00E+00	0.00E+00	0.00E+00
281711	0.00E+00	0.00E+00	0.00E+00	0.00E+00	0.00E+00	0.00E+00

[illegible]

* GROUP 15 RADAR ALTIMETER TERRAIN MODELING ERROR EAFB 35

TIME	POSITION R	ESTIMATE D	ERROR C	VELOCITY R	ESTIMATE D	ERROR C	PLATFORM R	TILT D	ESTIMATE C	ERROR C
2809.43	0.000E+00	0.000E+00	0.000E+00	0.000E+00	0.000E+00	0.000E+00	0.000E+00	0.000E+00	0.000E+00	0.000E+00
2809.43	2.671E+00	5.854E-03	2.905E-04	8.928E-08	5.998E-04	1.300E-04	0.000E+00	0.000E+00	0.000E+00	0.000E+00
2811.35	7.726E+00	1.510E-02	5.397E-04	4.175E-05	1.431E-03	3.249E-04	0.000E+00	0.000E+00	0.000E+00	0.000E+00
2813.27	5.634E+00	1.529E-02	8.633E-04	8.200E-05	1.168E-03	1.574E-04	0.000E+00	0.000E+00	0.000E+00	0.000E+00
2815.19	3.138E+00	1.178E-02	1.190E-03	1.097E-04	5.875E-04	3.312E-05	0.000E+00	0.000E+00	0.000E+00	0.000E+00
2817.11	8.796E-01	1.281E-02	2.252E-03	1.222E-04	5.748E-04	1.115E-04	0.000E+00	0.000E+00	0.000E+00	0.000E+00
TIME	U	V	W	U	V	W	U	V	W	
2809.43	0.000E+00	0.000E+00	0.000E+00	0.000E+00	0.000E+00	0.000E+00	0.000E+00	0.000E+00	0.000E+00	0.000E+00
2809.43	2.671E+00	2.498E-03	4.432E-04	1.749E-06	5.998E-04	1.300E-04	0.000E+00	0.000E+00	0.000E+00	0.000E+00
2811.35	7.726E+00	9.320E-03	1.585E-03	4.618E-05	1.430E-03	3.249E-04	0.000E+00	0.000E+00	0.000E+00	0.000E+00
2813.27	5.634E+00	2.702E-03	6.842E-04	8.569E-05	1.168E-03	1.574E-04	0.000E+00	0.000E+00	0.000E+00	0.000E+00
2815.19	3.138E+00	1.012E-03	2.731E-04	1.116E-04	5.872E-04	3.312E-05	0.000E+00	0.000E+00	0.000E+00	0.000E+00
2817.11	8.797E-01	9.943E-03	2.026E-03	1.241E-04	5.743E-04	1.139E-04	0.000E+00	0.000E+00	0.000E+00	0.000E+00

GROUP 15 RADAR ALTIMETER TERRAIN MODELING ERROR KSC 15

TIME	POSITION R	ESTIMATE D	ERROR C	VELOCITY R	ESTIMATE D	ERROR C	PLATFORM R	TILT D	ESTIMATE C	ERROR C
2809.43	0.000E+00	0.000E+00	0.000E+00	0.000E+00	0.000E+00	0.000E+00	0.000E+00	0.000E+00	0.000E+00	0.000E+00
2809.43	1.250E+00	2.739E-03	1.359E-04	4.177E-08	2.805E-04	6.111E-05	0.000E+00	0.000E+00	0.000E+00	0.000E+00
2811.35	4.841E+00	8.875E-03	3.105E-04	2.244E-05	8.517E-04	2.074E-04	0.000E+00	0.000E+00	0.000E+00	0.000E+00
2813.27	4.026E+00	1.028E-02	5.015E-04	5.274E-05	9.315E-04	1.539E-04	0.000E+00	0.000E+00	0.000E+00	0.000E+00
2815.19	3.804E+00	8.450E-03	8.183E-04	8.044E-05	4.875E-04	6.112E-05	0.000E+00	0.000E+00	0.000E+00	0.000E+00
2817.11	1.020E+00	8.275E-03	1.974E-03	9.485E-05	4.733E-04	1.074E-04	0.000E+00	0.000E+00	0.000E+00	0.000E+00
TIME	U	V	W	U	V	W	U	V	W	
2809.43	0.000E+00	0.000E+00	0.000E+00	0.000E+00	0.000E+00	0.000E+00	0.000E+00	0.000E+00	0.000E+00	0.000E+00
2809.43	1.250E+00	1.169E-03	2.074E-04	9.183E-07	2.805E-04	6.111E-05	0.000E+00	0.000E+00	0.000E+00	0.000E+00
2811.35	4.841E+00	6.593E-03	1.032E-03	5.508E-05	8.517E-04	2.074E-04	0.000E+00	0.000E+00	0.000E+00	0.000E+00
2813.27	4.026E+00	5.675E-03	8.738E-04	5.466E-05	9.315E-04	1.527E-04	0.000E+00	0.000E+00	0.000E+00	0.000E+00
2815.19	3.804E+00	3.818E-03	2.295E-04	8.199E-05	4.875E-04	6.112E-05	0.000E+00	0.000E+00	0.000E+00	0.000E+00
2817.11	1.020E+00	5.957E-03	1.704E-03	9.642E-05	4.728E-04	1.047E-04	0.000E+00	0.000E+00	0.000E+00	0.000E+00

GROUP 15 RADAR ALTIMETER TERRAIN MODELING ERROR KSC 33

TIME	POSITION R	ESTIMATE D	ERROR C	VELOCITY R	ESTIMATE D	ERROR C	PLATFORM R	TYLT D	ESTIMATE C
2809.43	0.000E+00	0.000E+00	0.000E+00	0.000E+00	0.000E+00	0.000E+00	0.000E+00	0.000E+00	0.000E+00
2809.43	0.000E+00	0.000E+00	0.000E+00	0.000E+00	0.000E+00	0.000E+00	0.000E+00	0.000E+00	0.000E+00
2811.35	0.000E+00	0.000E+00	0.000E+00	0.000E+00	0.000E+00	0.000E+00	0.000E+00	0.000E+00	0.000E+00
2813.27	0.000E+00	0.000E+00	0.000E+00	0.000E+00	0.000E+00	0.000E+00	0.000E+00	0.000E+00	0.000E+00
2815.19	0.000E+00	0.000E+00	0.000E+00	0.000E+00	0.000E+00	0.000E+00	0.000E+00	0.000E+00	0.000E+00
2817.11	0.000E+00	0.000E+00	0.000E+00	0.000E+00	0.000E+00	0.000E+00	0.000E+00	0.000E+00	0.000E+00
TIME	U	V	W	U	V	W	U	V	W
2809.43	0.000E+00	0.000E+00	0.000E+00	0.000E+00	0.000E+00	0.000E+00	0.000E+00	0.000E+00	0.000E+00
2809.43	0.000E+00	0.000E+00	0.000E+00	0.000E+00	0.000E+00	0.000E+00	0.000E+00	0.000E+00	0.000E+00
2811.35	0.000E+00	0.000E+00	0.000E+00	0.000E+00	0.000E+00	0.000E+00	0.000E+00	0.000E+00	0.000E+00
2813.27	0.000E+00	0.000E+00	0.000E+00	0.000E+00	0.000E+00	0.000E+00	0.000E+00	0.000E+00	0.000E+00
2815.19	0.000E+00	0.000E+00	0.000E+00	0.000E+00	0.000E+00	0.000E+00	0.000E+00	0.000E+00	0.000E+00
2817.11	0.000E+00	0.000E+00	0.000E+00	0.000E+00	0.000E+00	0.000E+00	0.000E+00	0.000E+00	0.000E+00

GROUP 15 RADAR ALTIMETER TERRAIN MODELING ERROR VAFB 12

TIME	POSITION R	ESTIMATE D	ERROR C	VELOCITY R	ESTIMATE D	ERROR C	PLATFORM R	TYLT D	ESTIMATE C
2809.43	0.000E+00	0.000E+00	0.000E+00	0.000E+00	0.000E+00	0.000E+00	0.000E+00	0.000E+00	0.000E+00
2809.43	0.000E+00	0.000E+00	0.000E+00	0.000E+00	0.000E+00	0.000E+00	0.000E+00	0.000E+00	0.000E+00
2811.35	0.000E+00	0.000E+00	0.000E+00	0.000E+00	0.000E+00	0.000E+00	0.000E+00	0.000E+00	0.000E+00
2813.27	0.000E+00	0.000E+00	0.000E+00	0.000E+00	0.000E+00	0.000E+00	0.000E+00	0.000E+00	0.000E+00
2815.19	0.000E+00	0.000E+00	0.000E+00	0.000E+00	0.000E+00	0.000E+00	0.000E+00	0.000E+00	0.000E+00
2817.11	0.000E+00	0.000E+00	0.000E+00	0.000E+00	0.000E+00	0.000E+00	0.000E+00	0.000E+00	0.000E+00
TIME	U	V	W	U	V	W	U	V	W
2809.43	0.000E+00	0.000E+00	0.000E+00	0.000E+00	0.000E+00	0.000E+00	0.000E+00	0.000E+00	0.000E+00
2809.43	0.000E+00	0.000E+00	0.000E+00	0.000E+00	0.000E+00	0.000E+00	0.000E+00	0.000E+00	0.000E+00
2811.35	0.000E+00	0.000E+00	0.000E+00	0.000E+00	0.000E+00	0.000E+00	0.000E+00	0.000E+00	0.000E+00
2813.27	0.000E+00	0.000E+00	0.000E+00	0.000E+00	0.000E+00	0.000E+00	0.000E+00	0.000E+00	0.000E+00
2815.19	0.000E+00	0.000E+00	0.000E+00	0.000E+00	0.000E+00	0.000E+00	0.000E+00	0.000E+00	0.000E+00
2817.11	0.000E+00	0.000E+00	0.000E+00	0.000E+00	0.000E+00	0.000E+00	0.000E+00	0.000E+00	0.000E+00

GROUP 15 RADAR ALTIMETER TERRAIN MODELING ERROR VAFB 30

TIME	POSITION R	ESTIMATE D	ERROR C	VELOCITY R	ESTIMATE D	ERROR C	PLATFORM R	TILT D	ESTIMATE D	ERROR C
2909.43	0.000E+00	0.000E+00	0.000E+00	0.000E+00	0.000E+00	0.000E+00	0.000E+00	0.000E+00	0.000E+00	0.000E+00
2909.43	0.000E+00	0.000E+00	0.000E+00	0.000E+00	0.000E+00	0.000E+00	0.000E+00	0.000E+00	0.000E+00	0.000E+00
2911.35	0.000E+00	0.000E+00	0.000E+00	0.000E+00	0.000E+00	0.000E+00	0.000E+00	0.000E+00	0.000E+00	0.000E+00
2913.27	0.000E+00	0.000E+00	0.000E+00	0.000E+00	0.000E+00	0.000E+00	0.000E+00	0.000E+00	0.000E+00	0.000E+00
2915.19	0.000E+00	0.000E+00	0.000E+00	0.000E+00	0.000E+00	0.000E+00	0.000E+00	0.000E+00	0.000E+00	0.000E+00
2917.11	0.000E+00	0.000E+00	0.000E+00	0.000E+00	0.000E+00	0.000E+00	0.000E+00	0.000E+00	0.000E+00	0.000E+00
TIME	U	V	W	U	V	W	U	V	W	W
2909.43	0.000E+00	0.000E+00	0.000E+00	0.000E+00	0.000E+00	0.000E+00	0.000E+00	0.000E+00	0.000E+00	0.000E+00
2909.43	0.000E+00	0.000E+00	0.000E+00	0.000E+00	0.000E+00	0.000E+00	0.000E+00	0.000E+00	0.000E+00	0.000E+00
2911.35	0.000E+00	0.000E+00	0.000E+00	0.000E+00	0.000E+00	0.000E+00	0.000E+00	0.000E+00	0.000E+00	0.000E+00
2913.27	0.000E+00	0.000E+00	0.000E+00	0.000E+00	0.000E+00	0.000E+00	0.000E+00	0.000E+00	0.000E+00	0.000E+00
2915.19	0.000E+00	0.000E+00	0.000E+00	0.000E+00	0.000E+00	0.000E+00	0.000E+00	0.000E+00	0.000E+00	0.000E+00
2917.11	0.000E+00	0.000E+00	0.000E+00	0.000E+00	0.000E+00	0.000E+00	0.000E+00	0.000E+00	0.000E+00	0.000E+00

GROUP 15 RADAR ALTIMETER TERRAIN MODELING ERROR AAFB NO. (NE APPROACH)

TIME	POSITION R	ESTIMATE D	ERROR C	VELOCITY R	ESTIMATE D	ERROR C	PLATFORM R	TILT D	ESTIMATE D	ERROR C
2909.43	0.000E+00	0.000E+00	0.000E+00	0.000E+00	0.000E+00	0.000E+00	0.000E+00	0.000E+00	0.000E+00	0.000E+00
2909.43	0.000E+00	0.000E+00	0.000E+00	0.000E+00	0.000E+00	0.000E+00	0.000E+00	0.000E+00	0.000E+00	0.000E+00
2911.35	0.000E+00	0.000E+00	0.000E+00	0.000E+00	0.000E+00	0.000E+00	0.000E+00	0.000E+00	0.000E+00	0.000E+00
2913.27	0.000E+00	0.000E+00	0.000E+00	0.000E+00	0.000E+00	0.000E+00	0.000E+00	0.000E+00	0.000E+00	0.000E+00
2915.19	0.000E+00	0.000E+00	0.000E+00	0.000E+00	0.000E+00	0.000E+00	0.000E+00	0.000E+00	0.000E+00	0.000E+00
2917.11	0.000E+00	0.000E+00	0.000E+00	0.000E+00	0.000E+00	0.000E+00	0.000E+00	0.000E+00	0.000E+00	0.000E+00
TIME	U	V	W	U	V	W	U	V	W	W
2909.43	0.000E+00	0.000E+00	0.000E+00	0.000E+00	0.000E+00	0.000E+00	0.000E+00	0.000E+00	0.000E+00	0.000E+00
2909.43	0.000E+00	0.000E+00	0.000E+00	0.000E+00	0.000E+00	0.000E+00	0.000E+00	0.000E+00	0.000E+00	0.000E+00
2911.35	0.000E+00	0.000E+00	0.000E+00	0.000E+00	0.000E+00	0.000E+00	0.000E+00	0.000E+00	0.000E+00	0.000E+00
2913.27	0.000E+00	0.000E+00	0.000E+00	0.000E+00	0.000E+00	0.000E+00	0.000E+00	0.000E+00	0.000E+00	0.000E+00
2915.19	0.000E+00	0.000E+00	0.000E+00	0.000E+00	0.000E+00	0.000E+00	0.000E+00	0.000E+00	0.000E+00	0.000E+00
2917.11	0.000E+00	0.000E+00	0.000E+00	0.000E+00	0.000E+00	0.000E+00	0.000E+00	0.000E+00	0.000E+00	0.000E+00

REPRODUCIBILITY OF THE
ORIGINAL PAGE IS POOR

GROUP 15 RADAR ALTIMETER TERRAIN MODELING ERROR AAFB NO. (SW APPROACH)

TIME	POSITION R	ESTIMATE D	ERROR C	VELOCITY R	ESTIMATE D	ERROR C	PLATFORM R	TILT D	ESTIMATE D	ERROR C
2909.43	0.000E+00	0.000E+00	0.000E+00	0.000E+00	0.000E+00	0.000E+00	0.000E+00	0.000E+00	0.000E+00	0.000E+00
2909.43	3.904E+00	8.554E-03	4.245E-04	1.305E-07	4.758E-04	1.902E-04	0.000E+00	0.000E+00	0.000E+00	0.000E+00
2911.35	2.789E+01	4.527E-02	1.549E-03	9.709E-05	4.481E-03	1.201E-03	0.000E+00	0.000E+00	0.000E+00	0.000E+00
2913.27	2.207E+01	5.004E-02	2.850E-03	2.570E-04	4.080E-03	8.268E-04	0.000E+00	0.000E+00	0.000E+00	0.000E+00
2915.19	1.176E+01	3.905E-02	4.460E-03	3.594E-04	2.175E-03	8.415E-04	0.000E+00	0.000E+00	0.000E+00	0.000E+00
2917.11	3.073E+00	4.288E-02	8.273E-03	4.031E-04	2.130E-03	4.337E-04	0.000E+00	0.000E+00	0.000E+00	0.000E+00
TIME	U	V	W	U	V	W	U	V	W	W
2909.43	0.000E+00	0.000E+00	0.000E+00	0.000E+00	0.000E+00	0.000E+00	0.000E+00	0.000E+00	0.000E+00	0.000E+00
2909.43	3.904E+00	3.650E-03	4.476E-04	2.555E-06	8.758E-04	1.911E-04	0.000E+00	0.000E+00	0.000E+00	0.000E+00
2911.35	2.789E+01	4.289E-02	6.120E-03	1.118E-04	4.481E-03	1.200E-03	0.000E+00	0.000E+00	0.000E+00	0.000E+00
2913.27	2.207E+01	2.045E-02	3.224E-03	2.699E-04	4.079E-03	6.255E-04	0.000E+00	0.000E+00	0.000E+00	0.000E+00
2915.19	1.176E+01	1.133E-03	1.229E-03	3.664E-04	2.174E-03	8.302E-05	0.000E+00	0.000E+00	0.000E+00	0.000E+00
2917.11	3.073E+00	3.287E-02	7.482E-03	4.103E-04	2.128E-03	4.352E-04	0.000E+00	0.000E+00	0.000E+00	0.000E+00

GROUP 15 RADAR ALTIMETER TERRAIN MODELING ERROR AAFB NO. (NE APPROACH)

TIME	POSITION R	ESTIMATE D	ERROR C	VELOCITY R	ESTIMATE D	ERROR C	PLATFORM R	TILT D	ESTIMATE D	ERROR C
2909.43	0.000E+00	0.000E+00	0.000E+00	0.000E+00	0.000E+00	0.000E+00	0.000E+00	0.000E+00	0.000E+00	0.000E+00
2909.43	6.500E+00	1.424E-02	7.048E-04	2.172E-07	1.458E-03	1.178E-04	0.000E+00	0.000E+00	0.000E+00	0.000E+00
2911.35	2.323E+01	4.203E-02	1.514E-03	1.140E-04	4.119E-03	9.842E-04	0.000E+00	0.000E+00	0.000E+00	0.000E+00
2913.27	1.741E+01	4.400E-02	2.524E-03	2.370E-04	3.470E-03	4.810E-04	0.000E+00	0.000E+00	0.000E+00	0.000E+00
2915.19	9.765E+00	3.442E-02	3.638E-03	3.213E-04	1.775E-03	8.358E-05	0.000E+00	0.000E+00	0.000E+00	0.000E+00
2917.11	2.560E+00	3.754E-02	6.776E-03	3.570E-04	1.737E-03	3.461E-04	0.000E+00	0.000E+00	0.000E+00	0.000E+00
TIME	U	V	W	U	V	W	U	V	W	W
2909.43	0.000E+00	0.000E+00	0.000E+00	0.000E+00	0.000E+00	0.000E+00	0.000E+00	0.000E+00	0.000E+00	0.000E+00
2909.43	6.500E+00	6.078E-03	1.078E-03	4.255E-06	1.458E-03	3.182E-04	0.000E+00	0.000E+00	0.000E+00	0.000E+00
2911.35	2.323E+01	3.049E-02	4.870E-03	1.267E-04	4.119E-03	9.842E-04	0.000E+00	0.000E+00	0.000E+00	0.000E+00
2913.27	1.741E+01	1.090E-02	2.265E-03	2.489E-04	3.475E-03	4.800E-04	0.000E+00	0.000E+00	0.000E+00	0.000E+00
2915.19	9.766E+00	2.931E-03	9.559E-04	3.270E-04	1.774E-03	8.267E-05	0.000E+00	0.000E+00	0.000E+00	0.000E+00
2917.11	2.560E+00	2.921E-02	6.119E-03	3.636E-04	1.736E-03	3.473E-04	0.000E+00	0.000E+00	0.000E+00	0.000E+00

GROUP 15 RADAR ALTIMETER TERRAIN MODELING ERROR AAFB SO. (SW APPROACH)

TIME	POSITION ESTIMATE ERROR C			VELOCITY ESTIMATE ERROR C			PLATFORM TILT ESTIMATE ERROR C		
	R	U	V	R	U	V	R	U	V
2809.43	0.000E+00	0.000E+00	0.000E+00	0.000E+00	0.000E+00	0.000E+00	0.000E+00	0.000E+00	0.000E+00
2809.43	1.083E+01	2.374E-02	1.174E-03	3.620E-07	2.430E-03	5.295E-04	0.000E+00	0.000E+00	0.000E+00
2811.35	6.202E-02	1.735E-02	7.571E-04	1.077E-04	1.280E-03	5.473E-05	0.000E+00	0.000E+00	0.000E+00
2813.27	1.115E+01	3.546E-03	6.334E-04	5.247E-05	3.820E-04	4.414E-04	0.000E+00	0.000E+00	0.000E+00
2815.19	7.617E+00	5.012E-04	8.224E-04	6.933E-06	7.066E-04	1.215E-04	0.000E+00	0.000E+00	0.000E+00
2817.11	2.030E+00	1.635E-03	3.142E-03	3.570E-05	6.776E-04	2.115E-04	0.000E+00	0.000E+00	0.000E+00
TIME	POSITION ESTIMATE ERROR C			VELOCITY ESTIMATE ERROR C			PLATFORM TILT ESTIMATE ERROR C		
	R	U	V	R	U	V	R	U	V
2809.43	0.000E+00	0.000E+00	0.000E+00	0.000E+00	0.000E+00	0.000E+00	0.000E+00	0.000E+00	0.000E+00
2809.43	1.083E+01	1.013E-02	1.797E-03	7.091E-06	2.430E-03	5.295E-04	0.000E+00	0.000E+00	0.000E+00
2811.35	6.196E-02	1.745E-02	7.679E-04	1.049E-04	1.279E-03	5.473E-05	0.000E+00	0.000E+00	0.000E+00
2813.27	1.115E+01	3.915E-02	3.716E-03	5.137E-05	3.832E-04	4.415E-04	0.000E+00	0.000E+00	0.000E+00
2815.19	7.617E+00	2.406E-02	1.284E-03	9.178E-06	7.066E-04	1.215E-04	0.000E+00	0.000E+00	0.000E+00
2817.11	2.039E+00	5.001E-03	2.598E-03	3.805E-05	6.776E-04	2.115E-04	0.000E+00	0.000E+00	0.000E+00

GROUP 15 RADAR ALTIMETER TERRAIN MODELING ERROR HAFB 8

TIME	POSITION ESTIMATE ERROR R	VELOCITY ESTIMATE ERROR R	VELOCITY ESTIMATE ERROR C	PLATFORM TILT ESTIMATE ERROR R	PLATFORM TILT ESTIMATE ERROR C
2809.43	0.000E+00	0.000E+00	0.000E+00	0.000E+00	0.000E+00
2809.43	6.750E+00	1.479E+02	7.340E-04	0.000E+00	0.000E+00
2811.35	5.245E+00	1.820E+02	7.095E-04	0.000E+00	0.000E+00
2813.27	2.220E+00	1.473E+02	8.173E-04	0.000E+00	0.000E+00
2815.19	8.608E-01	1.038E+02	7.674E-04	0.000E+00	0.000E+00
2817.11	4.038E-02	1.091E+02	1.166E-03	0.000E+00	0.000E+00
	U	V	W	U	V
2809.43	0.000E+00	0.000E+00	0.000E+00	0.000E+00	0.000E+00
2809.43	6.312E+00	6.312E+00	1.120E-03	0.000E+00	0.000E+00
2811.35	5.245E+00	1.620E+02	7.323E-04	0.000E+00	0.000E+00
2813.27	2.220E+00	7.636E-03	2.095E-04	0.000E+00	0.000E+00
2815.19	8.608E-01	7.607E-03	5.551E-04	0.000E+00	0.000E+00
2817.11	4.042E-02	1.078E-02	1.163E-03	0.000E+00	0.000E+00

GROUP 15 RADAR ALTIMETER TERRAIN MODELING ERROR HAFB 24

TIME	POSITION ESTIMATE ERROR R	VELOCITY ESTIMATE ERROR R	VELOCITY ESTIMATE ERROR C	PLATFORM TILT ESTIMATE ERROR R	PLATFORM TILT ESTIMATE ERROR C
2809.43	0.000E+00	0.000E+00	0.000E+00	0.000E+00	0.000E+00
2809.43	1.800E+00	3.944E-03	1.957E-04	0.000E+00	0.000E+00
2811.35	6.831E+00	1.245E-02	4.381E-04	0.000E+00	0.000E+00
2813.27	6.832E-01	9.541E-03	8.180E-04	0.000E+00	0.000E+00
2815.19	2.483E-02	6.659E-03	6.354E-04	0.000E+00	0.000E+00
2817.11	1.051E-03	7.122E-03	6.897E-04	0.000E+00	0.000E+00
	U	V	W	U	V
2809.43	0.000E+00	0.000E+00	0.000E+00	0.000E+00	0.000E+00
2809.43	1.800E+00	1.643E-03	2.986E-04	0.000E+00	0.000E+00
2811.35	6.831E+00	9.144E-03	1.440E-03	0.000E+00	0.000E+00
2813.27	6.833E-01	7.358E-03	6.325E-04	0.000E+00	0.000E+00
2815.19	2.485E-02	6.578E-03	6.323E-04	0.000E+00	0.000E+00
2817.11	1.084E-03	7.118E-03	6.948E-04	0.000E+00	0.000E+00

[illegible]

TIME	GROUP 15			RADAR ALTIMETER ANTENNA POINTING ERROR			PLATFORM TILT			ESTIMATE ERROR		
	POSITION R	ESTIMATE D	ERROR C	VELOCITY R	ESTIMATE D	ERROR C	U	V	U	V	U	V
28000.43	0.00E+00	0.00E+00	0.00E+00	0.00E+00	0.00E+00	0.00E+00	0.00E+00	0.00E+00	0.00E+00	0.00E+00	0.00E+00	0.00E+00
28000.43	0.42E-03	1.85E-05	9.21E-07	2.83E-10	1.90E-06	4.14E-07	0.00E+00	0.00E+00	0.00E+00	0.00E+00	0.00E+00	0.00E+00
28011.27	9.00E-01	1.25E-04	7.90E-07	9.69E-07	1.39E-05	3.49E-06	0.00E+00	0.00E+00	0.00E+00	0.00E+00	0.00E+00	0.00E+00
28011.27	1.00E-01	2.05E-04	7.90E-07	9.69E-07	1.39E-05	4.00E-06	0.00E+00	0.00E+00	0.00E+00	0.00E+00	0.00E+00	0.00E+00
28012.11	1.00E-01	1.91E-04	1.77E-05	1.74E-06	1.27E-05	2.34E-06	0.00E+00	0.00E+00	0.00E+00	0.00E+00	0.00E+00	0.00E+00
28012.11	3.23E-02	2.01E-04	4.97E-05	2.10E-06	1.16E-05	2.05E-06	0.00E+00	0.00E+00	0.00E+00	0.00E+00	0.00E+00	0.00E+00
28000.43	0.00E+00	0.00E+00	0.00E+00	0.00E+00	0.00E+00	0.00E+00	0.00E+00	0.00E+00	0.00E+00	0.00E+00	0.00E+00	0.00E+00
28000.43	0.42E-03	7.02E-06	0.00E+00	0.00E+00	0.00E+00	0.00E+00	0.00E+00	0.00E+00	0.00E+00	0.00E+00	0.00E+00	0.00E+00
28011.27	9.00E-01	1.42E-04	2.00E-05	3.27E-06	1.39E-05	3.47E-06	0.00E+00	0.00E+00	0.00E+00	0.00E+00	0.00E+00	0.00E+00
28011.27	1.00E-01	2.05E-04	2.00E-05	3.27E-06	1.39E-05	3.47E-06	0.00E+00	0.00E+00	0.00E+00	0.00E+00	0.00E+00	0.00E+00
28012.11	1.00E-01	1.65E-04	4.12E-05	1.78E-06	1.20E-05	2.37E-06	0.00E+00	0.00E+00	0.00E+00	0.00E+00	0.00E+00	0.00E+00
28012.11	3.23E-02	0.00E-05	4.12E-05	2.22E-06	1.10E-05	2.06E-06	0.00E+00	0.00E+00	0.00E+00	0.00E+00	0.00E+00	0.00E+00

GROUP 15 RADAR ALTIMETER TIMING DELAY

TIME	POSITION ESTIMATE ERROR R D	POSITION ESTIMATE ERROR C	VELOCITY ESTIMATE ERROR R D	VELOCITY ESTIMATE ERROR C	PLATFORM TILT ESTIMATE ERROR R D	PLATFORM TILT ESTIMATE ERROR C
2809.43	0.000E+00	0.000E+00	0.000E+00	0.000E+00	0.000E+00	0.000E+00
2809.43	1.757E-01	3.850E-04	5.872E-09	3.942E-05	0.000E+00	0.000E+00
2811.35	9.381E-02	4.140E-04	6.582E-07	3.441E-05	0.000E+00	0.000E+00
2813.27	6.204E-02	3.430E-04	1.125E-06	2.860E-05	0.000E+00	0.000E+00
2815.19	4.165E-02	2.480E-04	1.643E-05	7.103E-06	0.000E+00	0.000E+00
2817.11	1.740E-02	2.607E-04	1.614E-06	6.977E-06	0.000E+00	0.000E+00
TIME	U	V	W	V	U	W
2809.43	0.000E+00	0.000E+00	0.000E+00	0.000E+00	0.000E+00	0.000E+00
2809.43	1.757E-01	1.643E-04	2.914E-05	1.150E-07	0.000E+00	0.000E+00
2811.35	9.381E-02	1.175E-04	9.212E-06	7.660E-07	0.000E+00	0.000E+00
2813.27	6.205E-02	1.445E-04	5.437E-07	1.190E-06	0.000E+00	0.000E+00
2815.19	4.165E-02	1.137E-04	5.049E-06	1.459E-06	0.000E+00	0.000E+00
2817.11	1.740E-02	2.041E-04	2.179E-05	1.637E-06	0.000E+00	0.000E+00

GROUP 15 RADAR ALTIMETER RECEIVER NOISE

TIME	POSITION ESTIMATE ERROR R D	POSITION ESTIMATE ERROR C	VELOCITY ESTIMATE ERROR R D	VELOCITY ESTIMATE ERROR C	PLATFORM TILT ESTIMATE ERROR R D	PLATFORM TILT ESTIMATE ERROR C
2809.43	1.000E-10	1.000E-10	1.000E-10	1.000E-10	1.000E-10	1.000E-10
2809.43	2.244E-09	1.575E-09	2.805E-10	2.092E-10	1.000E-10	1.000E-10
2811.35	1.868E-09	1.070E-09	4.370E-09	4.445E-09	1.000E-10	1.000E-10
2813.27	3.620E-09	1.350E-09	8.950E-09	9.430E-09	1.000E-10	1.000E-10
2815.19	5.720E-09	3.118E-09	1.336E-08	1.329E-08	1.000E-10	1.000E-10
2817.11	1.043E-08	5.755E-09	1.781E-08	1.841E-08	1.000E-10	1.000E-10
TIME	U	V	W	V	U	W
2809.43	1.000E-10	1.000E-10	1.000E-10	1.000E-10	1.000E-10	1.000E-10
2809.43	2.421E-09	1.745E-09	2.912E-10	2.238E-10	1.000E-10	1.000E-10
2811.35	2.085E-09	8.019E-09	4.397E-09	4.825E-09	1.000E-10	1.000E-10
2813.27	3.711E-09	1.827E-08	8.982E-09	9.397E-09	1.000E-10	1.000E-10
2815.19	5.774E-09	5.053E-08	1.340E-08	1.324E-08	1.000E-10	1.000E-10
2817.11	1.060E-08	5.693E-08	1.784E-08	1.834E-08	1.000E-10	1.000E-10

[illegible][illegible]

Figure 1 displays a series of 12 vertical panels, labeled A through L, showing the time evolution of a quantum state. Each panel contains a grid of symbols (dots, crosses, and letters) representing the state at discrete time steps. The panels are labeled A through L on the left, and the vertical axis is labeled 'TIME' at the bottom. The symbols are arranged in a grid that changes over time, with some panels showing a clear pattern of dots and crosses, while others show a more complex arrangement of letters and symbols.

ADDITIONAL STATE ESTIMATES AT 20,000 FT (10 TO NP)
1.000E-10 3.157E+00 4.985E-05

GROUP 20 MLS TIMING ERRORS RANGE

TIME	POSITION ESTIMATE ERROR			VELOCITY ESTIMATE ERROR			PLATFORM TILT ESTIMATE ERROR		
	R	D	C	R	D	C	R	D	C
2723.03	0.000E+00	0.000E+00	0.000E+00	0.000E+00	0.000E+00	0.000E+00	0.000E+00	0.000E+00	0.000E+00
2723.03	9.168E+00	2.490E+01	1.792E+00	0.000E+00	1.469E-01	4.543E-03	3.175E-06	1.599E-06	3.795E-06
2734.55	9.990E+00	2.814E+01	5.474E-01	7.265E-02	2.612E-01	6.272E-02	1.550E-05	5.820E-06	1.382E-05
2742.23	9.970E+00	2.912E+01	5.426E-01	4.263E-01	2.043E-01	8.697E-02	1.819E-05	5.691E-06	1.017E-05
2749.03	9.973E+00	2.921E+01	8.893E-01	2.624E-02	1.027E-01	6.292E-02	1.577E-05	4.700E-06	7.346E-06
2757.59	9.612E+00	2.765E+01	7.215E-01	2.415E-01	8.118E-02	2.750E-02	1.574E-05	4.702E-06	7.370E-06
2767.19	8.195E+00	2.626E+01	4.688E-01	1.084E-01	1.197E-01	1.435E-02	1.578E-05	4.704E-06	7.371E-06
2776.79	6.526E+00	2.529E+01	4.236E-01	1.499E-01	1.071E-01	5.572E-03	1.578E-05	4.706E-06	7.384E-06
2786.39	4.718E+00	2.433E+01	4.368E-01	1.743E-01	1.011E-01	1.072E-03	1.575E-05	4.709E-06	7.397E-06
2794.01	2.874E+00	2.343E+01	4.693E-01	2.150E-01	7.974E-02	4.473E-03	1.574E-05	4.710E-06	7.403E-06
2801.75	8.714E-01	2.244E+01	4.914E-01	2.380E-01	1.539E-01	6.363E-03	1.574E-05	4.712E-06	7.405E-06
2809.43	4.830E-01	1.908E+01	4.913E-01	2.014E-01	3.122E-01	4.410E-03	1.574E-05	4.714E-06	7.408E-06
2811.35	3.645E-01	1.870E+01	4.798E-01	2.014E-01	3.503E-01	2.890E-03	1.574E-05	4.714E-06	7.408E-06
2813.27	6.951E-02	1.779E+01	4.720E-01	2.008E-01	3.791E-01	2.247E-03	1.574E-05	4.715E-06	7.410E-06
2815.19	5.294E-01	1.690E+01	4.629E-01	2.002E-01	4.009E-01	1.297E-03	1.574E-05	4.715E-06	7.413E-06
2817.11	2.857E-02	1.501E+01	4.558E-01	1.999E-01	4.171E-01	8.199E-04	1.574E-05	4.715E-06	7.414E-06
TIME	POSITION ESTIMATE ERROR			VELOCITY ESTIMATE ERROR			PLATFORM TILT ESTIMATE ERROR		
	R	D	C	R	D	C	R	D	C
2723.03	0.000E+00	0.000E+00	0.000E+00	0.000E+00	0.000E+00	0.000E+00	0.000E+00	0.000E+00	0.000E+00
2723.03	9.143E+00	2.021E+01	1.404E+01	0.000E+00	1.095E-01	9.811E-02	3.173E-06	3.670E-06	1.871E-05
2734.55	9.950E+00	2.665E+01	8.977E+00	7.237E-02	2.248E-01	1.472E-01	1.549E-05	1.014E-05	1.105E-05
2742.23	9.927E+00	2.807E+01	3.716E+00	4.255E-01	1.916E-01	1.092E-01	1.548E-05	6.801E-06	9.489E-06
2749.03	9.924E+00	2.925E+01	1.175E-02	2.698E-02	1.046E-01	5.971E-02	1.578E-05	4.698E-06	7.510E-06
2757.59	9.579E+00	2.765E+01	3.085E-01	2.420E-02	6.126E-02	1.538E-02	1.575E-05	4.622E-06	7.444E-06
2767.19	8.132E+00	2.626E+01	2.659E-01	1.082E-01	1.200E-01	1.323E-02	1.574E-05	4.670E-06	7.424E-06
2776.79	6.446E+00	2.531E+01	3.994E-01	1.496E-01	1.074E-01	5.440E-03	1.574E-05	4.773E-06	7.393E-06
2786.39	4.674E+00	2.418E+01	5.133E-01	1.741E-01	1.015E-01	7.956E-03	1.573E-05	4.773E-06	7.389E-06
2794.01	2.807E+00	2.384E+01	5.235E-01	2.148E-01	6.035E-02	4.303E-03	1.573E-05	4.775E-06	7.389E-06
2801.75	8.048E-01	2.245E+01	5.237E-01	2.176E-01	1.546E-01	6.208E-03	1.572E-05	4.769E-06	7.405E-06
2809.43	5.425E-01	1.908E+01	4.936E-01	2.004E-01	3.128E-01	2.848E-03	1.572E-05	4.765E-06	7.411E-06
2811.35	7.062E-01	1.870E+01	4.836E-01	2.003E-01	3.503E-01	2.379E-03	1.572E-05	4.765E-06	7.412E-06
2813.27	1.256E+02	1.779E+01	4.714E-01	1.998E-01	3.798E-01	2.310E-03	1.572E-05	4.764E-06	7.413E-06
2815.19	1.205E+02	1.689E+01	4.548E-01	1.993E-01	4.017E-01	1.483E-03	1.572E-05	4.762E-06	7.415E-06
2817.11	2.034E-02	1.507E+01	4.442E-01	1.986E-01	4.181E-01	1.189E-03	1.572E-05	4.761E-06	7.422E-06

D-42

REFERENCES

1. Jones, H.L. and Luders, G., "Space Shuttle Navigation Analysis," The Analytic Sciences Corp., TR-548-1, 12 December 1975.
2. Crawford, B.S., and Duiven, E.M., "Space Shuttle Post Entry and Landing Analysis," The Analytic Sciences Corp., TR-302-1, 20 July 1973.
3. Jones, H.L. and Crawford, B.S., "Space Shuttle Entry and Landing Navigation Analysis," The Analytic Sciences Corp., TR-302-2, 31 July 1974.
4. Jones, H.L. and Luders, G., "Quarterly Progress Report for the Period Ending 31 March 1975," The Analytic Sciences Corp., PR-548-9, 10 April 1975.
5. Pyle, R.H. and Rains, R.G., "Global Positioning System (Phase I) Error Analysis (ANSWER V)," The Analytic Sciences Corp., TR-428-1, 1 August 1974.
6. Roy, K.J. and Pyle, R.H., "Investigation of the Performance of Army Users of the NAVSTAR Global Positioning System," The Analytic Sciences Corp., TR-422-1, 15 September 1974.
7. Brammer, R.F., Himes, J.G. and Shields, J.D., "Evaluation of GPS Tactical Missile Guidance," The Analytic Sciences Corp., TR-625-2, 31 December 1975.
8. "User System Segment Specification for the NAVSTAR Global Positioning System Phase I," U.S. Air Force Space and Missile Systems Organization, SS-US-101A, Code Identification 07868, 3 April 1974.
9. Duiven, E.M., "Predicted Global Positioning System User Performance," Presented at the Seventh Biennial Test Symposium, Holloman Air Force Base, New Mexico, April 1975.
10. Mealy, G.L., "Time Standard Error Modeling with Applications to Satellite Navigation," Proc. of the 29th Annual Symposium on Frequency Control, (Atlantic City, New Jersey), May 1975.

THE ANALYTIC SCIENCES CORPORATION

11. "Specification for the Master Timing Unit," Rockwell International Document No. MC456-0051, 5 November 1973.
12. Hellwig, H., "Atomic Frequency Standards: A Survey," Proc. IEEE, Vol. 63, February 1975, pp. 212-229.
13. Fletcher, C.L. and Ferry, W.W., "Data Package for Shuttle Ascent Reference Trajectory Tape," Johnson Space Center IN No. 73-FM-139, October 1973.
14. "Ascent and AOA Navigation Input to Level C OFT Navigation Functional Subsystem Software Requirements," Johnson Space Center IN No. 75-FM-69, 22 October 1975.
15. Fang, B.T. and Gibbs, B.P., "TDRSS Era Orbit Determination System Review Study," EG and G/Washington Analytic Services Center, Inc. Report No. MT010-75, December 1975.
16. Keach, D.G. and Knoedler, J.L. "A Study of the Feasibility of Selected Systems for Shuttle Navigation Support. Volume II — The Tracking Data Relay Satellite System," Manned Spacecraft Center IN No. 71-FM-51.
17. Thibodeau, J.R. III, "Shuttle Navigation at Insertion," Johnson Space Center, FM83 (73-345), 21 November 1973.
18. "OFT Level C Functional Subsystem Software Requirements (FSSR). Inertial Measurement Unit," Rockwell International, Document No. SD-76-SH-0013, 4 June 1976.
19. Mealy, G.L. and Shipp, R.F., "Sensor Data Bank Development: AN/ASN-90 Test Data File and Error Models," The Analytic Sciences Corp., AFAL-TR-74-233, August 1974.
20. Sharples, W.K. and Shipp, R.F., "AN/ASN-90 Systems Improvement Final Report," The Analytic Sciences Corp., TR-353-10, 31 July 1974.
21. Feigen, M. et al., "Software Functional Requirements Document for Space Shuttle Inertial Measurement Unit," The Singer Company, Kearfott Division, Engineering Technical Report PDRD No. UA06, Document No. Y201A194A100, Rev. F, 9 January 1975.
22. Epple, R.G.E., "Shuttle IMU Math Model For Real Time Simulation," Rockwell International IL No. 392-240-76-231, 30 June 1976.

THE ANALYTIC SCIENCES CORPORATION

23. "IMU Mounting Base to Cluster Transformation Matrix," The Singer Company, Kearfott Division, Engineering Technical Report PDRD No. UA10, Document No. Y258A230, 19 July 1974.
24. "Orbiter IMU Error Source Model and Error Mnemonics," The Singer Company, Kearfott Division, Engineering Technical Report PDRD No. UA10, Document No. Y258A182, Rev. C, 29 March 1974.
25. Campbell, M.E. and Walker, R.A., "Shuttle IMU Error Model," Rockwell International IL No. 392-240-75-094.
26. Duiven, E.M. and Crawford, B.S., "LPMS/AIRS Calibration and Alignment Study (U)," The Analytic Sciences Corp., TR-340-2-1, September 1973 (SECRET).
27. "Orbiter Inertial Measurement Unit (IMU) Modification of Multi-Cal Calibration to Minimize Attitude Sensitivity," The Singer Company, Kearfott Division, Engineering Technical Report PDRD No. UA10, Document No. Y258A325, 29 January 1975.
28. "Specifications for Inertial Measurement Unit (IMU) — Orbiter," Rockwell International, Document No. MC409-0004, 1 June 1974.
29. Crawford, B.S., and Duiven, E.M., "A Study of Space Shuttle Approach and Landing Navigation with Conventional NAVAIDS," Presented at Institute of Navigation Aerospace Meeting, Dayton, Ohio, March 1974.
30. Lear, W.M., "The Multi-Phase Navigation Program for the Space Shuttle Orbiter," Johnson Space Center, IN 73-FM-132, 7 September 1973.
31. Kriegsman, B.A. and Tao, Y.C., "Shuttle Navigation System for Entry and Landing Mission Phase," AIAA Paper No. 74-866, August 1974.
32. Blazek, G. and Carrier, L.M., "Microwave Landing System for Space Shuttle Orbiter," AIAA Paper No. 74-907, 5 August 1974.
33. Lear, W.M., "Baro Altimetry and Associated Error Models for the Space Shuttle," TRW Report No. 27054-6004-TU-00, 8 November 1974.

THE ANALYTIC SCIENCES CORPORATION

34. "Microwave Scanning Beam Landing System Ground Station Progress Report," AIL Project A980, October 1975.
35. Madni, A., "Preliminary Mathematical Models for RF Nav Sensors," Rockwell International, Document No. 382-JBP-75-030, 16 April 1975.
36. "Altimeter Set, Electronic AN/APN-194(V), Test and Evaluation Under Hover Conditions," Naval Air Test Center, No. NATC-WST-40R-72, April 1972.
37. "Specifications for Radar Altimeter," Rockwell International, Document No. MC409-0015, 3 September 1974.
38. Daniels, G.E., ed., "Terrestrial Environment (Climatic) Criteria Guidelines for Use in Aerospace Vehicle Development, 1973 Revision," NASA TMX-64757, May 1971.
39. Gelb, A., ed., Applied Optimal Estimation, M.I.T. Press, 1974.
40. Escobal, P.R., Methods in Astrodynamics, Wiley, 1968.
41. Smart, W.M., Textbook on Spherical Astronomy, 4th ed., Cambridge University Press, 1960.
42. The American Ephemeris and Nautical Almanac, Nautical Almanac Office, U.S. Naval Observatory.
43. Schiesser, E.R., "SSV Mission Navigation Requirements," Johnson Space Center, FM83 (72-228), 30 August 1972.
44. Bellaire, R.G., "Statistics of the Geodetic Uncertainties Aloft," The Analytic Sciences Corp., presented at American Geophysical Union Fall Meeting (San Francisco), December 1971.
45. "Entry, TAEM, and Landing Navigation Input to Level C OFT Navigation Functional Subsystem Software Requirements," Johnson Space Center, IN No. 75-FM-39, 30 May 1975.
46. "Aerodynamic Design Data Books. Volume I Orbiter Vehicle Revision 3," Johnson Space Center Report No. SD-72-SH-0060-1J, 25 June 1976.
47. Eckelkamp, R.E. "OFT 1 Nominal Entry-Landing Test Case 1," Informal Memorandum, 1 April 1976.

THE ANALYTIC SCIENCES CORPORATION

48. Pixley, P.T., "Times of Output, Coordinate Systems, and Station Location Errors for TASC," FM82 (72-240), 6 September 1972.
49. "Navigation System Characteristics," MSC IN 72-FM-190, Rev. 1, 10 July 1973.
50. Cree, D., Johnson Space Center, Personal Communication to H.L. Jones, 12 December 1975.
51. "ALT Level C Functional Subsystem Software Requirements (FSSR)," Rockwell International, Document No. SD-74-SH-0269, 17 March 1976.
52. AN/APN-194(V) "Pulse Radar Altimeter Systems, Technical Description," Honeywell, Inc., January 1976.
53. Cole, A.E., "Distribution of Thermodynamic Properties of the Atmosphere Between 30 and 80 km," AFCRL-72-0477, August 1972.